Characterization of molecular targets for differential regulation of the type I and III interferon induction and signalling pathways by rotavirus NSP1

Thesis submitted in accordance with the requirements of the University of Liverpool for the degree of Doctor in Philosophy by

Gennaro Iaconis

September 2018

Table of contents

List of figures

List of tables

Acknowledgments

I would like to thank all the people that contributed to make this challenging scientific experience an incredible and unforgettable human and scientific challenging experience. Support, arguments, laughs, confrontation and much much more are in every single page of this work. Without you all this was not possible.

Per mia madre, semplicemente la persona piu' forte che conosco.

Per mio padre, che mi ha trasmesso la capacita' di mettermi in discussione.

Above all, this work is for you that after many years, are still able to surprise me.

Ad maiora.

Somewhere, something incredible is waiting to be known.

Declaration

I, Gennaro Iaconis, confirm that the work presented in this thesis is the result of my own work and effort. The material contained in the thesis has not been presented, nor is currently being presented, either wholly or in part, for any other degree or other qualification.

Research in this thesis was carried out at the Pirbright Institute (UK).

Characterization of molecular targets for differential regulation of the type I and III interferon induction and signalling pathways by rotavirus NSP1

Gennaro Iaconis

Abstract

Rotavirus (RV) is the leading cause of severe dehydrating diarrhoea in infants, infecting almost every child by 3-5 years of age and causing approximately 590,000 gastroenteritis-associated deaths world-wide both in developed and developing countries. The virus infects the young of all mammalian species and cross-species infections and zoonosis events have been reported. However, RV is host replication-restricted during heterologous infection for reasons that are not fully understood.

Type I and type III interferons (IFNs) constitute the first line of defence against viral infection. Their expression is triggered when specific viral components (Pathogen-Associated Molecular Patterns – PAMPs), such as dsRNA, are detected within the cells by specific host proteins, Pattern Recognition Receptors (PRR). Once secreted, IFNs bind their specific receptors inducing the expression of interferon stimulated genes (ISGs), establishing an antiviral state.

RV non-structural protein 1 (NSP1), exhibits the greatest sequence variability of any of RV protein. Although non-essential for RV replication in cell culture, NSP1 has been suggested as a virulence factor modulating the host innate immunity. RV NSP1-mediated ability to modulate the IFN response is conserved between strains infecting different species, however, it has been reported that targets within the induction and signalling pathways vary between strains. NSP1 derived from viruses infecting monkeys (RRV, SA) and mice (EW) appear to preferentially target IRF-3 to induce its proteasome-mediated degradation, while NSP1 of porcine origin (OSU) targets β-TrCP, preventing NF-κB activation. In contrast, NSP1 from RV strain UKtc infecting cattle appears to target both IRF-3 and β-TrCP.

In order to establish if the observed RV host-range restriction is related to the ability of NSP1 to selectively target different components of the IFN pathways, Y-2-H analysis were performed. A panel of NSP1 derived from RV infecting different mammal species were tested for their binding ability against components of the IFN induction pathway. Indeed NSP1 showed a strain-dependent ability to interact with IRF-3.

A series of luciferase reporters have shown that NSP1 was able to downregulate the induction of type I and type III IFNs at their transcriptional level and how this downregulation varied between NSP1 derived from different strains. In addition, NSP1 appeared to target the IFN signalling pathway, blocking ISGs transcription.

Moreover, NSP1 showed a strain-dependent expression level.

1 Introduction

1.1 Rotavirus

1.1.1 Historical Background

Diarrheal disease is one of the predominant cause of death in children under the age of five years in developing countries (Estes *et al.*, 2007; Martella *et al.*, 2010). The availability of clean water and adequate hospital treatment are key factors in determining the severity of diseases (Parashar *et al.*, 2003). In developed countries advanced sanitary conditions play a pivotal role in reducing transmission, however prevalence of infection is still very high (Tucker *et al.*, 1998).

Until the end of the sixties diarrheal diseases due to viral infection were not reported (Yow *et al.*, 1970). Only in 1969, Mebus's group reported the presence of virus particles, 65nm in diameter, in the faces of animals previously inoculated with bacteria-free filtrates of diarrhoeic faces *(Mebus et al., 1969)*, and in 1971 they were able to successfully cultivate Nebraska calf diarrhoea virus (NCDV) in primary foetal bovine cell culture (Mebus *et al.*, 1971). These early works in animals received little attention until electron-microscopic examination of biopsy material from children with acute non-bacterial gastroenteritis revealed the presence of orbivirus-like particles within epithelial cells of the duodenal mucosa (Bishop *et al.*, 1973). This first report was rapidly followed by others in which virus particles, morphologically indistinguishable from calf reo-like virus, were detected in the feces of children with gastroenteritis in England (Flewett *et al.*, 1973), Australia (Bishop *et al.*, 1974), Canada (Middleto.Pj *et al.*, 1974), and the U. S. (Kapikian *et al.*, 1974). Shortly afterwards, it became clear that rotaviruses were an important etiological agent of diarrhoea in infants and young children, causing up to the 50% of the gastroenteritis-related hospitalisation. Later in the in the eighties, the first successful cultivation of human rotaviruses in African green monkey cells MA104 was reported, facilitating the investigation of the virus at the molecular level (Wyatt *et al.*, 1980), allowing

further examination of the rotavirus replication cycle, epidemiology, pathogenesis and the nature of host resistance.

1.1.2 Classification

1.1.2.1 Reoviridae

Rotaviruses (RV) constitute the genus of *Rotavirus*, one of the 16 genera of Reoviridae, together with *Aquareovirus*, *Cardoreovirus*, *Coltivirus*, *Crabreovirus*, *Cypovirus*, *Dinovernavirus*, *Fijivirus*, *Idnoreovirus*, *Mimoreovirus*, *Mycoreovirus*, *Orbivirus*, *Orthoreovirus*, *Oryzavirus*, *Phytoreovirus* and *Seadornavirus* (International Committee on Taxonomy of *et al.*, 2012). The viruses of this family have a double-stranded RNA (dsRNA) genome divided in to 10, 11 or 12 segments, encapsidated within a non-enveloped icosahedral particle with a diameter spanning between 60 and 100nm. Reoviridae family can be further classified into two sub-families, based on the presence or the absence in the inner capsid (the core) of a "turret"- like protein, situated on the surface of the icosahedral core particle, one at the each of the five-fold axes. The *Spinareovirinae* (Spinae from Latin spike) sub-family contains Reoviridae members (*Aquareovirus*, *Coltivirus*, *Cypovirus*, *Fijivirus*, *Orthoreovirus*, *Idnoreovirus*, *Dinovernavirus*, *Oryzavirus*, *Mycoreovirus*) which show spikes or turrets on the surface of the core particle. In contrast, members of the *Sedoreovirinae* (*Cardoreovirus*, *Mimoreovirus*, *Rotavirus*, *Orbivirus*, *Phytoreovirus*, *Seadornavirus*), show a relatively smooth morphology (Sedo from Latin smooth).

Members of the *Reoviridae* family are the largest and the most diverse group of dsRNA viruses in terms of host range, infecting different species including human (Rotavirus), animals (African horse sickness viruses) and plants (rice dwarf virus) (International Committee on Taxonomy of *et al.*, 2012).

Table 1. Feature of members of the Reoviridae family.

Reoviridae genus	Number of genome segments	Hosts
	Spinareovinae	
Aquareovirus	11	fish, molluscs
Coltivirus	12	Mammals, arthropods
Cypovirus	10	Insect
Dinovernavirus	9	Insects
Fijivirus	10	Plants, insects
Idnoreovirus	10 or 11	Insects
Mycoreovirus	11 or 12	Fungi
Orthoreovirus	10	Vertebrates
Oryzavirus	10	Plants
	Sedoreovirinae	
Cardoreovirus	12	Crustaceans
Mimoreovirus	11	Marine photosynthetic protists
Orbivirus	10	Mammals, birds, arthropods
Phytoreovirus	12	Plants, insects
Rotavirus	11	Human and Vertebrates
Seadornavirus	12	Human, cattle, pig

Division of the Reoviridae family into two subfamilies based on the presence or absence of a turreted-like structure on the outer shell of the core particle.

1.1.2.1.1 Rotavirus

RV are classified serologically by a scheme that allows for the presence of multiple groups (serogroups, based on viral protein 6 -VP6- reactivity) and of multiple serotypes within each group (based on viral protein 4 -VP4- and viral protein 7 -VP7- neutralizing epitopes) (Estes *et al.*, 2007). RV are divided into seven distinct groups (A-G), now designated RVA (rotavirus A), RVB (rotavirus B), RVC (rotavirus C) etc. RVA, RVB, and RVC strains have been found in both humans and animals. To date, RV of groups D, E, F, and G have been found only in animals (Trojnar *et al.*, 2010). RV falling into each of the seven groups can be identified by cross-reactive antibodies to the viral structural protein 6 (VP6). The particular group a virus belongs to can be determined by a number of serological tests such as immune-fluorescence (IF) (Pedley *et al.*, 1986), enzyme-linked immunosorbent assay (ELISA) and immunoelectron-microscopy (IEM) (Estes *et al.*, 2007). Viruses within each group are

capable of genetic reassortment, however, such mechanisms do not occur between viruses in different groups, and thus RV groups are considered unique species (Yolken *et al.*, 1988).

The group A rotaviruses (RVA) have been studied most in depth because few strains belonging to the other groups have been successfully cultured *in vitro* (Matthijnssens *et al.*, 2011) and serotype A viruses are important paediatric and animal pathogens (Martella *et al.*, 2010; J. T. Patton, 2012). Within the RVA group, virus isolates have been divided into serotypes. This classification is based on plaque reduction or fluorescence foci reduction neutralization assays using hyper-immune serum prepared in antibody-negative animals targeting the outer capsid proteins, VP7 and VP4 (Hoshino *et al.*, 1996). Based on of this, currently 32 G-serotypes (G1 - G27) (G for glycoprotein VP7) and 74 P-types (P for protease sensitive protein VP4) have been described for RVAs (Crawford *et al.*, 2017). Among G-serotypes, G1-4 and G9 are the most common human strains worldwide (Angel *et al.*, 2012; Gentsch *et al.*, 2005; Santos *et al.*, 2005). RV are classified by a binary system similar to the one used for influenza viruses, in which distinct types of VP4 and VP7 are recognised (D. Y. Graham *et al.*, 1985; Hoshino *et al.*, 1984). The advent of deep sequencing has allowed a further classification of RVA, with the possibility to relate serotypes to genotypes. To integrate the P-serotype and genotype designation, an open Arabic number following P is used to denote serotype, an Arabic number in brackets is used to indicate genotype. To identify a specific virus first the P (VP4) number as determined by serotyping, then followed by the designated genotype number in brackets, after which the G (VP7) number is given. For example, using this system, the human Wa isolate is designated P1A[8]G1.

In April 2008, a new system of classification was developed for group A RV, based on nucleotide sequence. The system assigned a specific genotype to each of the 11 segments of the RV genome (VP7-VP4-VP6-VP1-VP2-VP3-NSP1-NSP2-NSP3-NSP4-NSP5/6 genes) based on nucleotide identity cut-off percentages (Maes *et al.*, 2009) (Table 2). Today RV classification is classified as followed: RV group/species of

origin/ country of identification/ common name/ year of identification/ G- and P-type (Matthijnssens *et al.*, 2011).

Table 2. Nucleotide identity percentage cut-off values defining genotypes for 11 RV gene segments of rotavirus A (RVA).

Gene product	Percentage identity cut-off values	Genotypes	Name of genotypes
VP7	80%	27 G types	Glycosilated
VP4	80%	37 P types	Protease sensitive
VP6	85%	18 I types	Inner capsid
VP1	83%	9 R types	RNA-dependent RNA polymerase
VP2	84%	9 C types	Core protein
VP3	81%	8 M types	Methyltransferase
NSP1	79%	18 A types	Interferon Antagonist
NSP2	85%	10 N types	NTPase
NSP3	85%	12 T types	Translation enhancer
NSP4	85%	15 E types	Enterotoxin
NSP5	91%	11 H types	phosphoroprotein

1.1.3 Epidemiology

RVs are the predominant etiological agent of acute viral gastroenteritis in the young of a wide range of mammalian and avian species (Tate *et al.*, 2016). Until the discovery of RVs, only a small portion of severe diarrheal illness in children was associated with a specific etiological agent (Yow *et al.*, 1970). With the development of world-wide accurate diagnosis, it has become clear that RVs are the major etiological agent of serious diarrheal in the young world-wide (Walker *et al.*, 2013). By the age of 5 years, almost every child has encountered a RV infection, with the highest incidence of infection occurring between 6 and 24 months of age (Angel *et al.*, 2012). Factors such as healthcare system and access to clean water lead to a dramatic difference in severity of disease in developed and developing countries. The impact of RV infection on infant mortality is 82% greater in poor regions of Asia, Africa and Latino America (Bresee *et al.*, 2005; Parashar *et al.*, 2009; Parashar *et al.*, 2006b; WHO, 2016). In the U.S. RVs cause about 5% to 10% of all diarrheal episodes in children under the age of 5 years, with 3 million cases reported, 500,000 visits to

a medical centre, 70,000 hospitalisations and 20-40 deaths (Desai *et al.*, 2011; Fischer *et al.*, 2007; Parashar *et al.*, 2006a). Similar results have been published in epidemiological studies in Europe (Soriano-Gabarro *et al.*, 2006). Hospital-based studies in developing countries have indicated that overall RVs are the leading cause of life-threating diarrhoea, causing more than 100 million episodes, 2 million hospitalisations and approximately 500,000 deaths in children younger than 5 years (Lanata *et al.*, 2013; Parashar *et al.*, 2003; Rheingans *et al.*, 2009) (Figure 1). Adults are frequently re-infected with RV, as suggested by the high titre of RV antibodies that can be found throughout (Lausch *et al.*, 2017). Usually these subsequent infections are asymptomatic, with minimal, moderate or no effects. RVs have been reported to be the cause up to 36% of the cases of the diarrhoea affecting adult travellers (Sheridan *et al.*, 1981) and symptomatic infection can also occur in parents and carers of children with RV gastroenteritis, immunocompromised persons and elderly adults.

Group A rotaviruses are the major cause of disease in humans, however, group B (C. M. Chen *et al.*, 1985; Sanekata *et al.*, 2003; Su *et al.*, 1986) and C also infect humans (Bridger *et al.*, 1987; Bridger *et al.*, 1986), whereas, sero-groups D and E have been reported to successfully infect only animals (Trojnar *et al.*, 2010).

The transmission of human RV is complex and differs greatly geographically. During the early stages of infection, the virus is highly contagious because of the low infectious dose that is sufficient to productively infect a susceptible individual (van Gaalen *et al.*, 2017). The virus is shed for several days at a very high concentration ($>10^{12}$ particles/gram) in the stool and vomit of infected individuals (Ward *et al.*, 1984) and because RV particles are highly resistant to environmental inactivation (temperature, pH) (Keswick *et al.*, 1983), they may persist on contaminated surfaces for several months. The faecal-oral route of transmission is the major one observed for RV infection. However, a respiratory route of transmission is suggested by temporal patterns of disease in temperate zones, with clear distinct winter peaks of incidence (van Gaalen *et al.*, 2017).

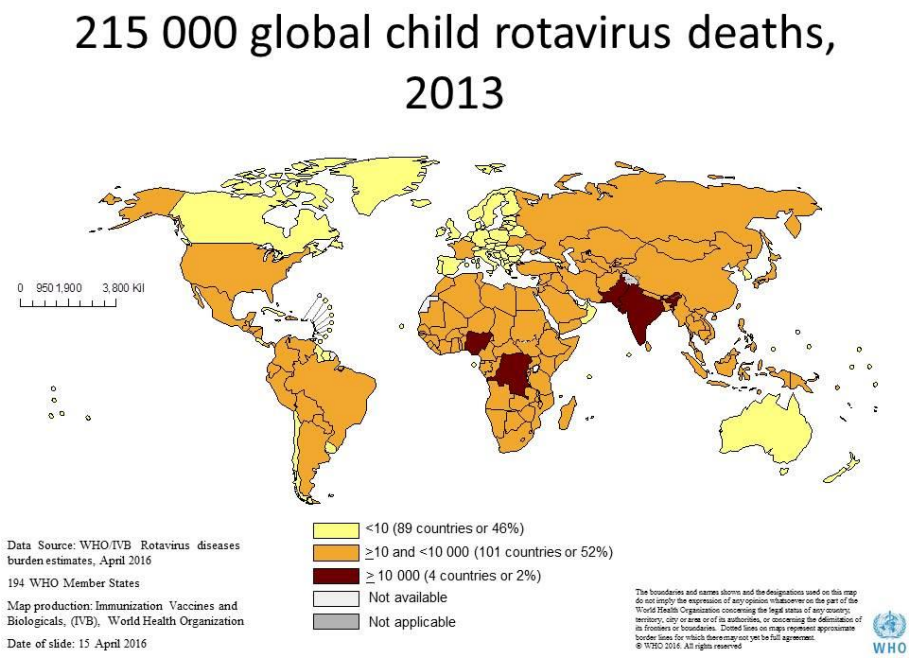

Figure 1. Map showing the global child deaths due to RV infection.

The burden of RV disease is unevenly distributed between developed and developing countries, probably for socioeconomic and epidemiological reasons, with the majority of deaths occurring in the developing countries (WHO, 2016).

1.1.4 Pathogenesis and pathology

The understanding of RV pathogenesis is based primarily on studies in animal models. *In vivo,* RV infects mainly mature enterocytes in the mid and top section of the villi of the small intestine, suggesting that fully differentiated enterocytes express molecules required for efficient infection and replication (Ramig, 2004). However, studies have demonstrated that RV can replicate in the liver, the biliary system and pancreas (Desselberger, 2014). In animal models, infection can have different outcomes, ranging from a few visible lesions of the intestine, to more severe pathology, as enterocyte vacuolization, villus blunting and crypt hyperplasia (Ramig, 2004). Severity of intestinal infection depend on both host and viral factors. Based on the relationship occurring between the virus and the host, two types of infection are possible, homologous and heterologous. Homologous strains (strains generally

isolated from the host species in question) tend to replicate efficiently, often causing diarrhoea at a very low inoculation dose, and spread efficiently in that host. In general, heterologous strains (not routinely isolated from that host in question but found frequently in another host species) replicate poorly compared to the homologous strains (Sen *et al.*, 2009). The replication rate for both homologous and heterologous strains seems to depend on the age of the animal at infection.

Loss of the absorption function of damaged intestinal villus enterocytes has been addressed as the major contributing factor to RV-induced diarrhoea (Estes *et al.*, 2007). Another study suggested that the diarrhoea resulted from epithelial damage caused by villus ischemia (Osborne *et al.*, 1988). However, studies in animal models have shown that diarrhoea was observed before the detection of damaged villi. The fact that gut lesions often do not correlate with the presence of diarrhoea suggest an alternative mechanism of diarrhoea induction. Later in infection, intracellular events, probably involving non-structural protein 4 (NSP4), cause the release of Ca^{2+} from the endoplasmic reticulum. This results in disruption of the microvillar cytoskeleton and increased permeability of the membrane to Ca^{2+} (Ramig, 2004; Tian *et al.*, 1994). Furthermore, the enteric nervous system (ENS) in the intestinal wall has also been shown to be involved in RV-induced diarrhoea (Lundgren *et al.*, 2000).

1.1.5 Rotavirus vaccine

RV infection is ubiquitous among mammals and the virus can acquire the ability to spread from animals to humans (Desselberger, 2014). However, RVs are usually replication restricted in heterologous host species, resulting in poor replication and reduced virulence compared to the homologous species (Sen *et al.*, 2009). This host range restriction and the observation that natural infection can protect against severe RV-induced acute and recurrent gastroenteritis (RVGE) (Angel *et al.*, 2012) were the basis for the development of the three live-oral-attenuated vaccines, Rotashiled (Wyeth), Rotarix® (GSK) and RotaTeq® (Merck). Rotashield was

the first one to be licensed in U.S., however, in 1998 was withdrawn due to a potential link between first vaccination and intussusception (Kapikian *et al.*, 2005). The two other vaccines released later in 2006, showed no significant risk of intussusception (Angel *et al.*, 2007). RotaRix® (designed as RV vaccine 1, RV1), was a monovalent vaccine derived from a virulent human G1P[8] strain attenuated by passaging in cell culture (Bernstein *et al.*, 1999; Phua *et al.*, 2005). RotaTeq® (designed as RV vaccine 5, RV5) was a pentavalent vaccine, containing a bovine strain and bovine-human mono-reassortant strains containing the common human RV G and P types (G1, 2, 4 and P[8]).

RV1 and RV5 are globally licensed and protect against strains that are not included in the vaccine reassortment (Armah *et al.*, 2010; Leshem *et al.*, 2014; Patel *et al.*, 2012; Steele *et al.*, 2012), however, the exact mechanism of protection remains unclear.

1.1.6 Virion Structure

The morphological appearance of RV by negative-stain electron microscopy is distinctive. The term “rotavirus” was given to the particle due to the sharply defined outline of the outer layer that resembled the rim of a wheel (rota from Latin means wheel) (Flewett *et al.*, 1974).

RV is a non-enveloped icosahedral, triple-layered virus of approximately 100 nm in diameter (Trask, Ogden*, et al.*, 2012). The triple-layered particles (TPLs) are composed of an outer layer characterized by the presence of protein spikes that protrude from the surface, an intermediate layer and an inner core. The use of cryo-electron microscopy (cryoEM) and high-resolution image processing techniques (x-ray crystallography) have allowed a detailed reconstitution of the particles to near atomic level (Settembre *et al.*, 2011). All three layers show an icosahedral organization: a T=13l (levo) for the two outer layer, while the innermost exhibits a unique T=1 icosahedral organization.

Starting from the inside of the virion, the architecture of the inner layer surrounding the viral genome is organized in 120 copies of VP2 proteins organized in dimers (Labbe *et al.*, 1991; Lawton *et al.*, 1997; Z. Li *et al.*, 2009). Of the two subunits, one (VP2A) points towards the fivefold axis, while the other (VP2B), fills the space between VP2A (Z. Li *et al.*, 2009), forming a decameric cap structure at the fivefold axis. The N-terminus of VP2 points towards the viral genome, where it is thought to interact with the dsRNA genome having shown RNA-binding capability (McDonald *et al.*, 2011; Steger *et al.*, 2018). Within the core the dsRNA genome is thought to exist in a super-coiled conformation around one of the 12 copies of the transcriptional complex (TC). TCs are formed by the viral protein 1, VP1, the RNA dependent RNA polymerase (RdRp) and the viral protein 3, VP3, the capping enzyme, found at the 5-fold axes (Jayaram *et al.*, 2004).

The VP2 layer is surrounded by 780 molecules of VP6 proteins organized in 260 trimers (Z. Li *et al.*, 2009). The particle formed by the inner core and the external VP2 shell is referred as double layered particle (DLP) and is about 705Å in diameter (Desselberger *et al.*, 2013). DLPs are transcriptionally active, but not infectious, and they are the structure delivered into the host cell upon infection (Desselberger *et al.*, 2013). VP6 may provide structural integrity for RV, enhancing long-term stability of the particle (Zeng *et al.*, 1996).

The outer layer is formed by VP4 and VP7: the first forms spikes that protrude from the virion surface while the second is a glycoprotein that constitutes the surface of the particle. VP7 is organized in 260 trimers, giving a T=13 icosahedral shape of the shell (Estes *et al.*, 2007). Sixty spikes composed of dimers of VP4 protrude for a length of around 120Å from the smooth surface and inward about 80Å (Z. Li *et al.*, 2009). VP7 interacts with the tips of VP6 trimers underneath to stabilize the outer most shell. VP4 is shown to be implicated in cell attachment and penetration (Diaz-Salinas *et al.*, 2013; Y. Li *et al.*, 2018; Trask *et al.*, 2013), haemaglutination (Fiore *et al.*, 1991), neutralization and virulence, and interacts with both VP6 and VP7 (Trask, Ogden*, et al.*, 2012). VP4 is subject to proteolytic cleavage, resulting in two distinct but still associated sub-units, VP8* (28kDa) and VP5*(60kDa) (Trask *et al.*, 2013).

A distinctive feature of the virion particles is the presence of 132 aqueous channels that span the 2 outer layers and link the outer surface with the inner core. There are three types of channels based on their position and size. There are twelve type-I channels with a diameter of 40 Å that run from the core of the virus to the outer surface. Sixty type-II channels are found at each of the pentavalent position of the fivefold axis. Another set of sixty type-III channels, 140Å in depth and 50Å wide at the outer surface of the virus. Type-I and –III channels are thought to import metabolites required for RNA transcription (Desselberger, 2014; Gridley *et al.*, 2014), while type-I are believed to be conduits for the export of messenger RNA (mRNA) (Periz *et al.*, 2013).

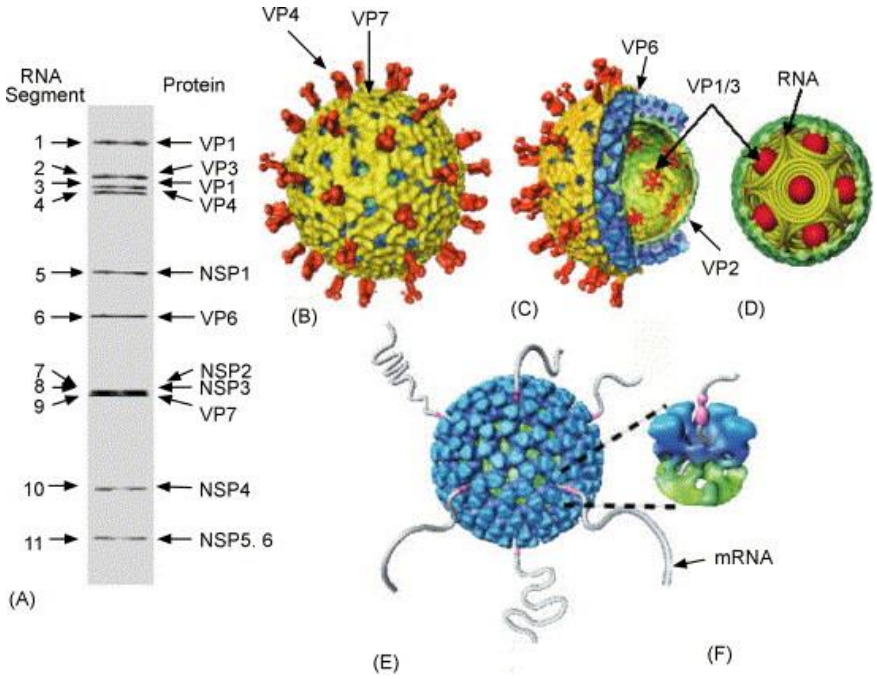

Figure 2. Rotavirus structure.

Architectural features of RV. **(A)** PAGE gel showing 11 dsRNA segments comprising the RV genome. The gene segments are numbered on the left and the proteins they encode are indicated on the right. The migration pattern observed, with segments grouped following a 4-2-3-2 scheme, is characteristic of RVA. **(B)** Cryo-EM reconstruction of the RV triple-layered particle. The spike protein VP4 is coloured in orange and the outermost VP7 layer in yellow. **(C)** A cutaway view of the RV TLP showing the inner VP6 (blue) and VP2 (green) layers and the transcriptional enzymes (shown in red) anchored to the VP2 layer at the five-fold axes. **(D)** Schematic depiction of genome organization in RV. The genome segments are represented as inverted conical spirals surrounding the transcription enzymes (shown as red balls) inside the VP2 layer in green. **(E and F)** Model from Cryo-EM reconstruction of transcribing DLPs. The endogenous transcription results in the simultaneous release of the transcribed mRNA from channels located at the five-fold vertex of the icosahedral DLP (Jayaram *et al.*, 2004) .

1.1.7 Genome organization

The RV genome is divided into eleven segments of double-stranded RNA (dsRNA). The genome segments range from 667 (segment 11) to 3302 base pairs (segment 1) (Estes *et al.*, 2007). In general the genome sequences of the dsRNA are A+U rich (from 58% up to 67%) and all segments are completely base paired (Estes *et al.*, 2007).

Analysis of the viral genome of the group A viruses using a polyacrylamide gel electrophoresis (PAGE) revealed a characteristic migration pattern: four high-molecular weight segments (1 to 4), two middle size segments (5 and 6), a peculiar triple of segments (7 to 9) and two smaller fragments (10 and 11) (Clarke *et al.*, 1981) (Figure 2-A). When this pattern, 4-2-3-2, is not observed, the virus analysed may be an avian serotype, a non-group A virus, a group A that was subjected to rearrangement or a new unique virus. Analysis of genomic electropherotypes could be a potential rapid technique for the genotypic characterization of the virus during outbreaks, however, because distinct RNA patterns can arise by different mechanisms (re-assortment, mutation, rearrangements) and RNA segments of different sequences may co-migrate, these profiles are not useful as a definitive criterion for classification of a virus strain.

Although some genes possess additional in-phase (genes 7, 9 and 10) or out-of-phase (gene 11) ORFs, evidence to date indicates that all segments are monocistronic, except gene 11 that encodes for two non-structural proteins, NSP5 and NSP6 (Desselberger, 2014). The open reading frame of each segment is flanked by 5’ and 3’ untranslated regions (UTRs) that are variable in length. UTRs are believed to play a role in genome replication, genome packaging and in the regulation of gene expression as a consequence of either their primary nucleotide sequences or their secondary structures. Although UTRs are not completely conserved among the different genome segments (and often differ in their length), terminal consensus sequences are common to all eleven genome segments: the 5’-terminal consensus 5’-GGC(A/U)7−3’ and the 3’-terminal consensus 5’-U(G/U)3(A/G)CC-3’. A work by Di

Lorenzo *et al* showed the 5'-UTR of several (but not all) genome segments of RV contain an inhibitory motif (IM) that downregulates expression of RV cDNAs when expressed from a T7 polymerase-encoding recombinant vaccinia virus (De Lorenzo *et al.*, 2016). The positive strand has a conserved 5'-cap sequence $m^7GpppG^{(m)}Gpy$ but it lacks a 3'- poly-A tail (Imai *et al.*, 1983). However, the 3'-end of the positive sense has the conserved sequences 5'-UGUGACC-3' as the minimal essential promoter for the negative strand RNA strand synthesis (J. T. Patton *et al.*, 1996; Wentz, Patton*, et al.*, 1996). For RV, as for all members of *Reoviridae* family, the positive strand mRNA has two functions: it is used for translation of viral proteins and also serves as templates for the synthesis of minus strand during genome replication (Ayala-Breton *et al.*, 2009; J. T. Patton *et al.*, 2004). Moreover, each mRNA must also contain a signal sequence that is unique to it alone, because each segment needs to be distinguished from the others during genome packaging. However, these sequences remain unknown.

1.1.8 Gene-protein coding assignments

The RV genome encodes six structural proteins, VP1-VP4, VP6 and VP7, and six non-structural proteins, NSP1-NSP6. The viral proteins VP5* and VP8* are generated by the proteolytic cleavage of VP4 (Trask *et al.*, 2013). Both the genome segments and the corresponding proteins are numbered based on their migration order on PAGE from the slowest to the fastest (Figure 2). But the absolute migration order of cognate genes does vary among viral strains.

The protein coding assignment for each segments were determined by (1) *in vitro* translation using mRNA or denatured dsRNA (Mason *et al.*, 1980; McCrae *et al.*, 1983), (2) analysis of reassortant viruses (Gombold *et al.*, 1985b; Gombold *et al.*, 1987; Kantharidis *et al.*, 1988; M. Liu *et al.*, 1988), and (3) immunological studies with specific antibodies (Both *et al.*, 1983; Dyall-Smith *et al.*, 1983) .

1.1.9 Rotavirus proteins

1.1.9.1 Rotavirus structural proteins (VPs)

1.1.9.1.1 VP1 (core)

Encoded by the gene segment 1, VP1 is a 125kDa basic protein which constitutes a minor component of the viral core. Several studies have proposed VP1 as the RNA dependent RNA polymerase (RdRp) (Estrozi *et al.*, 2013). The use of a baculovirus expression system has shown that a core-like particle containing VP1, VP2 and VP3 is able to transcribe RNA, as is a core-like particle containing VP1 and VP2 only. However, a core-like particle expressing VP2 alone or VP2 and VP3 is not able to transcribe RNA (Zeng *et al.*, 1996), indicating the essential role of VP1 in RNA transcription. Furthermore, it has been shown that prototype temperature-sensitive mapping mutations within VP1 are not able to produce RNA at non-permissive temperatures (D. Chen *et al.*, 1990). The nucleotide-binding activity of VP1 was established using cross-linking experiments. VP6 active particles (DLP) expressing VP1 and photosensitive nucleotide analogue [α-^{32}P] azido-adenosine triphosphate were unable to transcribe RNA in the presence of light (Valenzuela *et al.*, 1991). VP1 specifically binds the 3' end of viral RNA containing the *cis*-acting replication signals (J. T. Patton *et al.*, 1996). VP1 functions as both a viral replicase and transcriptase (J. T. Patton, 1995), and its activity appears to be dependent on the presence of VP2 (Mansell *et al.*, 1990).

1.1.9.1.2 VP2 (core)

VP2 is a 92 kDa protein that constitutes 12% of the viral core (M. K. Estes *et al.*, 1989). It forms the innermost of the three protein layers, encapsidating the dsRNA genome, VP1 and VP3 (Settembre *et al.*, 2011). VP2 has been shown to have sequence-dependent RNA binding activity and to associate with both ssRNA and dsRNA, but showing higher affinity for ssRNA rather than dsRNA (Boyle *et al.*, 1986), facilitating its role in viral replication and encapsidation (Boyle *et al.*, 1986; Mansell *et al.*, 1990). Potential binding domains have been mapped between amino acids 1-132 (Labbe *et al.*, 1994) and between amino acids 517-636 (Landschulz *et al.*, 1988).

VP2 is highly immunogenic, and serum antibodies to this protein are a good indicator of prior infection (Lopez-Guerrero *et al.*, 2018).

1.1.9.1.3 VP3 (core)

VP3 is an 88kDa protein localised in the core of the viral particle. A baculovirus expression system expressing core-like particles has shown that VP3 binds to the N-terminus of VP2, which is the domain of VP2 that binds RNA (Labbe *et al.*, 1994; Zeng *et al.*, 1998). It has been demonstrated that VP3 exhibits a sequence-independent affinity for ssRNA, but not for dsRNA (Boyle *et al.*, 1986; J. T. Patton *et al.*, 1999). VP3 is found in early replication intermediates in the viroplasms and associated with viral mRNA during early stages of viral replication cycle (J. T. Patton *et al.*, 1990). This could be due to the guanylyltransferase capping activity of VP3, which places a 5' cap onto viral mRNA (M. Liu *et al.*, 1992). This activity has been demonstrated to be non-specific with VP3 being able to cap any RNA initiating with either guanine or adenine residues. However, VP3 does preferentially bind uncapped RNA rather than capped RNA (J. T. Patton *et al.*, 1999). VP3 has also been shown to have methyltransferase activity (D. Chen *et al.*, 1999). Recent studies have shown how VP3 plays a role in subverting the host immune response targeting MAVS in a host-range-restricted manner (Ding *et al.*, 2018). Moreover, it has been shown that VP2 cleaves the IFN-inducible 2',5'-oligoadenylate (2-5A) synthetases (OASs), thereby preventing activation of RNase L (Silverman *et al.*, 2014; R. Zhang *et al.*, 2013).

1.1.9.1.4 VP4 (outer capsid protein)

VP4 is an 88kDa protein found in the outer most layer of the virus, where it forms sixty spikes which protrude from the virion surface (Anthony *et al.*, 1991; Prasad *et al.*, 1994). Each spike is a trimer, where two VP4 molecules form a rigid structure and the third is flexible (Mathieu *et al.*, 2001). VP4 is the haemagglutinin (Fiore *et al.*, 1991; Kalica *et al.*, 1978; Prasad *et al.*, 1990; Shaw *et al.*, 1993) and it has been proposed to be the viral protein involved in cell attachment (S. K. Mohanty *et al.*, 2017; Ruggeri *et al.*, 1991). Moreover, VP4 has been implicated in growth restriction in cell culture (Greenberg *et al.*, 1983), enhancement of viral infectivity

due to the cleavage of VP4 into VP8* and VP5*, virulence (Offit *et al.*, 1986), neutralisation and protective immune responses (Offit *et al.*, 1986). Studies in mice have shown how VP4 is the major determinant in modulating disease pathogenesis (Walther *et al.*, 2015; W. Wang *et al.*, 2011). The C-terminus of 'free' VP4 was identified as interacting with actin microfilaments (Condemine *et al.*, 2018). The acting-binding domain is highly conserved in rotavirus strains from species A, B and C suggesting that actin binding and remodelling is a general strategy for rotavirus exit.

1.1.9.1.5 VP6 (inner capsid protein)

VP6 is a non-glycosylated protein which forms the inner shell of the virion and accounts for 50% of the total viral proteins (Estes *et al.*, 2007). It can spontaneously associate into trimers and biochemical and 3-dimensional structural analysis experiments have shown that this is the native form adopted by the protein within the viral particle (Gorziglia *et al.*, 1985; Prasad *et al.*, 1988; Sabara *et al.*, 1987). Deletion mutagenesis experiments have mapped a region essential for trimerisation to between amino acid 246 and 314 (Affranchino *et al.*, 1997). VP6 shows great sensitivity to pH, and variation of few degrees lead to disaggregation of the trimers into round particles or hexamers (Tosser *et al.*, 1992). The resulting single-layered particle lacks RNA-transcriptase activity which can be restored by the addition of VP6 to the core particle, indicating that VP6 is required for viral-transcriptase activity (Bican *et al.*, 1982; Charpilienne *et al.*, 2002; Sandino *et al.*, 1986). VP6 interacts with VP2, VP4 and VP7 (Charpilienne *et al.*, 2002; Mathieu *et al.*, 2001). It is highly immunogenic and antigenic and contains RV group and subgroup determinates (Lopez-Guerrero *et al.*, 2018). VP6 is used as primary antigen detection in routine diagnosis of RV disease (Lappalainen *et al.*, 2017).

1.1.9.1.6 VP7 (outer capsid protein)

VP7 forms the smooth outer surface of the mature virion, and constitutes 30% of the viral proteins (Estes *et al.*, 2007). There are 780 copies of VP7 associated in trimers (Prasad *et al.*, 1988). It is known to be the major neutralisation antigen

(Sabara *et al.*, 1985) and it is the G-serotype determinant of RV classification (Greenberg *et al.*, 1983). VP7 is a glycoprotein with three potential sites for N-linked glycosylation, although only two of these appear to be used in different strains (Kouvelos *et al.*, 1984). The N-glycosylation takes place in the host, when the protein is inserted into the membrane of rough endoplasmic reticulum (RER) (Kabcenell *et al.*, 1985). The ORF of gene 9 that encodes VP7 has three potential ORFs. The first one which transcribes for the full length protein (376 amino acids) has a sub-optimal Kozak consensus sequence. The second ORF is -90 base downstream and it has a much stronger Kozak sequence. There is a potential third ORF downstream, however, this is found only is some strains. VP7 has been shown to interact with VP4 and NSP4 within infected cells and these interactions appear to be crucial for the formation of the outer layer (Maass *et al.*, 1990). Moreover, there is some evidence that suggests that VP7 binds to calcium ions and this may play a role in maintaining the stability of the virion (Cohen *et al.*, 1979).

1.1.9.2 Rotavirus non-structural proteins (NSPs)

1.1.9.2.1 NSP1

Non-structural protein 1 (NSP1), previously known as NS53, is a 55kDa basic protein transcribed by segment 5. NSP1 exhibits the greatest sequence variability of any of the RV proteins, being much higher than even the outer capsid proteins VP4 and VP7. This amino acid sequence variability is particularly evident among virus strains that infect different animal species (Dunn *et al.*, 1994). The open reading frame (ORF) of gene 5 of group A RV can vary considerably among different virus strains. As a result, NSP1 protein ranges in size from 486 to 496 amino acids for mammalian RV isolates, to 577 amino acids for avian isolates. In contrast with the overall sequences variability, sequencing analyses have identified highly conserved residues or regions, especially in the first 150 amino acids rather than the C-terminus (Bremont *et al.*, 1993; Mitchell *et al.*, 1990). The first 55 nucleotides, which include the 5'-UTR and the sequence transcribing for the first eight amino acids are highly

conserved (Hua *et al.*, 1994). The region between amino acids 42 and 72 in the N-terminus of the protein has been found to be conserved among most RV strains. This region is rich in cysteine and has been shown to contain two potential zinc fingers domains (Hua *et al.*, 1994; Okada *et al.*, 1999). Although the majority of the NSP1 sequences available are from isolates belonging to group A, the N-terminus cysteine rich region has been found in group C RV but not in group B (Bremont *et al.*, 1993). The consensus sequence for the cysteine domain is C-X2-C-X3-H-X-C-X2-C-X5-C (Bremont *et al.*, 1993; Hua *et al.*, 1994; Mitchell *et al.*, 1990). Other conserved regions span through the sequence of NSP1: a short sequence (15-30 residues each) of basic amino acids in proximity of the N-terminus (Hua *et al.*, 1994), a cluster of acid amino acids in the last 15 residues (Hua *et al.*, 1994; Mitchell *et al.*, 1990), and eleven isolated proline residues throughout the entire length of the gene (Hua *et al.*, 1994). Moreover, sequence analyses have identified conserved regions of NSP1 with RNA-binding activity: *in vitro* experiments have confirmed its capacity to bind the 5' ends of all 11 RV mRNA strands (Hua *et al.*, 1994).

Phylogenetic analyses have revealed that NSP1 sequences resolve within two classes, termed class I and II (Arnold *et al.*, 2011). It has been shown that NSP1 is implicated in counteracting the host immune response upon viral infection (Arnold *et al.*, 2009; Bagchi *et al.*, 2010; Barro *et al.*, 2005, 2007; Di Fiore *et al.*, 2015; Feng *et al.*, 2009; Morelli, Ogden*, et al.*, 2015). These phylogenetic analyses have revealed a kind of correlation between the NSP1 origin and the modality of IFN down-regulation. NSP1 members falling into class I seem to modulate IFN activation preferentially targeting interferon regulatory factors 3, 5 and 7 (IRF-3, IRF-5 and IRF-7). In contrast, NSP1 falling in class II seem to down-regulate IFN expression modulating NF-κB activation. However, some exceptions are observed within the two groups, as described later in this chapter (1.3). The amino acids sequence variability among different strains could underline adaptations to down-regulate the IFN response in different host species. Despite the sequence divergence, the presence of evolutionary conserved regions could constitute a selective advantage in animal infection.

Immunofluorescent staining of RV infected cells has shown that NSP1 is localized into the cytoplasm (Graff *et al.*, 2002) and it associates with the cytoskeleton when analysed by sub-cellular centrifugation (Hua *et al.*, 1994). NSP1 does not appear to be essential for RV replication in cell culture as mutants encoding truncated version of the protein can still replicate but produce smaller virus plaques (Kanai *et al.*, 2017; K. Taniguchi *et al.*, 1996).

NSP1 is one of the least abundant non-structural proteins, with a half-life of 45 min in infected cells (Mitzel *et al.*, 2003). In BSC-1 cell lines infected with rhesus RV (RRV), NSP1 was not detectable after 9 hours, and at 12 hpi the protein represented less than 0.1% of total protein synthesis (Johnson *et al.*, 1989). Experiments using a vaccinia expression system have shown that in BSC-1 cells in absence of other RV proteins, the susceptibility of NSP1 to proteasome degradation is the major determinant of the viral protein stability (Pina-Vazquez *et al.*, 2007). However, the sensitivity of NSP1 to proteasome-mediated degradation can be fully reversed by viral gene products, either viral proteins alone or in combination with viral mRNAs. Based on the knowledge that NSP1 binds *in vitro* to all eleven viral mRNAs and to other viral proteins, it has been proposed that such interaction could affect the susceptibility of NSP1 to be degraded (Brottier *et al.*, 1992; Hua *et al.*, 1994).

1.1.9.2.2 NSP2

As with all dsRNA viruses, RV do not release their genome in infected cells preventing the activation of the immune system. Two hours post infection, those cells are characterized by the presence of cytoplasmic occlusion bodies, defined as viroplasms (Altenburg *et al.*, 1980). These viroplasms have been shown to be sites for dsRNA synthesis and replication, the packaging of viral dsRNA into new cores and the early steps of viral morphogenesis which result in the formation of the double-layered particle (Fabbretti *et al.*, 1999; J. T. Patton *et al.*, 1997; Wentz, Zeng*, et al.*, 1996). The major component of these bodies is NSP2 (known also as NS35) (Fabbretti

et al., 1999; Petrie *et al.*, 1984), a 35kDa basic protein encoded by gene segment 8. It assembles in octamers (Schuck *et al.*, 2001) which is the functional form of the protein (Kattoura *et al.*, 1994; Z. F. Taraporewala *et al.*, 2002). Early studies using temperature sensitive mutants have shown that NSP2 is essential for viroplasms formation (Ramig *et al.*, 1984) and virus replication (Gombold *et al.*, 1985a). Viroplasms assembly appears to be driven by the interaction of NSP2-NSP5 (Afrikanova *et al.*, 1998), without the requirement of any other viral protein (Eichwald *et al.*, 2004; Fabbretti *et al.*, 1999). The interaction of NSP2 with NSP5 seems to be essential, because when NSP2 is transiently expressed alone tends to diffuse homogeneously in the cytoplasm (Eichwald *et al.*, 2004; Fabbretti *et al.*, 1999). In RV infected cells, NSP2 appears to be present in two different dorms that differentially interacts in a phosphorylation-dependent manner with NSP5 (Criglar *et al.*, 2014). Cytoplasmically dispersed NSP2 (dNSP2), is first detected in small puncta throughout the cytoplasm of infected cells and colocalizes with NSP5 in nascent viroplasms, and accumulates rapidly in the RV-infected cell at early times post-infection. The second previously known form, viroplasmic NSP2 (vNSP2) is detected only in viroplasms, and the amount steadily increases as viroplasms mature and increase in size. It has been shown that NSP2 exhibits great affinity to microtubules (Cabral-Romero *et al.*, 2006; Eichwald *et al.*, 2012). This interaction could lead to the association of the viroplasms with the microtubules network and its subsequent virus-induce de-polymerization (Cabral-Romero *et al.*, 2006; Martin *et al.*, 2010). Studies using siRNA to knock down the expression of NSP2 have shown that the loss of the viral protein leads to inhibition of viroplasms formation, genome replication, virion assembly and synthesis of other viral proteins (Silvestri *et al.*, 2004). Cross-linking assays have shown that NSP2 binds to VP1, (Arnoldi *et al.*, 2007). The interaction with the viral RdRp could be due to the multifunctional ability of NSP2, being involved in genome replication and packaging. Enzymatic studies have revealed that NSP2 possess nucleoside triphosphates (NTPase) (Z. Taraporewala *et al.*, 1999; Vasquez-Del Carpio *et al.*, 2006), RNA triphosphates (RTPase) (Z. F. Taraporewala *et al.*, 2001; Vasquez-Del Carpio *et al.*, 2006) and helix-destabilizing activity (Carpio *et al.*, 2004).

1.1.9.2.3 NSP3

NSP3 is a slightly acid protein of 36kDa which can be found distributed in the cytoplasm or associated with the cytoskeleton of infected cells (Mattion *et al.*, 1992). NSP3 is organized in two domains, the N-terminal domain that binds the 3'-consensus sequence of all viral mRNA, "GACC" (Poncet *et al.*, 1993; Poncet *et al.*, 1994), and a dimerization domain, localised between amino acids 163 and 237. Initially NPS3 was reported to function primarily in the shut-off of cellular protein expression following viral infection (Padilla-Noriega *et al.*, 2002). In eukaryotes, protein translation is initiated by the eukaryotic initiation factor 4E (e1F4E) which binds to the 5'-cap structure of the mRNA. Subsequently, the mRNA poly-A tail is recognised by poly-A binding protein (PABP). This is followed by the interaction of e1F4E and PABP and the subsequent circularisation of mRNA which is required for efficient initiation of translation (Imataka *et al.*, 1998; Tarun *et al.*, 1995). To interrupt this process, it is believed that NSP3 first recognises the consensus sequence of the viral mRNA and then interacts with e1F4G taking over the position of PABP and host mRNA evicting them from the cellular translational complex (Gratia *et al.*, 2015) and blocking host protein synthesis (Gratia *et al.*, 2016). However, contrasting results have shown that knock down of NSP3 using RNAi technology had little or no effect on the overall viral gene expression (Montero *et al.*, 2006).

1.1.9.2.4 NSP4

NSP4 is a 28kDa protein transcribed from genome segment 10. It is a transmembrane protein that localises in the ER. NSP4 has been shown to be implicated in viral morphogenesis and pathogenesis (Ericson *et al.*, 1982; Kabcenell *et al.*, 1985). It is both co-translationally and post-translationally glycosylated (Au *et al.*, 1989; Kabcenell *et al.*, 1985). The protein is characterized by three hydrophobic domains (H1, H2 and H3) localised in the N-terminus (Bergmann *et al.*, 1989). The H2 domain contains a predicted transmembrane domain that spans into the ER membrane, while H3 appears to lie on the cytoplasmic side of the ER membrane and is implicated in the recruitment of the DLPs to the ER lumen (Jagannath *et al.*, 2006). The C-terminus is hydrophilic and forms an extended cytoplasmic domain. It has been

proposed that the C-terminus contains the signal to mediate the transport of the DLP into the ER (Au *et al.*, 1993; Taylor *et al.*, 1992). Cross-linking experiments have shown that NSP4 oligomerizes in dimers and tetramers (Maass *et al.*, 1990) and it is involved in the removal of the transient membranes from the DLPs budding through the ER. NPS4 also contains a VP4 binding domain, suggesting a potential role in the assembling of the virions outer layer (Au *et al.*, 1993).

The second function of NSP4 appears to be related to its secretion from virus infected cells and the establishment of the viral pathogenesis. NSP4 was the first viral endotoxin documented and its effects were first observed when purified NSP4 proteins were inoculated intraperitoneally and caused age-dependent diarrhoea in mice (Tian *et al.*, 1996).

The mechanism by which NSP4 destroys epithelial cells is believed to happen through paracrine pathways which leads in the end with the secretion of intra-cellular calcium (Ca^{2+}) and chloride ions (Diaz *et al.*, 2012). The interaction of NSP4 with cellular integrins activates a cascade of events resulting in the release of Ca^{2+} from the ER and accumulation into the cytoplasm, causing disruption in the homeostasis of Ca^{2+} (Sastri *et al.*, 2014). Moreover, NSP4 appears to act as viroporin, creating a Ca^{2+} channel leading to the export of Ca^{2+} from the cell (Pham *et al.*, 2017). Cytoplasmic Ca^{2+} concentration plays a pivotal role in live cell osmosis and its disruption results in dysfunctional cellular molecules which leads to the death of bystander epithelia. Furthermore, Ca^{2+} stabilizes the outer capsid of the virion and induces cell death (Ruiz *et al.*, 2005). It has been proposed that the secretion of water and loss of electrolytes from the cells that contribute to the onset of diarrhoea can be triggered by the sudden changes in Ca^{2+} concentration (Pham *et al.*, 2017).

The amino acid sequences of NSP4 is highly conserved within groups, with 98% homology in RVA (S. L. Lin *et al.*, 2003)and 93% in RVB (Guzman *et al.*, 2005). However, this identity is much lower between groups, with less than 10% sequence identity occurring between group A and group B NSP4 (Guzman *et al.*, 2005). In

contrast with the sequence variability, there is a high level of secondary sequence similarity (Guzman *et al.*, 2005).

Immunization against NSP4 has been shown to be able to induce immunity that protects animals and children from viral challenge (Iosef *et al.*, 2002; Malik *et al.*, 2008). Anti-NSP4 antibodies have also been reported to be sufficient to block RV-induced diarrhoea in mice (Hou *et al.*, 2008).

1.1.9.2.5 NSP5

NSP5 is the primary translational product of gene segment 11 (Mattion *et al.*, 1991). It is a dimer which is post translationally O-glycosylated and phosphorylated (Afrikanova *et al.*, 1996). NSP5 has shown to be able to bind ssRNA and dsRNA with equal affinity (Vende *et al.*, 2002) and also to interact with the viral proteins VP1, VP2 and NSP2 (Afrikanova *et al.*, 1998; Berois *et al.*, 2003). Interaction with NSP2 has been reported to be sufficient to form viroplasm-like structures (Criglar *et al.*, 2014). Recently it has been reported that interactions of NSP5 with NSP2 and VP5 is able to drive the recruitment of all the other viral protein to the viroplasms (Contin *et al.*, 2010). This suggests a potential role of NSP5 in orchestrating the formation of viroplasms, the recruitment of the other viral proteins and viral RNA packaging (Martin *et al.*, 2013). NSP5 expression has bene shown to be essential for virus replication. siRNA experiments knocking-down expression levels of NSP5 in infected cells have been shown to reduce the number on viroplasm-associated proteins, result in a decrease in the synthesis of structural and non-structural proteins and a reduction of genomic dsRNA and infectious viral particles (Campagna *et al.*, 2005; T. Lopez, Rojas*, et al.*, 2005; Vascotto *et al.*, 2004).

1.1.9.2.6 NSP6

NSP6 is encoded by a +1 alternative reading frame in gene segment 11. NSP6 ORF is completely positioned within the ORF of NSP5 (Mattion *et al.*, 1991). The encoded protein is of 12kDa, with a length of 92 to 98 amino acids, depending by the viral strain. NSP6 appears to be expressed at low level, with high turnover rate (Mattion *et al.*, 1991; Rainsford *et al.*, 2007).

Yeast-2-hybrid and co-immunoprecipitation experiments have shown an interaction between NSP6 and NSP5, and both proteins appear to localize into the viroplasms (Torres-Vega *et al.*, 2000). However, this interaction has not been confirmed in virus-infected cells (Torres-Vega *et al.*, 2000). The C-terminal region of NSP5 has been shown to be essential for the interaction with NSP6 and to be involved in dimerization and phosphorylation (Torres-Vega *et al.*, 2000). Sequences analysis of gene 11 from different virus isolates has revealed that NSP6 is not encoded by all RV strains (Kojima *et al.*, 1996; Wu *et al.*, 1998). The absence of the start codon of NSP6 in two human strains, the truncated form of NSP6 found in porcine OSU (S. A. Gonzalez *et al.*, 1989) and lapine (Gorziglia *et al.*, 1989) and the absence of NSP6 reading frame in group B and group C (Trojnar *et al.*, 2010) suggest that NSP6 may play a non-essential role in regulation during the viral replication cycle (Komoto *et al.*, 2017).

1.1.10 Rotavirus replication cycle

RV replicate entirely in the cytoplasm and have a lytic replication cycle (Estes *et al.*, 2007). Most of the data generated on the replication cycle were obtained from studies with permissive cell lines. In monkey kidney cells (MA104), the virus reaches a maximum yield after 10 to 12 hpi (McCrae *et al.*, 1981). However in polarized intestinal epithelial cells (Caco-2) the replication appears to be much slower with a maximum virus yield detected at 20 to 24 hpi (Jourdan *et al.*, 1997). Both cell lines are highly permissive and Caco-2 cells in particular are thought to reflect RV *in vivo* infection (Ciarlet *et al.*, 2001). *In vivo*, the natural cell tropism for RV are mature enterocytes at the tip of the villi of the small intestine (Boshuizen *et al.*, 2003), suggesting these cells express specific receptor(s) for virus attachment (Ma *et al.*, 2014). However, extra -intestinal spread of virus also occurs in human and all animal models, demonstrating a wider range of host cells and additional receptors may be involved (Yu *et al.*, 2015). RV have been reported to replicate in the liver, the biliary system and pancreas (Saxena *et al.*, 2016).

The general features of RV replication based on studies on permissive cells line are summarised as followed: (a) *In vitro* cultivation of most RV strains required an extra step characterized by the addition of exogenous proteases to the culture medium to ensure the activation of the virus through the proteolytic cleavage of VP4, (b) the replication is completely cytoplasmic, and occurs in virus-synthesised structures, defined viroplasms, (c) the virus supplies all the enzymes required for the replication of the genomic dsRNA, the host lacks these enzymes, (d) viral mRNA transcripts are used both to translate viral proteins and as template for the production of negative-strand RNA, (e) replication occurs in nascent sub-viral particles, viroplasms (free dsRNA of free negative-stranded ssRNA is generally not found in infected cells), (f) sub-viral particles are produced in association with viroplasms, and these particles mature by budding through the membrane of the ER, (g) intracellular levels of calcium are important for controlling virus assembly and stability and (h) infectious particles (TLPs) are released by cells lysis (Long *et al.*, 2017).

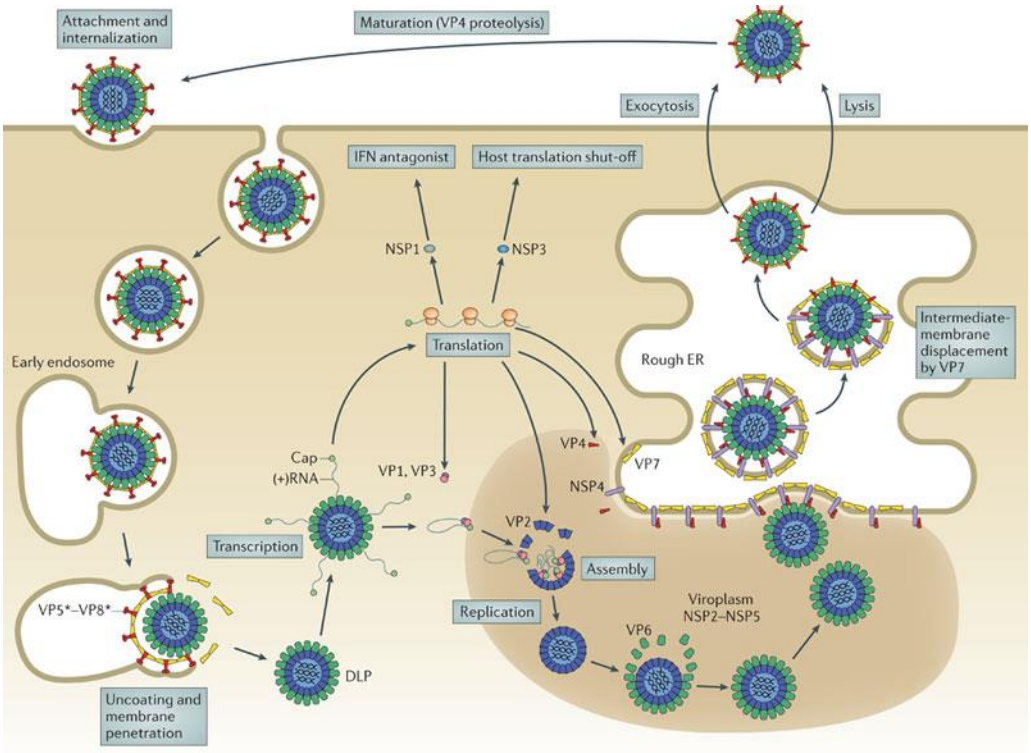

Figure 3. Rotavirus replication cycle.

RV virions attach to the surface of target cells sialic acids through VP8*, resulted from the cleavage of VP4 into VP5* and VP8* respectively. Once internalised, it is believed that variation in Ca^{2+} induce the uncoating of the TLPs and the release of DLPs. Loss of the outer shell activates the RdRp complexes (VP1 and VP3) that transcribe capped positive-sense RNA ((+)RNAs) from each of the 11 double-stranded RNA (dsRNA) genome segments. (+)RNAs serve either as mRNAs for synthesis of viral proteins by cellular ribosomes or as templates for synthesis of negative-sense RNA ((–)RNA) during genome replication. Two early-translated viral proteins, NSP2 and NSP5, interact to form large inclusions, defined viroplasms, where viral genome replication and assembly of new viral sub-particles take place. Through and undefined mechanism, new DLPs acquire a temporary outer membrane budding through the ER. Intermediate membrane displacement by VP7 leads the formation of mature TLPs that exit the cell by host cell lysis or by non-classical vesicular transport. TPLs released in the gut are exposed to trypsin-like proteases that cleave VP4 into VP5* and VP8*, producing a fully infectious virus (Trask, McDonald*, et al.*, 2012).

1.1.10.1 Virus attachment

RV attachment appears to be mediated by conformational changes occurring on the viral surface proteins upon interaction with host receptors (Estes *et al.*, 2007). RV attachment and entry are a multi-step processes which involve sialic acid containing receptors in the preliminary step to cell attachment and coordinated interactions with multiple receptors during the post attachment step (Ma *et al.*, 2014). TLPs particle have been reported to be the only viral form that is able to successfully infect cell (Long *et al.*, 2017). Cell attachment involves conformational changes of the proteins of the outer capsid, VP4 and VP7 (Trask *et al.*, 2013). VP4 is sensitive to proteolytic cleavage by proteases present in the gut of the host. Once activated, VP4 results in two distinct but still associated sub-units, VP5* and VP8* (Diaz-Salinas *et al.*, 2013). It is believed that the virus attachment is mediated by VP4 (Trask *et al.*, 2013) or by its cleavage product, VP5*(Zarate *et al.*, 2000). However, previous works have shown how the cleavage of VP4 seems not to be required for cell binding (Clark *et al.*, 1981; Fukuhara *et al.*, 1988), neither is the glycosylation of VP7 (Petrie *et al.*, 1983). A variety of potential receptors have been reported to be involved in binding process, including N-acetylneuramic acid (sialic acid), several integrins (α2β1, αvβ3, α4β1 and αxβ2) and the heat shock cognate (hsc70) (Ma *et al.*, 2014; Yu *et al.*, 2015). It has been proposed that during the early stages an interaction occurs between VP8* and sialic acid receptors (Hu *et al.*, 2012; S. Lopez *et al.*, 2004). It has been shown that VP8* of human and not human RV strains origin, goes under structural rearrangement upon glycan receptor binding (Yu *et al.*, 2015). The intrinsic structural flexibility of VP8* could provide crucial advantage in RV adaptation to intestinal replication in hosts which express different cellular glycans. Recently has been shown that VP8* that A-type HBGAs are receptors for human rotaviruses, although rotavirus strains vary in their ability to recognize these antigens (Bohm *et al.*, 2015; Yu *et al.*, 2015). VP8*- receptors interaction triggers a conformational change in VP4 to form the trimeric VP5* that through their DGE domains interact with integrin α2β1 (Fleming *et al.*, 2011; K. L. Graham *et al.*, 2003). After the initial interactions, VP8*- sialic acid receptors and VP5*- α2β1, another three host proteins

seem to be involved in many interactions: (i) the KID domain of VP5* and the ligand binding domain of hsc70 (Guerrero *et al.*, 2002; Zarate *et al.*, 2003), (ii) the CNP region of VP7 and integrin αvβ3 (Zarate *et al.*, 2004), and (iii) the GRP domain of VP7 and integrin αxβ2 (K. L. Graham *et al.*, 2003). However, the exact orders of these interactions remain unclear.

1.1.10.2 Penetration

Following the attachment to the cell surface, the virus initiates the internalization of the viral particle. Efficient entry of RV into cells requires conformational rearrangements of the spike proteins to facilitate membrane penetration. It has been reported that trypsinized particles enter the cells more rapidly than untreated (Kaljot *et al.*, 1988). Observations made by EM of RV-infected cells have shown that the viral particles were associated with coated pits and internalized in coated vesicles, suggesting that the virus entry was achieved via endocytosis (Ludert *et al.*, 1987). However, the same experimental techniques have reported that trypsin-treated viral particles entered the cells by direct membrane penetration. In these studies untreated particles were removed by the plasma membrane be endocytosis, giving a non-productive infection (Suzuki *et al.*, 1985). Later experiments using drugs that inhibited the acidification of the endosome and the transport of endocytic vesicles have shown no effect on the infectivity, suggesting that endocytosis is not involved in virus entry (S. Lopez *et al.*, 2006; Ludert *et al.*, 1987). By contrast, it has been reported that an inhibitor of the vacuolar proton-ATPase pump, bafilomic A, is able to block RV infectivity, supporting the endocytic mechanism for virus entry (Chemello *et al.*, 2002). Another mechanism of direct penetration of the cell membrane has been proposed for RV internalization. This was based on the observation that RV infection induces a rapid permeabilization of the cell membrane (Kaljot *et al.*, 1988). Taken together these studies suggest that different viral strains rely on different mechanisms for internalization (Arias *et al.*, 2015), but the exact mechanisms of each pathway remains unclear. Recent studies have shown that virions bind tightly upon contact with a cell, becoming relatively immobile on the cell surface in less than a minute. Within about 5 minutes of

attachment, the particles become inaccessible to EDTA (which releases accessible virions from the cell by dissociating VP7). In 5-7 min upon cell attachment, DLPs are released into the cytoplasm (Abdelhakim *et al.*, 2014).

1.1.10.3 Uncoating

The uncoating process of RV consists of the removal of the outermost layer proteins, VP4 and VP7, and the delivery of the transcriptionally active double-layered particles (DLPs) into the cytoplasm of infected cells (Abdelhakim *et al.*, 2014). This process can be achieved *in vitro* by the use of chelating agents such as EDTA or EGTA (Cohen *et al.*, 1979). *In vivo* it has been proposed that VP4 and VP7 are solubilized within endocytic vesicles because of the low calcium concentration (Salgado *et al.*, 2018). In support to that, the employment of the calcium ionophore A23187 seems to prevent the uncoating of porcine strain OSU (Ludert *et al.*, 1987). However, treatment of cells with A23187 appears to have no effect on the uncoating of some strains, as rhesus RRV and monkey SA (Cuadras *et al.*, 1997). Therefore, as for viral entry, the importance of calcium levels for the uncoating process might vary between different strains.

1.1.10.4 Transcription

The incoming RV double-layered particles (DLPs) contain the genomic dsRNA which is used for both the translation of viral proteins and as a template for the synthesis of new dsRNA genome (Long *et al.*, 2017). To initiate transcription, transcriptase complexes (TCs), which are formed of one copy of VP1 and VP3 each, utilize ATP (Spencer *et al.*, 1981) and viral dsRNA to generate capped, positive sense single-stranded RNA ((+)ssRNA) (Lawton *et al.*, 2001). The first is the RNA dependent RNA polymerase (RdRp) (Estrozi *et al.*, 2013), the latter is the capping enzyme, with guanylyltransferase and methyltransferase activities (D. Chen *et al.*, 1999; M. Liu *et al.*, 1992). It has been proposed that there are 12 VP1-VP3 heterodimers, one at each five axes fold anchored to the inner surface of the single-layered particle (SLP) by interactions with VP2 (Estrozi *et al.*, 2013). EM experiments have shown that the viral genome is organised into ordered concentric layers within the core structure and it

is been suggested that it winds around the TCs in spiral (Prasad *et al.*, 1996). The nascent RNA transcripts are capped at their 5'-ends ($^{m7}GpppG^{(m)}$) (Lawton *et al.*, 2001) and exit the viral core through the type I channels in the VP2 layers (Periz *et al.*, 2013). The transcription of each gene segment in different equimolar amount suggests that each TC unit functions independently (Gridley *et al.*, 2014). There is also evidence that there is a quantitative and temporal control of viral gene expression at both transcriptional and translational level (Gridley *et al.*, 2014; Long *et al.*, 2017).

1.1.10.5 Translation

The viral mRNA exits the double-layered particle (DLP) and hijacks the host translational machinery, recruiting cellular ribosomes for the translation of the twelve viral proteins (S. Lopez, Oceguera*, et al.*, 2016). For efficient translation, cellular mRNAs are circularized through the heterotrimer of eIF4E (eukaryotic translation initiation factor 4E) which binds the cap structure at the 5'of cellular mRNA, cellular poly-A binding protein (PABP) which binds the polyadenylated 3'-end, and eIF4G (eukaryotic initiation factor 4G), a scaffold protein (Imataka *et al.*, 1998; Preiss *et al.*, 1998).

RV mRNAs are capped but lack polyadenylation sequence. Nevertheless it has been shown that the last four bases of its mRNA (GACC) act as a translational enhancer. The lack of poly-A sequence implies a different mechanism for the circularization of viral mRNA. It has been shown that NSP3 regulates viral protein production shutting off cellular mRNA, leading to preferential translation of viral mRNA. The N-terminus of NSP3 interacts specifically with the 3'-consensus sequence (UGACC) of viral mRNA (Gratia *et al.*, 2016), while its C-terminus interacts with eIF4G as does PAPB, but with higher affinity (Contreras-Trevino *et al.*, 2017). It has been reported that NSP3-iF4G complex interacts with a cellular protein, RoXaN (RV X associated with NSP3) (Vitour *et al.*, 2004). RoXaN is a novel cellular protein containing at least five zinc binding domains, a paxillin leucine-aspartate repeat (LD) motif facilitating protein-protein interactions, and another protein-protein interaction domain called the tetratricopeptide repeat region (TRR) (Vitour *et al.*,

2004). Complex consisting of NSP3, RoXaN and eIF4G can be detected in RV-infected cells, indicating that RoXaN is involved in translation regulation. PAPB is known to shuttle between the nucleus and the cytoplasm: the lack of free eIF4G which is mostly bound to NSP3 due to the greater binding affinity of the viral protein, results in an immediate shuttle back of PAPB into the nucleus. All these events lead to enhancement of translation of RV mRNA and to the concomitant impairment of translation of cellular mRNAs.

1.1.10.6 Viroplasms formation and genome replication

The kinetics of the synthesis of positive and negative stranded RNA has been studied in RV-infected cells. Positive and negative RNAs are initially found during the first four hours of infection (Ayala-Breton *et al.*, 2009). Following a small linear increment of the synthesis of both RNAs, a logarithmic increase is observed later during the infection. This trend reflects the peculiarity RV replication cycle that can be divided into two waves of transcription. The first one occurs upon the infection with the delivery of double-layered particles (DLPs) into the cytoplasm of infected cells. DLPs produce a small amount of mRNA, which is translated and replicated, producing new DLPs. When new DLPs are assembled, these transcribe viral genome, initiating a secondary amplified wave of transcription.

RV proteins and RNA accumulate in cytoplasmic *foci*, called viroplasms which are sites of genome replication and DLPs assembly (Criglar *et al.*, 2014). Viroplasms appear 2 to 3 hpi (Stacy-Phipps *et al.*, 1987). The non-structural proteins NSP2 and NSP5 coordinate the formation of the viroplasms. It has been shown that those two viral proteins are able to self-assemble in viroplasms-like structure when co-transfected together (Criglar *et al.*, 2014). Experiments with RNAi that knocked-down the expression of either NSP2 or NSP5 confirmed the importance of viroplasms formation in RV replication. The experiments showed how knocking-down of either NSP2 or NSP5 resulted in a reduction in viral mRNA, proteins and progeny (T. Lopez, Rojas*, et al.*, 2005; Silvestri *et al.*, 2004). Replication and packaging within viroplasms happen in steps, during which a number of distinct replication intermediates (RI) can

be found, the pre-core RI, the core RI and the double-layered RI (Gallegos *et al.*, 1989; Z. F. Taraporewala *et al.*, 2004). The pre-core RI appears to be formed by viral RNA, the structural proteins VP1 and VP3 and the non-structural proteins NSP1 and NSP3. The core RI contains all the structural proteins found within the RV single-shelled particle (VP1, VP2 and VP3) and the non-structural proteins NSP2 and NSP5. The double-layered RI is identical to the core RI but it includes the VP6 proteins (Gallegos *et al.*, 1989). Recently published results hypothesize that within viroplasms two different species of positive sense RNAs are produced. One which exits the viroplasms and act as mRNA to translate viral proteins and another that is retained within the particle and is utilised as template for minus strand synthesis and formation of dsRNA (Silvestri *et al.*, 2004).

Cis-acting signals involved in genome replication have been identified in the 5'- and 3'-UTR regions and it is believed that they act by complementary binding to promote RNA replication (De Lorenzo *et al.*, 2016).

Although *in vitro* replication systems have shown that the structural proteins of the cores (VP1, VP2, and VP3) are capable of synthesizing dsRNA (D. Chen *et al.*, 1994; J. T. Patton *et al.*, 1997), only replication systems that include NSP2 and NSP5 are able to package the dsRNA into cores (J. T. Patton *et al.*, 2000). NSP6 may also be involved in genome packaging because it is located within viroplasms and interacts with NSP5 (R. A. Gonzalez *et al.*, 1998; Mattion *et al.*, 1991).

1.1.10.7 Virion assembly, maturation and release

The selective packaging mechanism which leads to the presence of equimolar genome segments within the infectious particle remain unknown for RV as for all the members of R*eoviridae (McDonald et al., 2016)*. Recent results based on the study of *Bluetongue virus* (BTV), a 10-segmented genome virus belonging to the genus of *Orbivirus*, suggested the presence of specific signals within the RNA sequences that drive the RNA-RNA interactions necessary for the presence of a single copy of each segment within the viral particle (Boyce *et al.*, 2016). Biochemical and structural studies of RV replication suggest that the selection 11 distinct RNA segments must

involve interactions occurring between RNA segments and viral proteins (Fajardo *et al.*, 2015): these RNA-RNA and RNA-proteins interactions require the binding of NSP2 with RNA strands, the subsequent remodelling of RNA structure which stabilize interaction between RNA molecules (Borodavka *et al.*, 2017; Borodavka *et al.*, 2016).

RV morphogenesis is a process that involves the sequential assembly of the VP2 layer being applied to the pre-core particle, followed by the coating with the VP6 layer to form double-layered particle (DLPs). Once generated, DLPs move from the cytoplasm to the lumen of the ER where they acquire the VP7 external layer, forming mature TLPs. EM experiments have shown that the viral core (VP1, VP2 and VP3) accumulate in viroplasms (Garcés Suárez *et al.*, 2018). The assembly of VP1 and VP2 is dependent on both their high affinity for ssRNA and their interaction with NSP2 and NSP5 (Arnoldi *et al.*, 2007; Colomina *et al.*, 1998; J. T. Patton *et al.*, 2006). VP2 forms the structural basis of the viral core and the simultaneous associations with VP1 and VP3 direct the formation of a functional core (Zeng *et al.*, 1998). The formation of DLPs is achieved by adding VP6 to the viral core. Co-expression of VP2 and VP6 in insect cells results in the formation of DLPs, indicating the intrinsic ability of VP6 to associate with the viral core (Zeng *et al.*, 1996). During DLPs formation in infected mammalian cells, it has been observed that VP6 accumulates in the exterior region of viroplasms which allowing its association with newly assembled viral cores to form DLPs that move from the periphery of the viroplasms toward the ER (T. Lopez, Camacho*, et al.*, 2005).

NSP4 acts as an intracellular receptor on the membrane of the ER membrane where it binds newly made DLPs released from viroplasms and mediates their budding into ER lumen. This process leaves a transient membrane around the DLPs that will be replaced by the final addition of VP7 and VP4 (T. Lopez, Camacho*, et al.*, 2005). It has been proposed that the removal of the transient envelop is mediated by variation in calcium concentration (Poruchynsky *et al.*, 1991). Calcium appears to be involved also in RV maturation: studies in cell maintained in low level of Ca^{2+} have revealed decreased RV production and the inability of the virus to bud through the ER (Poruchynsky *et al.*, 1991; Shahrabadi *et al.*, 1986).

The release of infectious triple-layered particles (TLPs) appears to be cell-specific, with substantial differences occurring in differentiated and undifferentiated cell lines. In MA104, undifferentiated green money kidney epithelial cell lines, virus release seems to happen through cytolysis (Musalem *et al.*, 1985; Perez *et al.*, 1998). In contrast, in Caco-2, differentiated human colon cell lines, virions have been shown to be released from the apical surface of the cells through a vesicular transport process that bypass the Golgi system (Gardet *et al.*, 2007; Jourdan *et al.*, 1997). The apical release has been reported to involve actin and lipid rafts (Gardet *et al.*, 2007; Sapin *et al.*, 2002). However, it has been reported that the infection of Caco-2 cells could lead to the disruption of the cellular cytoskeleton, in particular the actin network (Brunet *et al.*, 2000). The same effect was reported when NSP4 was exogenously expressed (Berkova *et al.*, 2007). In addition, RV infection causes alteration in tight junctions, independently on the effect on cytoskeleton (Dickman *et al.*, 2000; Obert *et al.*, 2000).

1.2 Interferon

The ability to sense and respond to the environment is crucial to life. Cells respond to stress in a variety of ways activating pathways ranging from promoting cells survival to eliciting programmed cell death. Typically, signalling pathways act to alter transcriptional responses to generate both transient and/or sustained changes. Rapid changes in gene expression are mediated by transcriptional factors (TFs) such as members of interferon regulated factors (IRF)-family or nuclear factor kappa-light-chain-enhancer of activated B cells (NF-κB) that induce production of interferon (IFNs) and subsequent expression of a variety of interferon stimulated genes (ISGs) (R. E. Randall *et al.*, 2008; Schneider *et al.*, 2014). Thus the activation of IFN represents one of the first barriers of innate immunity that viruses face during infection. IFNs are biologically active signalling proteins that are produced and secreted by host cells upon pathogen recognition, with 3 major functions. First, they induce an antimicrobial state in infected and surrounding uninfected cells, limiting the spread of infectious agents, such as viral pathogens. Second, they modulate the innate immune response promoting antigen presentation and natural killer cell functions. Third, they activate the adaptive immune system and consequently contribute to immunological memory (Ivashkiv *et al.*, 2014).

Human interferon classification is based on the type of receptors through which they signal. Three major types have been identified: (1) Type I (IFNα, β, ε, κ, δ, ζ and ω) that binds to IFN α/β receptors (IFNAR), (2) Type II (IFNγ) that binds to interferon-gamma receptors (IFNRG) and (3) Type III (IL-28A, IL-28B , IL-29) that binds to a complex consisting of the interleukine 10 receptor beta (IL10RB) and interferon lambda receptor 1 (IFNLR1).

Type I IFNs, including multiple IFN-α isoforms and IFN-β (IFNα/β) are a key component of the host-defence against viral infections and possess potent antiviral properties. Recently type III IFN-λ has also been shown to have a non-redundant role in antiviral responses (Wells *et al.*, 2018). Innate immune cells, such as macrophages and plasmacytoid dendritic cells are the primary producers of IFN-α (Cao *et al.*, 2007),

while non-immune cells, such as fibroblasts and epithelial cells produce IFN-β (Ivashkiv *et al.*, 2014).

The early IFN response occurs when specific viral components, defined as pathogen-associated molecular patterns (PAMPs), are recognized in infected cells by specific host proteins called pattern recognition receptors (PRRs) (Mogensen, 2009; R. E. Randall *et al.*, 2008). PAMPs are molecular structures such as glycoproteins, lipopolysaccharides, proteoglycans and nucleic acid motifs that are broadly shared by different microorganisms (R. E. Randall *et al.*, 2008). Nucleic acids (RNA, mRNA, replication intermediates and dsRNA) make up the largest class of PAMPs and depending on their form, length and localization they are detected by different PRRs. Members of the PPR family can be distinguished by ligand specificity, cellular localization and activation of unique, but downstream converging, signalling pathways (Takeuchi *et al.*, 2010). Two major classes of PPRs are specifically activated by RNA viruses and they include the cytosolic retinoic acid-inducible gene-like receptors (RLRs) and membrane-bound Toll-like receptors (TLRs) (Said *et al.*, 2018).

Toll-like receptors comprise a gene family of only 10 members in humans (12 in mice). These receptors cover an impressive range of PAMPs involved in the recognition of parasites, fungi, bacteria, and viruses (Vidya *et al.*, 2018). Members of the RLR family, such as RIG-I and MDA5, sense cytoplasmic 5'-uncapped dsRNA and transmit this signal to MAVS (VISA/Cardif/IPS-1) which induces phosphorylation and activation of IRF-3/-7 NF-κB. These transcriptional factors migrate into the nucleus where, along with c-jun/ ATF-2 bind to and activate the promoters of type IFN genes, ultimately leading to IFN expression. Recently, it has been shown that nucleotide-binding oligomerization domain-containing (NOD)-like receptors (NLRs) can also detect infection with RNA viruses (Kim *et al.*, 2016).

IFNs can act in both an autocrine and paracrine manner binding to their heterodimeric transmembrane receptors (IFNAR) in infected and surrounding uninfected cells. Engagement with IFNAR leads to the activation of signal transducer and activator of transcription 1 (STAT1) and STAT2 which dimerise and associate with

IRF-9. This trimolecular complex, called IFN-stimulated gene factor 3 (ISGF3) moves into the nucleus where it binds to its cognate DNA sequences, activating the transcription of ISGs and establishing an antiviral state, which slows down the replication and the spread of the virus. To date hundreds of ISGs have been characterized that often target conserved aspects of viral infection and replication cycle, such as the use of the host cell translation machinery. It has been showed that ISGs are also involved in apoptosis (Kotredes *et al.*, 2013), inhibition of cell growth and innate and adaptive immune cell activation (Kamada *et al.*, 2018). Some of the most well-studied antiviral genes induced by type I IFNs include the adenosine deaminize acting on RNA, 2′,5′-oligoadenylate synthetase, RNase L and Myxovirus Resistance Gene A (MxA) proteins (R. E. Randall *et al.*, 2008; Schneider *et al.*, 2014; Schoggins *et al.*, 2011).

Similar to type I IFNs, type III IFNs are induced following stimulation of PRRs. In humans this family of cytokines consists of 3/4 members, IFN-λ_1 (IL-29), IFN-λ_2 (IL-28A) and IFN-λ_3 (IL-28B). Recently it has been reported that human hepatocytes upon viral infection produce a new type-III interferon that was not reported before, IFN-λ_4 (Prokunina-Olsson *et al.*, 2013). This interferon is a frame-shift variant of IFN-λ_3. Type III IFNs are structurally separate from type I IFN and also bind to a different class of receptors. Type III IFNs signal through a heterodimeric cellular surface receptor complex composed of two chains: IFNLR1 and IL-10RB (Wack *et al.*, 2015). The IL-10RB chain is also an essential component of the receptor complexes for IL-10, IL-22, and IL-26 (Donnelly *et al.*, 2004), however, the IFNLR-1 is a unique receptor complex that is used only by INF-λ. IL-10RB shows a broad expression pattern (Josephson *et al.*, 2001), whereas in contrast IFNLR-1 shows much more restricted cellular distribution. Several studies showed how fibroblast, splenocytes, bone marrow derived macrophages (Lasfar *et al.*, 2006) and endothelial cells (Sommereyns *et al.*, 2008) do not respond to IFN-λ due to lack/low expression of IFNLR-1. However, epithelium-rich organs such as the stomach (Doyle *et al.*, 2006), intestine (Brand *et al.*, 2005; Kotenko *et al.*, 2003), skin (Zahn *et al.*, 2011) and lung (Ioannidis *et al.*, 2012) show high expression of IFNLR-1 and high response to IFN-λ. IFNLR-1 shows

expression mainly in epithelial cells, however, some responses to IFN-λ are also reported in non-epithelial cells. Among these cells, conventional or classical dendritic cells (cDCs) (S. Zhang *et al.*, 2013) and plasmacytoid dendritic cells (pCDs) (Yin *et al.*, 2012) express IFNLR-1 and are IFN-λ-stimulation sensitive. IFN-λ binds initially to the IFN-λR1 chain, and the binary complex formed by the association of IFN-λ with the IFN-λR1 chain causes a rapid conformational change that facilitates recruitment of the second receptor chain, IL-10RB, to the complex. Once the assembly of the ternary complex is complete, the receptor-associated *Janus* tyrosine kinases, Jak1 and Tyk2, mediate *trans*-phosphorylation of the receptor chains which results in the formation of phosphotyrosine-containing peptide motifs sites for latent preformed cytosolic STAT proteins, including STAT1 and STAT2. Signalling of type III IFN, as for type I IFN, results in the formation of a transcription factor complex known as IFN-stimulated gene factor 3 (ISGF3) (Schneider *et al.*, 2014). Once assembled, ISGF3 translocates to the nucleus where it binds to IFN-stimulated response elements in the promoters of various ISGs. Signal transduction and gene activation profiles are almost indistinguishable from those of type I IFN. Moreover its ubiquitous expression has made it difficult to attribute a specific non-redundant role to type III IFN. However, the spectrum of responsive cells is different with the expression of type III IFN receptors mostly on epithelial cells (Siegel *et al.*, 2011).

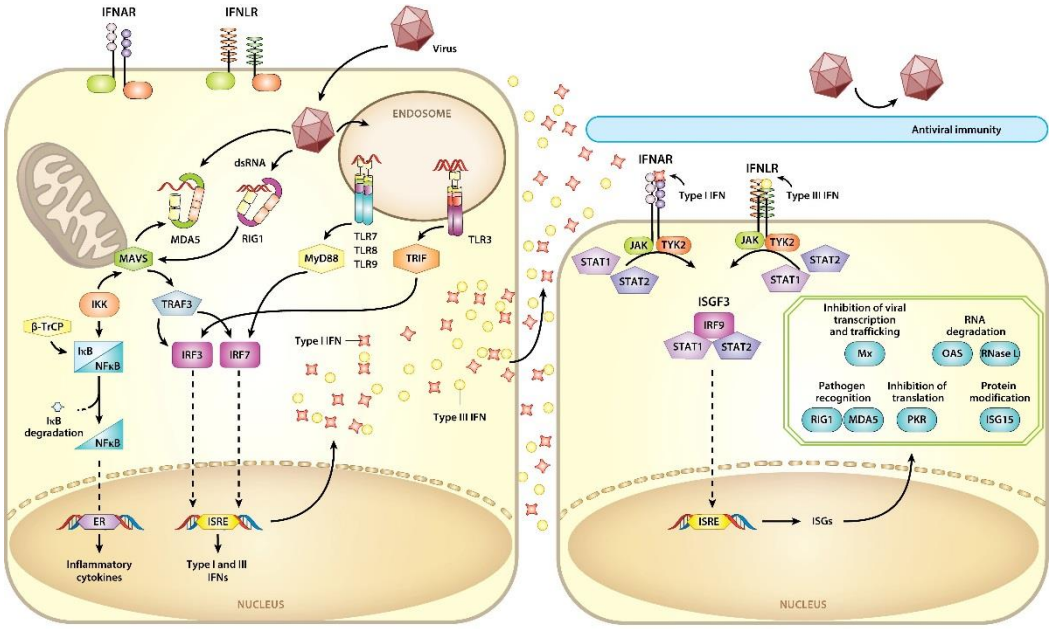

Figure 4. Detection of viral RNA in intestinal epithelial cells and induction of innate responses.

Following cells infection, RV double-layered particles are released into the cytoplasm, triggering transcriptions. Despite replication and virus packaging take place within the virioplasms, a population of dsRNA or uncapped mRNA are released and sensed by specific host proteins, Pattern Recognition Receptors (PRRs). Two major classes of PPRs include the cytosolic retinoic acid-inducible gene-like receptors (RLRs) and membrane-bound Toll-like receptors (TLRs). Members of the RLR family, such as RIG-I and MDA5, sense cytoplasmic dsRNA through a conserved DExD/H-box helicase and C-terminal domain (CTD). RIG-I recognizes 5'-triphosphorylated blunt ends of short (<300 bp) dsRNA, whereas MDA5 lacks end specificity and binds to internal sites on long (>1000 bp) dsRNA. Upon ligand binding, RIG-I and MDA5 signal through the mitochondrial antiviral sensor protein MAVS (VISA, Cardiff or IPS-1). MAVS leads to the activation of Tbk1 or IKKε and the subsequent phosphorylation of IRF-3/-7. IRF-3 is constitutively expressed in cells, where it accumulates at elevated levels in the cytoplasm. In contrast, IRF-7 is present in most cells at low levels, and its expression is amplified by type I IFN. Both IRF-3 and IRF-7 reside in inactive forms in the cytoplasm and undergo activation through phosphorylation. These active forms of IRF-3 and IRF-7 undergo dimerization and are imported to the nucleus, where they interact with specific promoters to enhance the transcription of IFN. MAVS also induces the activation of NF-κB. NF-κB regulation is governed by a number of positive and negative elements. In the "resting" state, NF-κB dimers are held inactive in the cytoplasm through association with IκB proteins. Incoming stimuli from MAVS induces the phosphorylation of IκB by Ικκα and Ικκβ. Phosphorylated IκB becomes a target of β-TrCP that induces its ubiquitination and degradation. Free NF-κB dimers can then translocate to the nucleus, bind specific DNA sequences and promote transcription of target IFNs genes. IFNs bind to heterodimeric transmembrane receptors, IFNAR. Cellular responses to IFNAR ligation are cell-type and context-dependent and can vary during the

course of the immune response. Engagement of IFNAR activates the receptor-associated protein tyrosine kinases Janus kinase 1 (JAK1) and tyrosine kinase 2 (TYK2), which phosphorylate the latent cytoplasmic transcription factors STAT1 and STAT2. Tyrosine-phosphorylated STAT1 and STAT2 dimerize and associate with IRF-9. This trimolecular complex, ISGF3, translocate to the nucleus, binds to its cognate DNA sequences, activating the transcription of ISGs and establishing an antiviral state. STAT1 can also translocate to the nucleolus as active homodimers and it can stimulate expression of a sub-set of ISGs (S. Lopez, Sanchez-Tacuba*, et al.*, 2016).

1.2.1 Toll-like receptors

Toll-like receptors (TLRs) are a family of innate immune receptors acting in the frontline detection of viral PAMPs. The human TLR multigene family comprises 10 members, of which TLR2, -3, -4, -7, and -8 are thought to be of importance in the recognition of structural components of RNA viruses, including viral double-stranded RNA (dsRNA), single-stranded RNA (ssRNA), and surface glycoproteins (Vidya *et al.*, 2018).

TLRs are transmembrane glycoprotein receptors with an N-terminal extracellular PAMP-binding region and a C-terminal intracellular signalling region. All TLRs contain an extracellular leucine-rich repeat (LRR) domains which participate in ligand recognition, and an intracellular TIR (Toll-interleukin (IL)-1 receptor) domains. It is believed that the extracellular ligand recognition induces the TLR dimerization, bringing together the cytoplasmic TIR domains. This leads to the induction of the downstream signalling processes. The activation of the TLRs leads to the expression of 3 major pathways: mitogen-activated protein kinases (MAPKs), one or more IRFs and NF-κB (De Nardo, 2015) (Figure 5).

RNA virus infections can induce up-regulation of type I IFN expression via TLR3, TLR7 and TLR8. TLR7 and TLR8 recruit a TIR-containing adaptor named myeloid differentiation primary response gene 88 (MyD88) to the cytoplasmic TIR domain of the receptor (Figure 5) . MyD88 consists of a TLR-binding TIR domain in the C-terminal portion and a death domain in the N-terminal part, and through the latter it forms a

complex with two interleukin-1 receptor-associated kinases (IRAKs), IRAK-4 and IRAK-1. Upon activation, IRAK-4 phosphorylates IRAK-1, that once activated binds the C-terminal domain of TNF receptor-associated factor 6 (TRAF6). The IRAK-1/TRAF6 complex then dissociates from the TLR. Upon activation TRAF6 polyubiquitinates the tumour growth factor beta (TGF-β) activated kinase 1 (TAK1) and the IκB kinase gamma (IKKγ, known also as NEMO) (Oeckinghaus *et al.*, 2011; C. Wang *et al.*, 2001). IKKγ subsequently associates with IKKα and IKKβ (Hinz *et al.*, 2012), leading to the IKK-mediated phosphorylation of IκB on specific serine residues in a conserved degron motif (DSGΦxS [Φ, hydrophobic residue](Kanarek *et al.*, 2012). Under resting condition, IκB proteins sequester inactive NF-κB complexes in the cytoplasm (Kanarek *et al.*, 2012). Phosphorylated IκB is a substrate for $SCF^{\beta\text{-}TrCP}$, an E3 ubiquitin ligase of the Skp-Cullin-F-box (SCF) family that recognizes this phosphodegron through its F-box subunit, β-transducin repeat-containing protein (β-TrCP) (Ghosh *et al.*, 1998). Polyubiquitinated IκB is targeted for proteasome-mediated degradation, releasing NF-κB. The family of NF-κB is composed of two sub-families, the NF-κB proteins and the Rel proteins (Kanarek *et al.*, 2012). They all share a conserved 300 amino acid long amino-terminal Rel homology domain (RHD). Sequences within the RHD are required for dimerization, DNA binding, IκB interaction and nuclear translocation (Baldwin, 1996; Ghosh *et al.*, 1998). The Rel subfamily includes c-Rel, RelB, RelA (known also as p65) (Oeckinghaus *et al.*, 2009).

Members of the NF-κB sub-family include p105 and p100. These two proteins need to be activated through proteolysis or arrested translation, generating p50 from p105 (Moorthy *et al.*, 2006) and p52 from p100 (Giardino Torchia *et al.*, 2013) respectively. However, the active forms of these proteins are not usually able to activate transcription, except when they form dimers with members of Rel sub-family (Oeckinghaus *et al.*, 2009). Only p65, c-Rel, and RelB possess C-terminal transactivation domains (TADs) that confer the ability to initiate transcription. Although p52 and p50 lack TADs, they can positively regulate transcription through heterodimerization with TAD-containing NF-κB subunits or interaction with non-Rel proteins that have transactivating capability. Alternatively, p50 and p52 homodimers

can negatively regulate transcription by competing with TAD-containing dimers for binding to κB sites. These p50 and p52 dimers may also constitutively occupy some κB sites and thus enforce an activation threshold for certain NF-κB target genes (Hayden *et al.*, 2012). The activation of NF-κB dimers is the result of IKK-mediated, phosphorylation-induced degradation of the IkB inhibitor, which enables the NF-κB dimers to enter the nucleus and activate specific gene expression.

Unlike TLR7 and TLR8, TLR3 does not require MyD88. Upon ligand binding, TLR3 brings together the TIR domains of TLR3s leading to the recruitment of TIR domain-containing adaptor protein inducing IFN-β (TRIF) (Vidya *et al.*, 2018). TRIF recruits TRAF6 and RIP-1 (receptor-interacting protein 1) and activates NF-κB, following the same TAK-1 dependent pathway as TLR7 and TLR8. In addition, it has been shown that the complex TRIF/TRAF6/RIP-1 can activate NF-κB in a TAK-1 independent way (Meylan *et al.*, 2004). TRIF also recruits TRAF3 and associates with the complex TANK/NEMO IKKγ. This complex recruits TBK1 that once activated associates with IKKε. TBK1/IKKε subsequently phosphorylates IRF-3 that then dimerizes and translocates to the nucleus to initiate transcription of type I IFNs (Thwaites *et al.*, 2014).

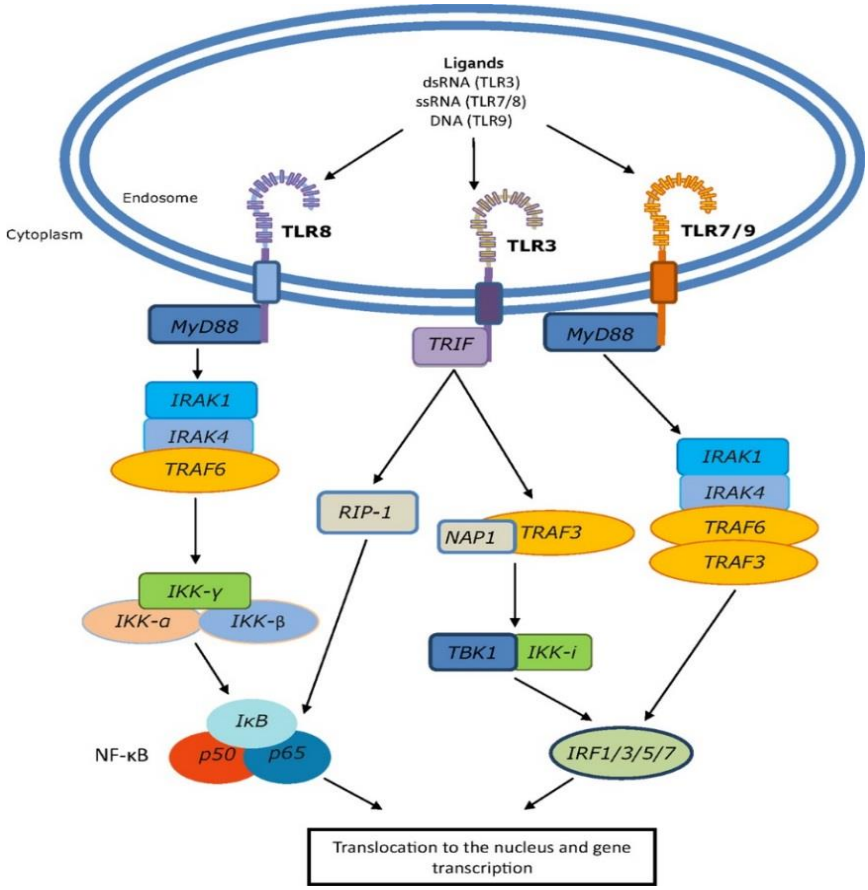

Figure 5. Recognition of double stranded RNA and activation of NF-κB and IRFs by Toll-like receptors.

Following activation, Toll-like receptors (TLRs) 7 (TLR7) and 8 (TLR8) recruit the adaptor protein myeloid differentiation primary response gene 88 (MyD88) to the cytoplasmic TIR domain of the receptor. MyD88 initiates a signalling cascade involving IL-1R associated kinase (IRAK) and TNFR-associated factor 6 (TRAF6) proteins, which converge at the activation of the IκB kinase (IKK) family members. Once activated, they lead to the IKK-mediated phosphorylation of Iκβ, that when phosphorylated becomes the substrate for β-TrCP, an E3 ubiquitin-ligase enzyme that induces its proteasome-mediated degradation. Upon the degradation of Iκβ, NF-κB dimers can translocate into the nucleus, activating gene expression. Alternatively, TRAF6 can associate with TRAF3 recruiting TBK1 that phosphorylates and activates IRF-3. In contrast, TLR3 does not require MyD88. Upon activation, TLR3 recruits TRIF that activates the complex TRAF6-/RIP-1 (receptor-interacting protein 1) and activates NF-κB, following the same TAK-1 dependent pathway as TLR7 and TLR8 (Thwaites *et al.*, 2014).

1.2.2 RIG-I receptors

The RIG-I-like receptors (RLRs) include the retinoic acid-inducible gene I product (RIG-I), melanoma differentiation-associated antigen 5 (MDA5), and laboratory of genetics and physiology 2 (LGP2). RIG-I receptors play a major role in pathogen detection and defence. They sense RNA-virus infection and are involved in establishing and modulating antiviral immunity (G. Liu *et al.*, 2018). RLRs belong to the family of aspartate-glutamate-any amino acid-aspartate/histidine (DExD/H)-box helicases and detect viral RNA ligands or processed self RNA in the cytoplasm to trigger innate immune responses and inflammation (G. Liu *et al.*, 2018). RLRs are critical sensors of viral infection and in many cell types detection of intracellular pathogens relies on a tight collaboration with TLRs. However, the possible interplay between these two systems has not been elucidated.

Although TLR-mediated signalling pathways are relatively well characterized in human pDCs (Bao *et al.*, 2013), the expression and the functional importance of RLRs in this cell type have been poorly characterised. Initial data from murine models indicated that pDCs preferentially use the TLR system rather than RIG-I for the detection of viral infections (H. Kato *et al.*, 2005) and unlike monocytes, pDCs express only marginal levels of RIG-I under steady-state conditions (Ablasser *et al.*, 2009). Recent data have shown how the expression of RIG-I is rapidly and dramatically up-regulated upon stimulation of TLR7 or TLR9. Moreover, the ability of pDCs to detect 5’-triphosphate double-stranded RNA (5’-ppp-dsRNA) seems to take place only following the activation by endosomal TLRs (Szabo *et al.*, 2014). RLRs cooperate in signalling crosstalk networks with Toll-like receptors and other factors involved in the induction of innate immune responses and the modulation of the adaptive immune response (Kawai *et al.*, 2008).

1.2.2.1 RIG-I

Retinoic acid-inducible gene I (RIG-I) contains a ssRNA/dsRNA (ss/dsRNA)-binding C-terminal domain (CTD) which, when unbound, functions as a repressor domain (RD) (Gack, 2014). During viral infections, the detection of viral components leads to the exposure of two repeats of a cysteine-aspartic protease (caspase)-recruiting domain (CARD)-like region at the N-terminus. This CARD domain can interact with proteins containing the same motif leading to the activation of downstream signalling pathways. RIG-I has a DExD/H helicase motif and an ATP-ase binding domain in its middle portion. Under resting conditions, the CARD domain is unexposed. However, during viral infection the RD recognises non-self RNA structures (associated with viral replication) such as ds RNA and 5'-triphosphate RNA (Gack, 2014). It has also been shown that RIG-I detects triphosphorylated blunt ends of short (<300 bp) dsRNA (Holloway *et al.*, 2013; Hiroki Kato *et al.*, 2008). The recognition of non-self RNA combined with the ATP binding unmasks the CARD domain of RIG-I, allowing its interaction with the CARD domain mitochondrial antiviral-signalling protein (MAVS) (Kawai *et al.*, 2005).

1.2.2.2 MDA5

Melanoma differentiation-associated antigen 5 (MDA5) shows a high degree of homology to RIG-I. They exhibit the same overall domain structure, with 23 and 35% amino acids identities in N-terminal CARD and C-terminal helicase domain respectively (Dias Junior *et al.*, 2018). MDA5 is able to detect long segments of dsRNA but it lacks the specificity for 5'-triphospate ends present in RIG-I. MDA5 has been shown to be important for the recognition of Sendai virus, rabies virus, dengue virus and RV (Faul *et al.*, 2010; Fredericksen *et al.*, 2008; Loo *et al.*, 2008; Sen *et al.*, 2011).

1.2.2.3 LGP2

Laboratory of genetics and physiology 2 (LPG2) shows 31% and 41% amino acids identities to the helicase domain of RIG-I and MDA5 respectively (Hansen *et al.*, 2011) but completely lacks the region encoding CARD, prejudicing its ability to

transmit the signal downstream to MAVS. It has been shown that LPG2 binds to dsRNA 5'-triphosphate signatures and it could compete with RIG-I binding of dsRNA, acting as negative feedback (Pippig *et al.*, 2009). In contrast, it has been reported that MDA5 ability to detect long dsRNA is augmented in presenceof LGP2 (Pippig *et al.*, 2009). The absence of the CARD motif and the strong inhibition of the virus-induced gene activation suggest that LPG2 could act as negative feedback regulator (Yoneyama *et al.*, 2005).

1.2.3 MAVS

Signalling via RIG-I and MDA5 converges to mitochondrial antiviral-signalling protein (MAVS), known also as VISA (virus-induced signalling adapter), IPS-1 (interferon promoter stimulator) or Cardif (Vazquez *et al.*, 2015). Once activated, MAVS recruits TNF receptor-associated death domain (TRADD), initiating two distinct pathways. In one, TRAAD forms a complex with the FAS-associated death domain (FADD) recruiting RIP-1 for the nuclear translocation of NF-κB (as described above in section 1.2.1). In the other pathway, MAVS/TRADD complexes recruit TRAF3, which together with TANK and IKKγ/NEMO initiates the activation of IKKs, ending in the phosphorylation and nuclear translocation of IRF-3, as reported for TLRs (Vazquez *et al.*, 2015). The convergence of RLR and TLR signalling on MAVS leads to the activation of a similar profile of gene expression, inducing synthesis and release of IFN and pro-inflammatory cytokines, establishing an antiviral response (R. E. Randall *et al.*, 2008).

1.2.4 Regulation of the IFN: promoters and induction

1.2.5 Structure of the promoter of Type I IFN

The induction of type I IFN is regulated primarily at the transcriptional level, wherein IFN regulatory factors (IRFs) play a central role (T. Taniguchi *et al.*, 2001). The promoter region of type I IFN (IFN-β and IFNα/β) contains at least 4 regulatory *cis*-elements, termed positive regulatory domains (PRDs) I, II, III and IV (Goodbourn *et al.*, 1988) (Figure 6). The PRD I and PRD III elements found within the promoter region of IFN-β are recognised and activated by members of the IRF family (IRF-3, IRF-7) (Leblanc *et al.*, 1990; T. Taniguchi *et al.*, 2001). Within the same regions, PRD II and PRD IV recognition elements were identified: these sequences are activated by NF-κB and ATF-2/c-JUN respectively (Fujita *et al.*, 1989). The promoter region of IFN-α is characterised by PRD I and PRD IV elements. Within the same region, PRD III-like elements (PRD III-LEs) have been identified: these sequences could bind to other transcriptional factors of the IRF family, however the exact nature remains unclear (Raj *et al.*, 1989; Ryals *et al.*, 1985).

IFN-β, the prototypical type I IFN, is induced by the combined actions of the transcription factors AP-1, IRF-3, IRF-7 and NF-κB. The binding sites for each set of transcription factors are localized in close proximity to each other and IFN-β expression requires the cooperative binding of all activators in a complex, the enhanceosome (Panne, 2008; Thanos *et al.*, 1995).

1.2.6 Structure of the promoter of Type III IFN

Although IFN-λ (IL-28A, IL-28B, IL-29) differ genetically from type I IFN, their similar antiviral functions gives reason to assume that their expression is regulated in a similar fashion and that their promoter sequences share common features. Both IFN-λ_1 and IFN-λ_3 promoter elements present IRFs and NF-κB binding sites (Osterlund *et al.*, 2007). In contrast with type I, they present alternative binding sites for IRFs, IFN-stimulated response elements (ISREs) (Figure 6). In contrast with type I IFN, only IRF-3, IRF-7 and NF-κB are required for type III IFN induction (Odendall *et al.*, 2014;

Onoguchi *et al.*, 2007). However, recent studies have identified a distal NF-κB binding site (-1137. -1182) responsible for a potent induction of IFN-λ (Thomson *et al.*, 2009). In the same work, they have showed how a depletion of NF-κB RelA protein significantly reduced the expression of IFN-λ. Importantly, while IFN-β is induced by coordinated action of a multifactor enhanceosome, and IFN-α expression is activated by multiple IFN regulatory factor (IRF)-binding *cis*-promoter elements, the type III IFNs are induced through independent actions of IRFs and NF-κB, with the latter having a predominant role (Iversen, Ank*, et al.*, 2010; Iversen & Paludan, 2010).

Although both IFN-λ and IFN-β are induced downstream of PRR sensing and activation of MAVS, IFN-λ production is favoured when activated MAVS localizes to the peroxisome, whereas IFN-β production is dominant when MAVS localizes to the mitochondria (Odendall *et al.*, 2014). The relative abundance of peroxisomes in epithelial cells suggests a mechanism for preferential production of IFN-λ instead of IFN-β in response to viral infection at epithelial surfaces.

IFN-λ regulation is more flexible than IFN-α/β, which could allow expression of type III IFNs in response to a wider range of stimuli compared with type I IFNs. Such flexibility will potentially render expression of type III IFNs less sensitive to microbial evasion strategies targeting the IRF pathway. Thus, the mechanisms governing type III IFN expression play an important part in dictating the biology of this antiviral cytokine.

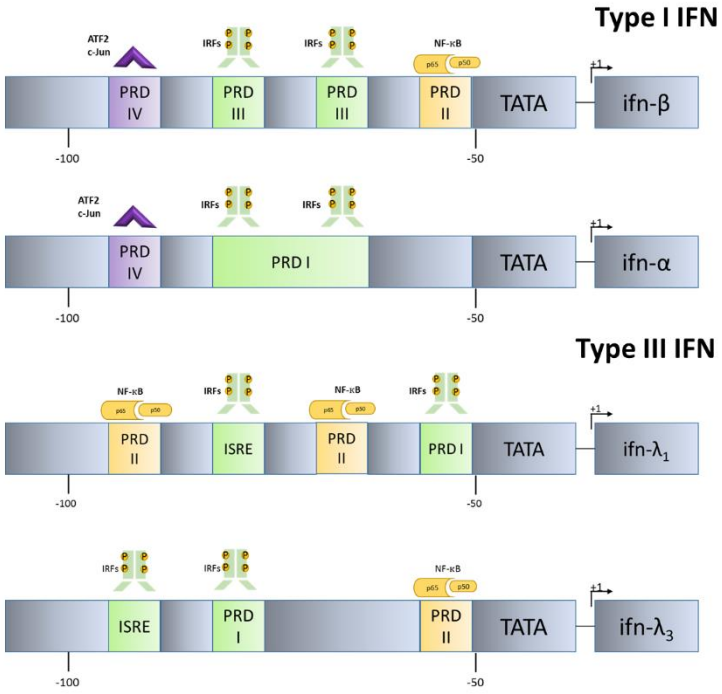

Figure 6. Schematic representation of the promoter regions of type I and type III interferon.

The precise transcription of IFN gene is often controlled by more than one specific activator. Several activators can bind together in close proximity, forming an "enhanceosome" at the enhancer binding sites of genes, to stimulate transcription. The highly evolutionarily conserved enhancer of interferons span in a compact 55 bp stretch upstream of the coding sequence and comprises 4 regulatory cis-elements namely the positive regulatory domains (PRDs) I-IV. Upon virus infection, the PRDs have been shown to facilitate the cooperative assembly of a multiprotein regulatory complex involving NF-κB (RelA/p50), IFN regulatory factors (IRF) 3/7 and activating transcription factor (ATF) 2/c-Jun to form a stable enhanceosome complex. In contrast with resemblance in the pattern of induction and biological activity of type I and type III interferon, the structure of their the 5-'UTR are different. IFN-β promoter region contains the binding site sequences for IRF-3 and IRF-7 (PDR-III and PDR-I respectively), however, for an efficient induction, the activation of NF-κB (PDR-II) and ATF2 c-Jun (PDR-IV) is required. By contrast, the promoter region of IFN-α presents the binding sites for IRF-7 (PRD-I) and ATF2 c-Jun (PDR-IV). Compared to type I, the induction of type III interferon is driven by the transcriptional activity of NF-κB (PDR-II). INF-λ_1 has two NF-κB binding sites and one for IRF-3. IFN-λ_3 present one binding site for IRF-3 and one for NF-κB. Moreover, in contrast with type I, type III interferons promoter region present alternative binding sites for IRFs, defined IFN-stimulated response elements (ISREs). Assembling of the enhanceosome in correspondence of the binding sequences leads to the recruitment of histone acetyl transferases (HATs) and RNA polymerase II machinery to the promoter in correspondence of the TATA box, which constitutes the site of preinitiation complex formation, the first step in eukaryotes transcription.

Type I and III IFNs are produced following recognition of viral ligands, most prominently nucleic acids, by a wide range of pattern recognition receptors. These pathways involve TLRs, RLRs, MAVS and TBK1, as described in 1.2.1. However, the subcellular localization of MAVS determines which IFN species is produced. MAVS is an adapter of the RLR pathway that was first identified as being localized on mitochondria and was later shown to also localize to peroxisomes and mitochondrial-associated endoplasmic reticulum membranes. From peroxisomes, MAVS is able to induce ISGs and control viral infections independently of type I IFNs. In addition, the function and abundance of peroxisomes and mitochondria determines the quality of the IFN response. Increasing peroxisomal abundance or inhibiting mitochondrial function favours the expression of type III over type I IFNs (Odendall *et al.*, 2014). This observation could reflect what happens physiologically in epithelia. Indeed, polarization of epithelial cells increases peroxisome abundance and type III IFN responses to viral infections, while the number of mitochondria and type I IFN expression are unaffected.

Despite differences in the enhanceosome sequences and in the temporal and spatial activation of IFN-β and IFN-λ, a two-step model for their induction has been proposed. In this model, early-induced IFNs exercise a positive feedback for the induction of later IFNs in order to establish a robust and long-lasting immune response (Figure 7). This model also underlines the essential role of IRF-3 in both early and late phases of IFN induction. In early phase, which is mostly IFN independent, IRF-3 senses the incoming infection and induces the transcription of early-stage IFN (IFN-β and IFN-λ). During the late phase of infection IRF-3 is critical for 2 reasons: for the augmentation of the early-stage induced IFN, and for the full procurement of all IFN family members (IFN-α) by cooperating with IRF-7, underling the essential role of IRF-7 in the late induction phase (Hwang *et al.*, 2013; Sato *et al.*, 1998; Sato *et al.*, 2000).

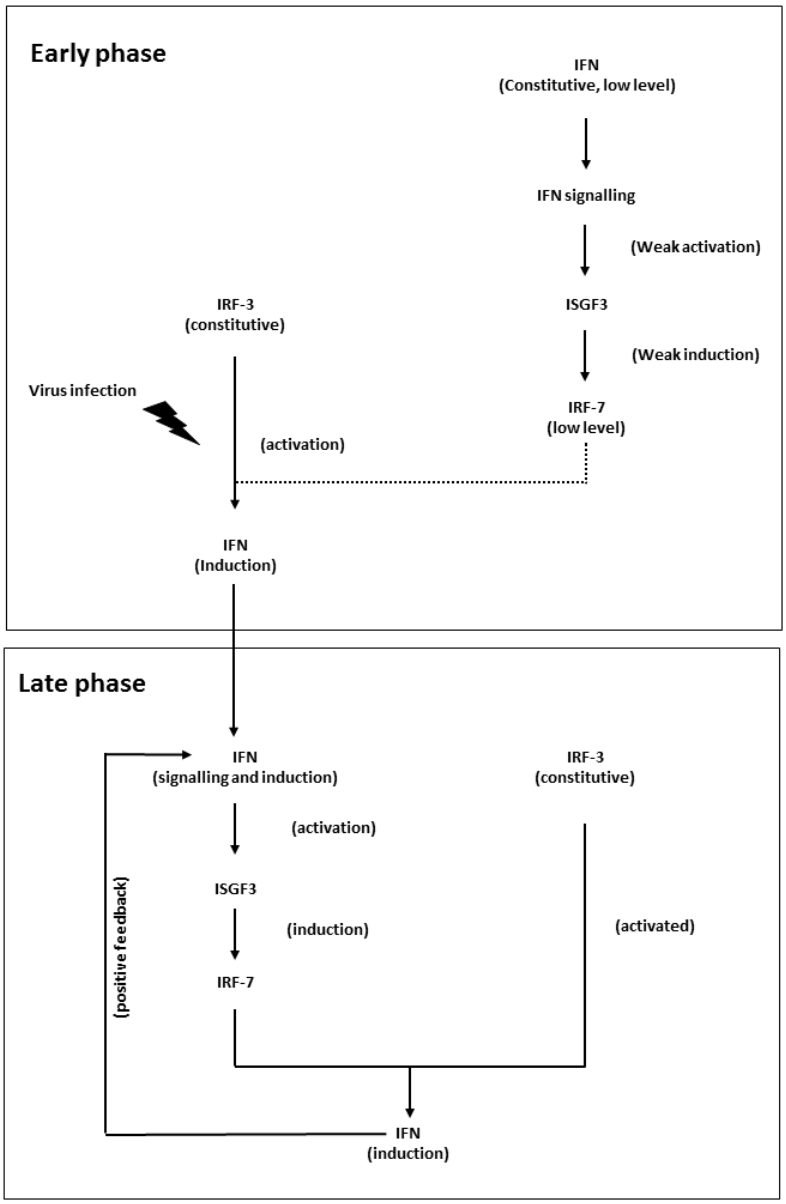

Figure 7. Schematic representation of the biphasic mechanism of IFN gene induction mediated by IRF-3 induced IRF-7.

The expression of IRF-7 is ubiquitous, however, it is totally dependent on IFN signalling, whereas IRF-3 expression is constitutive and remains essentially unaffected by virus and IFNs. In the early phase, constitutively expressed IRF-3 is activated by virus infection, and this activation results in activations of type I and type III IFN. In this phase, IRF-7 is expressed only at very low levels by spontaneous IFN signalling. Induction of IFN results in a strong induction of IRF-7 expression through activation of ISGF3 by IFN signalling. Thus, in the late phase, IRF-3 and IRF-7 cooperate with each other for amplification of IFN gene induction, resulting in the full procurement of the normal mRNA induction profile of the IFN gene subfamily (Sato *et al.*, 2000).

1.2.7 JAK / STAT pathway

The Janus kinase/signal transducers and activators of transcription (JAK/STAT) pathway is a complex signalling pathway involved in development and in maintaining homeostasis in animals (Aaronson *et al.*, 2002; Darnell, 1997). Extracellular signalling polypeptides, such as growth factors or cytokines, are recognized by specific transmembrane receptors or receptor complexes on target cells leading to fast reprogramming in gene expression. In mammals, there are seven STAT genes, *STAT1*, *STAT2*, *STAT3*, *STAT4*, *STAT5A*, *STAT5B*, and *STAT6*, with different distribution among tissues.

In the absence of specific extracellular signals, STAT proteins are normally inactive in the cytoplasm. After receptor-binding interaction, they are rapidly activated and recruited to the intracellular domain of the cytoplasmic –associated protein from the JANUS kinase (JAK) (Leonard, 2001). In mammals there are 4 JAK kinases: Jak1, Jak2, Jak4 and Tyk2. JAK activation occurs upon ligand –mediated conformational changes. When two JAK proteins are brought into closer proximity, they trans-phosphorylate, creating a STAT docking site. Once activated JAKs is able to phosphorylate additional targets, including STATs. STATs are latent transcription factors that reside in the cytoplasm until activated. Phosphorylation of STATs on tyrosine residues leads to STAT homo- and hetero-dimerization and subsequent translocation to the nucleus by importin α-5 (also called nucleoprotein interactor 1) or the Ran nuclear import pathway. Once in the nucleus, STAT recognises target promoter sequences, increasing the transcription of the cognate gene (Aaronson *et al.*, 2002; Darnell, 1997) (Figure 4).IFN-mediated activation of the JACK/STAT pathway is mechanistically distinct from the majority of STAT pathways. In this pathway, upon the phosphorylation of STATs by JAK, STAT1 and STAT2 form a heterodimer that binds interferon regulatory factor 9 (IRF-9) forming the heterotrimeric complex Interferon-stimulated gene factor 3 (ISGF3) (Fu *et al.*, 1990; Kessler *et al.*, 1990). The ISGF3 transcriptional factor enters the nucleus and binds to the IFN stimulated response element (ISRE) to activate the transcription of interferon stimulated genes (Holloway *et al.*, 2014).

1.3 Modulation of the host innate immunity by rotavirus NSP1

The importance of innate immunity in controlling viral replication means that most viruses have evolved strategies to counteract IFN-mediated innate responses, including interference with components of the IFN induction and/or signalling pathways. In common with other dsRNA viruses, RV do not release their genomic RNA when it enters cells, preventing recognition by PPRs and the subsequent activation of IFN induction pathway through this route (Estrozi *et al.*, 2013). However, during transcription, the RNA-capping activity of VP3 is not completely efficient, which results in populations of uncapped and partially capped viral transcripts that can activate the host innate immune response through RLRs and TLRs (Uzri *et al.*, 2013). Moreover, it has been shown that VP4 and VP8* can activate NF-κB through a TRAF2-NF-κB-inducing kinase signalling pathway (LaMonica *et al.*, 2001)VP4 and VP8* both contain three TNFR-associated factor (TRAF) binding motifs. When expressed *in vivo* VP4 and VP8* both caused a 5 to 7 fold increase in NF-κB activity and upregulated TRAF2-mediated NF-κB activation. This suggests that RV actively changes cellular signalling and directly affects cellular transcriptional responses.

Although the virus is capable of triggering IFN production, infection of permissive cell lines with wild type (wt) RV strains does not result in high levels of IFN transcription or secretion, suggesting that the virus encodes proteins that antagonize the IFN induction pathways (Feng *et al.*, 2009). The key viral protein involved in the downregulation of IFN expression is the non-structural protein 1 (NSP1) (Arnold, Sen*, et al.*, 2013). Consistent with the role in down-regulating the type I IFN response, the loss of a complete NSP1 (ORF) has been found to produce a slow growth phenotype in cell culture (Silvestri *et al.*, 2004). The presence of the RING domain to drive the proteasome-mediated degradation of the target proteins (Graff *et al.*, 2007), a high specificity for its substrate and auto-regulation via self-ubiquitination support the hypothesis that NSP1 has E3 ubiquitin-ligase activity (Barro *et al.*, 2007; Graff *et al.*, 2009).

The NSP1-mediated ability of RV to modulate the IFN response is conserved between strains infecting different species. However, it has been reported that targets within the induction and signalling pathways vary between strains.

1.3.1 IRFs

Recent studies have identified a host cell-specific interaction between RV NSP1 and IRF-3 using the yeast two-hybrid system (Barro *et al.*, 2005). Expression of NSP1 from the bovine RV strains UK and NCDV in COS7 and 293T cells directed the proteasome-mediated degradation of IRF-3, however, such regulation was missing in in mouse embryonic fibroblast (MEFs) 3T3 cells (Sen *et al.*, 2009). In contrast, expression of NSP1 encoded by rhesus (RRV), simian (SA11) and murine (EW) strains is capable of driving IRF-3 degradation in 3T3 cells (Sen *et al.*, 2009) and Caco-2 cells (Barro *et al.*, 2005). Interestingly, the human strains Ku, DS-1, AU-1 and Wa (Arnold *et al.*, 2011; Barro *et al.*, 2007) and porcine Osu (Graff *et al.*, 2007; Sen *et al.*, 2009) have been reported to have no effects on the levels of IRF-3 in 293T and MA104 cell lines. However, infection with these strains leads to a downregulation in IFN-β expression, suggesting the use of alternative strategies by the virus to down regulate IFN expression. It has also been shown that simian Sa-11 NSP1 expression can interfere directly with the accumulation of the activated (homodimerized) form of IRF-3 and its nuclear translocation in Caco-2 cell line (Barro *et al.*, 2005, 2007). Given the role of IRF-3 in initiating IFN-β expression and IRF-7 as the “master regulator” of type I IFN, downregulation of IRF-7 would also interfere with the ability of the host to activate the IFN-dependent antiviral state. Consistent with this, RV NSP1 has also been shown to induce proteasome-mediated degradation of IRF-7 (Barro *et al.*, 2007).

The adaptor proteins STING, MAVS, and TRIF contain a conserved motif, pLxIS (in which p represents a hydrophilic residue, x represents any residue, and S represents a phosphorylation site), that is phosphorylated by TBK1 or IKKε and mediates the recruitment of IRF-3 to the signalling complexes. Moreover, IRF-3 itself also contains a pLxIS motif that is crucial for phosphorylation-induced dimerization

and activation of IRF-3 (S. Liu *et al.*, 2015). Mutation of the serine in the phosphorylation site within the pLxIS motif of STING, MAVS, and TRIF abolish the induction of type I IFNs in their respective signalling pathways (S. Liu *et al.*, 2015). BLAST searches revealed that NSP1 isolates from different hosts contains a conserved pLxIS domain (B. Zhao *et al.*, 2016). This domain falls in the last 17 amino acids residues located in the C-terminal of NSP1, which is essential for targeting IRF-3 (Barro *et al.*, 2005). Recent studies have identified that L486 and I488 are essential residues in the NSP1-mediated degradation of IRF-3 (B. Zhao *et al.*, 2016). Similar results have been reported by Kobayashi's group (Kanai *et al.*, 2017), which used an entirely plasmid-based RV reverse genetic system to shown that the C-terminus region of NSP1 is responsible for the IRF-3 interaction.

1.3.2 RIG-I, MDA5 and MAVS

It has been shown that porcine (OSU) NSP1 interacts with RIG-I, inducing its degradation in a proteasome-independent way (Qin *et al.*, 2011). With its position within the type I IFN induction pathway, downstream of viral detection and upstream of IκB and IRF-3 phosphorylation, MAVS has an essential role in establishing an early antiviral response. It has been reported that MAVS is also targeted by NSP1 leading to its proteasome-mediated degradation (Broquet *et al.*, 2011; Kawai *et al.*, 2005; Nandi *et al.*, 2014) in a strain independent manner, which is independent of the IRF degradation.

1.3.3 NF-κB

NF-κB is a transcription factor that is known to play an important role in the induction of elements of the immune response. NF-κB also acts broadly to influence gene expression events that impact cell survival, differentiation, and proliferation (Hayden *et al.*, 2012). RV NSP1 has a conserved C-terminal domain that mimics the IκB phosphodegron recognised by β-TrCP. NSP1 uses this sequence, defined phosphodegron-like (PDL) motif to interact with β-TrCP, driving its proteasome-mediated degradation (Davis *et al.*, 2017a; Morelli, Dennis*, et al.*, 2015) resulting in an inactive form of NF-κB dimers that are unable to translocate to the nucleus and

activate IFN transcription. This mechanism is strain dependent, with porcine OSU, bovine NCDV and human D, DS-1, Ku, P, Wa strains able to induce the degradation of β-TrCP, while porcine Gottfried and YM, and human IAL28, ST3 and WI16, lack this mechanism (Di Fiore *et al.*, 2015; Graff *et al.*, 2009). In addition, certain RV strains show the ability to sequester NF-κB p65 subunit in viroplasms during infection or interfere with NF-κB nuclear accumulation (Holloway *et al.*, 2009), potentially blocking NF-κB signalling pathways in a β-TrCP-independent manner.

1.3.4 STAT1 and STAT2

NSP1 from rhesus RV (RRV) and the porcine strain, SB1A can interfere with IFN signalling by blocking STAT1/2 nuclear localization (Holloway *et al.*, 2009). NSP1 antagonizes IFN mediated STAT1 Y701 phosphorylation, and the inactivated complex is unable to translocate to the nucleus (Holloway *et al.*, 2014; Sen *et al.*, 2014).

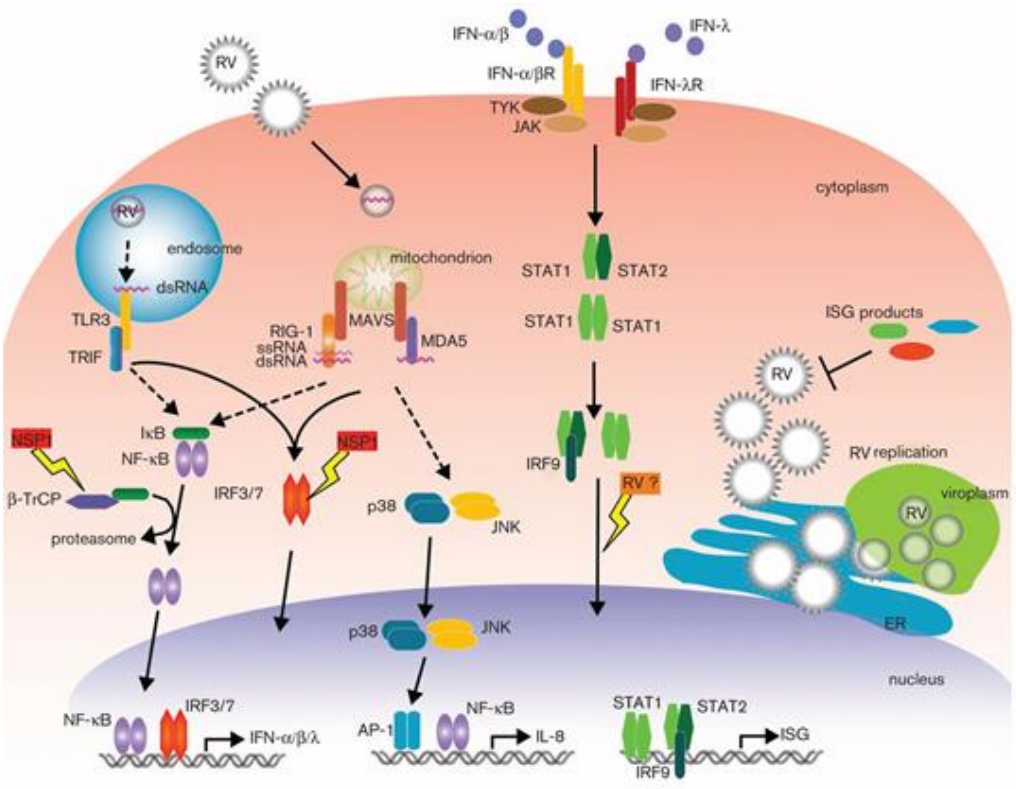

Figure 8. Modulation of type I IFN induction and signalling by rotavirus NSP1.

RV NSP1 is able to modulate the induction of IFN by targeting members of the induction and signalling pathways and inducing their proteasome-mediate degradation. The ability of NSP1 to modulate the IFN response is conserved among species, however, the specific targets vary among strains. Moreover, *in vitro* experiments have underlined how the ability of NSP1 to induce the degradation of its targets depends on the cellular context. Overall, the human, bovine and murine strains are likely to preferentially target the IRFs (IRF-3,-5,-7 and 9). The porcine strains appears to target the helicase RIG-I and MDA-5 and β-TrCP which regulates the activation of NF-κB. Monkey strains appear to preferentially target the IFN signalling pathway, blocking the nuclear translocation of STA1/2.

1.4 Aims

NSP1 is the most variable protein expressed by RV, however, the kind of selective pressure the protein is subject to remains unknown. It has been shown that NSP1 is essential in subversion of immune responses, targeting members of IFN induction and signalling pathways. This role is well conserved among strains that infect different host species, but the specific targets of NSP1 vary. This may be a major contributor to the observed host range specificity for which the molecular mechanisms remain unattributed. In order to evaluate if NSP1 from different host species downregulates the induction and signalling of interferon by targeting different host proteins in this signalling pathway or if all NSP1s target a set of proteins which are the common targets irrespective of the host species:

Objectives:

1. Determine if NSP1 proteins, from strains of RV that infect different mammalian species, differentially interact with members of the IFN induction and IFN signalling pathways (RIG-I, MDA5, MAVS, IRF-3, IRF-7, β–TrCP, and TBK1) using the yeast-2-hybrid system (Y2H).
2. Determine if NSP1 proteins derived from different RV strains show a strain-dependent expression level and stability.
3. Determine if NSP1 proteins derived from RV strains which infect different mammalian species, can differentially antagonise type I and III IFN induction and signalling in cell lines derived from host and non-host species.

Material and Methods

2 Material and methods

2.1 Cell Culture

2.1.1 Cell lines

Unless otherwise stated, cells were cultured in GMEM-BHK21 (Thermo Fischer Scientific, #11710035) or DMEM (Thermo Fischer Scientific #41965-039)cell culture media supplemented with 5% foetal bovine serum (FBS) (Thermo Fisher Scientific, #10270106), penicillin (100 U/mL) and streptomycin (100 µg/mL) (Sigma, #P4333).

Table 3. List of cell lines used in this study

Cell line	Comments	Culture medium	Splitting ratio	ACC	Source
BSC-1	African green monkey kidney cells	GMEM-BHK21	1 in 4	ATCC® CCL-26™	Mark Boyce
MA104	African green monkey kidney cells	GMEM-BHK21	1 in 10	ATCC® CRL-2378.1™	Mark Boyce
Caco-2	Homo sapiens Colon Colorectal cells	DMEM	1 in 4	ATCC® HTB-37™	Miren Iturriza-Gomara
HEK293T	Human embryonic kidney cells expressing large T-antigen of	DMEM	1 in 5	ATCC® CRL-1573™	Julian Seago
HT-29	Homo sapiens Colon Colorectal cells	DMEM	1 in 4	ATCC® HTB-38™	Miren Iturriza-Gomara
PK-15	Porcine kidney epithelial cells	DMEM	1 in 5	ATCC® CCL-33™	Julian Seago
Pk-15 GFP-N^{pro}	Porcine kidney epithelial cells stably expressing CSFV N^{pro}	DMEM	1:4		Julian Seago
MDBK	Madin–Darby Bovine Kidney cell	DMEM	1 in 10	ATCC® CCL-22™	Julian Seago
MDBK-t/2	Madin Derby bovine kidney cells stably transfected with Mx-CAT	DMEM + 10µg/ml blasticidin	1 in 10		Julian Seago
BSRT-7/5	BHK-derived cell line stably expressing T7 RNA polymerase	DMEM + 10µg/ml/geneticin	1:10		Julian Seago
TS20	Balb3T3-derived cell line harbouring a temperature-sensitive allele of the ubiquitin-activating enzyme E1	DMEM/F12 +10%FCS	1:5	ATCC® MYA-3861™	Julian Seago

2.1.2 Maintenance of cells in tissue culture

Cells were maintained at 37°C with 5% CO_2 in a humidified incubator in 75 cm^2 flasks using the appropriate media. When confluent, the cells were passaged as follows: cells were washed twice with Hank's Balanced Salt Solution (HBSS, Thermo Fisher Scientific, #14170070), incubated with 3 ml trypsin-EDTA (Sigma, #T3924) for 5min at 37°C, or until they were no longer adherent, and then pelleted by centrifugation at 500 x g for 5min at RT. Cells were re-suspended in the appropriate medium and re-seeded at the required density (Table 3). All manipulations were performed under sterile conditions in a class II laminar flow cabinet using standard aseptic techniques.

2.1.3 Maintenance of stable cells in tissue culture

Blasticidin was purchased from Sigma (#15205) and used to maintain selection pressure on MDBK-t/2 cell lines.

2.1.4 Transfection

Relevant cell lines were grown to 80% confluency in 6-, 12- or 24-well plates. For each well 200 ng of DNA diluted at 15 ng/µl in Opti-MEM® (Gibco, #31985-062) was incubated with 1 µl of Lipofectamine2000® (Thermo Fisher, #11668030) - Opti-MEM®mix (ratio 1:1) at RT for 20min. The mix was then added to the wells and incubated at 37°C for 4h, after which the media was removed and replaced with fresh complete GMEM media. Cells were then incubated overnight at 37°C/5% CO_2.

Alternatively, cells were transfected using TransIT®-LT1 transfection reagent (Mirus biolab, #Mir 2300) as follows: 50 µl of DMEM without FCS and penicillin/streptomycin was incubated with 1 µl of transfection reagent at RT for 5min. Plasmids were added to the transfection mix and incubated at RT for 30min. During the incubation period, growth media was removed from the cells and they were washed with PBS before the addition of 300 µl of media without FCS and penicillin/streptomycin. The transformation mix was then added to the cells, followed by an incubation period for 4h at 37°C/5% CO_2. 2 ml of complete media was

added, and cells were maintained overnight at 37°C in order to express exogenous proteins.

2.2 Viruses

2.2.1 Sendai virus

Sendai Virus (SeV), Cantell Strain (ATCC VR-907 Parainfluenza 1), used for induction of IFN in HEK-293, Caco-2, HT-29, MA-104, BSC-1, PK-15 and MDBK cell lines (2.1.1) was purchased from Charles River, Wilmington MA, USA (#10100773) at a titre of 4000 HA tube titre/mL.

2.2.2 Classical Swine fever Virus

Classical Swine fever Virus (CSFV) strain Alfort 187 used to knock-down the expression of IRF-3 was available within the Molecular Virology group, having been originally provided by the EU reference laboratory, Hannover, Germany. The virus was stored at -80^{o}C in 1 ml single use aliquot

2.2.3 CSFV infection of PK-15 cell lines

PK-15 cells were seeded in 6-well plates at 3 x 10^5 cells/ml with DMEM media. Once cells reached 80% confluency, media was removed and replaced with 750 µl of fresh DMEM without FCS and penicillin/streptomycin. 50 µl (200 HA) of CSFV was added to the cells and incubated for 1h at 37°C. Media was then removed and replaced with 3 ml of fresh DMEM. An incubation period of 48h at 37°C followed.

2.2.4 Modified Vaccinia Ankara –T7 polymerase (MVA-T7)

Modified vaccinia virus Ankara-T7 polymerase (MVA-T7) is an attenuated vaccinia virus strain encoding the bacteriophage T7 polymerase gene (Sutter *et al.*, 1995). The virus was used to promote higher levels of expression of RV NSP1 from the T7 promoter in the pcDNA3.1 derived construct. For T7 driven expression, cells were grown to 90% confluency in 6-well plates and infected with MVA-T7 1h prior to transfection. Briefly, growth media was removed, cells were washed with PBS and

250 µl of fresh GMEM without FCS and penicillin/streptomycin was added. 50 µl MVA-T7 was added directly to the growth medium and cells were incubated for 1h at 37°C. Supernatant was removed and replaced with complete media. Cells were transfected using TransIT®-LT1 transfection reagent (Mirus biolab, #Mir 2300) as described in 2.1.4. Cells were incubated at 37°C for 16h before cell lysates were prepared and protein expression checked by Western blot analysis as described in section 2.7.

2.3 Cloning and plasmid preparation

2.3.1 Polymerase chain reaction (PCR)

DNA was amplified by PCR in 0.5 ml centrifuge tubes in a 100 µl reaction containing 10 ng of DNA template, 10 µl of 10X buffer, 200 µM dNTPs, 1.5 mM $MgSO_4$, 0.3 pmol/µl of forward and reverse primers (Table 7) and 1U KOD polymerase (Merck Millipore, #71085-3) adjusted to the final volume with dH_2O.

Alternatively, PCR was carried out in a final volume of 50 µl containing 25 µl of Taq 2X master mix (Thermo Scientific, #K1081), 0.5 µM forward and reverse primers and dH_2O to the final volume. In some cases, adjustments in thermal cycling parameters were necessary to improve amplification specificity and DNA yield.

PCR was carried out under the following cycling condition:

Table 4. Standard PCR thermal cycling conditions

Stage	Temperature and Time	Number of cycles	Step
1	95°C for 1min	1	Initial denaturation
2	94°C for 30sec	30 to 35	Denaturation
3	55°C to 60°C for 30sec		Annealing *
4	72°C 60 sec/kb		Elongation
5	Go to step 2		
6	72°C for 5min	1	Final elongation
7	rt	hold	

* The annealing temperature was adjusted based on the Tm of the primers.

2.3.2 Agarose gel electrophoresis

DNA fragment size was determined by agarose gel electrophoresis using 0.8% - 1.2% (w/v) agarose gels (Invitrogen UltraPure™ Low Melting Point Agarose, #16520-100) dependent on the size of the products being resolved. Agarose was dissolved in 1X Tris-Acetate EDTA (TAE) (40 mM Tris, 20 mM acetic acid, and 1mM EDTA, pH 8.0) (Severn Biotech, #20600110) or Tris-Borate EDTA (TBE) (0.9 M Tris-base, 0.9 M Boric acid, 0.02 M EDTA) (Ambion,#AM9863) and heated until dissolved. Melted agarose was cooled down and supplemented with 1 µg/ml ethidium bromide (ThermoFisher, #15585011). Gel loading buffer was added to DNA samples and run alongside a 1 kb ladder (Promega, #G5711 or New England BioLabs, #N3232L) in 1X TAE or 1X TBE buffer at 90 mA for a sufficient time to obtain a clear separation of the products.

2.3.3 Gel purification of DNA

DNA was visualized using UV trans-illuminator at 365 nm (UV-A range) and the bands of interest were excised. DNA was recovered using the Wizard® SV Gel and PCR Clean-Up System (Promega, #A9281) or QIAquick® gel extraction kit (Qiagen, #28704), according to the manufacturer's instructions.

2.3.4 Restriction enzyme digestion of DNA

Analytic digestions were performed in 1 ml microcentrifuge tubes in a reaction volume of 5 µl. For each, 150 ng of DNA was digested with 1U of appropriate restriction enzyme, 0.5 µl of the corresponding 10X buffer and 0.5 µl of 10X Bovine Serum Albumin (BSA). Reactions were incubated for 2-3h at 37^{o}C.

Preparative digestions of 5-20 µg were performed in 1 ml micro-centrifuge tubes in a reaction volume of 30 µl, using 5-10 U of appropriate restriction enzyme, 3 µl of the corresponding 10X buffer and 3 µl of 10X BSA. Reactions were incubated overnight at 37°C but time was adjusted for efficiency or to reduce star activity. DNA was purified as described in 2.3.3

2.3.5 Dephosphorylation of vector DNA

The 5'-phoshate groups were removed from the digested DNA Vector using FastAP Alkaline Phosphatase (ThermoFisher scientific, #EF651) following the manufacturer's protocol. Briefly, 1U of FastAP was added to purified DNA and incubated 10 min at 37 °C. FastAP was inactivated with an incubation for 5min at 75°C. DNA was purified as described in 2.3.3.

2.3.6 DNA ligation

Ligations were performed in 1 ml microcentrifuge tubes in a reaction volume of 20 µl. 100 ng (~1 µl) of vector DNA was incubated with a 3:1 molar excess of insert DNA, 1 µl of 10X T4 DNA ligase buffer (New England BioLabs, #B0202S), 20U of T4 DNA ligase (New England BioLabs,#M0202S) and dH_2O to the final volume. For each ligation, a "vector only" control was performed using the same quantity of vector DNA, buffer and T4 DNA ligase excluding the insert DNA. Ligation reactions were performed at room temperature (RT) overnight.

2.3.7 Transformation

For each transfection 2 µl of ligation or control was added to 50 µl of chemically competent XL1-Blue MRF' supercompetent *E.coli* in a 1 ml microcentrifuge tube. 0.7µl of *β*-mercaptoethanol was then added and incubated on ice for 40min. The mix was heat shocked at 42°C for 45sec and placed on ice for 2min. 0.5 ml of Luria Broth (LB) was then added and the *E.Coli* were incubated at 37°C for 1h with shaking (200rpm). Transformation of Subcloning Efficiency™ DH5α, One Shot® TOP10 Chemically Competent or Rubidium Chloride chemically competent *E.coli* was carried out as previously described, with the exception of the administration of *β*-mercaptoethanol. Following incubation, the transformed *E.coli* were plated onto selective LB agar plates (in-house) supplemented with either Kanamycin (50 µg/ml (w:v)) (Sigma Aldrich #0879) or Ampicillin (100 µg/ml (w:v)) (Thermo Fisher, # 11593027) selective antibiotics and incubated at 37°C for 16h.

2.3.8 Small scale plasmid DNA preparation (mini prep)

For each plasmid preparation, an individual bacterial colony was used to inoculate 5 ml LB medium containing the appropriate antibiotic before incubation for 16h at 37°C with shaking (200rpm). Plasmid DNA was then purified using a QIAprep Miniprep Kit (QIAGEN, #27104) following the manufacturer's protocol. Briefly, each overnight bacterial culture was pelleted by centrifugation at 17,900 x g for 15min at RT. Supernatant was discarded and the pellet re-suspended in 250 µl of buffer P1 in a 1 ml microcentrifuge tube. 250 µl of Lysis buffer P2 was then added. 350 µl of Neutralization buffer N3 was added, gently mixed and the sample was centrifuged at 17,000 x g for 10min at RT. The supernatant was transferred to a QIAprep 2.0 spin column and centrifuged at 17,000 x g for 1min at RT. The flow-through was then discarded, 500 µl of Binding buffer PB was added and the column centrifuged at 17,000 x g for 1 min at RT. The flow-through was discarded, 750 µl of Washing buffer PE was added and the column centrifuged at 17,000 x g for 1min at RT. The flow-through was discarded and an additional centrifugation performed, before the column was transferred to a clean 1 ml microcentrifuge tube and the plasmid DNA eluted by the addition of 50 µl of DNase/RNase free dH_2O and centrifugation for 1 min at 17,000 x g, RT.

2.3.9 Permanent bacterial stock

One ml aliquot of the overnight culture generated in 2.3.7 was inoculated in 5 ml of fresh LB media containing the appropriate antibiotic resistance and cells were incubated with shaking (200 rpm) at 37°C for 3h. 500 µl of 100% glycerol (VWR International, #24388.260) was added and the culture aliquoted in 1.5 ml cryogenic vials and stored at -80°C.

2.3.10 Bacterial strains used for the amplification of plasmid DNA

Subcloning Efficiency™ DH5α™ E.coli (F^- Φ80*lac*ZΔM15 Δ (*lac*ZYA-*arg*F) U169 *rec*A1 *end*A1 *hsd*R17(r_k^-, m_k^+) *pho*A *sup*E44 *thi*-1 *gyr*A96 *rel*A1 λ^-) (ThermoFisher Scientific, #18265017) were used to amplify plasmid DNA.

One Shot® TOP10 Chemically Competent E. coli F- mcrA Δ (mrr-hsdRMS-mcrBC) Φ80lacZΔM15 Δ lacX74 recA1 araD139 Δ (araleu)7697 galU galK rpsL (StrR) endA1 nupG (ThermoFisher Scientific, #C404003) were used to amplify plasmid DNA.

XL1-Blue MRF' supercompetent E.coli (Δ (mcrA) 183Δ (mcrCB-hsdSMR-mrr)173 endA1 supE44 thi-1 recA1 gyrA96 relA1 lac[F´ proAB acIqZΔM15 Tn10(Tet r) (Agilent, #200230) were used to amplify plasmid DNA.

XL10-Gold Ultracompetent cells, XL10-Gold β-ME (TetrΔ(mcrA)183 Δ(mcrCB-hsdSMR-mrr)173 endA1 supE44 thi-1 recA1 yrA96 elA1 lac Hte [F' proABlacIqZΔM15 Tn10(Tetr) Amy Camr]

Rubidium competent *E.coli* strain JM109 (*endA1, recA1, gyrA96, thi, hsdR17 rk–, mk+*), *relA1, supE44, Δ*(*lac-proAB*), [*F´ traD36, proAB, laqIqZΔM15*]), (in-house) were used to amplify plasmid DNA.

Bacterial strains were grown in LB media in presence or absence of appropriate antibiotic.

2.3.11 DNA sequencing

DNA concentrations were determined by measuring the OD_{260} using a NanoDrop spectrophotometer (NanoDrop™ 2000/2000c). 100 ng of plasmid DNA was sequenced in-house using the BigDye® Terminator v3.1 Cycle Sequencing Kit (Thermo Fischer Scientific, #4337454). Briefly, for each reaction 200 ng of plasmid (1.5 µl) and 4.8 µL of dH_20 were added to a 0.5 ml microcentrifuge tube and heated at 94°C for 4 min to denature DNA prior to placing on ice for 2 min. 1.9 µl of BigDye® 10X buffer, 0.5 µl of sequencing mix, 1.5 µl of primer (at 3.4 pmol/µl) were then added before PCR was performed under the conditions reported in Table 5:

Table 5. PCR protocols to amplify DNA sequences using BigDye® Terminator v3.1 Cycle Sequencing Kit.

Stage	Temperature and Time	Number of Cycles	Step
1	95°C for 1min	1	Initial denaturation
2	94°C for 45sec	25	denaturation
3	50°C for 10sec		annealing
4	60°C for 4min		elongation
5	Go to step 2		
6	4°C	hold	

Following PCR, 5 µl of EDTA (100 mM) was added to stop the amplifying reaction. 70 µl of 100% ethanol (v/v) was then added and the sample centrifuged at 16,000 x g for 30min at 4°C, to precipitate the DNA. The supernatant was removed and 400 µl of 70% ethanol (v/v) was added before centrifugation at 16,000 x g for 10min at 4°C. The supernatant was then discarded and the pellet air dried for 10min prior to storage at -20°C. The pellet was re-suspended in 20 µl Hi-Di™ Formamide and sequenced in-house using an ABI 3730 DNA analyser (Applied Biosystem). Sequence electropherograms were analyzed using Chromas Lite® software.

2.3.12 Site-directed mutagenesis

Site-direct mutagenesis was performed using QuikChange Lightning Site-Directed Mutagenesis Kit (Agilent, # 210518) following the manufacturer's protocol.

Briefly, PCR was performed in a 0.5 µl microcentrifuge tube in a 50 µl reaction containing 1 µl of DNA template (~150 ng), 5 µl of 10X reaction buffer, 2 µl of forward and reverse primers (150 ng each primer), 1 µl of dNTPs mix, 1.5 µl of quick solution reagents, 1 µl of quick change enzyme and the total volume was made up to 50 µl with dH_2O. PCR amplification was set up under the conditions reported in Table 6.

Table 6. PCR protocols to perform site-direct mutagenesis using the Quickchange® Lightening Site-Directed Mutagenesis Kit

Stage	Temperature and time	Number of cycles	Step
1	95°C for 2min	1	Initial denaturation
2	95°C for 20sec	18	denaturation
3	60°C for 10sec		annealing
4	68°C for 30sec/kb		elongation
5	Go to step 2		
6	68°C for 5min	hold	

2 µl of β-mercaptoethanol were added to 45 µl of XL-Gold Ultracompetent cells and incubated for 5 minutes on ice. 2 µl of *Dpn*-I restriction endonuclease was added to the PCR reaction and incubated at 37°C for 5min. 2 µl of *Dpn*-I-treated DNA was added to the cells and incubated on ice for 30min. Cells were heat-shocked at 42°C for 40sec and incubated on ice for 2min. 500 µl of SOC was added and bacteria were incubated for 1h at 37°C with shaking. After incubation, 100 µl of the bacteria were plated on an LB agar plate containing the appropriate antibiotic resistance.

2.4 Yeast Two-Hybrid

The Y-2-H technique is based on the observation that many eukaryotic transcriptional factors (TFs) are formed of a discrete and separable DNA-binding domain (BD) and a transcriptional-activation domain (TD) (Fields *et al.*, 1989). The system utilizes the reconstitution of an active TF to assay for protein-protein interaction. The fusion of each protein to separate TF domains reconstitutes an active TF when test proteins interact. The expression of reporter genes, that contain an upstream element to which the DNA binding domain binds, can be monitored to detect the interactions.

2.4.1 Yeast strains

The *Saccharomyces cerevisiae* strain AH109 (Matchmaker Y-2-H System 3) was used (Clontech). AH109 yeast use 4 reporter genes under the control of distinct GAL4 upstream activating sequences; two auxotropic reporter genes –(ADE2, HIS3) that facilitate growth on selective media and two reporter genes (LacZ and MEL1) (Aho *et al.*, 1997) that process chromogenic substrates to produce blue coloured colonies.

2.4.2 Yeast media

Yeast growth media and supplements, dropouts (DO), double dropouts (DDO) (#630317), triple dropouts (TDO) (#630319) and quadruple dropouts (QDP) (#630323) were sourced from Clontech.

2.4.3 Small-scale LiAc yeast transformation

An aliquot of -80°C *Saccharomyces cerevisiae* stock was streaked on a fresh YPDA agar plate (Clontech, #630465) and incubated at 30°C to allow yeast colonies to grow. A sterile inoculation loop was used to scrape a single colony, which was then resuspended in 200 ml of YPDA medium (Clontech, #630464). An incubation period of 18h at 30°C with shaking (250rpm) followed, after which the absorbance at 600 nm (OD_{600}) was confirmed to be above 1.5. 30 ml of the overnight culture was

transferred to a new flask containing 300 ml of YPD, giving an OD_{600} between 0.2-0.3. An incubation period of 3h at 30°C with shaking (250rpm) followed. The OD_{600} was checked to be between 0.4-0.6.

Cells were placed in 50 ml tubes and centrifuged at 1000 x g for 5 min at RT. The supernatant was discarded and the pellet resuspended in a 50 ml of dH_2O. The cells were centrifuged again at 1000 x g for 5 min at RT, the supernatant was discarded and the cells were resuspended in freshly prepared sterile 1X TE/ 1X LiAc.

1 µl of the "bait" and "prey" plasmids were mixed together with 10 µl of carrier DNA. 100 µl of yeast competent cells were added to each tube and mixed well by vortexing. Each tube was inoculated with 600 µl of freshly prepared sterile 1X PEG/ 1X TE/ 1X LiAc solution and vortexed for 10sec and incubated for 30min at 30°C with shaking (250rpm), after which 70 µl of DMSO was added and mixed gently. The cells were then heat-shocked by incubation for 15min at 42°C, followed by placement on ice for 2min. The cells were pelleted by centrifugation at 17,000 x g for 1min at RT. The supernatant was removed and the cells were resuspended in 500 µl of sterile 1X TE buffer. Finally, 150 – 200 µl of transformed cells were plated on the appropriate agar plate. Yeast -2-hybrid screening experiments were carried out with:

A positive control co-transforming competent yeast cells with a "bait" plasmid pGBKT7-53 and a "prey" plasmid pGADT7-T. pGBKT7-53 encodes the Gal4 DNA-BD fused with murine p53 while pGADT7-T encodes the Gal4 AD fused with SV40 large T-antigen. Since p53 and large T-antigen are known to interact in a yeast two-hybrid (B. Li *et al.*, 1993), mating yeast with pGBKT7-53 and pGADT7-T will result in cells containing both plasmids that can activate all four reporters and grow on DDO media (*-Leu,-Trp*) and QDO media (*-Leu, -Trp, -Ade, -His*).

A negative control co-transforming competent yeast cells with a "bait" plasmid pGBKT7-Lam (which encodes the Gal4 BD fused with lamin) and a "prey" plasmid pGADT7-T. Yeast containing pGBKT7-Lam and pGADT7-T will grow on DDO media (*-Leu,-Trp*) but not on QDO media (*-Leu, -Trp, -Ade, -His*).

2.5 Mx/CAT assay

2.5.1 Interferon induction in cell lines

Cells were seeded in 6-well plates at 2 x 10^5 cells/well with 2 ml of DMEM and incubated for 18h at 37°C/5% CO_2. At 80% confluence, media was removed, cells washed twice with PBS and 2 ml of fresh DMEM were added. Synthetic dsRNA (poly I:C; Sigma, #P0913) was added directly to the media and the cells were incubated for a further 18h at 37°C/5% CO_2. Alternatively, poly I:C was transfected into cells using a TransIT-LT1 kit (Geneflow, #E7-004). Briefly, the required concentration of poly I:C was mixed with 7.5 µl of TransIT-LT1 reagent in 250 µl of media without FCS and penicillin/streptomycin and incubated for 30min at RT. The mix was then added to the cells, which were incubated for a further 18h at 37°C/5% CO_2.

SeV infection was performed by washing cells twice with 1X PBS and adding 600 µl of DMEM without FCS and penicillin/streptomycin plus 50 µl (200 HA) of SeV, followed by a 2h incubation at 37°C/5% CO_2. The media containing SeV was removed and 2 mL of fresh DMEM was added. Cells were incubated for a further 18h at 37°C/5% CO_2. Supernatant was removed and stored at -20˚C for quantification of IFN using the Mx/CAT assay.

2.5.2 Mx/CAT reporter assay

MDBK-t2 cells, in which the chloramphenicol acetyltransferase (CAT) gene is under the control of the human MxA promoter (Fray *et al.*, 2001) were used to determine the presence of biologically active IFN.

MDBK-t2 cells were seeded in 6-well plates at 2 x 10^5 cells/well in 2 ml of DMEM. At 80% confluence, media was removed and replaced with 800 µl fresh DMEM containing 1% FCS. 200 µl of sample cell culture supernatant generated in 2.5.1 was added to the cells and mixed gently. A standard curve of recombinant bovine IFN-α (Novartis) was separately prepared in 1.5 ml microcentrifuge tubes at a dilution of 90, 30, 10, 3.3 , 1.1 , 0.31, 0.123 IU/ml in GMEM containing 2% FCS. 200

µl of each dilution and 800 µl of complete DMEM were then added to duplicate wells of the MDBK-t2 cell plate. The cells were incubated for 24h at 37°C/5% CO_2 to allow for induction of the MxA promoter and the expression of chloramphenicol acetyltransferase (CAT) enzyme in the reporter cell line. After 24h, supernatant was removed and cells washed twice with 1X PBS. After removal of the supernatant 1 ml of lysis buffer (Sigma, #11363727001) was then added to the cells and the plate was incubated for 20min at RT. Lysates were collected in glass vials and stored at -80°C before assaying for CAT levels by ELISA

2.5.3 Chloramphenicol acetyltransferase (CAT) ELISA

A CAT ELISA (Sigma, #11363727001) was used to indirectly measure IFN production (Fray *et al.*, 2001). 200 µl of supernatant generated in 2.5.2 was added in to duplicate wells in the anti-CAT micro-plates, sealed and incubated for 1h at 37°C. Supernatants were removed and wells washed five times with 200 µl/well washing buffer provided with the kit. 200 µl per well of anti-CAT DIG were added to each well, the micro-plates were sealed and incubated for 1h at 37°C. Supernatants were removed and wells washed three times as previously described. 200 µl of anti-DIG POD was added to each well and the plates were sealed and incubated for 1h at 37°C. Supernatants were removed and wells washed as previously described. 200 µl of POD substrate was added to each well and plates were incubated a RT till until colour development. ELISA plates were read at an absorbance 405 nm (reference wavelength: 409 nm) using a Dynex MRXII ELISA reader and Revelation V4.25 software.

2.6 NSP1 sequences

NSP1 cDNAs derived from different RV species were cloned into a mammalian expression vector to investigate their functions. The sequences of NSP1s derived from RV isolated from human and pig were kindly provided by Professor Miren Ituriza-Gomara (University of Liverpool). Based on phylogenetic analysis (0), the relative nucleotide sequences were ordered from GeneArt gene synthesis (Thermo Fisher).

2.6.1 Cloning of NSP1s in mammalian expression vector pcDNA

PCR was performed in 0.5 microcentrifuge tubes in a final volume of 25 µl. Reactions contained 1 µl of template DNA (~300 ng/µl), 6.2 µl (2 µM) of each forward and reverse primer (Table 7) and 12.5 µl of master mix reaction (Promega, GoTaq® Long PCR, #4021). PCR was carried out using the cycling conditions reported in Table 4. PCR products were gel purified using the GFX™ PCR DNA and Gel Band Purification Kit (Healthcare, #28-9034-70) as described in 2.3.3. Products were then ligated into the pcDNA3.1/V5-His-TOPO® plasmid (Invitrogen, K4800-01) under the following conditions: 1 µl of vector was mixed with 3 µl of purified PCR product and 1 µl of salt solution and incubated at RT for 30min. Competent cells were transformed as described in (2.3.7). Transformed rubidium competent *E.coli* were plated on agar plates supplemented with Ampicillin (100 µg/ml) and incubated at 37°C for 16h.

2.6.2 *In vitro* transcription and translation

In a 1.5 ml microcentrifuge tube, 1 µl (~300 ng) of plasmid was mixed with 40 µl of TnT® Quick master mix (Promega, #L5061), 2 µl of [^{35}S]methionine (EasyTag; Perkin Elmer) and a final volume of 50 µl was reached with nuclease-free water. The reaction was incubated at 30°C for 90min. 5µl of each TnT® reaction was added to 20 µl of Lamelli lysis buffer and heated at 95°C for 5min. Samples were resolved by SDS-PAGE as indicated in 2.7.1.

The SDS gel was then incubated in fixing solution (50% methanol, 10% glacial acetic acid, 40% water) with shaking for 30min. The fixing solution was removed and the gel was immersed in 10% glycerol for 5min to prevent cracking during drying. The gel was placed on Whatman 3MM filter paper (ThermoFisher, # 05-716-E), covered with plastic wrap and dried at 80°C for 60min, after which it was placed in an exposure cassette with CL-XPosure™ Film (Thermo Fisher, #34089) for 24h or until the desired proteins were detected.

2.7 Protein analysis

2.7.1 Sodium dodecyl sulphate polyacrylamide gel electrophoresis (SDS-PAGE)

Gradient SDS-PAGE gels were used to separate proteins according to size. Cells were seeded in 6-well plates at a density of 2 x 10^5 cells/well with 2 ml of culture media and maintained at 37°C with 5% CO_2. When confluent, 200 µl of Laemmli lysis buffer was added, lysates were collected and heated for 5 min at 95°C. 20 µl of each lysate was loaded on a 4-20% universal gel (NuSep, #NG21-420) and run at 150 V for 60min. Protein sizes were determined by comparison to a full range molecular weight rainbow marker (Sigma, # RPN800E).

2.7.2 Immunoblotting analysis

Resolved protein bands were transferred onto a nitrocellulose membrane (Amersham™ Protran™, #10600016) in 1X Western blot buffer for 60min at 100 V (200 mA). Following transfer, membranes were first blocked in 5% milk solution (milk powder, 0.1% tween, dissolved in PBS) for 1h at RT with shaking (40 rpm) to prevent non-specific binding. Membranes were incubated with primary antibody diluted in milk solution (referred to table 2.13 dilution/concentration) overnight at 4°C with shaking (40 rpm). Membranes were then washed three times with milk solution, each time for 10min, prior to incubation with secondary antibody HRP conjugates (diluted in milk solution) for 1h at RT with shaking (40 rpm). Membranes were washed three times, each time for 10 min, in 1X PBS (0.1% TWEEN) and then washed once in 1X PBS. Residual solution was removed from membranes and 1 mL of pre-mixed

SuperSignal® West Pico 86 Chemiluminescent Substrate (Pierce, #34087) or Immobilion™ Western chemiluminescent substrate (Millipore, #WBKLS0500) was added to each membrane and incubated for 5min at RT. Membranes were placed in an exposure cassette with CL-XPosure™ Film (Thermo Fisher, #34089) for 5sec to 10min, then incubated in developing solution (AGFA, #HT536) for 2 min, briefly washed in water and finally incubated in fixing solution (AGFA, #2828q) for 2min. Autoradiography film were washed then rinsed with water, air dried and scanned using An EPSON Selection V600 scanner.

2.8 Dual Luciferase reporter assays

Luciferase promoter reporter assays were used to investigate the ability to plasmid-encoded NSP1 proteins to downregulate the promoter activity of type I and III IFN (5.2.1.1, 5.2.1.2), NF-κB (5.2.1.3) and Mx (5.2.1.4). A dual luciferase system relies on the detection of two different reporter genes, *Renilla* (*Renilla reniformis*) and firefly luciferase (*Photinus pyralis*), to evaluate regulated genes expression. One reporter is used as an internal control to which measurement of the other reporter is normalized. The experimental reporter is coupled to a regulated promoter to study the structural or physiological basis of regulated gene expression. Relative changes in the expression of reporter activity correlate to changes in the transcriptional activity of the coupled regulated promoter. To provide an internal control for transcriptional activity, the second reporter gene is constitutively expressed. Cells were co-transfected with respective luciferase reporters and NSP1 as described in 2.1.4. In order to prevent detachment of HEK293 cells, wells were treated with 1X Poly-D-lysine (Sigma, #P6407-5MG) for 30min at RT prior to use. Depending on the promoter investigated, cells were treated with different stimuli (SeV, TNFα, IFNα) as stated. After induction, cells were washed in 1X PBS and lysed in 100 µl of passive 1X lysis buffer for 30min at RT. Supernatants were collected and luciferase values were obtained using the Dual-Luciferase® Reporter (DLRTM) Assay System (Promega, #E1910) and a spectrophotometer (Biotek, #Synergy 2). 30 µl of each lysate was added to a white sided, white flat bottom Greiner CELLSTAR® 96 well plate (Sigma, #

CLS3912) in triplicate. 40 µl of Luciferase Assay Buffer II was injected and firefly luciferase was automatically read for 8 seconds, then 40 µl of Stop & Glo® Buffer was added and *Renilla* luciferase values were automatically read. Values for firefly luciferase luminescence were then normalised to the expression of *Renilla* luciferase within the same sample. Values were converted into percentage expression of the positive control (stimulated cells containing empty vector only).

2.9 Bionformatics

ApE- A plasmid Editor (http://jorgensen.biology.utah.edu/wayned/ape/) was used to design primes.

Vector NTI Advance™ 11.5.3 (LifeTechnologies) was used to align sequences and draw phylogenetic trees.

ExPASy: SIB Bioinformatics Resource Portal was used to translate protein sequences (https://web.expasy.org/translate/).

Basic Local Alignment Search Tool (BLAST) was used to align primary biological sequence information, such as the amino-acid sequences of proteins or the nucleotides of DNA sequences (https://blast.ncbi.nlm.nih.gov/Blast.cgi)

Ensemble alignment tool was used to gain information about promoter sequences (http://www.ensembl.org/index.html)

2.10 Statistical analysis

Where required, t-test statistical analysis was performed with Graph Pad PRISM 7.00.

2.11 Graphical presentation

Dual luciferase reporter charts were generated using Graph Pad PRISM 7.00

2.12 List of primers

Table 7 lists the main oligonucleotides used in this report. Oligonucleotide primers were synthesised by Sigma-Aldrich and stock solutions of 100 pmol/µl were made using RNase/DNase freeH_2O (Sigma, #4502).

Table 7. Primers used for this study.

Primer name	Sequence (5'to 3')	use
βTrCPFwNed1	ACTATACATATGGACCCGGCCGAGGC	To clone β-TrCP in pGADT7 (forward)
βTrCPRevBamhI	TGATATGGATCCTTATCTGGAGATGTAGGTGTA TGTTCGAGAAGG	To clone β-TrCP in pGADT7 (reverse)
3' DNA-AD Sequencing	AGATGGTGCACGATGCACAG	To sequence of pGADT7 (reverse)
3' DNA-BD Sequencing	ATCATAAATCATAAGAAATTCGCC	Sequencing of pGBKT7 (reverse)
pCDNA3.1_NSP1_Re	TTATGCGGCCGCTGCAGG	To clone NSP1s in pcDNA™3.1/V5-His-TOPO® (reverse)
pCDNA3.1_NSP1_Fw	CAGAGGAGGACCTGCATATG	To clone NSP1s in pcDNA™3.1/V5-His-TOPO® (forward)
T7	TAATACGACTCACTATAGGǴ	To sequence NSP1s cloned in pcDNA™3.1/V5-His (forward) To sequence amplicons cloned in pGADT7 and pGBKT7 (forward)
BGH Reverse	TAGAAGGCACAGTCGAGǴ	To sequence NSP1s cloned in pcDNA™3.1/V5-His (reverse)
pCDNA_human_NSP1_18A(Fw)	CTCCTAGATGTAGAGTATTCACGC	To sequence human NSP1 strain 18A annealing within the sequence (forward)
pCDNA_human_NSP1_1M0(Fw)	ACCAGATGTAGAATGTTTACGC	To sequence human NSP1 strain 1M0 annealing within the sequence (forward)
pCDNA_human_NSP1_TC(Fw)	GCTTCTTGGCTGGAATGAAGC	To sequence human NSP1 strain TC annealing within the sequence (forward)
pCDNA_porcine_NSP1_G10P5(Fw)	TGGGATCGTATCAAGACTGG	To sequence porcine NSP1 strain G10P5 within the sequence (forward)
pCDNA_porcine_NSP1_A8(Fw)	AGGTGCAGAATGTTTACGC	To sequence porcine NSP1 strain A8 within the sequence (forward)
pCDNA_rhesus_NSP1_RRV(Fw)	CTCATCAAATCATTGGCAACC	To sequence rhesus NSP1 strain RRV within the sequence (forward)
pCDNA_bovine_NSP1_Uktc(Fw)	CATTATGAACTCATCGTATACCG	To sequence bovine NSP1 strain UKtc within the sequence (forward)
TC_FW_HIStag_kpn1	TGGCTAGTTAAGCTTGGTACCATGCATCACCATCACCATCAC AAAAGTCTTGTGGAAGCCATG	To clone HIS tag human NSP1 strain TC in pcDNA3.1 (forward)
18A_FW_HIStag_kpn1	TGGCTAGTTAAGCTTGGTACCATGCATCACCATCACCATC ACAAAAGTCTTGTGGAAGCCATG	To clone HIS tag human NSP1 strain 18A in pcDNA3.1 (forward)
1M0_FW_HIStag_kpn1	TGGCTAGTTAAGCTTGGTACCATGCATCACCATCACCATCACAAAAG TCTTGTGGAAGCCATG	To clone HIS tag human NSP1 strain 1M0 in pcDNA3.1 (forward)
G10P5_Fw_HIStag_kpn1	TGGCTAGTTAAGCTTGGTACCATGCATCACCATCACCATCACGCGACT TTTAAAGACGCTTGT	To clone HIS tag porcine NSP1 strain G10P5 in pcDNA3.1 (forward)

A8_FW_HIStag_kpn1	TGGCTAGTTAAGCTTGGTACCATGCATCACCATCACCATCACAAAAG TCTTGTGGAAGCCATG	To clone HIS tag porcine NSP1 strain A8 in pcDNA3.1 (forward)
Uktc_FW_HIStag_kpn1	TGGCTAGTTAAGCTTGGTACCATGCATCACCATCACCATCACGCGACT TTTAAAGACGCTTGC	To clone HIS tag bovine NSP1 strain UKtc in pcDNA3.1 (forward)
TC-18A-1M0_FW_HAGtag_kpn1	TGGCTAGTTAAGCTTGGTACCATGTACCCATACGACGTACCAGATTA CGCTAAAAGTCTTGTGGAAGCCATG	To clone HA tag human NSP1 strain 18A, 1M0 and TC in pcDNA3.1 (forward)
G10P5_Fw_HAtag-kpn1	TGGCTAGTTAAGCTTGGTACCATGTACCCATACGACGTACCAGATTA CGCTGCGACTTTTAAAGACGCTTGTTATC	To clone HA tag porcine NSP1 strain G10P5 in pcDNA3.1 (forward)
A8_Fw_HAtag-kpn1	TGGCTAGTTAAGCTTGGTACCATGTACCCATACGACGTACCAGATTA CGCTAAAAGTCTTGTGGAAGCCATGG	To clone HA tag porcine NSP1 strain A8 in pcDNA3.1 (forward)
UKtc_Fw_HAtag-kpn2	TGGCTAGTTAAGCTTGGTACCATGTACCCATACGACGTACCAGATTA CGCTGCGACTTTTAAAGACGCTTGC	To clone HA tag bovine NSP1 strain UKtc in pcDNA3.1 (forward)
NSP1s_Rev_not1	GCCCTTTTATGCGGCCGC	To clone HIS and HA tag human 18A, 1M0 and TC strains , porcine G10P5 and A8 strains and bovine UKtc strain in pcDNA3.1 (reverse)
G10P5_extra_Fw	TCAGAGGAGGACCTGCATATGAAAAGTCTTGTGGAAGCCATGGCGA CTTTTAAAGACGCT	To insert extra bases at the 5'-end of the porcine NSP1 G10P5 (forward)
G10P5_extra_Rev	AGCGTCTTTAAAAGTCGCCATGGCTTCCACAAGACTTTTCAT ATGCAGGTCCTCCTCTGA	To insert extra bases at the 5'-end of the porcine NSP1 G10P5 (reverse)
E1a_Fw	TCAAGCCTCAGACAGTGGTTC	To sequence rhesus (RRV) NSP1 cloned in pEF/flag-_RRV_NSP1
RRV_NSP1_inside	CATGATTTAAATTTGGGGAG	To sequence rhesus (RRV) NSP1 cloned in pEF/flag-_RRV_NSP1
RRV_NSP1_ inside(2)	TGAATTCACCTGGGATTCTCAAACTG	To sequence rhesus (RRV) NSP1 cloned in pEF/flag-_RRV_NSP1
hIRF3_EcoRI_Fw	GCGCGCGAATTCATGGGAACCCCAAAGCC	To clone the human IRF-3 in pGADT7 (Fw)
hIRF3_XhoI_Rev	AAATTTCTCGAGTCAGCTCTCCCCAGGG	To clone the human IRF-3 in pGADT7 (Rev)
pIRF3_Fw_Nde1	AATCATATGGGAACTCAGAAGCCTCGAATCC	To clone the porcine IRF-3 in pGADT7 (Fw)
pIRF3_Rev_BamH1	AATGGATCC CTAGAAATCCATGTCCTCCACCAGG	To clone the porcine IRF-3 in pGADT7 (Rev)

2.13 Primary and secondary antibodies used in this study

Table 8 lists the primary and secondary antibody used in this study.

Table 8. Primary and secondary antibodies used in this study.

Protein	Primary antibody	Secondary antibody
IRF-3	Anti- IRF-3 rabbit polyclonal IgG, 1:3000 (Santa Cruz , #9082)	Goat-α-rabbit IgG-HRP Conjugate, 1:5000 (Promega, # W401)
γ -tubilin	α-γ-tubulin mouse monoclonal Clone GTU-88 (IgG1) 1:5000 (Sigma, #T6557)	Goat-α-mouse-HRP Conjugate, 1:5000 (Promega, # W402B)
N^{PRO}	α-DS14 rabbit 1:50 (IAH in-house)	Alexa Flour 594 goat anti rabbit IgGI 1:500 (Molecular probes, #A11011)
HIS-tag	Anti-HIS mouse monoclonal, 1:3000 (GE Healthcare, #27-4710-01)	Goat-α-mouse-HRP Conjugate, 1:5000 (Promega, # W402B)
HIS-tag	Anti-6X His tag® mouse monoclonal, 1:3000 (Abcam, #ab18184)	Goat-α-mouse-HRP Conjugate, 1:5000 (Promega, # W402B)
HA-tag	Anti-HA Affinity Purified Antibody goat monoclonal, 1:3000 (QED Bioscience, #18849)	Donkey Anti-Goat IgG (H+L), HRP Conjugate, 1:5000 (Promega, #V8051)
MYC-tag	Anti-MYC rabbit polyclonal IgG, 1:3000 (Thermofisher, #PA1981)	Goat-α-mouse-HRP Conjugate, 1:5000 (Promega, # W402B)

2.14 Plasmids vectors

Table 9 lists the plasmids used in this study.

Table 9. Plasmids vectors used in this study.

Plasmid	Function	Resistance	Source
pGADT7/bIRF-3	Expression of bovine IRF-3 prey protein fused to the GAL4 AD domain protein	A	Steve Goodbourn
pGADT7/mIRF-3	Expression of monkey IRF-3 prey protein fused to the GAL4 AD domain protein	A	Michele Hardy
pGADT7/hMAVS	Expression of human MAVS prey protein fused to the GAL4 AD domain protein	A	Steve Goodbourn
pGADT7/hTBK1	Expression of human TBK1 prey protein fused to the GAL4 AD domain protein	A	Steve Goodbourn
pGADT7/hRIG-I	Expression of human RIG-I prey protein fused to the GAL4 AD domain protein	A	Steve Goodbourn
pGADT7/hβTrCP	Expression of human β-TrCP prey protein fused to the GAL4 AD domain protein	A	This study
pGADT7/hMDA5	Expression of human βTrCP prey protein fused to the GAL4 AD domain protein	A	Steve Goodbourn
pMA-T16AAM42P/NSP1-1M0	Plasmid containing the sequences encoding the human RV NSP1 (1M0)		GeneART®
pMA-T16AAM42P/NSP1-TC	Plasmid containing the sequences encoding the human RV NSP1 (tissue cultured adapted, TC)	A	GeneART®
pMA-RQ16AAM44P/NSP1-18A	Plasmid containing the sequences encoding the human RV NSP1 (18A)	A	GeneART®
pMAT16AAUNRP/NSP1-A8	Plasmid containing the sequences encoding the porcine RV NSP1 (A8)	A	GeneART®
pMA-RQ16AAUNSP/NSP1-G10P5	Plasmid containing the sequences encoding the porcine RV NSP1 (G10P5)		GeneART®
pGBKT7/hNSP1(1M0)	Expression of the human RV NSP1 (strain 1M0) bait protein fused to the GAL4 BD protein	K	This study
pGBKT7/hNSP1(TC)	Expression of the human RV NSP1 (Tissue cultured adapted, TC) bait protein fused to the GAL4 BD protein	K	This study
pGBKT7/hNSP1(18A)	Expression of the human RV NSP1 (strain 18A) bait protein fused to the GAL4 BD protein	K	This study
pGBKT7/pNSP1(A8)	Expression of the porcine RV NSP1 (strain A8) bait protein fused to the GAL4 BD protein	K	This study
pGBKT7/pNSP1(G10P5)	Expression of the porcine RV NSP1 (strain G10P5) bait protein fused to the GAL4 BD protein	K	This study
pGBKT7/RRV-NSP1	Expression of the rhesus RV NSP1 (strain RRV) bait protein fused to the GAL4 BD protein	K	Steve Goodbourn

pGBKT7/UKtc-NSP1	Expression of the bovine RV NSP1 (strain UKtc) bait protein fused to the GAL4 BD protein	K	Steve Goodbourn
pCNV5_ β-TrCP	Plasmid containing the sequence encoding the human β-TrCP	A	Steve Goodbourn
pcDNA3.1/V5-His-TOPO-human NSP1(18A)	Expression of the human RV NSP1 (strain 18A) in mammalian cell lines	A	This study
pcDNA3.1/V5-His-TOPO-human NSP1(1M0)	Expression of the human RV NSP1 (strain 1M0) in mammalian cell lines	A	This study
pcDNA3.1/V5-His-TOPO-human NSP1(TC)	Expression of the human RV NSP1 (strain TC) in mammalian cell lines	A	This study
pcDNA3.1/V5-His-TOPO-porcine NSP1(G10P5)	Expression of the porcine RV NSP1 (strain G10P5) in mammalian cell lines	A	This study
pcDNA3.1/V5-His-TOPO-porcine NSP1(A8)	Expression of the porcine RV NSP1 (strain A8) in mammalian cell lines	A	This study
pcDNA3.1/V5-His-TOPO-bovine NSP1 (UKtc)	Expression of the bovine RV NSP1 (strain UKtc) in mammalian cell lines	A	This study
pcDNA3.1/V5-His-TOPO-human HA-NSP1(18A)	Expression of the HA-tag human RV NSP1 (strain 18A) in mammalian cell lines	A	This study
pcDNA3.1/V5-His-TOPO-human HA-NSP1(1M0)	Expression of the HA-tag human RV NSP1 (strain 1M0) in mammalian cell lines	A	This study
pcDNA3.1/V5-His-TOPO-human HA-NSP1(TC)	Expression of the HA-tag human RV NSP1 (strain TC) in mammalian cell lines	A	This study
pcDNA3.1/V5-His-TOPO-porcine HA-NSP1(G10P5)	Expression of the HA-tag porcine RV NSP1 (strain G10P5) in mammalian cell lines	A	This study
pcDNA3.1/V5-His-TOPO-porcine HA-NSP1(A8)	Expression of the HA-tag porcine RV NSP1 (strain A8) in mammalian cell lines	A	This study
pcDNA3.1/V5-His-TOPO-bovine HA-NSP1 (UKtc)	Expression of the HA-tag bovine RV NSP1 (strain UKtc) in mammalian cell lines	A	This study
pcDNA3.1/V5-His-TOPO-rhesus HA-NSP1 (RRV)	Expression of the HA-tag rhesus RV NSP1 (strain RRV) in mammalian cell lines	A	This study
pcDNA3.1/V5-His-TOPO-human HIS-NSP1(18A)	Expression of the HIS-tag human RV NSP1 (strain 18A) in mammalian cell line	A	This study
pcDNA3.1/V5-His-TOPO-human HIS-NSP1(1M0)	Expression of the HIS-tag human RV NSP1 (strain 1M0) in mammalian cell lines	A	This study
pcDNA3.1/V5-His-TOPO-human HIS-NSP1(TC)	Expression of the HIS-tag human RV NSP1 (strain TC) in mammalian cell lines	A	This study
pcDNA3.1/V5-His-TOPO-porcine HIS-NSP1(G10P5)	Expression of the HIS-tag porcine RV NSP1 (strain G10P5) in mammalian cell lines	A	This study
pcDNA3.1/V5-His-TOPO-porcine HIS-NSP1(A8)	Expression of the HIS-tag porcine RV NSP1 (strain A8) in mammalian cell lines	A	This study
pcDNA3.1/V5-His-TOPO-bovine HIS-NSP1 (UKtc)	Expression of the HIS-tag bovine RV NSP1 (strain UKtc) in mammalian cell lines	A	This study

pEF/flag h-IRF-3	Plasmid containing the sequence encoding human IRF-3		Steve Goodbourn
pGADT7/hIRF-3	Expression of human IRF-3 prey protein fused to the GAL4 AD domain protein	A	This study
pGBKT7/pNSP1(G10P5) extra	Expression of the porcine RV NSP1 (strain G10P5) with extra aa sequence at the 5'-end bait protein fused to the GAL4 BD	K	This study
pEF-flag-hIRF3	Plasmid containing the sequence encoding the human IRF-3	A	Steve Goodbourn
pGADT7/hIRF-3	Expression of human IRF-3 prey protein fused to the GAL4 AD domain protein	A	This study
pGL2/hIFNβ	Luciferase reporter vector under the control of the human IFNβ promoter.	A	Steve Goodbourn
pRL-CMW Renilla	pRL Renilla Luciferase control reporter vector under the control of the CMV promoter	A	Promega (#E2261)
pcDNA3.1/V5-His-TOPO-N^{pro}	Expression of the Classical Swine Fever N-terminal protease (N^{pro}) in mammalian cell lines	A	Julian Seago
pGL2/hIFNλ_1	Luciferase reporter vector under the control of the human IFN λ_1 promoter.	A	Julian Seago
pGL2/hIFNλ_3	Luciferase reporter vector under the control of the human IFN λ_3 promoter.	A	Julian Seago
pGL2/hIFNα	Luciferase reporter vector under the control of the human IFNα_4 promoter.	A	Julian Seago
pGL2/pMx_2	Luciferase reporter vector under the control of the porcine Mx_2 promoter.	A	Christ Netherton
pcdnaV5_RPV_Sa_VCStop	Expression of the V protein encoded by rinderpest virus (RPV) Saudi/81 strain in mammalian cell lines	A	Michael Baron
pMA-RQ/pigIRF-3	Plasmid containing the sequence encoding the porcine IRF-3	A	GeneART®
pGADT7/pIRF-3	Expression of porcine IRF-3 prey protein fused to the GAL4 AD domain protein	A	This study
pMC159	Expression of the MC159 protein encoded by Molluscum Contagiosum in mammalian cell lines	A	Johanna Shisler
pGL3-Mx1P-luc	Luciferase reporter vector under the control of the murine Mx_1 promoter.	A	Georg Kochs
P6kB-LUC-NF-κB	Luciferase reporter vector under the control of the human NF-κB promoter.	A	Julian Seago
pEGFP-C1-IRF-7	Plasmid containing the sequence encoding the human IRF-7	K	Julian Seago
pEF-OSU_NSP1	Expression of the porcine RV NSP1 (OSU) in mammalian cell lines	A	Steve Goodbourn

pc-CMV-P50	Expression of p50 (NF-κB subunit) in mammalian cell lines	A	Julian Seago
pRC- Ikkα	Expression of Ikkα in mammalian cell lines	A	Julian Seago
pc-CMV-P65	Expression of p65 (NF-κB subunit) in mammalian cell lines	A	Julian Seago
pRC- Ikkβ	Expression of Ikkβ in mammalian cell lines	A	Johanna Shisler
pcDNA3.1/V5-His-TOPO-MYC-18A	Plasmid containing the sequence encoding the MYC-tag RV NSP1 (18A)	A	GeneArt
pcDNA3.1/V5-His-TOPO-MYC-1M0	Plasmid containing the sequence encoding the MYC-tag RV NSP1 (1M0)	A	GeneArt
pcDNA3.1/V5-His-TOPO-MYC-TC	Plasmid containing the sequence encoding the MYC-tag RV NSP1 (TC)	A	GeneArt
pcDNA3.1/V5-His-TOPO-18AUKtc	Expression of recombinant NSP1 carrying the N-termini region of the human strain 18A and the C-termini region of the bovine strain UKct in mammalian cell lines	A	GeneArt
pcDNA3.1/V5-His-TOPO-UKtc18A	Expression of recombinant NSP1 carrying the N-termini region of the bovine strain UKct and the C-termini the human strain 18A region of in mammalian cell lines	A	GeneArt

Antibiotic resistance: A=Ampicillin, K=Kanamycin

2.15 Buffers, solutions and culture media

Table 10 lists buffers, solutions and culture media used in this study

Table 10. Buffers, solutions and culture media used in this study.

Solutions	Recipe	Use
LB media	Tryptone (Oxoid,#LP0042) 4gr Yeast extract (Oxoid,#LP0021) 2gr Formulation for 400ml	Culturing transformed bacterial cells
LB Agar	Tryptone (Oxoid,#LP0042) 4gr Yeast extract (Oxoid,#LP0021) 2gr Bacto Agar (Sigma,#A5306) Formulation for 400ml	Culturing transformed bacterial cells
S.O.C.	2% tryptone 0.5% yeast extract 10 mM NaCl 2.5 mM KCl 10 mM $MgCl_2$ 10 mM $MgSO_4$ 20 mM glucose	Recovery medium used during bacterial transformation
Tris-Acetate EDTA (TAE) 1X	40mM Tris 20mM acetic acid 1mM EDTA, pH 8.0	DNA gel electrophoresis
Tris-Borate EDTA (TBE)	0.9 M Tris-base 0.9 M Boric acid 0.02 M EDTA	DNA gel electrophoresis
Loading buffer 10X	100 mg Orange G (Sigma,# O3756) Glycerol 15ml (Sigma,#G5516) Formulation for 50ml	DNA gel electrophoresis: loading samples
Laemelli buffer	4% SDS 20% glycerol 10% 2-mercaptoethanol 0.004% bromphenol blue 0.125 M Tris HCl, pH 6.8.	Lysing cells
SDS-running buffer 10X	TRIS base (Sigma,#1503) 30gr Glycine (AnalaR Normapur,#101194M) 144gr SDS (Sigma,#L3771) 10gr Formulation for 1000ml To be used at 1X	Protein manipulation: proteins resolution
Transfer buffer 10X	TRIS base (Sigma,#1503) 30gr Glycine (AnalaR Normapur,#101194M) 144gr Formulation for 1000ml To be used 1X: 100ml of 10X solution, 200ml isopropanol, 700ml H_20	Protein manipulation: transfer of resolved protein from the gel to membrane
Washing buffer	0.1% Tween (Sigma,#P1379) in PBS	Protein manipulation: washing western blot membrane
Blocking buffer	5% skimmed milk powder in washing buffer	Protein manipulation: prevention of unspecific bindings of the antibody
Tris-EDTA (TE) 10X	10 mM Tris-HCl 1 mM EDTA pH 8.0	Yeast-two-hybrid assay
40%PEG, LiAc, TE	PEG50% 8ml LiAc 1M 1ml TE 10X 1ml	Yeast-two-hybrid assay
LiAc, TE	TE 10X 1ml LiAc 1M 1ml 8ml H_2O	Yeast-two-hybrid assay

Result chapter 1

Analysis of NSP1 interaction using a yeast-two-hybrid

3 Strain-dependent interaction between IRF-3 and rotavirus NSP1

Purpose

This chapter describes experiments performed in order to identify host proteins involved in interferon induction which may interact with RV NSP1. A strain-specific interaction was observed between a panel of NSP1 proteins from RV isolates and IRF-3 proteins from different mammalian species. These observations provide the foundations for the investigations in the following chapters.

Introduction

The role of NSP1 in modulating the host innate immune response suggests that the protein is required by the virus during first steps of its replication cycle (Desselberger, 2014). Successful replication of RV in its target cells is partially due to the ability of the virus to modulate the IFN induction through the expression of NSP1. It has been shown that NSP1 from the bovine strain UKtc is able to interact with IRF-3, driving its proteasome-mediated degradation (Sen *et al.*, 2009). By contrast, porcine NSP1 OSU is able inhibit NF-κB transcriptional activity targeting β-TrCP (Di Fiore *et al.*, 2015). The ability of RV to downregulate the expression of IFN is conserved among different species, however, targets within the IFN pathways varies between strains (Arnold *et al.*, 2011). In order to determine if NSP1s from different host species downregulate interferon induction by targeting different host proteins in this signalling pathway, or if all NSP1s target a set of proteins which are the common targets irrespective of the host species of origin, a yeast-2-hybrid (Y-2-H) assay was used. A panel of NSP1, encoded by RV isolated from different species (human, pigs, cattle and rhesus) were screened against host proteins involved in the induction of interferon.

3.1 Generation of reagents to identify interactions between NSP1 and members of the IFN -induction pathway using a Y-2-H assay

3.1.1 Construction of "bait" plasmid pGBKT/NSP1

The Y-2-H "bait" plasmid pGBKT7 containing the sequences encoding the bovine NSP1 (UKtc) (GU808570) and the rhesus NSP1 (RRV) (U08433.1) were a gift from Professor Steve Goodbourn (St. George's, University of London). In order to include NSP1 derived from RV infecting human and pigs in the Y-2-H screening, plasmids encoding their sequences were ordered from GeneART/Thermo Fisher Scientific and sub-cloned into the "bait" yeast plasmid pGBKT7.

Selection and cloning of NSP1 from human RV isolates

Three NSP1 proteins encoded by human RV isolates were selected following the analysis of an alignment of thirteen different NSP1 amino acid sequences; the alignment included the NSP1 sequences of six human isolates belonging to the A2 genotype (BID18A, BID1RU, BID1JK, BID156, BID1PP, BID2Q5) and seven human isolates belonging to the A1 genotype (BID1CH, BID2JS, BID225, BID1M0, BID2D5, BID2BM, WA) (Matthijnssens *et al.*, 2008).

Based on alignment divergence, one within A1 genotype group (1M0 (G12P[8], Ku048673)) and one representing the A2 genotype group (18A (G1P[8], MG181761)) were selected. The TC-tissue cultured adapted (G1P[8], JX406751.1) was included in the screening (Figure 9). GeneART/Thermo Fisher plasmids encoding the sequences for the human NSP1 were amplified, the insert corresponding to NSP1 released and cloned into the MCS of the "bait" pGBKT7 plasmid using *Nde*I and *Bam*HI restriction sites. Restriction digestion analysis and sequencing confirmed the presence of the NSP1 genes and regeneration of the ligation junctions.

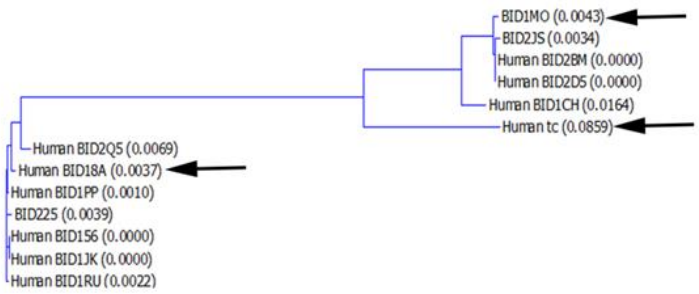

Figure 9. Phylogenetic tree derived from the amino acid alignment of NSP1 proteins from human rotavirus isolates.

The amino acid sequences of thirteen NSP1 proteins were aligned and strains were selected based on divergence. Arrows indicate the three NSP1 proteins selected for use in Y-2-H analysis. 1M0 and Wa (referred as TC-adapted) belong to the Wa-like group, while 18A belongs to DS-1-like group.

NSP1 isolates derived from rotavirus infecting pigs

The amino acid sequences of four NSP1 proteins from porcine RV isolates were aligned and based on sequence divergence the A8 (KJ482247.1) and G10P5 (AB972862.1) isolates were selected to perform Y-2-H analysis (Figure 10). Their respective nucleotide sequences were ordered from GeneART/Thermo Fisher. Plasmids encoding NSP1 sequences were amplified and inserted corresponding to NSP1 sub-cloned into the MCS of the "bait" plasmid pGBKT7 plasmid using *Nde*I and *Bam*HI restrictions sites. Digestion analysis and sequencing confirmed the presence of the NSP1 genes in frame within the sequence of pGBKT7 yeast plasmid.

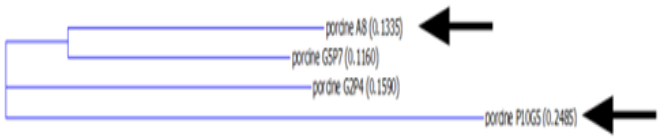

Figure 10. Phylogenetic tree derived from the amino acid alignment of NSP1 proteins from porcine rotavirus isolates.

The amino acid sequences of four NSP1 proteins were aligned and two strains were selected based on divergence. Arrows indicate the two porcine NSP1 that were chosen for use in Y-2-H analysis

Analysis of the NSP1 amino acid sequence of the porcine G10P5 RV isolate revealed the absence of seven N- terminal amino acids present in the other porcine

RV isolate (A8) and all three human RV isolates (1M0, 18A and TC). In order to evaluate whether these seven amino acids could influence the interaction of G10P5 NSP1 protein with "prey" proteins, the respective nucleotide sequence present in porcine A8 and human 1M0, 18A and TC NSP1 was inserted into the previously generated pGBKT7/G10P5 plasmid using a site-direct mutagenesis kit (Figure 11, Panel A). Sequence analysis confirmed the insertion of these additional nucleotides into the porcine NSP1 G10P5 open reading frame (ORF) (Figure 11, Panel B). This new "bait" plasmid was termed pGBKT7/G10P5extra and its encoded protein G10P5extra.

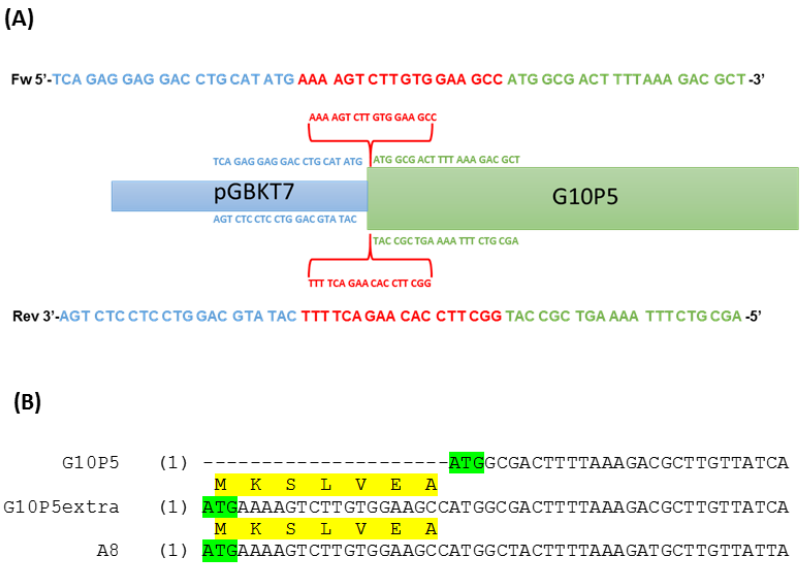

Figure 11. Insertion of seven amino acids into the N-terminus of the porcine NSP1 G10P5.

(**A**) Strategy used to insert seven amino acids using a Site-Directed Mutagenesis Kit. The Fw primer annealed within the yeast plasmid pGBKT7 (blue) and extended into the coding sequence of G10P5 (green). The nucleotide sequence encoding the seven extra amino acids was inserted (red) immediately downstream of the translation initiation start codon. (**B**) Alignment of the NSP1 N-terminal nucleotide sequences of porcine G10P5 and A8 RV isolates and the G10P5 isolate containing seven additional N-terminal amino acids (MKSLVEA) shown in yellow. The start codon (ATG) is highlighted in green.

3.1.2 Construction of "prey" pGADT7 plasmids encoding human β-TrCP, human IRF-3 and porcine IRF-3

A number of "prey" pGADT7 plasmids were kindly provided by Steve Goodbourn (St. George's, University of London), including bovine-IRF-3 (bIRF-3), human IRF-7 (hIRF-7), human-MAVS (hMAVS), human-TBK1 (hTBK-1), human-RIG-I (hRIG-I) and human MDA5 (hMDA5). The "prey" plasmid pGADT7, encoding the sequence for green monkey (*Cercopithecus aethiops*) IRF-3 (mIRF-3), was a gift from Professor Michelle Hardy (Washington State University).

Given the essential role of β-TrCP in the establishment of the host innate immune response, it is not surprising that some viruses have evolved strategies to counteract its activity (Bour *et al.*, 2001; Mansur *et al.*, 2013; Tang *et al.*, 2003). β-TrCP has been shown to be targeted for degradation by NSP1 proteins derived from the porcine OSU, the bovine NCDV and the human D, DS-1, Ku, P and Wa RV strains (Di Fiore *et al.*, 2015; Graff *et al.*, 2009). In order to determine if in a Y-2-H system β-TrCP interacts with NSP1 proteins encoded by RV isolates from different species, its cDNA was amplified from pCNV5_ β-TrCP (Table 7) and cloned into the MCS of the yeast "prey" plasmid pGADT7. Restriction digestion analysis and sequencing confirmed the presence of the β-TrCP gene and regeneration of the ligation junctions.

In order to include the human IRF-3 (hIRF-3) and the porcine IRF-3 (pIRF-3) in the panel of host proteins screened against RV NSP1, the nucleotide sequences of the 2 transcriptional factors were sub-cloned in to the yeast "prey" plasmid pGADT7. The sequence encoding hIRF-3 was amplified from pEF-flag-hIRF3 (Steve Goodbourn, St. George's, University of London) (Table 7) and inserted into the MCS of pGADT7. Restriction digestion analysis and sequencing confirmed the presence of the hIRF-3 gene and regeneration of the ligation junctions (Figure 12, Panel A). The nucleotide sequences encoding pIRF-3 (NM_213770.1) was ordered from GeneART/Thermo Fisher Scientific. The sequence ordered included the following silent substitutions: 21G>A and 683G>A. These two silent mutations were inserted to remove *BamHI*

restrictions sites present in the original coding sequence. GeneART containing pIRF-3 was PCR amplified, and inserted into the “prey” pGADT7 plasmid using *Nde*I and *Bam*HI restriction sites. Restriction digestion analysis and sequencing confirmed the presence of the pIRF-3 gene and regeneration of the ligation junctions (Figure 12, Panel B).

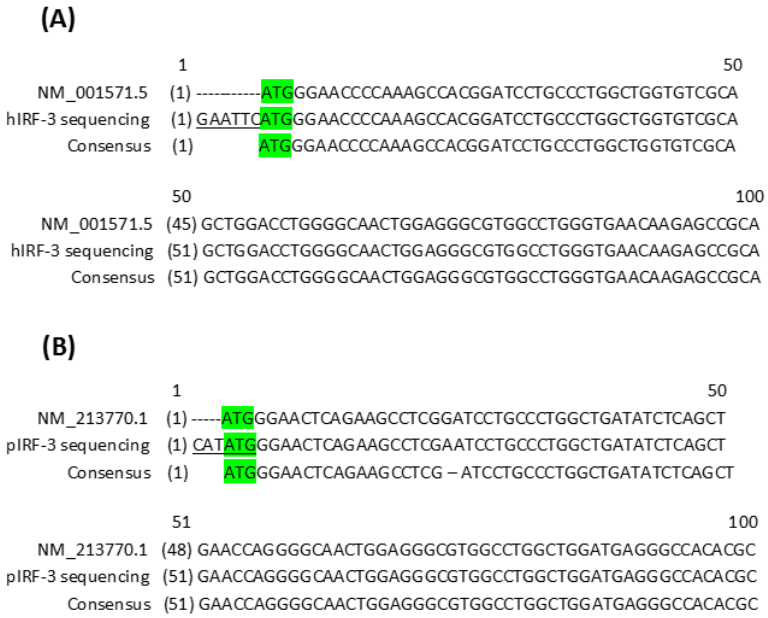

Figure 12. Construction of "prey" pGADT7 plasmids encoding human IRF-3 (hIRF-3) and porcine IRF-3 (pIRF-3).

(**A**) Sequencing alignment of the hIRf-3 cloned in pGADT7 and the reference sequence. The ATG is represented in green. Underlined the EcoRI cloning site to insert the hIRF-3 cDNA in the MCS of pGADT7. (**B**) Sequencing analysis of the pIRF-3 cloned in pGADT7. The ATG is represented in green. Underlined the NdeI cloning site to insert the hIRF-3 cDNA in the MCS of pGADT7. Here shown the first 100 nucleotides.

3.2 Y-2-H interactions between components of the IFN induction pathway and RV NSP1 proteins.

Before analysing putative interactions occurring between a panel of NSP1 (1 3.1.1) and proteins involved in the host innate immune response (3.1.2), preliminary experiments were performed in order to check for auto-activation of the GAL4 reporter promoter in the Y-2-H system. NSP1 “baits” were tested for self-activation when expressed alone or when co-transfected with the empty “prey” vector (pGADT7- expressing only the GAL4 activation domain). The reciprocal controls were performed to check for auto-activation by IFN components: “prey” plasmids were tested against the empty “bait” protein (pGBKT7- expressing only the GAL4 binding domain) and for self-activation when expressed alone. These experiments revealed that the porcine NSP1 A8 was able to self-activate the system, being able to grow on selective media when transfected alone or co-transfected in yeast with an empty “prey” plasmid (Figure 13, Panel A). The hIRF-7 was also shown to self-activate the system, generating yeast colonies on selective plates when co-transfected with an empty “bait” plasmid or transfected alone (Figure 13, Panel B). For this reason, IRF-7 was excluded from further investigation involving the Y-2-H. Transformation of competent yeast with the porcine A8 was included in the Y-2-H screen as an additional positive control.

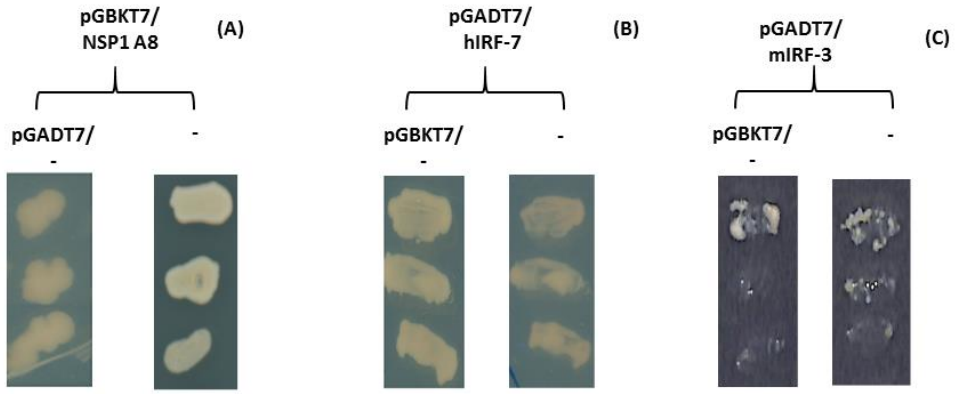

Figure 13. Human IRF-7 and the porcine A8 NSP1 self-activate the Y-2-H system.

Competent yeast were co-transformed as follows: (**A**) porcine NSP1 A8 together with an empty pGADT7 plasmid or alone, (**B**) human IRF-7 with an empty pGBKT7 plasmid or alone or (**C**) monkey IRF-3 with an empty pGBKT7 plasmid or alone and plated on DDO media. Once colonies had reached sufficient size (~5-7days), 5 were re-streaked from the original DDO media onto fresh QDO media (here reported). In the absence of an interaction between prey and bait proteins, yeast growth on selective quadruple dropout (QDO) media indicates the ability of a protein to self-activate the Y-2-H system (A and B). The inability of the mIRF-3 (C) to grow on QDO in absence the "prey" counterpart confirmed the validity of the system.

3.2.1 Y-2-H analysis between components of the IFN induction pathway and NSP1 proteins from bovine (UKtc) and rhesus (RRV) RV isolates

Once self-activating controls had been performed, the interactions occurring between NSP1 encoded by RV infecting cattle and monkeys and proteins involved in the IFN induction pathway were investigated.

"Bait" plasmids expressing either rhesus (RRV) or bovine (UKtc) NSP1 were individually co-transformed into competent AH109 yeast cells with a "prey" plasmid expressing either bovine-IRF-3 (bIRF-3), monkey IRF-3 (mIRF-3), human-MAVS (hMAVS), human-TBK1 (hTBK1), human-RIG-I (hRIG-I), human β-TrCP (hβ-TrCP) or human MDA5 (hMDA5). Following transformation, the yeast were plated on the appropriate selective media: double drop-out ((DDO) *-Leu,-Trp*) to confirm the correct co-expression of both plasmids in a single yeast cell, and quadruple drop-out ((QDO) *-Leu, -Trp, -Ade, -His*) to identify a putative interaction between encoded proteins.

The results of this assay are shown in Figure 14. Competent yeast were successfully co-transformed with the "bait" and "prey" plasmids (Figure 14, Panel A). The co-expression of bovine NSP1 UKtc with either bIRF-3 or mIRF-3 resulted in the growth of colonies on QDO media (Figure 14, Panel B), suggesting the proteins were interacting. No interaction was observed between bovine NSP1 and hMAVS, hTBK1, hRIG-I, hβ-TrCP or h-MDA5. Co-transformation of rhesus NSP1 RRV with any of the individual "prey" proteins did not result in growth on QDP plates (Figure 14, Panel B), suggesting no interactions occurred.

The ability of yeast colonies to grow on QDO plates when co-transformed with a "bait" plasmid pGBKT7-53 and a "prey" plasmid pGADT7-T confirmed transformation was successful. Co-transformation of competent yeast with a "bait" plasmid pGBKT7-Lam and a "prey" plasmid pGADT7-T was used as negative control.

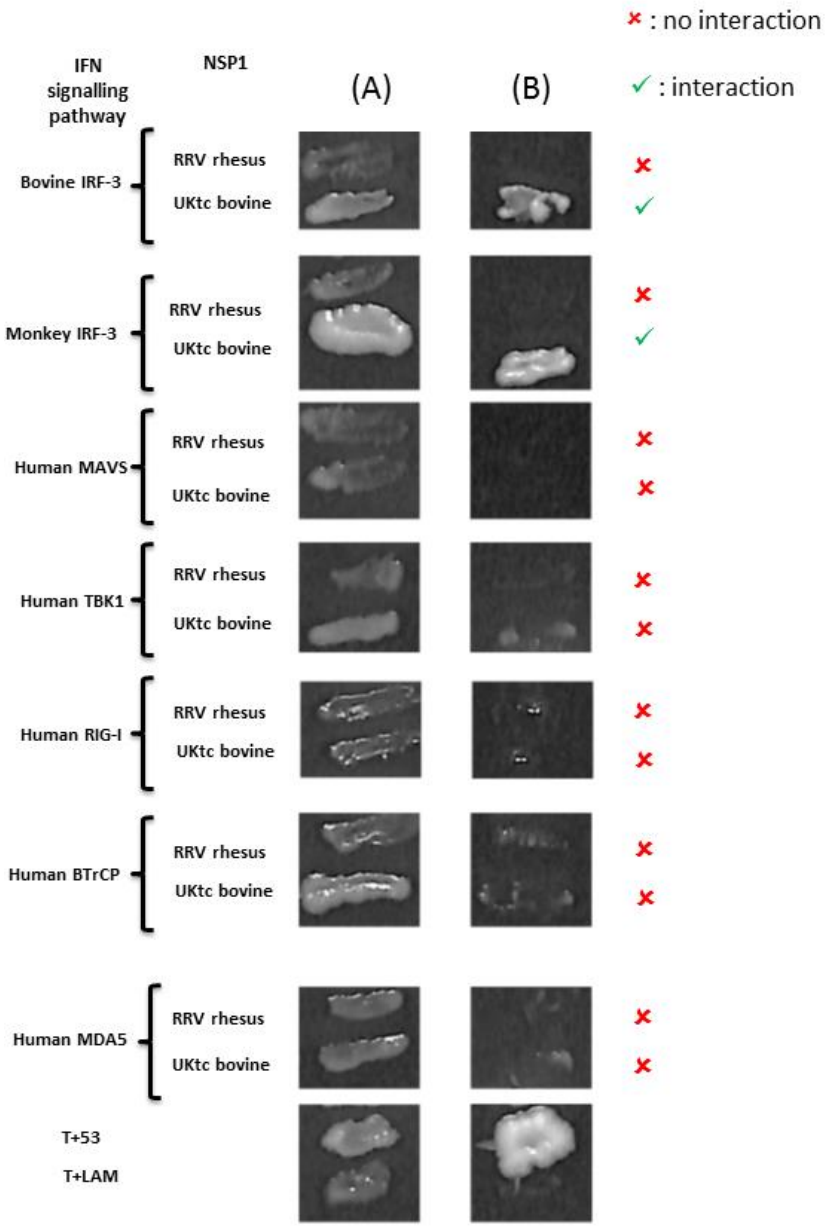

Figure 14. Y-2-H screening between rhesus (RRV) or bovine (UKtc) NSP1 and proteins of the IFN induction pathway, (bIRF-3, mIRF-3, hMAVS, hTBK1, hRIG-I, hBTrCP or hMDA5).

Aliquots of transformed yeast were plated on DDO (-Leu,-Trp) selective media. Once colonies had reached sufficient size (~5-7days), 5 colonies were re-streaked from the original DDO media onto fresh DDO media (*-Leu,-Trp*) (panel A) as well as QDO media (*-Leu, -Trp, -Ade, -His*) (panel B). The ability of yeast to grow on DDO selective media indicated that both the "bait" and the "prey" plasmids had been successfully co-transformed into a single yeast cell. The ability of yeast to grow on QDO plates indicated that the proteins encoded by the yeast-expression plasmids interacted. Co-transfection of vectors pGBKT7-53 with pGADT7-T and pGBKT7-Lam with pGADT7-T were used as positive and negative controls, respectively. Each single colony is representative of 5 colonies.

3.2.2 Y-2-H analysis between components of the IFN induction pathway and NSP1 proteins from porcine RV isolates: G10P5 and A8

Y-2-H analyses were then performed to determine if the NSP1 proteins from three porcine RV isolates (G10P5, G10P5extra and A8) interact with proteins involved in the interferon induction pathway. In order to do this, previously generated "bait" plasmids encoding the sequences for NSP1 G10P5, G10P5 and NSP1 A8 (0) were screened against "prey" plasmids expressing either bIRF-3, mIRF-3, hMAVS, hTBK1, hRIG-I, hβ-TrCP or hMDA5. Competent yeast cells were co-transformed with a "bait" and a "prey" plasmid expressing components of the IFN induction pathway as previously described (3.2.1).

Figure 15 shows the results of the Y-2-H assays between the two porcine RV isolates, G10P5 and A8 and components of the IFN induction pathway. The ability of yeast to grow on DDO plates (*-Leu, -Trp*), confirmed that cells were successfully transformed (Figure 15, Panels A). The co-expression of porcine NSP1 G10P5 with mIRF-3 resulted in growth on QDO media, indicating that a putative interaction occurred. Y-2-H analyses involving the "bait" porcine G10P5 NSP1 and "prey" human RIG-I, β-TrCP, MAVS, TBK1 and bIRF-3 proteins did not result in growth on QDO media, suggesting no interactions occurred. The growth of yeast colonies co-expressing G10P5 and MDA5 suggested a possible interaction occurred, however these colonies took longer to growth on QDO media compared to the other positive interactions, suggesting a possible weaker interaction.

Previous control experiments have shown the ability of the "bait" porcine A8 NSP1 to self-activate the expression of the reporter genes in absence of a true interaction (false positive) (Figure 13, Panel A). Co-transformation of competent yeast with porcine A8 and any on the "prey" plasmid was used as a further positive control (Figure 13, Panel B). In order to increase the stringency levels of Y-2-H screening involving the porcine A8 and to further corroborate its ability to self-activate the system, QDO media was administered with 3-Amino-1,2,4-triazole (3-AT) (Figure 15, Panel C) .3-AT is a competitive inhibitor of the imidazole-

glycerolphosphate dehydratase (HIS3) gene product (Durfee *et al.*, 1993) and yeast are capable of growing only if the production of histidine overcomes its inhibitory effect. Higher level of gene expression can be achieved only under the transcription of a full transcriptional factor, thus, the inability of yeast to grow on media containing 3-AT indicated that yeast contained only the DNA BD carried by pGBK7.

To determine if the additional 7 amino acids present in the N-terminus of G10P5extra NSP1 (0) could alter the interaction profile of the G10P5 NSP1 protein, Y-2-H screening was carried out using porcine G10P5extra NSP1 and the previously used components of the IFN induction pathway. Figure 16 shows that the insertion of the extra amino acids at the N-terminus of G10P5 did not alter the proteins binding profile to the "prey" proteins, and the only observable interaction was with mIRF-3 (Figure 15).

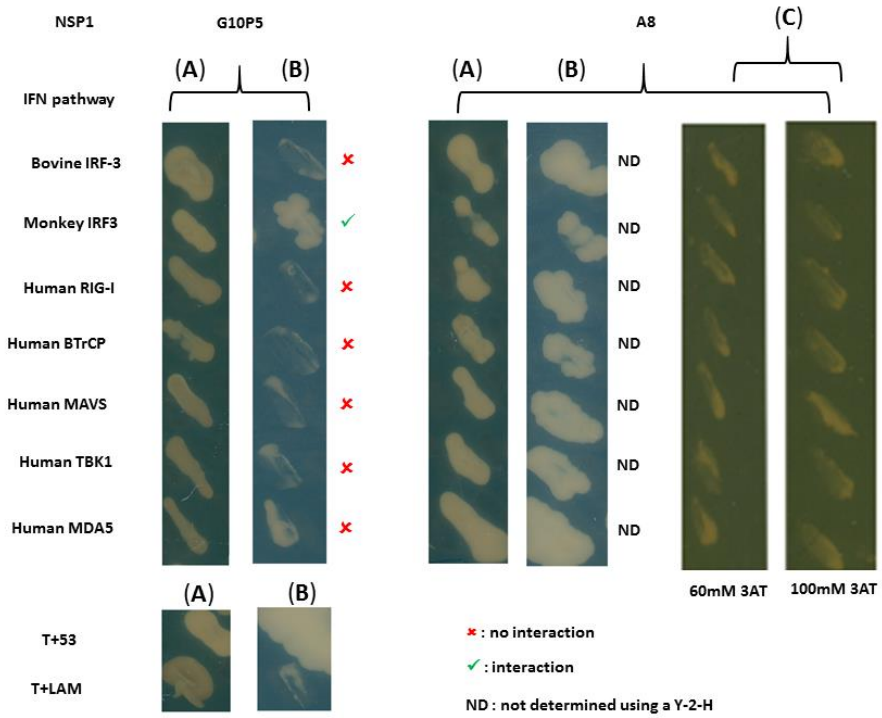

Figure 15. Y-2-H screening between the porcine G10P5 or A8 NSP1 proteins and components of the IFN induction pathway (bIRF-3, mIRF-3, hRIG-I, hBTrCP, hMAVS, hTBK1 or hMDA5.

Aliquots of transformed yeast were plated on DDO (*-Leu,-Trp*) selective media. Once colonies had reached sufficient size (~5-7days), 5 colonies were re-streaked from the original DDO media onto fresh DDO media (*-Leu,-Trp*) (panel **A**) as well as QDO media (*-Leu, -Trp, -Ade, -His*) (panel **B**). The ability of yeast to grow on DDO selective media indicated that both the "bait" and the "prey" plasmids had been successfully co-transformed into a single yeast cell. The ability of yeast to grow on QDO plates indicated that the proteins encoded by the yeast-expression plasmids interacted. (C) Yeast colonies re-streaked from QDO media onto QDO media supplemented with 60 mM or 100 mM 3AT. Co-transfection of vectors pGBKT7-53 with pGADT7-T and pGBKT7-Lam with pGADT7-T were used as positive and negative controls, respectively. Each single colony is representative of 5 colonies.

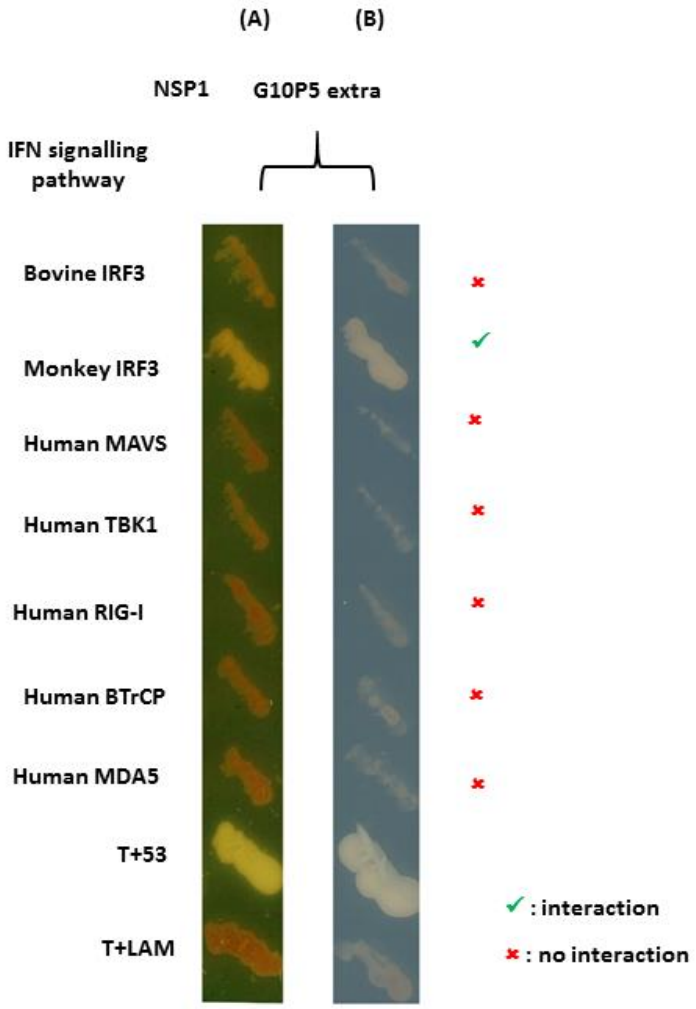

Figure 16. Y-2-H screening between the porcine G10P5extra NSP1 protein and components of the IFN induction pathway (bIRF-3, mIRF-3, hRIG-I, hBTrCP, hMAVS, hTBK1 or hMDA5.

Aliquots of transformed yeast were plated on DDO (*-Leu,-Trp*) selective media. Once colonies had reached sufficient size (~5-7days), 5 colonies were re-streaked from the original DDO media onto fresh DDO media (*-Leu,-Trp*) (panel **A**) as well as QDO media (*-Leu, -Trp, -Ade, -His*) (panel **B**). The ability of yeast to grow on DDO selective media indicated that both the "bait" and the "prey" plasmids had been successfully co-transformed into a single yeast cell. The ability of yeast to grow on QDO plates indicated that the proteins encoded by the yeast-expression plasmids interacted. Each single colony is representative of 5 colonies. The vectors pGBKT7-53 plus pGADT7-T and pGBKT7-Lam plus pGADT7-T were used as positive and negative controls, respectively.

The porcine NSP1 G10P5extra was constructed by inserting the nucleotide sequence encoding for the seven amino acids (METKSLVEA) at the 5- end of the porcine NSP1 G10P5. This sequence is present in the porcine NSP1 A8 and in the human 1M0, TC and 18A used in this study.

3.2.3 Y-2-H analysis between hIRF-3 and NSP1 proteins from porcine (G10P5, A8), bovine (UKtc) and rhesus (RRV) RV isolates

Having established that the bovine and monkey IRF-3 were cellular partners of NSP1 (3.2.1, 3.2.2), the next step was to evaluate whether the cross-species ability of RV to subvert host innate immunity was due to the ability of NSP1 to target IRF-3.

The initial Y-2-H assays established that the NSP1 proteins encoded by RV infecting cattle and monkeys interacted with the monkey IRF-3 and/or the bovine IRF-3. To extend these observations, the ability of rhesus (RRV), bovine (UKtc) and porcine (G10P5, G10P5extra and A8) NSP1 proteins to interact with hIRF-3 and pIRF-3 (3.1.2) was investigated. Yeast were successfully co-transformed with a plasmid encoding hIRF-3 and either porcine (G10P5, G10P5extra and A8) bovine (UKtc), or rhesus (RRV) NSP1 (Figure 17, panel A). The co-expression of hIRF-3 with the porcine NSP1s G10P5 and G10P5 extra and the bovine UKtc NSP1 resulted in growth on QDO plates. The ability of the porcine A8 to self-activate the Y-2-H reporter compromised the possibility to assess whether a real interaction with hIRF-3 was taking place. Nevertheless, the data implies an interaction between porcine (G10P5) or bovine (UKtc) NSP1s with hIRF-3. The growth on QDO of yeast co-transfected with the hIRF-3 and G10P5extra agreed with previous results (3.2.2, Figure 16) showing that the extra amino acid sequence had no effect on the binding activity of NSP1. No interaction was observed between the rhesus NSP1 protein and hIRF-3, as judged by a lack of yeast growth on QDO.

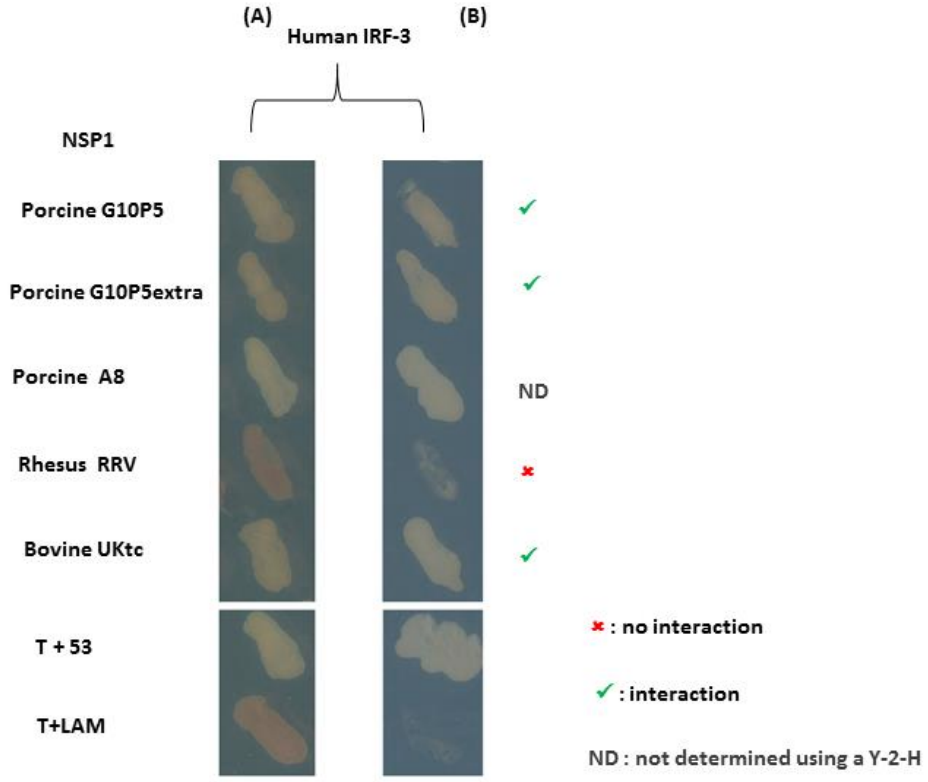

Figure 17. Y-2-H screening between porcine G10P5, G10P5extra, A8, rhesus RRV and bovine UKtc NSP1s and hIRF-3.

Aliquots of transformed yeast were plated on DDO (*-Leu,-Trp*) selective media. Once colonies had reached sufficient size (~5-7days), 5 colonies were re-streaked from the original DDO media onto fresh DDO media (*-Leu,-Trp*) (panel **A**) as well as QDO media (*-Leu, -Trp, -Ade, -His*) (panel **B**). The ability of yeast to grow on DDO selective media indicated that both the "bait" and the "prey" plasmids had been successfully co-transformed into a single yeast cell. The ability of yeast to grow on QDO plates indicated that the proteins encoded by the yeast-expression plasmids interacted. Each single colony is representative of 5 colonies. The vectors pGBKT7-53 plus pGADT7-T and pGBKT7-Lam plus pGADT7-T were used as positive and negative controls, respectively.

3.2.4 Y-2-H analysis between pIRF-3 and NSP1 proteins from porcine (G10P5, A8), bovine (UKtc) and rhesus (RRV) RV isolates.

Yeast were successfully co-transformed with a plasmid encoding pIRF-3 and either a porcine (G10P5, G10P5extra, or A8) bovine (UKtc), or rhesus (RRV) NSP1 (Figure 18, panel A). The co-expression of pIRF-3 with the porcine G10P5 or the bovine UKtc resulted in growth on QDO plates, indicating potential interactions. No interaction was observed between the rhesus NSP1 protein and hIRF-3, as judged by a lack of yeast growth on QDO. The ability of the porcine A8 to self-activate the Y-2-H reporter compromised the possibility to assess whether a real interaction with pIRF-3 was taking place.

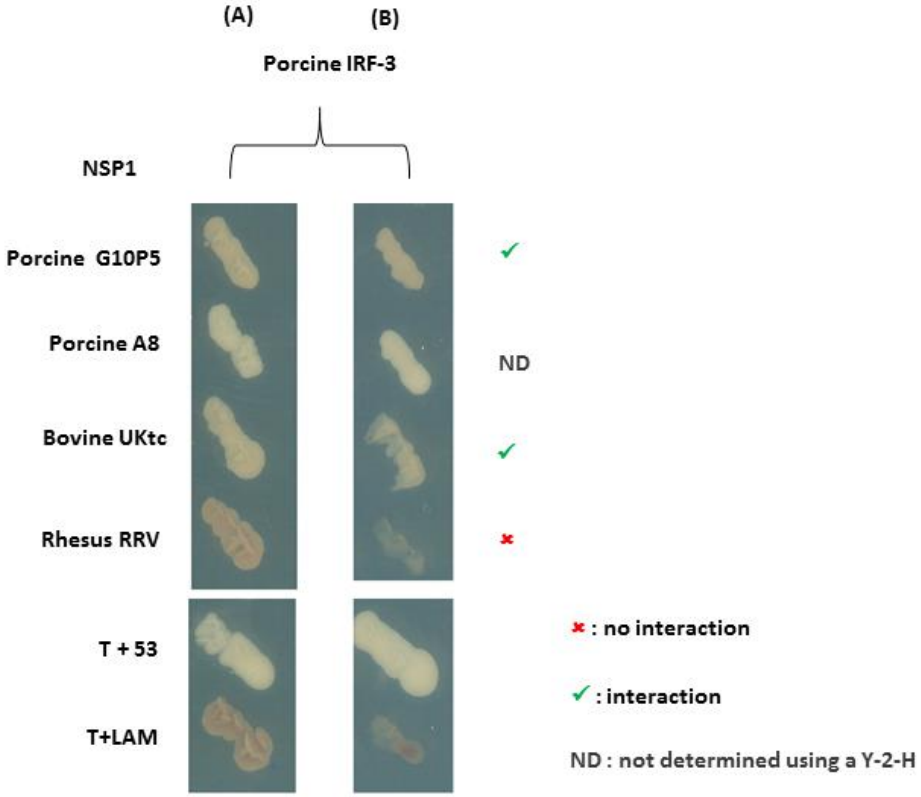

Figure 18. Y-2-H screening between porcine G10P5 and A8, rhesus RRV and bovine UKtc NSP1s and pIRF-3.

Aliquots of transformed yeast were plated on DDO (*-Leu,-Trp*) selective media. Once colonies had reached sufficient size (~5-7days), 5 colonies were re-streaked from the original DDO media onto fresh DDO media (*-Leu,-Trp*) (panel **A**) as well as QDO media (*-Leu, -Trp, -Ade, -His*) (panel **B**). The ability of yeast to grow on DDO selective media indicated that both the "bait" and the "prey" plasmids had been successfully co-transformed into a single yeast cell. The ability of yeast to grow on QDO plates indicated that the proteins encoded by the yeast-expression plasmids interacted. Each single colony is representative of 5 colonies. The vectors pGBKT7-53 plus pGADT7-T and pGBKT7-Lam plus pGADT7-T were used as positive and negative controls, respectively.

3.2.5 Y-2-H analysis between components of the IFN induction pathway and NSP1 proteins from human RV isolates: 18A, 1M0 and TC

Y-2-H analyses were performed to determine if the NSP1 proteins from three human RV isolates (1M0, 18A and TC) interacted with proteins involved in the interferon induction pathway. Previously generated “bait” plasmids encoding the human NSP1 (0) were screened against “prey” plasmids expressing components of the IFN induction pathway. The ability of yeast colonies to grow on DDO media confirmed the competent yeast cells had been successfully co-transformed with “bait” and “prey” (Figure 19, panel A). However, the inability of yeast colonies to grow on QDO plates indicated that no interactions occurred (Figure 19, panel B).

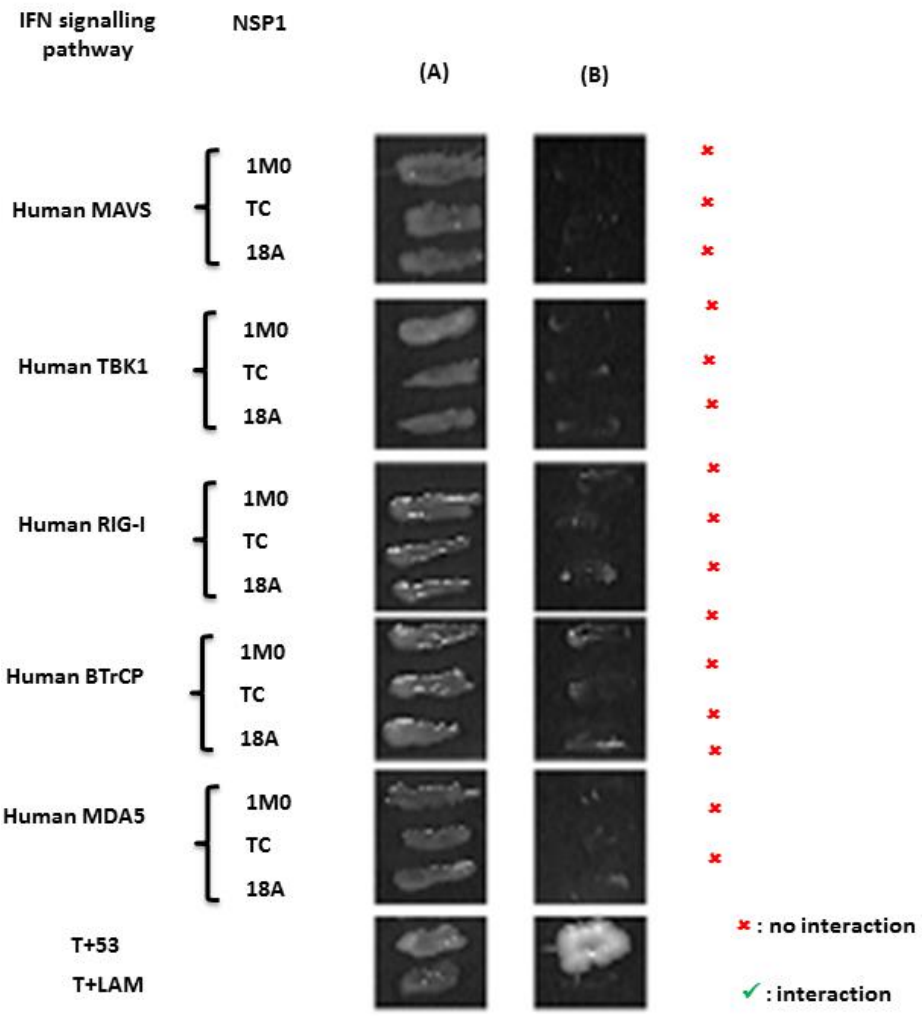

Figure 19. Y-2-H screening between human NSP1 (1M0, 18A and TC) and proteins of the IFN induction pathway, (bIRF-3, mIRF-3, hMAVS, hTBK1, hRIG-I, hBTrCP or hMDA5).

Aliquots of transformed yeast were plated on DDO (*-Leu,-Trp*) selective media. Once colonies had reached sufficient size (~5-7days), 5 colonies were re-streaked from the original DDO media onto fresh DDO media (*-Leu,-Trp*) (panel **A**) as well as QDO media (*-Leu, -Trp, -Ade, -His*) (panel **B**). The ability of yeast to grow on DDO selective media indicated that both the "bait" and the "prey" plasmids had been successfully co-transformed into a single yeast cell. The ability of yeast to grow on QDO plates indicated that the proteins encoded by the yeast-expression plasmids interacted. Each single colony is representative of 5 colonies. The vectors pGBKT7-53 plus pGADT7-T and pGBKT7-Lam plus pGADT7-T were used as positive and negative controls, respectively.

Further Y-2-H assays were performed to establish if the above mentioned panel of IRF-3 proteins (hIRF-3, pIRF-3, bIRF-3 and mIRF-3) could interact with the NSP1 proteins encoded by the three human RV isolates, 1M0, 18AA and TC. Competent cells were co-transformed with a “bait” plasmid expressing a single human NSP1 protein and a “prey” plasmid expressing either the human, porcine, bovine or monkey IRF-3. The ability of yeast colonies to grow on DDO media confirmed the competent yeast cells had been successfully co-transformed with “bait” and “prey” plasmids (Figure 20, panel A). However, the inability of yeast colonies to grow on QDP plates (Figure 20, panel B), suggested that no strong interactions were occurring between the human NSP1 and IRF-3s.

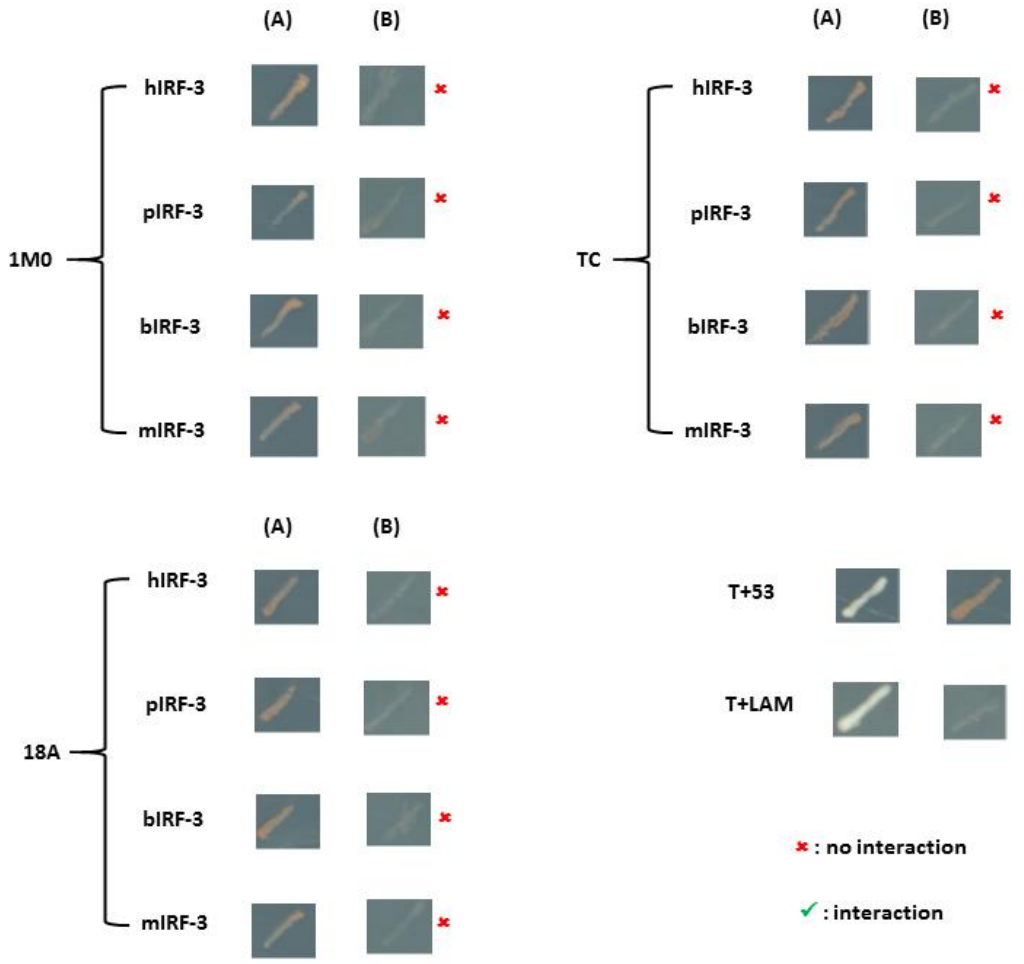

Figure 20. Y-2-H screening between human NSP1 (1M0, 18A or TC) and hIRF-3, pIRF-3, bIRF-3 and mIRF-3.

Aliquots of transformed yeast were plated on DDO (*-Leu,-Trp*) selective media. Once colonies had reached sufficient size (~5-7days), 5 colonies were re-streaked from the original DDO media onto fresh DDO media (*-Leu,-Trp*) (panel **A**) as well as QDO media (*-Leu, -Trp, -Ade, -His*) (panel **B**). The ability of yeast to grow on DDO selective media indicated that both the "bait" and the "prey" plasmids had been successfully co-transformed into a single yeast cell. The ability of yeast to grow on QDO plates indicated that the proteins encoded by the yeast-expression plasmids interacted. Each single colony is representative of 5 colonies. The vectors pGBKT7-53 plus pGADT7-T and pGBKT7-Lam plus pGADT7-T were used as positive and negative controls, respectively.

The Y-2-H screen indicated that no strong interactions were occurring between the NSP1 proteins from different human RV isolates and human, porcine, bovine or monkey IRF-3. In order to investigate whether these NSP1 transiently or weakly interact with IRF-3, the assays were repeated at a lower-stringency. As previously described, yeast were co-transformed with plasmids encoding one of the human NSP1 proteins and either the human, porcine, bovine or monkey IRF-3, and then plated on DDO media. Once colonies of sufficient size had grown (~5-7 days), yeast were re-streaked on lower-stringency media deficient for three instead of the possible four amino acids; triple drop out (TDO), *-Leu,-Try,-Ade* (-L,-W,-A) or TDO -*Leu,-Try,-His* (-L,-W,-H) (Figure 21).

The growth of yeast colonies on TDO plates co-expressing the human NSP1 1M0 or TC and the bIRF-3 (Figure 21 Panel A and B) suggested that a weak interaction did indeed occur. 1M0 also appeared to weakly interact with the hIRF-3 (Figure 21 Panel A) and the pIRF-3 proteins, while TC interacted weakly with the mIRF-3 (Figure 21 Panel B). The screening of the human 18A on plates with lower stringency did not result in growth of yeast colonies, suggesting that it does not interact with IRF-3 in the Y-2-H system.

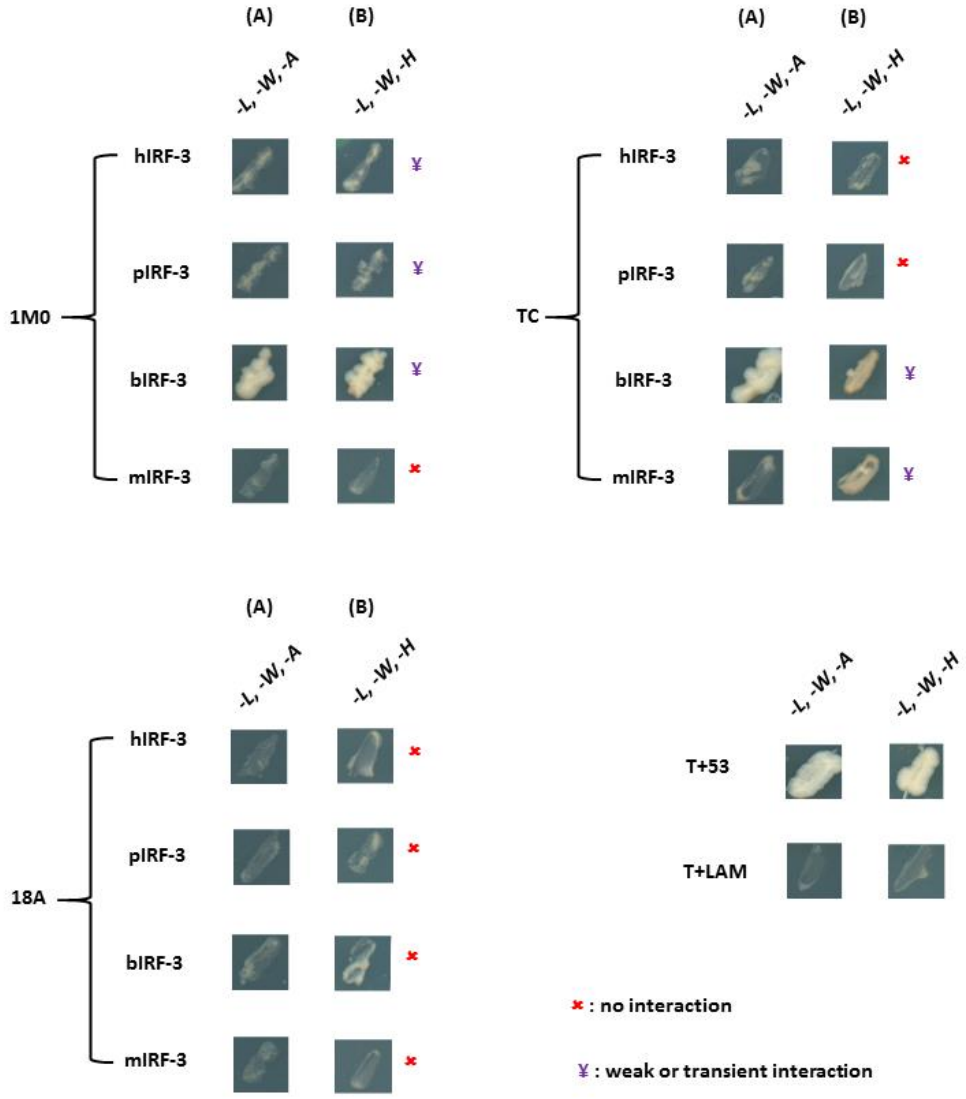

Figure 21. Y-2-H screening between human NSP1 (1M0, 18A or TC) and hIRF-3, pIRF-3, bIRF-3 and mIRF-3.

Aliquots of transformed yeast were plated on DDO (*-Leu,-Trp*) selective media. Once colonies had reached sufficient size (~5-7days), 5 colonies were re-streaked from the original DDO media onto fresh TDO media, **(A)** "-L, -W, A" (*-Leu,-Try, - Ade*), **(B)** -L, -W, -H (*-Leu, -Try, -His*). The ability of yeast colonies to grow on TFO media indicated a weaker and/or a transient interaction was occurring. Each single colony is representative of 5 colonies. The vectors pGBKT7-53 plus pGADT7-T and pGBKT7-Lam plus pGADT7-T were used as positive and negative controls, respectively.

3.3 Summary of Y-2-H interactions

Results obtained in this chapter have shown how NSP1 encoded by different RV is able to target IRF-3 in a strain-specific manner. Interactions with the IRF-3 encoded by different mammal species varied not only in terms of the relationship occurring between the host and the virus representing the scenario of a possible homologous or heterologous infection, but even in terms of the potency of the interactions. Y-2-H assay revealed that strong or weak interactions were occurring on species-specificity fashion.

Table 11 shows a summary of the interactions that occurred between the various NSP1 and IRF-3 proteins. The bovine-derived NSP1 (UKtc) showed a more promiscuous activity, being able to strongly interact with IRF-3 encoded by each of the mammalian species tested. By contrast, the rhesus RRV was not able to interact with any of the IRF-3 proteins in the Y-2-H system. The NSP1 G10P5, derived from RV infecting pigs, was able to bind to the homologous IRF-3 and the one encoded by monkeys. The G10P5extra, that carried the extra amino acid sequence at its N-terminus, showed no differences in binding affinity compared to the parental G10P5 NSP1. The other swine-derived NSP1, A8, self-activated the system, therefore an interaction with IRF-3 could not be assessed. Preliminary experiments involving the human-derived NSP1 reported no interactions with any IRF-3 occurred. However, lower stringency screening revealed that 1M0 weakly interacted with the human, bovine and porcine IRF-3, whereas TC NSP1 showed a weak interaction with only the monkey and bovine derived IRF-3 and 18A NSP1 did not interact with any of the IRF-3 proteins used in the screen.

Table 11.Summary of interactions occurring between NSP1 and IRF-3 using a Y-2-H assay.

"Preys"	Human IRF-3	Rhesus IRF-3	Bovine IRF-3	Porcine IRF-3	
"Baits"					Stringency levels
Human NSP1 1M0	x	x	x	x	QDO
	+	x	+	+	TDO
Human NSP1 TC	x	x	x	x	QDO
	x	+	+	x	TDO
Human NSP1 18A	x	x	x	x	QDO
	x	x	x	x	TDO
Porcine NSP1 G10P5	++	++	x	++	QDO
Porcine NSP1 G10P5extra	++	++	++	ND	QDO
Porcine NSP1 A8	ND	ND	ND	ND	QDO
Bovine NSP1 UKtc	++	++	++	++	QDO
Rhesus NSP1 RRV	x	x	x	x	QDO

Summary of interactions occurring between NSP1 proteins from virus infecting human, pigs, cattle and monkey and the IRF-3s encoded by the same species. Screening involving human NSP1 were further classified based on stringency levels: QDO (quadruple dropout) media (*-Leu, -Trp, -Ade, -His*) and TDO (triple dropout) media (*-Leu,-Try, - Ade* or *-Leu, -Try, -His*).

Result chapter 2

Analysis of NSP1 expression and stability

4 NSP1 shows strain-dependent expression level

Purpose

This chapter describes experiments performed in order to construct a panel of eukaryotic expression plasmids encoding the sequences for RV NSP1. A series of different experimental approaches confirmed an efficient expression of NSP1, however, a strain-specificity was observed. The employment of a series of tags together with the enhancement of transcription through Modified Vaccinia Ankara (MVA) infection allowed detection of NSP1, however contrasting results were obtained based on the strain origin. Overall data present in this chapter confirmed the ability to express a full length NSP1. This allowed the investigation of plasmid-encoded NSP1 on the downregulation of host innate immunity discussed in the following chapter.

Introduction

Following infection of target host cells, NSP1 is one of the less abundant non-structural proteins expressed by rotavirus (Johnson *et al.*, 1989; Mitzel *et al.*, 2003). Studies about the function and the role of the protein have been hampered by its poor expression level in infected cells: the protein is usually undetectable or barely detectable by metabolic labelling of rotavirus-infected cells, representing less than 0.1% of the total protein, with a half-life of 45 min (Johnson *et al.*, 1989; Mitzel *et al.*, 2003). The stability of NSP1 seems to be related to the presence of other rotavirus proteins and it appeared further reduced when expressed on its own due to an increase in susceptibility to proteasome-mediated degradation. By contrast, the simultaneous expression of either other viral proteins or viral mRNA appears to increase NSP1 stability (Brottier *et al.*, 1992; Hua *et al.*, 1994). Given the low expression of NSP1 and its short half-life, it was important to confirm its expression before investigating the downregulation of the host innate immunity.

4.1 Expression of NSP1 in mammalian cell lines

Preliminary experiments were performed in order to characterize the expression levels and stability of plasmid-encoded NSP1 by Western blot analysis. In order to do this, NSP1 constructs were first prepared by sub-cloning the respective NSP1 ORFs from plasmids used for the Y-2-H assays into mammalian expressing plasmids. The NSP1 sequences from human (18A, 1M0,TC), pig (G10P5, A8), bovine (UKtc) and rhesus (RRV) rotavirus isolates were amplified from the respective "bait" pGBKT7 plasmids with GoTaq® Long PCR Master Mix and "TA-cloned" into the mammalian expressing plasmid pcDNA3.1/V5-His-TOPO®.

Due to the lack of commercial antibodies against NSP1, and to optimize potential detection of an epitope tagged NSP1 two further approaches were used. A similar set of plasmids were constructed with either the HIS epitope tag or an HA epitope tag (YPYDVPDYA) inserted 5' to the NSP1 ORFs. PCR amplification was carried out using the pcDNA3.1/NSP1 plasmids generated above as templates (3.1) and primers that included the HIS-tag or the HA-tag sequences (Table 7). PCR products were then "TA-cloned" into pcDNA3.1/V5-His-TOPO®. Sequencing analysis confirmed the HIS-tag or the HA-tag were in frame with the respective ORF of each NSP1.

In preliminary experiments, HEK293 cells were transfected with plasmids encoding HIS-tagged or HA-tagged NSP1 proteins and at 16h post transfection whole cell lysates were prepared and analysed by Western blot. However, neither HIS- or HA-tagged NSP1 proteins could be detected with the respective antibodies.

In the following experiments, a number of strategies were employed in an attempt to enhance the expression levels of plasmid-encoded NSP1 proteins. First, the BSRT-7/5 cell line was used; this is a BHK-derived cell line that constitutively expresses the bacteriophage T7 RNA polymerase (Buchholz *et al.*, 1999), facilitating higher levels of protein expression from plasmids that contain the T7 promoter. Second, cells were infected with modified vaccinia virus Ankara (MVA-T7), an

attenuated vaccinia strain that also encodes the T7 polymerase (Sutter *et al.*, 1995). Third, the proteasome inhibitor MG132 (12h treatment at 25 μM) was used to reduce proteasome-mediated degradation of NSP1, which has been reported to be the main route of degradation for the viral protein (Pina-Vazquez *et al.*, 2007).

BSRT-7/5 cells were seeded in 6-well plates at a density of 3 x 10^5 cells/well and grown until 90% confluent. Prior to transfection, cells were first infected with MVA-T7, then 3h later transfected with a plasmid encoding the HIS-tagged NSP1 protein from either the porcine G10P5 or the bovine rotavirus UKtc isolate. Finally, the infected transfected cells were treated with MG132. At 16 h post MG132 treatment, whole cell lysates were prepared and analysed by Western blot for the expression of HIS-tagged NSP1 proteins using a monoclonal anti-mouse HIS antibody (Figure 1, Panel A and B, lanes 4). Experimental controls included non-transfected and transfected cells that received no other treatment (Figure 22, Panel A and B, lanes 3 and 7), or were also either infected with MVA-T7 (Figure 22, Panel A and B, lanes 1 and 5) or treated with MG132 (Figure 22, Panel A and B, lanes 2 and 6).

In the absence of MVA-T7 infection and/or MG132 treatment NSP1 protein could not be detected in the whole cell lysate samples prepared from transfected cells (Figure 22, Panels A and B, lanes 7). NSP1 levels were not detectable in samples prepared from transfected cells treated with MG132, suggesting proteasome inhibition does not influence NSP1 expression (Figure 22, Panels A and B, lanes 6). In contrast, infection of BSRT-7 cells with MVA-T7 resulted in the detection of HIS-tagged NSP1 proteins (Figure 22, Panels A and B, lanes 5). However, NSP1 was undetectable if cells were treated with MG132 following MVA-T7 infection (Figure 22, Panels A and B, lanes 4). Similar transfection and Western blot experiments were carried out using the other plasmids encoding HIS-tagged human (18A, 1M0, TC), porcine (A8) or rhesus (RRV) NSP1, however, even with MG132 treatment or MVA-T7 infection, these proteins could not be observed by Western blot analysis (data not shown).

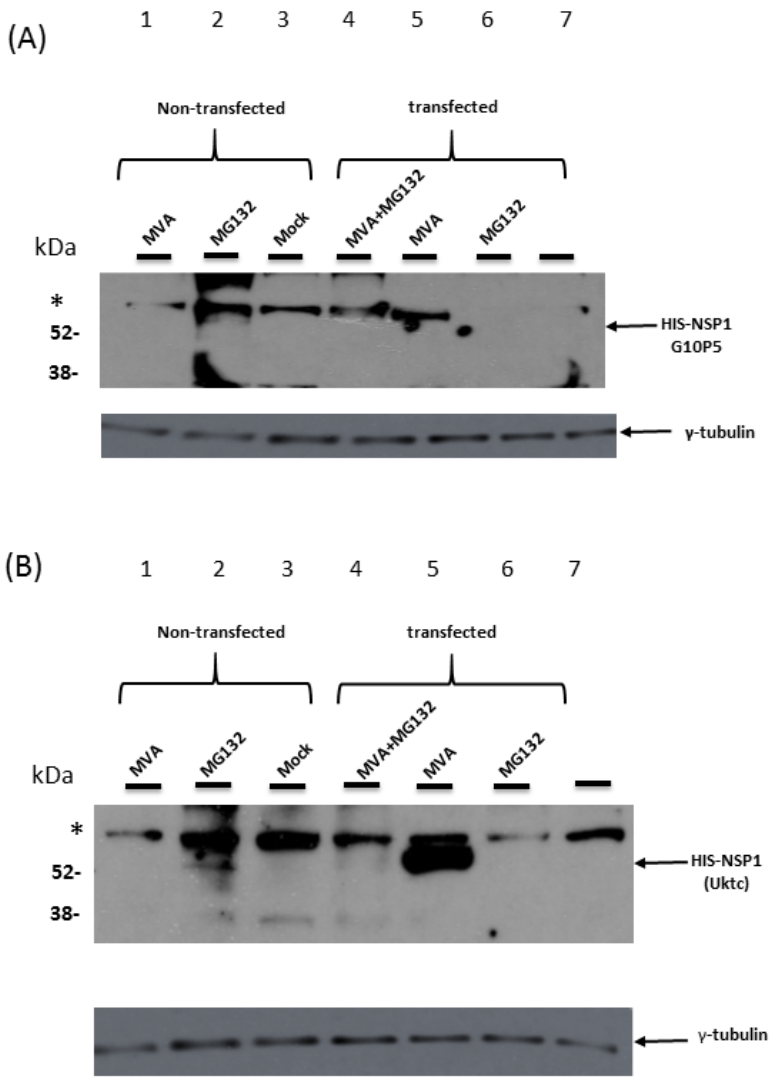

Figure 22. Western blot analysis of HIS- NSP1 expression in BSRT-7/5 cells.

To investigate plasmid-based expression of the HIS-tagged NSP1 protein from the (**A**) porcine G10P5 rotavirus isolate or (**B**) the bovine UKtc rotavirus isolate, BSRT-7/5 cells were subjected to different treatments in combination with transfection. Cells were infected with MVA-T7 prior to transfection and/or treated with MG132 as indicated. Whole cell lysates were prepared and analysed by Western Blot using an anti-HIS antibody. Blots were then re-probed for γ-tubulin as a loading control. The highest level of NSP1 expression was observed in transfected cells that had been infected with MVA-T7.

The predicted molecular weight of the HIS-tagged NSP1 protein is ~54 kDa. The asterisk indicates a non-specific protein that is cross-reactive with the anti-HIS antibody.

Due to the inability to detect HIS-tagged NSP1 in the absence of MVA-T7 infection and the high background observed when using the HIS antibody, the expression and detection of HA-tagged NSP1 proteins was next investigated. As before, BSRT-7/5 cells were first infected with MVA-T7, then 3h later transfected with a plasmid encoding the HA-tagged NSP1 protein from either the porcine G10P5 or the bovine UKtc rotavirus isolate. Finally, the infected transfected cells were treated with MG132. At 16 h post transfection, whole cell lysates were prepared and analysed by Western blot for the expression of HA-tagged NSP1 proteins using a mouse monoclonal anti- HA antibody. Experimental controls included non-transfected and transfected cells that received no other treatment (Figure 23, Panels A and B, lanes 3 and 8) or were also either infected with MVA-T7 (Figure 23, Panels A and B, lanes 1 and 6) or treated with MG132 (Figure 23, Panels A and B, lanes 2 and 7). An additional control consisted of non-transfected cells that were both infected with MVA-T7 and treated with MG132 (Figure 23, Panel A and B, lanes 4 and 5).

In contrast to the results obtained using the His-tagged NSP1 constructs (Figure 22), the stability of HA-tagged NSP1 increased when cells were treated with the proteasome inhibitor MG132 and the expression levels of the viral protein were further enhanced in presence of the T7 RNA polymerase encoded by MVA-T7.

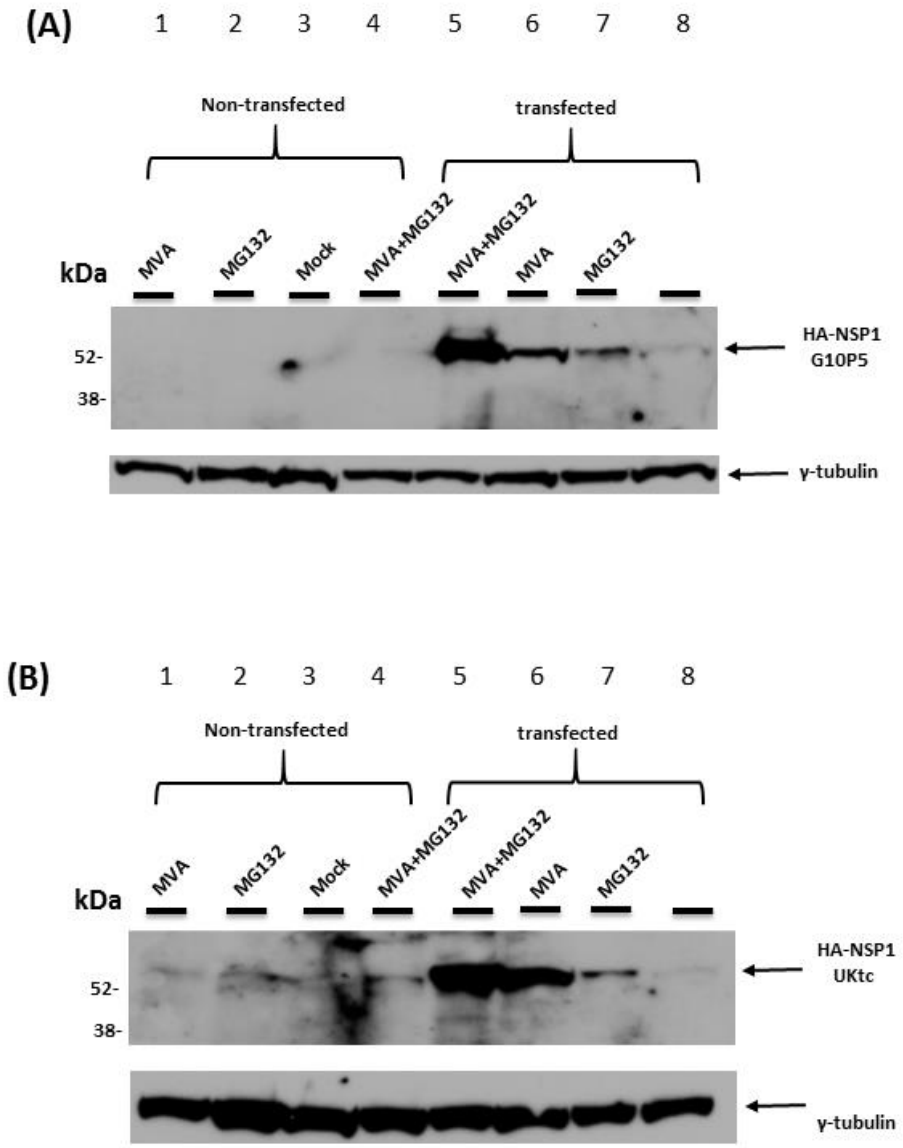

Figure 23. Western blot analysis of HA-NSP1 expression in BSRT-7/5 cell lines.

To investigate plasmid-based expression of the HA-tagged NSP1 protein from the (A) porcine G10P5 rotavirus isolate or (B) the bovine UKtc rotavirus isolate, BSRT-7/5 cells were subjected to different treatments in combination with transfection. Cells were infected with MVA-T7 and/or treated with MG132 as indicated. Whole cell lysates were prepared and analysed by Western Blot using an anti-HA antibody. Blots were then re-probed for γ-tubulin as a loading control. The highest level of NSP1 expression was observed in transfected cells that had been infected with MVA-T7 and treated with the proteasome inhibitor MG132.

The predicted molecular weight of the HA-tagged NSP1 proteins is ~54 kDa.

Additional transfections were carried out to investigate the respective expression levels of the HA-tagged NSP1 proteins from rhesus (RRV), porcine (A8) and human (1MO and 18A) rotavirus isolates (Figure 24). A high level of expression of the HA-tagged Rhesus (RRV) NSP1 protein was observed even when cells were not infected with MVA-T7 or treated with MG132 (Figure 24, Lane 1). Interestingly, both MVA-T7 infection and MG132 treatment led to a comparative reduction in NSP1 protein levels (Figure 24, Lanes 6 and 7). The observed decrease in RRV protein levels in presence of MVA infection could be explained with the downregulation of gene expression by the Vaccinia Virus D10 Protein (Shors *et al.*, 1999). This effect was only observed for the RRV strain, which has a comparatively divergent amino acid sequence to all the other NSP1 used in this study (data not shown). Following MVA-T7 infection and MG132 treatment, expression of the HA-tagged porcine (A8) NSP1 protein was observed by Western blot analysis (Figure 24, Lane 4). However, the expression of NSP1 proteins from human rotavirus isolates (18A, 1M0 and TC) was not detectable by Western blot, even after combined MVA-T7 infection and MG132 treatment (Figure 24, Lanes 2 and 3; TC data not shown).

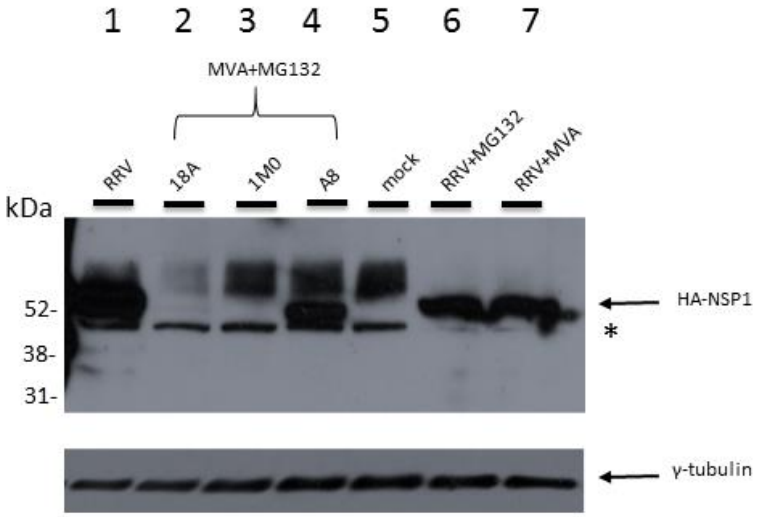

Figure 24. Western blot analysis of HA-NSP1 expression in BSRT-7/5 cell lines.

To investigate plasmid-based expression of the HA-tagged NSP1 protein from the rhesus RRV (1, 6 and 7), the porcine A8 (4), or the human 18A (2) and 1M0 (3) rotavirus isolates, BSRT-7/5 cells were subjected to different treatments in combination with transfection. Cells were infected with MVA-T7 and/or treated with MG132 as indicated. Whole cell lysates were prepared and analysed by Western Blot using an anti-HA antibody. Blots were then re-probed for γ-tubulin as a loading control.

The predicted molecular weight of the HA-tagged NSP1 proteins is ~54 kDa. The asterisk indicates a non-specific protein that is cross-reactive with the anti-HA antibody.

In the above described experiments, an increase in the expression level of some NSP1 proteins was observed following inhibition of proteasome-mediated degradation by MG132 treatment. To determine if the lack of expression exhibited by the remaining NSP1 proteins was due to their ubiquitin-dependent proteasome-mediated degradation, similar transfection experiments were performed using the TS20 cell line. TS20 is a Balb3T3-derived cell line in which ubiquitination is inhibited by restrictive temperature (Chowdary *et al.*, 1994).

TS20 cells were plated at a density of 0.3 x 10^6 cells/well in 6-well plates and transfected with plasmid DNA encoding HA-tagged NSP1 derived from human (18A, 1M0, TC), porcine (G10P5, A8), bovine (UKtc) or rhesus (RRV) rotavirus isolates. 16 h post-transfection, cells were left untreated or treated with proteasome inhibitor (MG132, 25 μM) and incubated overnight at permissive (34°C) or non-permissive (39°C) temperature. Whole cell lysates were then prepared and analysed by Western blot for the HA epitope tag as an indication of NSP1 expression (Figure 25).

The expression levels of plasmid-encoded NSP1 proteins in the TS20 cell line appeared to be higher compared to those reported in BSRT-7/5 (Figure 22, Figure 23 and Figure 24). However, although bands corresponding to the predicted molecular weight (54 kDa) of the HA-tagged NSP1 proteins were observed, other bands of slightly smaller size were also present. These bands did not appear to be unspecific, as they were absent in lanes corresponding to the mock-transfected cells. In all cases, the growth of the transfected TS20 cells at the non-permissive temperature of 39°C led to a reduction in the expression levels of the putative NSP1 protein bands.

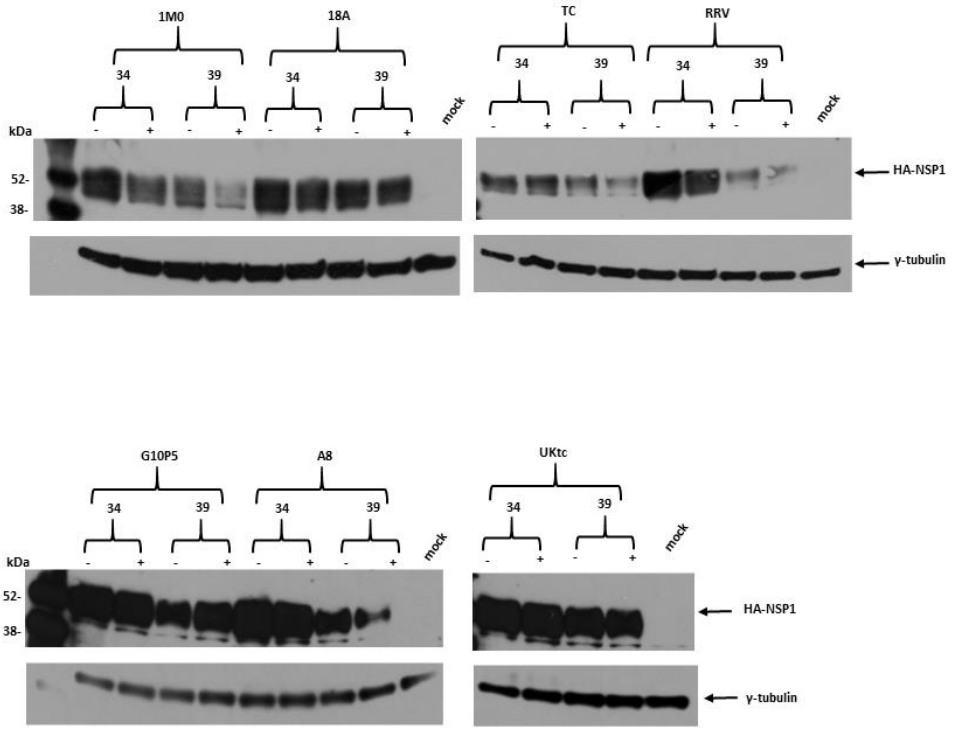

Figure 25. Western blot analysis of HA-NSP1 expression in TS20 cell lines at permissive and non-permissive temperatures.

TS20 cells were transfected with plasmids encoding HA-tagged NSP1 proteins from human (1M0, 18A or TC), porcine (G10P5 or A8), bovine (UKtc) or rhesus (RRV) rotavirus isolates. 16h post transfection, cells were left untreated or treated with the proteasome inhibitor MG132, (25 µM) and incubated for a further 16h at 34°C (permissive temperature) or 39°C (non-permissive temperature). Whole cell lysates were prepared and analysed by Western blot analysis using an anti-HA antibody. Blots were then re-probed for γ-tubulin as a loading control.

The predicted molecular weight of the HA-tagged NSP1 proteins is ~54 kDa. "+/-" indicates treatment with 25 µM MG132. "34 and 39" indicates 34°C or 39°C.

4.2 Expression of NSP1 in cell-free system

In order to determine if full length HA-tagged NSP1 proteins from human rotavirus isolates (1M0, 18A and TC) could be expressed by the corresponding plasmids, the TnT® quick system from Promega was used. This kit provides the necessary components for T7 promoter-mediated transcription and subsequent translation of ^{35}S-radiolabelled proteins. Figure 26 shows an autoradiograph of the TnT® results in which bands corresponding to the expected molecular weight (~54kDa) were observed for each NSP1 protein. The employment of a TnT® system confirmed the ability to express full length NSP1 proteins derived from RV infecting humans.

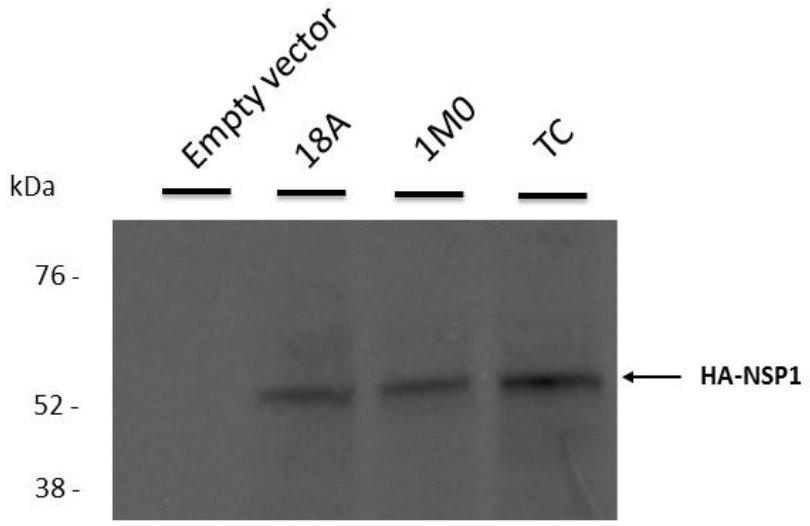

Figure 26. In vitro transcription/translation assay of human NSP1 18A, 1M0 and TC.
The use of a TnT® system confirmed the expression of a full length NSP1 derived from RV infecting humans.

4.3 NSP1 shows expression levels based on the strain of origin

Results obtained in this chapter suggest that RV NSP1 proteins are expressed from plasmids in a strain-specific manner. The level of protein expression varied not only between NSP1 isolates from different species (human, pigs, cattle and rhesus) but also between isolates infecting the same species.

NSP1 is the least abundant RV non-structural protein and experiments involving the bovine strain UKtc have reported that it has an estimated half-life of 45 min in infected cells (Mitzel *et al.*, 2003). In BSC-1 cells infected with RRV strain, NSP1 was not detected after 9 hpi and at 12 hpi the protein represented less than 0.1% of total protein synthesis (Johnson *et al.*, 1989). Moreover, it has been shown that NSP1 is much more susceptible to proteasome-mediate degradation if the viral protein is expressed on its own, without viral proteins or RNAs (Pina-Vazquez *et al.*, 2007). Based on these reports, a number of strategies were employed in this in this study to enhance the expression levels and the stability of plasmid-encoded NSP1 proteins.

Studies involving the bovine UKtc, porcine OSU and the rhesus RRV have used a specific polyclonal rabbit antiserum termed C19. The serum was raised against the oligopeptide NH2-CGTLTEEFELLISNSEDDNE-COOH, which includes the last 19 amino acids of the simian SA 11 NSP1 (previously referred to as the NS53 protein due to its molecular weight) (Hua *et al.*, 1994). The C19 antibody has been used for a series of experiments to characterize NSP1 (Bagchi *et al.*, 2010; Barro *et al.*, 2007; Ding *et al.*, 2016; Kearney *et al.*, 2004; Nandi *et al.*, 2014; J. Patton *et al.*, 2009; J. T. Patton, 1995) and the employment of specific antibody raised against conserved regions at either amino or carboxyl regions of NSP1 has been extensively used (Bagchi, Bhowmick*, et al.*, 2013; Bagchi, Nandi*, et al.*, 2013; Bhowmick *et al.*, 2013; Graff *et al.*, 2009; Kanai *et al.*, 2017).

The lack of an antibody for the detection of RV NSP1 required the addition of a series of an N-terminal epitope tag. Relatively short epitope tags such as FLAG, hemagglutinin (HA), histidine (His) and c-Myc, are used for the detection of fusion

proteins *in vitro*. Their short, linear recognition motifs rarely affect the properties of the heterologous protein of interest and are usually very specific for their respective primary antibodies. In some cases, the tags may not only ease protein purification but also help in protein expression, folding, and/or solubility (Structural Genomics *et al.*, 2008).

Indeed tagged NSP1 derived from each of the rotavirus strains was detected, however, contrasting results in their expression levels were obtained. In BSRT7/5 cell lines, His-tagged and HA-tagged NSP1 encoded by RV isolates that infect animals appeared to have higher levels of expression compared to isolates that infect humans. Compared to the other strains, the rhesus-derived (RRV) NSP1 showed a higher level of expression, being detected even in the absence of transcription enhancer (MVA infection) or proteasome inhibitor treatment (MG132) (Figure 24, lane 3). Low levels of porcine-derived G10P5 and the bovine-derived (UKtc) NSP1 were detected in untreated cells, however, administration of MG132 or MVA infection resulted in increased levels of NSP1 proteins. Synergic effects on the level of HA-tagged NSP1 expression were observed when MG132 treatment followed MVA infection (Figure 23, Panels A and B, lanes 5, 6 and 7). Treatment of cells with MG132 appeared to increase the stability of the porcine HA-tagged NSP1 A8 (Figure 24, lane 4). The attempts to detect the HA-tagged NSP1 from human rotavirus isolates (1M0, 18A and TC) in transfected BSRT-7/5 were not successful (Figure 24, lanes 2 and 3). The simultaneous inability to detect the human-derived NSP1 suggested a common molecular mechanism related to low expression levels and/or stability of the human-derived strains in the cell lines used; full-length plasmid-encoded proteins could only be detected using an *in-vitro* system (Figure 26).

The His tag does not offer increased expression or solubility levels, due to its relatively small size (~2.5 kDa) in comparison to NSP1 (54kDa) and it was hoped that N-terminal fusion would not interfere with the function and structure of the NSP1 proteins. His_6 tag may be attached to the target protein internally, or at either the N- or C-terminus, and it has been believed to date that most proteins are functional with the tag attached (Uhlen *et al.*, 1992). However, there is an increase in reports

indicating this assumption may be wrong (Ledent *et al.*, 1997; Majorek *et al.*, 2014; Sabaty *et al.*, 2013). The variation of the length and the position of the tag appear to affect the expression and production of protein (A. K. Mohanty *et al.*, 2004). His tags may affect the oligomeric states of proteins as well as their function (Araujo *et al.*, 2000; Majorek *et al.*, 2014; Panek *et al.*, 2013). Significant reductions in the enzymatic activity of several different enzymes were observed upon the incorporation of a His-tag (Araujo *et al.*, 2000; Majorek *et al.*, 2014; Panek *et al.*, 2013). Booth and colleagues (Booth *et al.*, 2018) reported the impact of an N-terminal polyhistidine tag on protein stability; they analysed the stability and the expression of various recombinant proteins when tagged or untagged at different pH and salt concentrations. In most cases (65%) the presence of the His tag decreased the thermal stability of the protein. When the His-tag epitope was inserted at the C-terminus of PhoP of *Salmonella enterica*, the biochemical proprieties of the protein were affected, mostly likely as result of conformation changes (Perron-Savard *et al.*, 2005). Previous work carried out in the Molecular Virology group on the N^{pro} protein of Classical Swine Fever Virus (CSFV) has shown that the His tag is not accessible to anti-His antibodies and that this is probably caused by folding of the epitope at the N-terminus (unpublished data). To exclude the possibility that the His tag was affecting expression or detection of NSP1, it was substituted for a HA-tag.

Contrasting results were obtained when NSP1 was fused at its N-terminus with the HA-tag from the influenza virus A, which has been extensively used in various experimental contexts of cell biology and biochemistry to track proteins of interest within cells, to isolate them and to co-precipitate binding partners (Lapaque *et al.*, 2009; Strunk *et al.*, 2011; Zhang *et al.*, 2002). The condition of cell-lines has been reported to influence the ability to detect HA-tagged proteins. Schembri and colleagues showed that HA-tagged protein levels were drastically reduced in cells which were undergoing apoptosis (Schembri *et al.*, 2007). This was due to the Caspase-3 and/or Caspase-7 mediated cleavage of the epitope tags from their fused proteins. The presence of a N-terminal HA-tag may have influenced the solubility and the stability of NSP1, however, the luciferase assay results (5.2) suggest the NSP1

proteins were functional and numerous studies have used tagged NSP1 proteins for functional assays.

Other epitopes, such as the Myc (EQKLISEEDL) or FLAG (DYKDDDDK) tags could have been used to detect NSP1. The Myc tag has been used to study the expression levels of bovine and swine NSP1 (Graff *et al.*, 2007) and the FLAG tag has been adopted to characterise the functionality of NSP1 isolates from RV infecting human, pigs and monkeys (Di Fiore *et al.*, 2015; Holloway *et al.*, 2009; B. Zhao *et al.*, 2016). Recently, a Halo-Tag has been used to identify proteins interaction occurring between NSP1 and host proteins involved in the ubiquitin-proteasome pathway (Lutz *et al.*, 2016). Other work employed a GFP-tag fused to NSP1 to increase the stability of porcine (OSU) and simian (SA11) NSP1, facilitating the analysis of the levels and localization of the viral protein (Qin *et al.*, 2011). GFP-tag has been used also to study by fluorescence microscopy the stability of NSP1 in COS7 murine-derived cell lines. Since expression of the HA-tagged NSP1 proteins had been confirmed and HA-tagged NSP1 proteins have been used in other functional studies of NSP1, the use of other epitope or fluorescent tags was not investigated further (Ding et al., 2016).

Cell-free protein synthesis (CFPS) allows generation of functional proteins independent of cell culture. CFPS systems derived from crude cell extracts have been used for decades as a research tool in fundamental and applied biology, having been used in 1961 to decipher the mechanism behind the genetic code (Nirenberg *et al.*, 1961). More recently, CFPS has shown remarkable utility as a protein synthesis technology (Katzen *et al.*, 2005; Swartz, 2006) including the production of pharmaceutical proteins (Goerke *et al.*, 2008; Swartz, 2006) and high-throughput production of protein libraries for protein evolution and structural genomics (Madin *et al.*, 2000; Takai *et al.*, 2010). This method is especially attractive for proteins that are difficult to synthesize in traditional cell culture due to problems associated with cellular toxicity, low expression or aggregation (Katzen *et al.*, 2005; Katzen *et al.*, 2009). To produce proteins of interest, CFPS systems harness an ensemble of catalytic components necessary for energy generation and protein synthesis from crude lysates of microbial, plant, or animal cells. Crude lysates contain the necessary

elements for transcription, translation, protein folding and energy metabolism (e.g., ribosomes, aminoacyl-tRNA synthetases, translation initiation and elongation factors, ribosome release factors, nucleotide recycling enzymes, metabolic enzymes, chaperones, foldases, etc). Activated catalysts within the cell lysate act as a chemical factory to synthesize and fold desired protein products upon incubation with essential substrates, which include amino acids, nucleotides, DNA or mRNA template encoding the target protein, energy substrates, cofactors, and salts. After initiation of cell-free protein synthesis, production typically continues until one of the substrates (e.g., ATP, cysteine, etc.) is depleted or by product accumulation (e.g., inorganic phosphate) reaches an inhibitory concentration (Lewin, 1975).

Rabbit reticulocyte lysates (RRL) has been a useful CFPS tool for the enhancement of viral transcription of bovine-isolated RV proteins (Vende *et al.*, 2000) or virion assembly of simian RV (Clapp *et al.*, 1991). Due to its low expression, a TandT® system has been employed in previous studies to dissect the expression and stability of NSP1 derived from RV infecting monkeys (SA11), birds (Ch2) and mice (EDIM) (Pina-Vazquez *et al.*, 2007). Studying involving comparative analysis between NSP1 derived from different strains employed cell lines stably expressing the viral protein. Transfection of HEK293 with plasmids encoding NSP1 derived from RV strains RRV (simian), EDT (murine) or Wa (human) resulted in higher level of expression (Ding *et al.*, 2016).

Transcriptional control is mediated by transcription factors, RNA polymerase and a series of *cis*-acting elements located in the DNA, such as promoters, enhancers, silencers and locus-control elements, organized in a modular structure and regulates the production of pre-mRNA molecules, which undergo several steps of processing before they become functional mRNAs. UTRs are known to play crucial roles in the post-transcriptional regulation of gene expression, including modulation of the transport of mRNAs out of the nucleus and of translation efficiency (van der Velden *et al.*, 1999) , subcellular localization (Jansen, 2001) and stability (Bashirullah *et al.*, 2001). Regulation by UTRs is mediated in several ways and nucleotide patterns or motifs located in 5'-UTRs and 3'-UTRs can interact with specific RNA-binding proteins.

The open reading frame of each segment of RV genome is flanked by 5’ and 3’ untranslated regions (UTRs) that are variable in length. Although UTRs are not completely conserved among the different genome segments (and often differ in their length), terminal consensus sequences are common to all eleven genome segments; these consist of the 5’-terminal consensus 5’-GGC(A/U)7−3’ and the 3’-terminal consensus 5’-U(G/U)3(A/G)CC-3’. Work by Patton *et al* has shown how an insertion of an extra A in the 3’-UTR region of NSP1 sub-optimally affected its *in vitro* gene replication and expression (J. T. Patton *et al.*, 2001). The insertion of the extra A had a negative impact on the replication of gene 5 (which encodes NSP1), causing a significant decrease in the expression of the ORF of the chimeric RNA. However, the insertion appeared to have no effects on the biology of the viruses, since RV carrying the mutation replicated at higher titer compared to wt viruses. This suggested that in cell culture NSP1 contributed to viral replication cycle and that the UTRs are not required for genome packing. A work by Kearney *et al* has shown how the sequence 5’-TGACC-3’ in the 3’-UTR is specifically recognised by NSP3. One of the roles of NSP3 is to facilitate the transcription of viral (Deo *et al.*, 2002; Poncet *et al.*, 1993; Poncet *et al.*, 1994), thus mutation in the 3’-UTR region of NSP1 resulted in decreased binding affinity with NSP3 and subsequent lower efficiency in NSP1 transcription (Kearney *et al.*, 2004). Sequences analyses of the 3’-UTR regions of NSP1 considered in this study revealed the presence of the conserved domain 5’-TGACC-3’, with the exception of the porcine strain A8, which sequences of the 3’-UTR appeared incomplete (Figure 27). The absence of the motif from plasmid-encoded NSP1 may have resulted in lower expression of the viral protein.

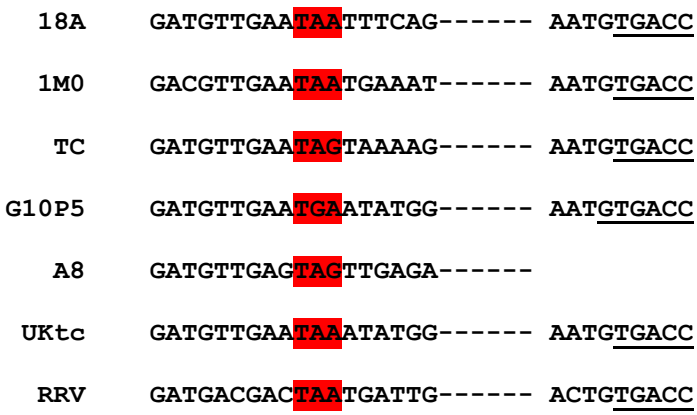

Figure 27. Alignment of the 3'-UTR region of NSP1 reveals the presence of the conserved domain5'-TGACC-3'.

Sequences analysis of the alignment of the 3'-UTR regions of the NSP1 revealed the presence of the conserved motif 5'-TGACC-3', here underlined. The stop codon is deciphered in red. The distance between the stop codons and the motif are representative and do not reflect real distances, which vary between strains.

A variety of expression systems have been developed to overproduce proteins in mammalian cells. Viral vectors are particularly powerful tools because they have inbuilt mechanisms to subvert the cellular machinery in their favour. Modified vaccinia virus Ankara-T7 polymerase (MVA-T7) is an attenuated vaccinia virus strain encoding the bacteriophage T7 polymerase gene. Vaccinia virus (VACV), the prototype of the Poxviridae family, has been widely used as an expression vector (Mackett *et al.*, 1992). In numerous strategies for expression of foreign genes using VACV, the gene of interest has been positioned downstream of VACV early or late promoters. However, the highest expression levels have been achieved when the gene encoding the RNA polymerase from the bacteriophage T7 was integrated into the VACV genome (MVA-T7) and the foreign gene of interest was under the control of a bacteriophage T7 promoter (Sutter *et al.*, 1995).

The cloning strategy in this study used pcDNA3.1-V5-HIS-TOPO®, a mammalian expressing vector containing a T7 promoter upstream of its MCS. Thus infection with MVA-T7 promoted higher levels of expression of NSP1. When MVA-T7

infection was used to increase expression of HIS-tagged NSP1, the viral protein was detected only in vaccinia-infected cells.

The MG132 treatment following infection resulted in the inability to detect protein levels. These results may have been due to the fact that MG132 treatment has been reported to block the expression of viral intermediate and late genes (Satheshkumar *et al.*, 2009). However, an increase in HA-tagged NSP1 (UKtc and G10P5 isolates) expression was observed when transfected cells were first infected with MVA-T7 and then treated with MG132. Although the constructs used in this study did not contain the 5'-UTR of NSP1, it has been shown that T7 polymerase-driven expression of RV cDNAs can be strongly inhibited due to the presence of an inhibitory motif (IM) within the long 5'-UTR regions of 8 genome segments. IM was mapped to the 5' terminal 6-nucleotide long pyrimidine-rich tract 5'-GGY(U/A)UY-3'(De Lorenzo *et al.*, 2016).

MG132 has been used to increase the level of GFP-tagged NSP1 in HT29 (Sen *et al.*, 2014) and has been employed to study proteasome-mediated degradation of NSP1 derived from bovine (B641) and porcine (OSU) RV strains. The use of the proteasome inhibitor resulted in a 2.5 fold increase in NSP1 compared to untreated cells. However, the expression of OSU NSP1 in untreated HEK293 was higher than B641 NSP1, even when expressed from the same construct (Graff *et al.*, 2007), indicating a strain-dependent level of expression. Moreover, MG132 appeared to increase the level of GFP-tagged NSP1 in HT29 (Sen *et al.*, 2014). Transient transfection with GFP-tagged NSP1 derived from RRV or EW (murine) resulted in poor expression levels compared to GFP-tagged UKtc. Treatment with MG132 resulted in higher expression levels of both GFP-tagged RRV and EW. In contrast, GFP-UKtc was stable and expressed to similar levels in the presence or absence of MG132 (Sen *et al.*, 2009). Thus, in contrast to the unstable nature of RRV and EW NSP1s, UK NSP1 does not appear to be susceptible to proteasome-mediated degradation in COS7 cells although it can efficiently degrade IRF-3 in these cells. Degradation of IRF-3 by GFP-tagged NSP1 has also been reported (Sen *et al.*, 2014).

The 26S proteasome catalyses the great majority (at least 80%) of the protein degradation in growing mammalian cells, including both the rapid degradation of misfolded and regulatory proteins and most of the slower breakdown of the bulk of cellular proteins (J. Zhao *et al.*, 2015). Since the discoveries of the critical role of ubiquitin (Ub) in protein turnover (Hershko *et al.*, 1980) and of the 26S complex in digesting ubiquitin conjugates (Hough *et al.*, 1987), it has been generally assumed that rates of proteolysis by this pathway are regulated solely through protein ubiquitination. However, it is now clear that ubiquitination and even the association of an ubiquitylated protein with the proteasome do not necessarily lead to its degradation (Crosas *et al.*, 2006). Thus, the proteasome is not simply a machine for efficient, automatic destruction of ubiquitin conjugates and ubiquitin recycling, but its properties also determine whether an ubiquitylated protein undergoes degradation or survives intact. In addition, the proteasome's degradative capacity and selectivity are not fixed, but are precisely regulated by multiple post-synthetic mechanisms.

The TS20 cell lines harbour a thermo-sensitive E1 ubiquitin activating enzyme. Since ubiquitin conjugating enzymes E2 (UBE2) are incapable of using ubiquitin without an E1 enzyme, the TS20 cells are unable to support ubiquitin conjugation at the non-permissive temperature, resulting in an accumulation of proteins usually targeted for ubiquitin-dependent degradation through the proteasome. Western blot analyses of whole cell lysates prepared from transfected TS20 cell lines treated with MG132 suggested a marginal role for ubiquitin-driven proteasome-mediated degradation of NSP1 (Figure 25). These results are consistent with previously published data where the MG132 treatment has no significant impact on NSP1 protein levels (Bhowmick *et al.*, 2013). The Western blot analyses also revealed the presence of a ladder of proteins with molecular weights ($\geq$40kDa and <54kDa) smaller than that predicted for the tagged NSP1 proteins (54kDa). These could be degradation intermediates, but they did not increase following MG132 treatment. Furthermore, they are unlikely to be caused by the presence of internal start codons,

as the N-terminal HA-tag was detected and the predicted molecular weights for proteins generated from alternative start codons do not correlate.

When BSC-1 cell lines were infected with vaccinia virus expressing rhesus RRV NSP1 (vNSP1), the protein was highly susceptible to proteasome-mediated degradation, since a 4-fold increase in the expression of NSP1 was observed after treatment with the proteasome inhibitor clasto-lactacystine-βlactone (CLL) and a 2.5-fold increase following MG132 treatment (Pina-Vazquez *et al.*, 2007). The susceptibility to proteasome degradation and half-life of NSP1 in cells expressing vNSP1 was affected by the simultaneous co-transfection with total RRV mRNAs. In the presence of total RRV mRNAs NSP1 was stabilised and became less susceptible to proteasome degradation, since identical amounts of NSP1 were obtained regardless of treatment with the proteasome inhibitor MG132. Moreover, the same work showed that the half-life of NSP1 was 90 min, and the protein showed an increased stability compared to previous results. These data are in contrast with the reported stability of NSP1, as determined by pulse-chain analysis of RV-infected cells (Johnson *et al.*, 1989; Mitzel *et al.*, 2003; Pedley *et al.*, 1984).

Specifically, Mitzel *et al* investigated the mechanism of regulation of RV gene expression of two differentially expressed viral mRNA: NSP1 and VP6. These two genes were chosen as models for analysis of rotavirus gene regulation because: (1) both are expressed early in infection; (2) VP6 is expressed at higher levels than NSP1, approximately 25-fold molar excess; and (3) the mRNAs and ORFs are similar in size, thus minimizing potential variations in expression due to mRNA length. They concluded that the difference in amount of NSP1 was due to poor translation efficiency of the mRNA compared to VP6. Due to contrasting results observed in the stability and half-life were observed for NSP1, which appeared for VP6, indicate that pulse-chase analysis cannot be used alone to determine the intracellular stability of NSP1.

Differences in the stability of NSP1 and its susceptibility to proteasome-mediated degradation have been reported by Sen *et al* (Sen *et al.*, 2009). When COS7

cell lines were transfected with GFP-tagged NSP1 from simian (RRV), bovine (UKtc) or murine (EW) RV and treated with PYR-41, an E1 ligase inhibitor that blocks the activation and subsequent transfer of polyubiquitin to the substrates (Yang *et al.*, 2007), an in increased levels of the murine and rhesus NSP1 were observed, but not for the bovine.

COPII coated vesicles are responsible for sorting and trafficking cargo out of the ER and into the Golgi apparatus (Campbell *et al.*, 1997). Multiple host and pathogen proteins contain the orthodox COPII sorting motif, composed of a transmembrane (TM) domain, a tyrosine residue and a spaced diacidic signal. Two such motifs were reported to present in Wa-NSP1, one within the N-terminal RING-finger domain and the other at the very C-terminus (Ding *et al.*, 2016). In their work they showed how the human isolate Wa was localised to the Golgi, however, the role of the COPII sequence was not proven. A further examination of NSP1 sequences revealed evolutionary conservation of these motifs. The Golgi is home to a multitude of glycosyltransferases (GTs), glycosidases, and nucleotide sugar transporters that function together to complete the synthesis of glycans from founding sugars covalently attached to protein or lipid in the endoplasmic reticulum (ER). Thus, glycoproteins, glycosphingolipids (GSLs), proteoglycans and glycophosphatidylinositol (GPI) anchors acquire their final sugar complement during passage through the Golgi (Stanley, 2011). Bioinformatics analyses have revealed the presence of putative glycosylation sites within NSP1 sequences (data not shown). However, no additional bands with molecular weights higher than that predicted for the tagged NSP1 proteins were observed.

Result chapter 3

NSP1-mediated downregulation on IFN response

5 NSP1 shows a strain-dependent ability to differentially target components of IFN induction and signalling pathways

Purpose

This chapter describes experiments performed in order to characterize the ability of RV NSP1 to modulate IFN expression. Strain-specificity of plasmid-encoded NSP1 to downregulate type I and type III IFN was observed due to the ability of the viral protein to differentially target host proteins within the IFN and NF-κB pathways. By contrast, the NSP1 proteins from all species investigated were able to inhibit the activation of Mx promoter following stimulation with type-I IFN.

Introduction

The ability of the host to sense incoming viral infection and answer rapidly and efficiently to the virus spread is crucial for life. The importance of innate immunity in controlling viral replication means that most viruses have evolved strategies to counteract IFN-mediated innate responses, including interference with components of the IFN induction and/or signalling pathways. Despite RV infection resulting in activation of the host innate immune response, wild type strains are capable of spreading from the site of infection to surrounding cells and tissues (Feng *et al.*, 2009). Infected cells have been shown to express very low levels of IFN transcription or secretion, suggesting that the virus encodes proteins that antagonize the IFN pathways.

NSP1-defective strains replicates in cell culture to titers close to those of their wild-type counterparts, but they yield small- to minute-plaque phenotypes. This suggests NSP1 could play a role in modulating the host innate immune response. A series of luciferase reporter assays were used to evaluate the effects of plasmid-encoded NSP1 derived from different mammalian species (human, pigs, cattle and monkey) on the induction and signalling of type I and type III IFN.

5.1 Cell lines evaluation

In order to evaluate the ability of NSP1 to downregulate IFN expression in the context of a homologous or heterologous infection, a set of human, monkey, pig and cattle-derived cell lines were first checked for (1) endogenous expression of IRF-3 and (2) the ability to induce an IFN response.

In order to check for endogenous IRF-3 expression in untreated cells, whole cell lysates obtained from human (HEK293, Caco-2 and HT29), monkey (BSC-1 and MA104), bovine (MDBK) and porcine (PK15) cell lines were prepared and analysed by Western blot using an antibody against IRF-3. As reported in Figure 28 Panel A, HEK293 Caco-2, HT-29, , BSC-1, MA104 MDBK and PK15 expressed IRF-3, with bands of expected migration size (47kDa) being observed. In order to confirm that the observed bands corresponded to IRF-3, PK15 cells were infected with Classical Swine Fever Virus (CSFV) and blotted for IRF-3 expression. CSFV is known to induce the degradation of IRF-3 through the expression of the viral protein N^{pro} (Seago *et al.*, 2007). 48h post-infection CSFV infection resulted in the complete abrogation of the expression of IRF-3. Similar results were obtained when IRF-3 expression levels were evaluated in a cell line stably expressing the CSFV N^{pro} protein (data not shown) (courtesy of Molecular virology group–The Pirbright Institute).

Differences in the observed migration profiles were observed between samples and this was likely due to species-specific differences in the size of IRF-3 (human IRF-3 427 aa, monkey IRF-3 422 aa, bovine IRF-3 417 aa and pig IRF-3 423 aa). The higher band observed in PK15-CSFV infected cells may beeen a phosphorylated form of IRF-3 re-localised to the nucleus following viral infection, as previously reported for bovine viral diarrhoea pestivirus (Hilton *et al.*, 2006). Doublets observed for Caco-2 and HT29 could be due to polymorphisms of the IRF-3 locus.

Next, employing an MX/CAT reporter assay, the ability to induce IFN in Caco-2, HT29, HEK293, MA104, BSC-1, PK15 and MDBK cell lines upon Sendai virus (SeV) infection was evaluated (Strahle *et al.*, 2003). At 3h, 6h and 16hpi cell culture

supernatants were collected and analysed for IFN production using MDBK-t2 IFN-reporter cells (2.5). The respective amount of IFN produced by each cell type was quantified using regression analysis following the preparation of a standard curve (2.5.2).

As reported in Figure 28 Panel B the human HT29 and HEK293 cell lines produced IFN, however, expression profiles were different: HT29 reached the peak of induction at 16hpi, while in HEK293 the highest induction was observed during the first 3h of infection, with the following 13h showing a basal expression of IFN. The human Caco-2 appeared not to induce IFN upon SeV infection. African green monkey-derived cell lines MA104 and BSC1 showed a similar profile, with the highest levels of IFN induction observed at 16hpi (~30 IU/ml). Similarly, the highest levels of IFN expression for both bovine MDBK and porcine PK15 cell lines was observed at 16hpi (~140 IU/ml).

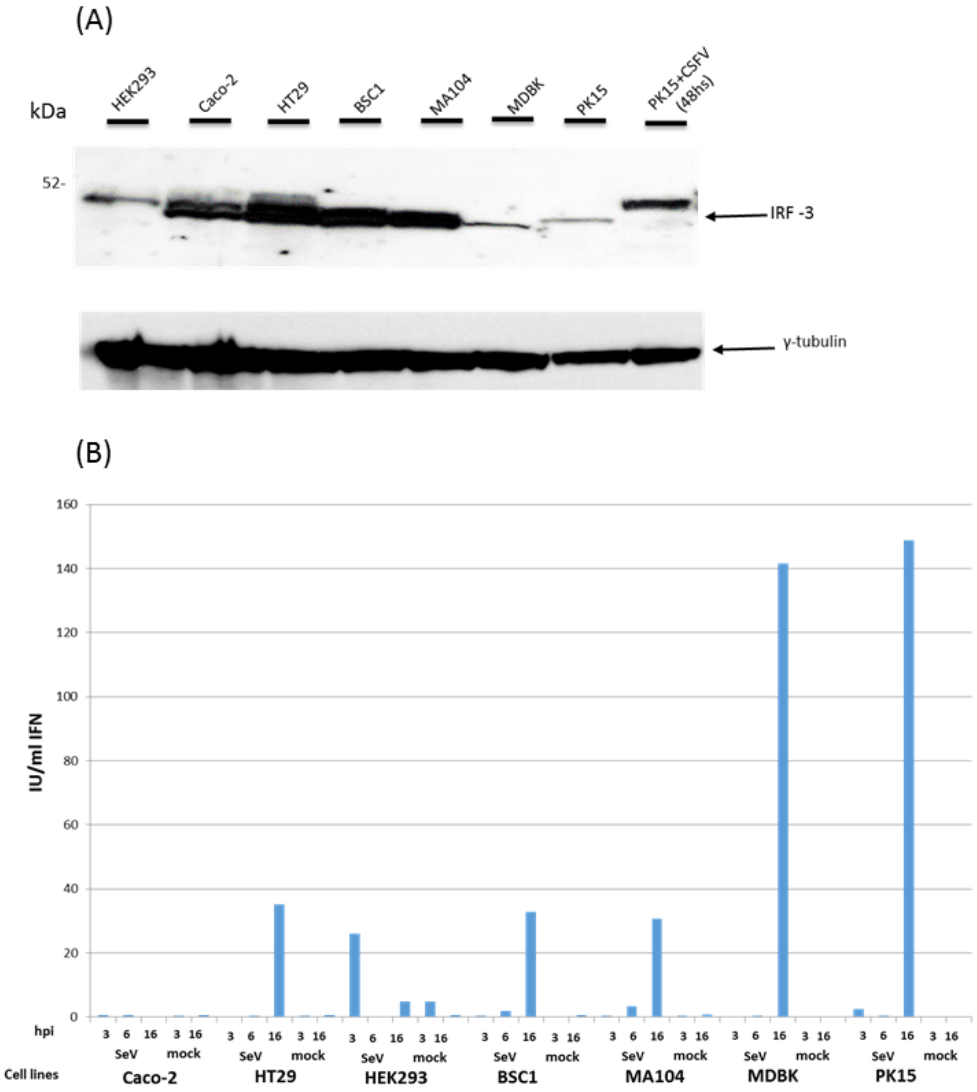

Figure 28. Analysis of different cell lines for IRF-3 expression and IFN induction following SeV infection.

(**A**) Whole cell lysates prepared from HEK293, Caco-2, HT-29 (human), BSC-1, MA104 (monkey), MDBK (bovine) and PK15 (swine) were analysed by Western blot using an antibody against IRF-3. Bands appeared to be at the expected size-related migration (~47 kDa). Infection of PK cell lines with CSFV results in the complete degradation of IRF-3. Overall protein expression was confirmed by probing for γ-tubulin. (**B**) Media samples were collected from Caco-2, HT29, HEK293, MA104, BSC1, PK15 and MDBK cell lines 3h, 6h and 16 hpi with SeV and analysed for the presence of IFN using MDBK-t2 MX-CAT reporter cells.

5.2 NSP1-mediated antagonization of the host innate immunity: Dual-luciferase reporter assay

Once the expression of full length plasmid-encoded NSP1 variants had been confirmed (4.1, 4.2) and the ability of relevant cell lines to express IRF-3 and produce IFN was established (Figure 28), the next step was to evaluate the effect of NSP1 in modulating the host innate immune response. To do this a Dual-Luciferase® Reporter (DLR™) Assay System (Promega) was used. This system involves co-transfecting mammalian cells with a firefly luciferase reporter under the control of a promoter region of interest, a plasmid encoding constitutively expressed *Renilla* luciferase (referred to herein as *Renilla* plasmid) and a plasmid encoding a putative effector protein. The co-transfected cells are then stimulated to induce expression of the firefly luciferase reporter, the activity of which can be rapidly quantified in a luminometer. *Renilla* luciferase activity is then quantified and used to normalise firefly activity to account for differences in transfection efficiency. The ability of the effector protein to increase or reduce transcriptional activity is then assessed.

In this study, firefly luciferase reporters containing the promoter regions of host factors involved in the establishment of host innate immunity (IFN-β, IFN-α IFN-λ, NF-κB, Mx_2) were used (2.14), and NSP1 plasmids prepared in (2.6), encoded the effector proteins that were investigated. Cells were treated with different stimuli (Sendai virus, TNFα, IFNα) depending on the nature of the region promoter and unstimulated cells provided background levels of luciferase.

Human HEK293 cell lines, which can be induced to produce IFN (Figure 28) and are known to have high transfection efficiency, were initially used. In order to assess the optimal concentration of NSP1 plasmid that could be transfected before observing cytotoxicity, a range of concentrations was first tested. To do this, cells were co-transfected with 250 ng of IFN-β reporter plasmid, 25 ng of *Renilla* plasmid and either 250 ng, 500 ng or 1µg of empty pcDNA3.1 vector (negative control), a plasmid encoding NSP1 (1M0), or a plasmid encoding the CSFV N^{pro} protein (positive control) (Seago *et al.*, 2007) respectively. 24h later the cells were infected with 50 µl

SeV (4000HA/ml) for a further 16h to induce expression of the firefly luciferase reporter. Cells were then harvested and firefly luciferase activity values were determined (Figure 29); from herein firefly luciferase will be referred to as luciferase.

Although SeV infection of cells transfected with different amounts of the empty vector all led to an increase in luciferase activity, a sequential decrease in activity was observed with increasing amounts of plasmid. The luciferase activity values obtained for the empty vector control were then compared to those determined for cells transfected with either NSP1 or N^{pro} plasmid. Interestingly, luciferase activity was downregulated when 250 ng and 500 ng of NSP1 plasmid were used, but not using 1 µg. Transfection of increasing amounts of N^{pro} plasmid led to a reduction in luciferase activity in each assay, however the use of 250 ng produced the highest inhibition. Based on these results, subsequent dual-luciferase reporter assays were performed using 250 ng of NSP1 plasmid.

(A)

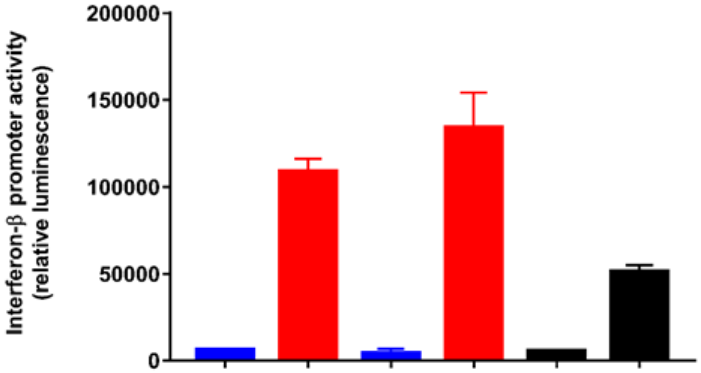

SeV	-	+	-	+	-	+
1M0	250	250	/	/	/	/
pcDNA	/	/	250	250	/	/
Npro	/	/	/	/	250	250

(B)

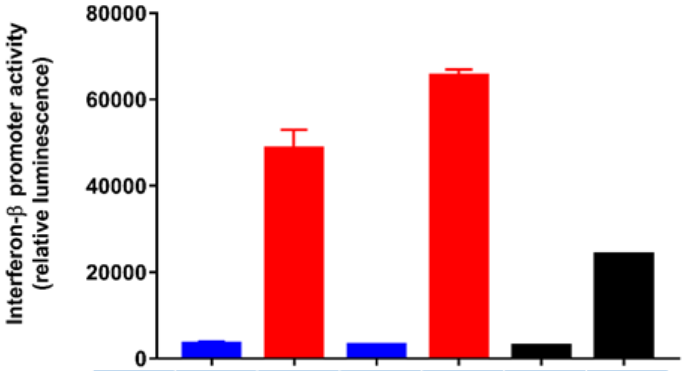

SeV	-	+	-	+	-	+
1M0	500	500	/	/	/	/
pcDNA	/	/	500	500	/	/
Npro	/	/	/	/	500	500

(C)

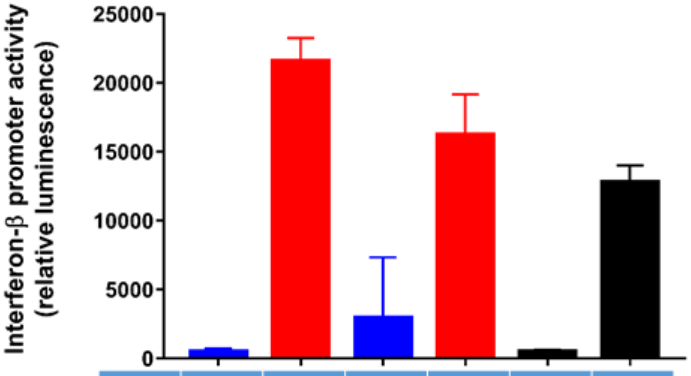

SeV	-	+	-	+	-	+
1M0	1000	1000	/	/	/	/
pcDNA	/	/	1000	1000	/	/
Npro	/	/	/	/	1000	1000

Figure 29. Evaluation of the optimal concentration of plasmid-encoded NSP1 to be transfected for dual-luciferase reporter assays.

HEK-293 cells were co-transfected with 250 ng of a IFN-β reporter, 25 ng of *Renilla* luciferase plasmid and either (**A**) 250 ng, (**B**) 500 ng or (**C**) 1 µg of a plasmid encoding the human rotavirus NSP1 (1M0), a plasmid encoding the CSFV N-terminal protease (N^{pro}) or an empty vector. 24 h later cells were infected with SeV, or mock infected for a further 16h, after which luciferase values were determined. Luminescence was normalised by comparing *Renilla* luciferase activity. Data are presented as the mean of three independent experiments (+/- SD).

5.2.1.1 The effects of plasmid-encoded NSP1 on the promoter of Type I IFN

5.2.1.1.1 IFN-β

HEK293 cells were co-transfected with IFN-β reporter and *Renilla* plasmids and a plasmid expressing either a single human (1M0, 18A and TC), porcine (G10P5 and A8), bovine (UKtc) or rhesus (RRV) NSP1 protein. A plasmid expressing CSFV N^{pro} and empty pcDNA3.1 vector served as positive and negative controls, respectively. 24h after co-transfection, cells were mock-infected or infected with SeV for 16h. Cells were harvested and respective luciferase activities were then determined (Figure 30). Luciferase activity values for NSP1 were compared to those obtained for the empty vector control (designated as 100% luciferase activity). The expression of each NSP1 protein led to a reduction in luciferase activity, with the exception of the porcine A8. The human 1M0, 18A and TC, together with the porcine G10P5, were able to reduce the level of luciferase activity to ~50% ($P<0.05$ and <0.01), while the bovine UKtc and rhesus RRV decreased the activity to ~40% ($P<0.01$). CSFV N^{pro} was able to knock down IFN-β promoter activity to ~40% ($P<0.001$).

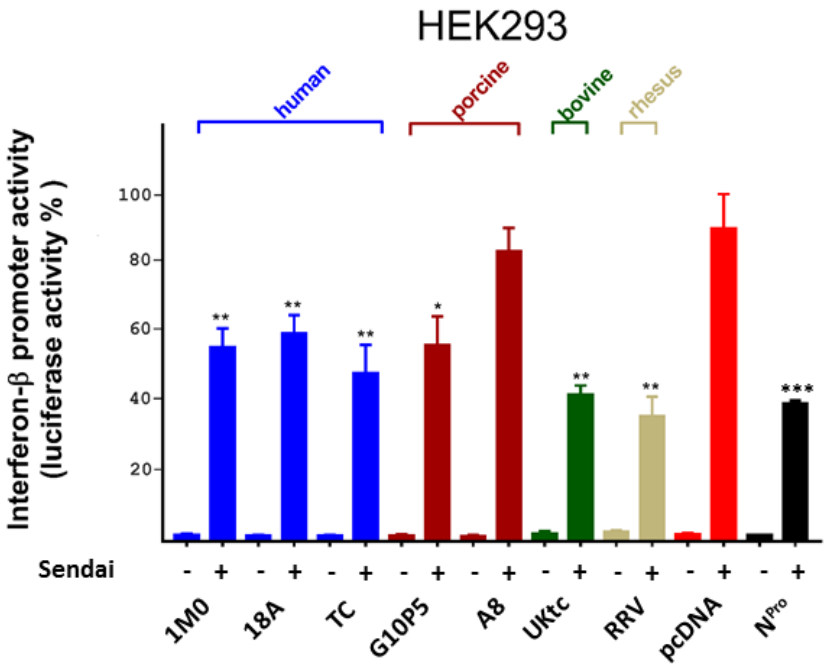

Figure 30. IFN-β downregulation by plasmid-encoded NSP1 in human HEK293 cell lines.

HEK293 cells were co-transfected with plasmids encoding either human (1M0, 18A, TC) porcine (G10P5, A8), bovine (UKtc) or rhesus (RRV) NSP1 proteins along with an IFN-β reporter and *Renilla* luciferase plasmid. Controls included transfection with an empty vector (pcDNA3.1) and plasmid expressing CSFV N^{PRO}. Cells were then infected with SeV, or mock infected for a further 16h, after which luciferase values were determined. Activation of the IFN-β promoter (expressed in percentage) was determined by normalising the luciferase activity to *Renilla* and comparing the signals in cells transfected with NSP1 and cells expressing an empty vector. Data are presented as the mean of four independent experiments (+/- SD) and analysed with Student T-test *P<0.05, **P<0.01, ***P<0.001.

IFN-β, the prototypical type I IFN, is induced by the combined actions of the transcription factors AP-1, IRF-3, IRF-7 and NF-κB (1.2.4). The binding sites for each set of transcription factors are localized in close proximity to each other and IFN-β expression requires the cooperative binding of all activators in a complex, the enhanceosome (Panne, 2008). In order to evaluate if the previously observed downregulation of IFN-β (Figure 30) was due to the ability of NSP1 to specifically target IRF-3, a PRD-III IFN-β reporter plasmid was used. This reporter plasmid expresses firefly luciferase under the control of only the IRF-3 binding sites (PRD-III) in the human IFN-β promoter.

HEK293 cells were co-transfected, infected with SeV, harvested as previously described (5.2.1.1.1) and luciferase activity was measured (Figure 31). Compared to the results showed in Figure 30, the human 1M0 and rhesus RRV NSP1 proteins mediated a further ~20% decrease in luciferase activity ($P<0.001$ and $P<0.0001$ respectively). Both porcine NSP1 proteins, G10P5 ($P<0.0001$) and A8 ($P<0.001$), were able to reduce the activity a further ~30%, while the human 18A ($P<0.001$) and the bovine UKtc ($P<0.0001$) were able to reduce luciferase activity to ~50% and ~30% respectively (Figure 30). CSFV N^{pro} was able to knock down PDRIII IFN-β promoter activity to ~20% ($P<0.0001$).

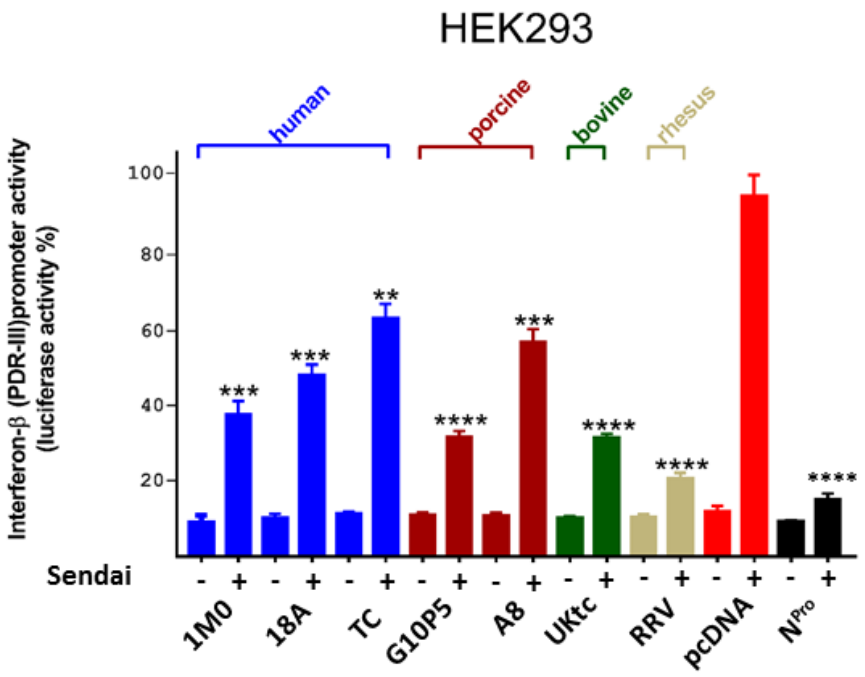

Figure 31. IFN-β (Luc IRF-3/PDRII) downregulation by plasmid-encoded NSP1 in human HEK293 cell line.

HEK293 cells were co-transfected with plasmids encoding either human (1M0, 18A, TC) porcine (G10P5, A8), bovine (UKtc) or rhesus (RRV) NSP1 proteins along with a PDRIII IFN-β reporter (in which the promoter region is under the control of only IRF-3) and *Renilla* luciferase plasmid. Controls included transfection with an empty vector (pcDNA3.1) and plasmid expressing CSFV N^{PRO}. Cells were then infected with SeV, or mock infected for a further 16h, after which luciferase values were determined. Activation of the IFN-β promoter (expressed in percentage) was determined by normalising the luciferase activity to Renilla and comparing the signals in cells transfected with NSP1 and cells expressing an empty vector. Data are presented as the mean of four independent experiments (+/- SD) and analysed with Student T-test **P<0.01, ***P<0.001, ****P<0.0001.

In order to assess the ability of NSP1 to downregulate the IFN-β promoter reporter in other cell lines, transfections of HT29 and Caco-2 human cell lines were carried out. However, these were unsuccessful, yielding non detectable luciferase values. The PK15 porcine cell line was next evaluated. Cells were transfected as previously described, infected with SeV and luciferase activity was determined (Figure 5). Consistent with results obtained with Y-2-H screening in which NSP1 was able to interact with IRF-3 independently of its host origin, no differences were observed in luciferase activity in PK15, and all the NSP1 proteins were able to significantly inhibit the induction of IFN-β (P**P<0.01, ***P<0.001, ****P<0.0001). The only observed difference was related to the porcine G10P5 (P<0.001), which was able to reduce the expression by 80% of that observed for the empty vector control. In PK15 cell lines, CSFV N^{pro} was able to completely knock down IFN-β promoter activity to more than ~90% (P<0.0001).

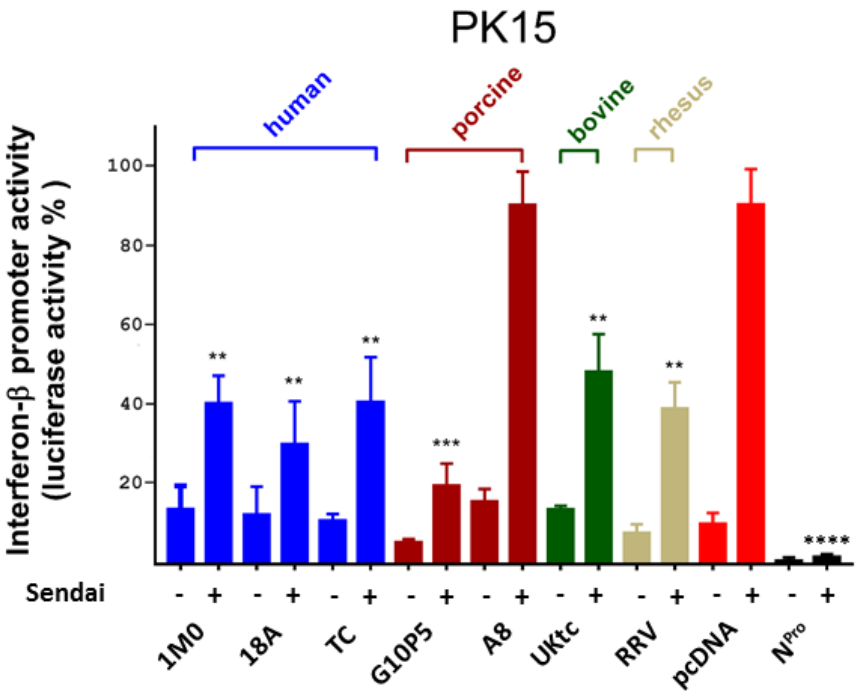

Figure 32. IFN-β downregulation by plasmid-encoded NSP1 in porcine PK15 cell lines.

PK15 cells were co-transfected with plasmids encoding either human (1M0, 18A, TC) porcine (G10P5, A8), bovine (UKtc) or rhesus (RRV) NSP1 proteins along with an IFN-β reporter and *Renilla* luciferase plasmid. Controls included transfection with an empty vector (pcDNA3.1) and plasmid expressing CSFV N^{PRO}. Cells were then infected with SeV, or mock infected for a further 16h, after which luciferase values were determined. Activation of the IFN-β promoter (expressed in percentage) was determined by normalising the luciferase activity to *Renilla* and comparing the signals in cells transfected with NSP1 and cells expressing an empty vector. Data are presented as the mean of four independent experiments (+/- SD) and analysed with Student T-test **P<0.01, ***P<0.001, ****P<0.0001.

Yeast-2-hybrid analyses (3.2.1) showed how bovine NSP1 UKtc was able to interact with IRF-3 encoded by human, pigs, cattle and monkeys. By contrast, the human 18A was not able to bind to any of the IRF-3 proteins, even in lower stringency conditions (3.2.5). Previous studies have shown how the C-terminus of NSP1 is important for the interaction of the viral protein with its targets (Barro *et al.*, 2007; Graff *et al.*, 2002; B. Zhao *et al.*, 2016). In order to confirm that the C-terminus of NSP1, which has been reported to contain a putative IRF-3 interaction site (B. Zhao *et al.*, 2016), was crucial in the binding ability of the viral protein to modulate the expression of IFN-β, two chimeric NSP1 were generated: 18A-UKtc (499aa), containing the N-terminus of the NSP1 protein from the human18A RV isolate and the C-terminus of the NSP1 protein from the bovine UKtc RV isolate, and UKtc-18A (487aa) containing the reciprocal terminus of either protein. A buffering area to swap domains was chosen based on a region of conserved amino acids, corresponding to the peptide sequence - L R Y F S K -. This sequence occurs between residues 640 to 658 in 18A, but between 619 to 637 in UKtc. The sequences encoding the two chimeric NSP1 were ordered from GeneART® in the mammalian expression vector pCDNA3.1.

Next, the effect of the swapped domains on the downregulation of IFN-β induction was evaluated using the DLR™ Assay System and HEK293 cells. Assays were performed alongside parental NSP1 proteins for comparison (Figure 33). Contrasting results were obtained on the effect of plasmid-encoded NSP1 on the downregulation of IFN-β. The human 18A either reduced luciferase activity to only ~80% or mediated no effect at all on, contrasting with the ~50% reduction previously reported (Figure 30). The effect of the bovine UKtc appeared more remarkable, dropping from the previously observed reduction of ~60% to ~30%. Since the effect of N^{pro} on luciferase activity was consistent and the expected luciferase activity was observed for the empty vector control, it is possible that this issue may have been due to the quality of NSP1 plasmid preparations. Due to unreproducible experiments, it was impossible to evaluate the effect of swapped-regions in chimeric NSP1 on the IFN downregulation.

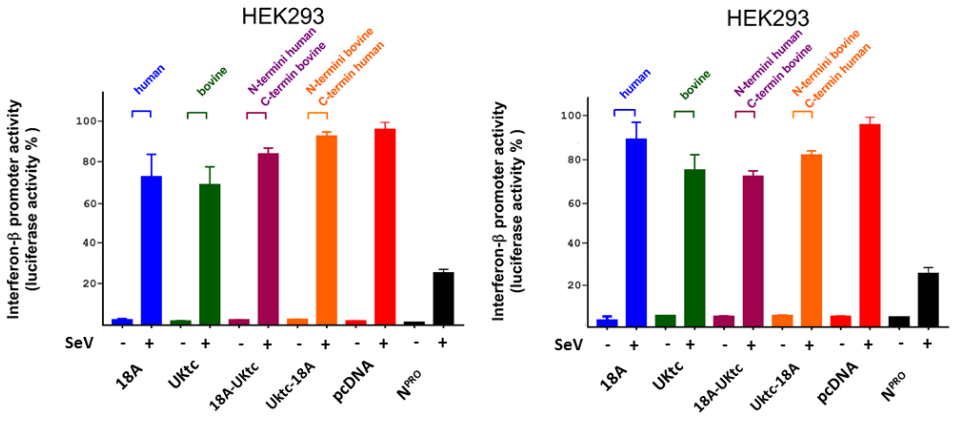

Figure 33. IFN-β downregulation by plasmid-encoded NSP1 in human HEK293 cell lines: swapped domains between the human 18A and the bovine UKtc.

HEK293 cells were co-transfected with plasmids encoding either the human NSP1 18A, the bovine NSP1 UKtc, the recombinant 18AUKtc or the recombinant UKt18A along with IFN-β reporter and *Renilla* luciferase plasmid Controls included transfection with an empty vector (pcDNA3.1) and plasmid expressing CSFV N^{PRO}. Cells were then infected with SeV, or mock infected for a further 16h, after which luciferase values were determined. Activation of the IFN-β promoter (expressed in percentage) was determined by normalising the luciferase activity to *Renilla* and comparing the signals in cells transfected with NSP1 and cells expressing an empty vector. Data are presented as the mean of three independent experiments (+/- SD).

The recombinant NSP1 18AUKtc of 499 aa in length has the N-terminus region (212 aa) from the human 18A and the C-terminus (287 aa) from the bovine UKtc. The recombinant UKtc18A of 487 aa in length has the N-terminus (220 aa) from the bovine UKtc and the C-terminus (267 aa) from the human 18A.

5.2.1.1.2 IFN-α

Recent studies have shown how NSP1 was able to induce the degradation of IRF-7 (Barro *et al.*, 2007). In order to investigate if the presence of NSP1 results in the downregulation of IFN-α promoter activity, the expression of which is IRF-7 dependent (Osterlund *et al.*, 2007), a luciferase reporter assay was used in which the firefly luciferase was under the control of the human IFN-α_4 promoter region. Preliminary experiments were performed in order to evaluate the induction of IFN-α_4 promoter; HEK293 cells were co-transfected with the IFN-α_4 reporter and *Renilla* plasmids and either a plasmid encoding CSFV N^{pro} or the empty pcDNA3.1 vector. Cells were then mock infected or infected with SeV.

Infection of HEK293 cells with SeV seemed to poorly induce IFN-α_4 transcription, with no substantial differences occurring between stimulated and unstimulated cells (Figure 34). These results are consistent with data published by Osterlund, who investigated the ability of IRFs and NF-κB family members to activate type I and type III IFN promoters (Osterlund *et al.*, 2007).

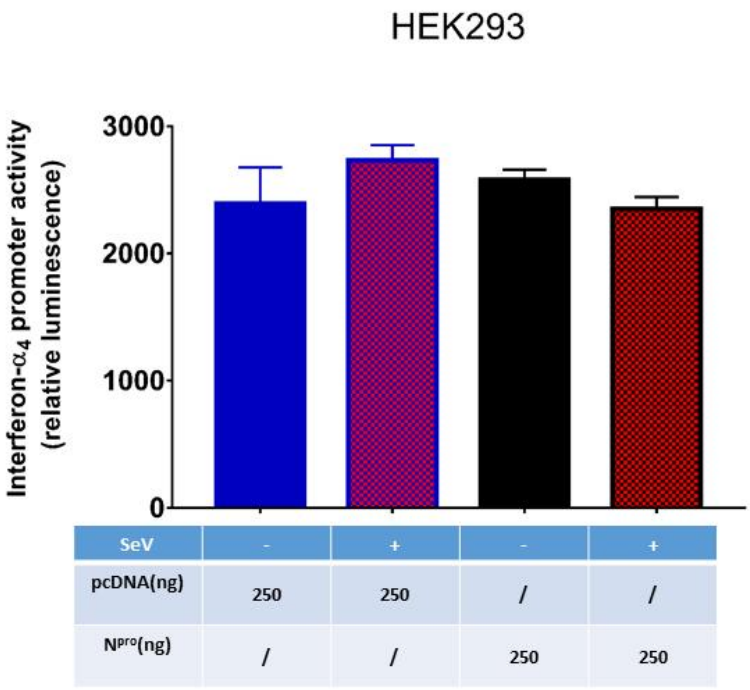

Figure 34. IFN-α induction in human HEK293 cell lines.

HEK293 were co-transfected with plasmid encoding either an empty vector (pCDNA3.1) or CSFV N^{pro} along with an inducible firefly luciferase reporter under human IFN-α_4 promoter region and a non-inducible plasmid encoding *Renilla*. After 24h interferon response was induced infecting cells with SeV for 16h or mock infected. Cells were harvested and luciferase values were read. Activation of IFN-α_4 promoter was evaluated by normalising luciferase activity to *Renilla* comparing the signals in cells infected with SeV and mock infected. Data are presented as the mean of two independent experiments (+/- SD).

Having confirmed that SeV was not able to induce IFN-α_4, the exogenous expression of IRF-7 was investigated. To facilitate this, HEK293 were co-transfected as previously described along with 50 ng, 100 ng or 200 ng of pEF-C1/EGFP-IRF7 plasmid encoding human IRF-7. 8 h post-transfection, cells were infected with SeV or mock-infected and 18 h later cells were harvested and luciferase levels measured (Figure 35). The administration of exogenous IRF-7 clearly activated the IFN-α_4 promoter reporter in HEK293 cells, with a two fold increase in luciferase activity observed between 50 ng and 100 ng. However, when increased to 200 ng, no further increase was observed. No difference in luciferase activity profiles were observed between cells only transfected with IRF-7 and those transfected and then infected with SeV.

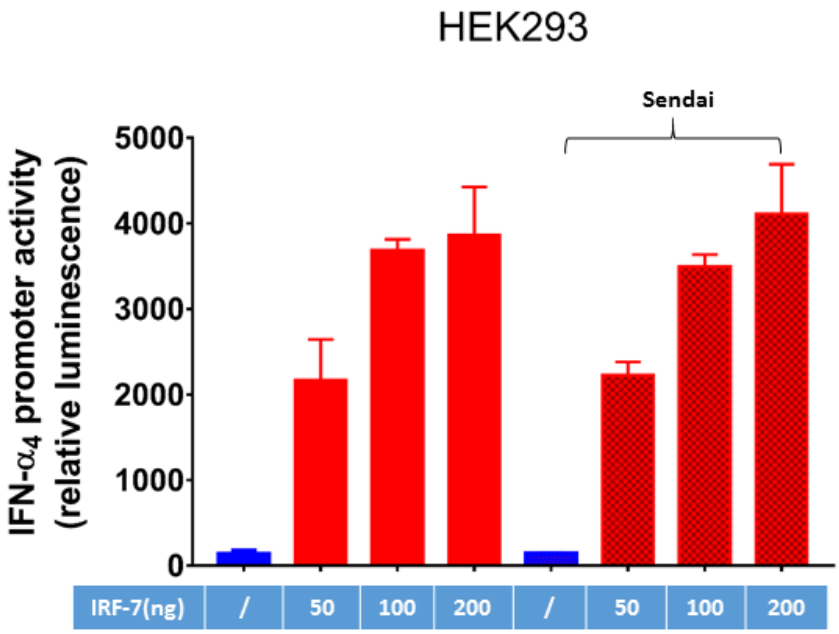

Figure 35. IRF-7 mediated induction of IFN-α4 in human HEK293 cell lines.

HEK293 were co-transfected with plasmid encoding either an empty vector (pCDNA3.1) or CSFV N^{pro} along with a IFN-α4 reporter and *Renilla* plasmid and 50 ng, 100 ng or 200 ng of human IRF-7. Cells were allowed to express plasmid-encoded proteins for 8h and infected with SeV overnight or mock infected before being harvested and luciferase values read. Luminescence was normalised by comparing *Renilla* luciferase activity. Induction of the human IFN-α4 promoter was evaluated comparing the signals in cells stimulated to produce interferon with the ectopic expression IRF-7 and those subsequently infected with SeV. Data are presented as the mean of two independent experiments (+/- SD).

Having confirmed exogenous IRF-7 activated the IFN-α_4 promoter reporter, assays were carried out using 100 ng of IRF-7 and plasmids expressing human (1M0, 18A and TC), porcine (G10P5 and A8), bovine (UKtc) and rhesus (RRV) NSP1. The rotavirus NSP1 proteins had no effects on induction of the IFN-α_4 promoter reporter, with the exception of the bovine UKtc, with a reduction to ~60 % ($P<0.05$) (Figure 36). As previously reported, CSFV N^{pro} is able to target IRF-7 (Fiebach *et al.*, 2011; Gottipati *et al.*, 2016), and this was evident by a reduction of ~80% in luciferase activity ($P<0.05$).

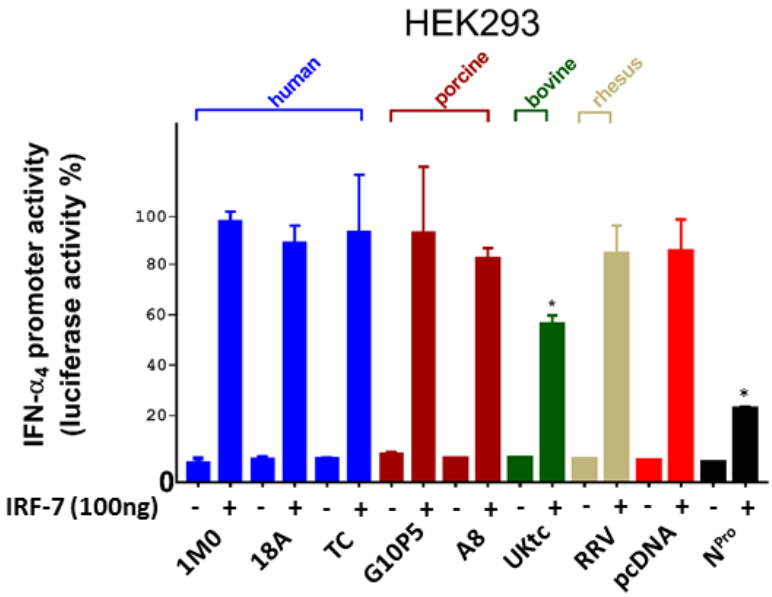

Figure 36. IFN-α_4 downregulation by plasmid-encoded NSP1 in human HEK293 cells.

HEK293 cells were co-transfected with plasmids encoding either human (1M0, 18A, TC) porcine (G10P5, A8), bovine (UKtc) or rhesus (RRV) NSP1 proteins along with an IFN-α_4 reporter and *Renilla* luciferase plasmid. Controls included transfection with an empty vector (pcDNA3.1) and plasmid expressing CSFV N^{PRO}. Interferon response was induced transfecting cells with 100 ng of human IRF-7. 16h post-transfection cells were harvested and luciferase values were read. Activation of IFN-α_4 promoter (expressed in percentage) was determined by normalising the luciferase activity to *Renilla* and comparing the signals in cells transfected with NSP1 and cells expressing an empty vector. Data are presented as the mean of three independent experiments (+/- SD) and analysed with Student T-test *$P<0.05$.

5.2.1.2 The effects of plasmid-encoded NSP1s on the promoter of Type III IFN

In vivo, RV infects predominantly mature enterocytes in the mid and top section of the villi of small intestine (Estes *et al.*, 2007) being able to replicate and spread in these cells. Moreover, it has been shown that IFN-λ knocked-out mice are more susceptible to RV infection compared to the wild-type or IFN-β knock-out mice (Hernandez *et al.*, 2015). Given the close relationship between IL-22 and IFN-λ and their concerted action on the defence of epithelial cells, and due to the high tropism of RV to a specific niche of cells, the ability of the virus to modulate IFN-λ promoter activity was investigated using an IFN-λ promoter reporter plasmid.

5.2.1.2.1 IFN-λ_1

HEK293 were co-transfected with a reporter plasmid encoding firefly luciferase under the control of the human IFN-λ_1 promoter, R*enilla* plasmid and a plasmid expressing either human (1M0, 18A and TC), porcine (G10P5 and A8), bovine (UKtc) or rhesus (RRV) NSP1. A plasmid expressing CSFV N^{pro} and the empty pcDNA3.1 vector served as positive and negative controls, respectively. Cells were mock infected or infected with SeV (Figure 37). All the NSP1 proteins derived from human RV isolates reduced luciferase activity to ~40% (1M0 $P<0.01$, 18A $P<0.01$ and TC $P<0.001$). The swine-derived G10P5 was able to reduce luciferase activity to ~30% ($P<0.001$), and rhesus RRV to ~20% ($P<0.001$). By contrast, the porcine A8 ($P<0.05$) and the bovine UKtc ($P<0.01$) decreased the IFN-λ_1 expression to ~60%. CSFV N^{pro} was able to knock down IFN-λ promoter activity to ~40% ($P<0.001$)

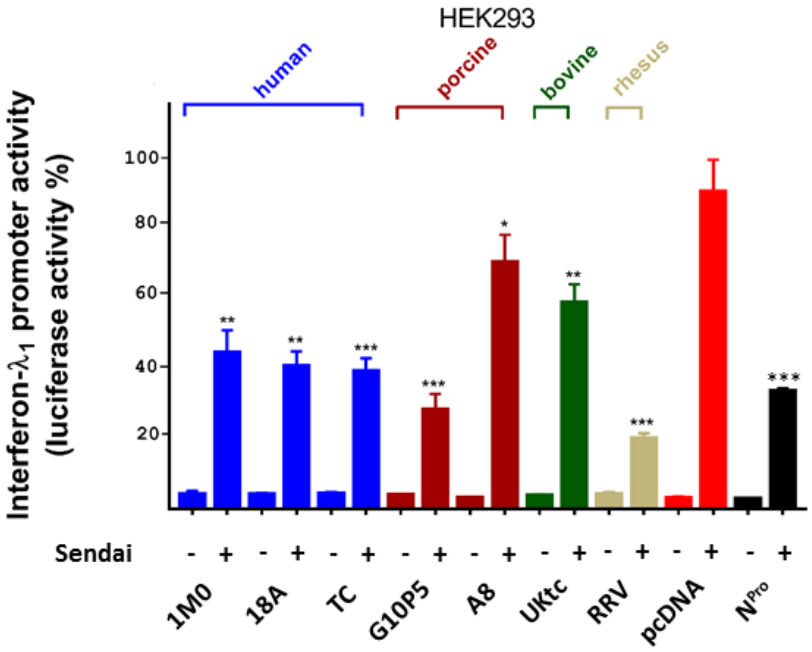

Figure 37. IFN-λ$_1$ downregulation by plasmid-encoded NSP1 in human HEK293 cell lines.

HEK393 cells were co-transfected with plasmids encoding either human (1M0, 18A, TC) porcine (G10P5, A8), bovine (UKtc) or rhesus (RRV) NSP1 proteins along with an IFN-λ$_1$ reporter and *Renilla* luciferase plasmid. Controls included transfection with an empty vector (pcDNA3.1) and plasmid expressing CSFV N^{PRO}. Cells were then infected with SeV, or mock infected for a further 16h, after which luciferase values were determined. Activation of the IFN-λ$_1$ promoter (expressed in percentage) was determined by normalising the luciferase activity to *Renilla* and comparing the signals in cells transfected with NSP1 and cells expressing an empty vector. Data are presented as the mean of four independent experiments (+/- SD) and analysed with Student T-test *P<0.05, 0*P<0.01, **P<0.01, ***P<0.001.

The ability of NSP1 to inhibit IFN-λ_1 promoter activity was investigated in other human cell lines, however transfections of HT-29 and Caco-2 human-derived cell lines were unsuccessful, yielding non detectable luminescence values. The PK15 porcine cell line was next evaluated. Cells were co-transfected as previously described, infected with SeV and firefly luciferase activity under the control of IFN-λ_1 promoter was measured (Figure 38). The human-derived 18A and TC ($P<0.05$), as well as the porcine G10P5 and the rhesus RRV ($P<0.01$), were able to reduce luciferase activity to ~40%. 1M0 reduced luciferase activity to ~60% ($P<0.05$), while the bovine was less efficient (reduced to ~80%, $P<0.01$).The porcine A8 did not reduce luciferase activity, suggesting an inability to inhibit activation of the type III IFN promoter following SeV infection. Similarly to data observed for IFN-β (Figure 32), in PK 15 cell lines, CSFV N^{pro} appeared to completely abolish induction of IFN- ($P<0.001$).

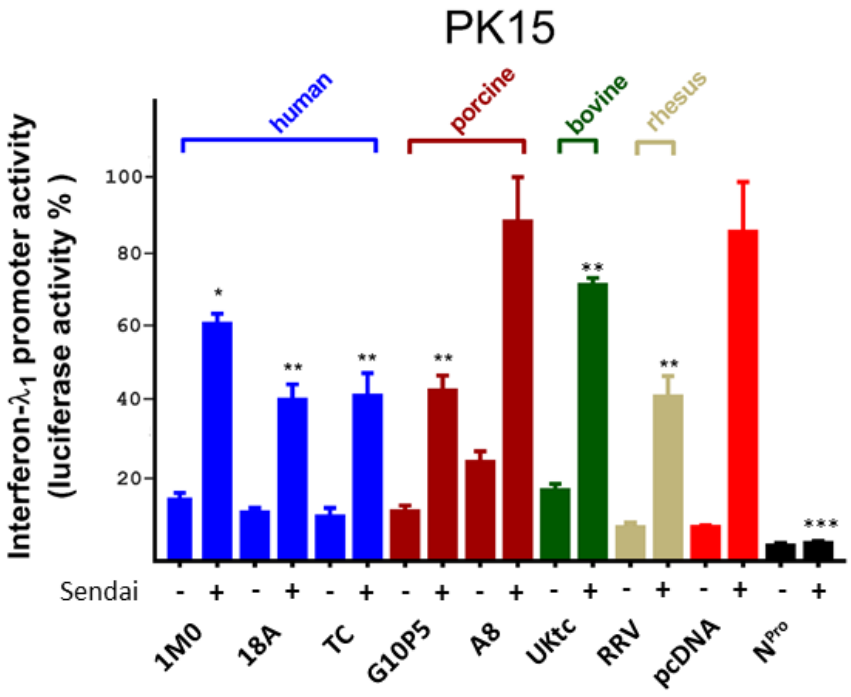

Figure 38. IFN-λ_1 downregulation by plasmid-encoded NSP1 in porcine PK15 cell lines.

PK15 cells were co-transfected with plasmids encoding either human (1M0, 18A, TC) porcine (G10P5, A8), bovine (UKtc) or rhesus (RRV) NSP1 proteins along with an IFN-λ_1 reporter and *Renilla* luciferase plasmid. Controls included transfection with an empty vector (pcDNA3.1) and plasmid expressing CSFV N^{PRO}. Cells were then infected with SeV, or mock infected for a further 16h, after which luciferase values were determined. Activation of the IFN-λ_1 promoter (expressed in percentage) was determined by normalising the luciferase activity to *Renilla* and comparing the signals in cells transfected with NSP1 and cells expressing an empty vector. Data are presented as the mean of four independent experiments (+/- SD) and analysed with Student T-test **P<0.05, **P<0.01, ***P<0.001.

Next, the previously generated chimeric NSP1 plasmids (18AUKtc or UKtc18A) were used to assess the ability of the encoded proteins to inhibit activation of the IFN-λ promoter in HEK293 cells following SeV infection. Figure 39 shows that swapping domains between the human 18A and the bovine UKtc appeared not to compromise the functionality of the viral protein, which was still able to downregulate type III IFN promoter reporter activity. The chimeric 18AUKtc, which had the 18A N-terminus and the UKtc C-terminus, showed a luciferase activity profile similar to that of the parental UKtc NSP1 protein, being able to reduce expression to ~50% ($P<0.0001$). By contrast, the UKtc18A, which had the UKtc N-terminus and the 18A C-terminus, showed a profile similar to the parental strain 18A, with a downregulation to ~60% of the total expression ($P<0.001$). Taken together this data confirmed the pivotal role of the C-terminus region of NSP1. As previously shown (Figure 37), CSFV N^{pro} was able to knock down IFN-λ promoter activity to ~20% ($P<0.0001$).

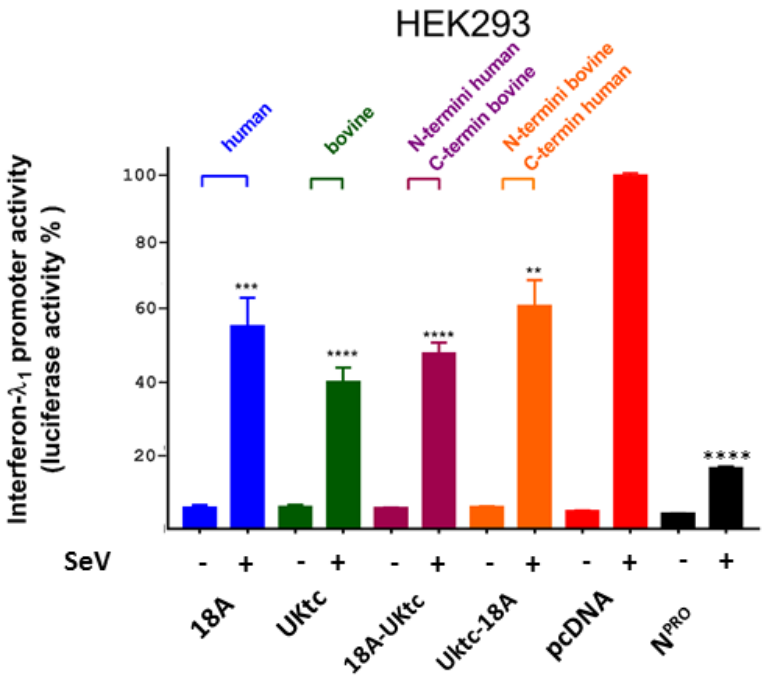

Figure 39. IFN-λ1 downregulation by plasmid-encoded NSP1 in human HEK293 cell lines: swapped domains between the human 18A and the bovine UKtc.

HEK293 cells were co-transfected with plasmids encoding either the human NSP1 18A, the bovine NSP1 UKtc, the recombinant 18AUKtc or the recombinant UKt18A along with IFN-λ1 reporter and *Renilla* luciferase plasmid Controls included transfection with an empty vector (pcDNA3.1) and plasmid expressing CSFV N^{PRO}. Cells were then infected with SeV, or mock infected for a further 16h, after which luciferase values were determined. Activation of the IFN-λ1 promoter (expressed in percentage) was determined by normalising the luciferase activity to *Renilla* and comparing the signals in cells transfected with NSP1 and cells expressing an empty vector. Data are presented as the mean of three independent experiments (+/- SD) and analysed with Student T-test **P<0.01, ***P<0.001, ****P<0.0001.

The recombinant NSP1 18AUKtc of 499 aa in length has the N-terminus region (212 aa) from the human 18A and the C-terminus (287 aa) from the bovine UKtc. The recombinant UKtc18A of 487 aa in length has the N-terminus (220 aa) from the bovine UKtc and the C-terminus (267 aa) from the human 18A.

5.2.1.2.2 IFN-λ_3

Like type I IFNs, type III are strongly induced by double stranded (ds) RNA or viral infection, suggesting common regulatory factors. Recently, it has been demonstrated that the IFN-λ_1 gene, similar to the gene encoding IFN-β, is regulated by virus-activated IRF-3 and IRF-7. In contrast, IFN-λ_2 and IFN-λ_3 gene expression is mainly controlled by IRF-7, similar to the activation of IFN-α (Osterlund *et al.*, 2007). Both IFN-λ_1 and IFN-λ_3 are able to activate STAT1 signalling. Microarray analysis has shown a profile of similar gene inductions by both cytokines and many of them play a role in antiviral immunity (Dickensheets *et al.*, 2013).

In order to evaluate if RV can affect IFN-λ_3 promoter activity through the expression of NSP1, a luciferase reporter was employed. The role of IRF-7 in the late induction of IFN-α has been previously discussed, and analogies in the promoter sequences with IFN-λ_3 presume a similar activation profile. Due to this, preliminary experiments were performed in order to evaluate the inducibility of IFN-λ_3 promoter using a plasmid encoding IRF-7. HEK293 cells were co-transfected as previously described for IFN-α_4 (5.2.1.1.2) and 8h post-transfection, cells were mock-infected or infected with SeV. 18 hpi cells were harvested and luciferase activity determined (Figure 40). Indeed the exogenous expression of IRF-7 induced activation of IFN-λ_3 promoter, as reported for IFN-α_4 (Figure 35), and as previously reported, the infection with SeV without the presence of IRF-7 was not able to induce the promoter activity. However, if SeV infection followed IRF-7 transfection, differences in the activation of IFN-λ_3 promoter activity were observed compared to when cells were only transfected with IRF-7. These results differed from those obtained studying the inducibililty of IFN-α_4 promoter, where the subsequent SeV infection of HEK293 cells transfected with IRF-7, had no impact on the induction of the promoter activity.

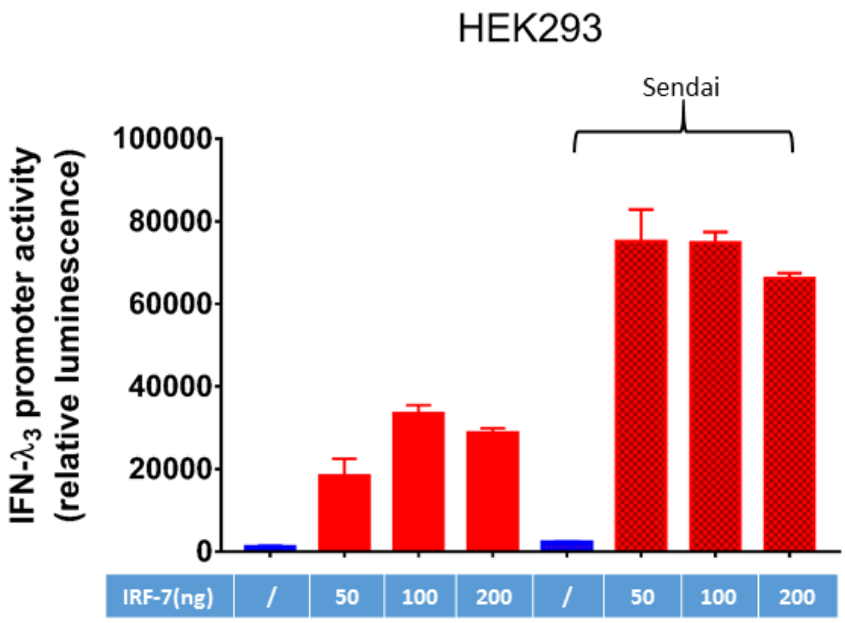

Figure 40. IRF-7 mediated induction of IFN-λ3 in human HEK293 cell lines.

HEK293 cells were co-transfected with an empty vector pcDNA3.1 along with an IFN-λ3 reporter, *Renilla* plasmid and 50 ng, 100 ng or 200 ng of human IRF-7. Cells were allowed to express plasmid-encoded proteins for 8h and where required infected with SeV overnight or mock- infected. Cells were then harvested and luciferase values were read. Induction of the human IFN-λ3 promoter was evaluated by normalising the luciferase activity to *Renilla* and comparing the signals in cells stimulated to produce interferon with the exogenous expression of IRF-7 and those expressing IRF-7 and infected with SeV. Data are presented as the mean of two independent experiments (+/- SD).

Given the two temporal differences in the activation of the IFN-λ_3 promoter depending on the nature of the induction (IRF-7 acts as an ISG, mimicking a later phase of infection, while SeV induces IRF-3 activation, resembling an early stage of infection), the ability of NSP1 to downregulate the type III IFN promoter was evaluated in HEK293 cells only transfected with IRF-7, as well as in cells transfected with IRF-7 and then infected with SeV (Figure 41). The human NSP1 1M0, 18A and TC proteins, together with the porcine A8, appeared to have no significant effects on luciferase activity of following IRF-7 expression in the absence or presence of SeV infection. The porcine G10P5 and rhesus RRV exhibited a reduction in luciferase activity to approximately ~80% ($P< 0.05$ and $P<0.01$, respectively), however, when cells were infected with SeV, RRV showed a slight higher ability to know down its expression. The bovine UKtc was able to reduce luciferase activity to ~50% ($P<0.01$). Interestingly, N^{pro} mediated a greater reduction in luciferase activity in cells which were subsequently infected with SeV, in comparison to those expressing only IRF-7 ($P<0.05$).

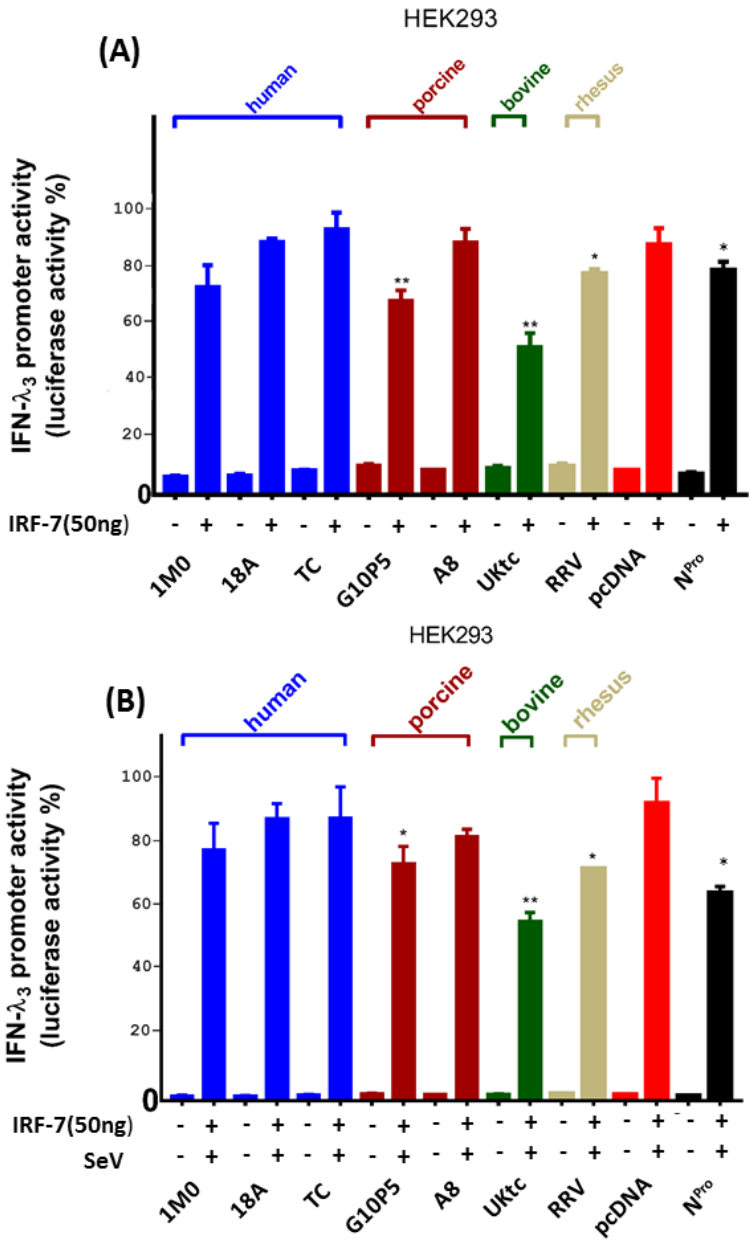

Figure 41. IFN-λ3 downregulation by plasmid-encoded NSP1 in human HEK293 cell lines.

HEK293 cells were co-transfected with plasmid encoding either human (1M0, 18A, TC) porcine (G10P5, A8), bovine (UKtc), rhesus (RRV) NSP1 proteins, and 50 ng of human IRF-7 along with an IFNλ3 reporter *Renilla* luciferase plasmid. Controls included transfection with an empty vector (pcDNA3.1) and plasmid expressing CSFV N^{pro}. Where required, 24h post-transfection, cells were infected with SeV for 16h, before being harvested and luciferase values were read. Activation of the IFNλ3 promoter (expressed in percentage) was determined by normalising the luciferase activity to *Renilla* and comparing the signals in cells transfected with NSP1 and cells expressing an empty vector. Data are presented as the mean of two independent experiments (+/- SD) and analysed with Student T-test *P<0.05, **P<0.01.

5.2.1.3 The effects of plasmid-encoded NSP1 on the activity of NF-κB

Preliminary experiments were performed in order to evaluate the inducibility NF-κB promoter activity. To facilitate this, the luciferase reporter plasmid pKB6tkluc, containing 6 NF-kB multimeric responsive upstream of the firefly luciferase gene under the control of the Herpes Simplex thymidine kinase promoter, was used (Traenckner *et al.*, 1995).

HEK293 cells were co-transfected with p*K*B6tkluc, R*enilla* plasmid and either an empty vector (pcDNA3.1) or a plasmid encoding the sequence of Molluscum Contagiosum virus (MCV) MC159 protein as positive control (C. M. Randall *et al.*, 2012). 24h after co-transfection cells were administered with 5 ng/ml, 10 ng/ml or 20 ng/ml of pig TNFα (gift from Chris Netherton, The Pirbright Institute) or infected with SeV for a further 18h to induce NF-κB transcription of or mock-treated. Cells were then harvested and luciferase activity was determined (Figure 42). The administration of TNFα clearly induced the transcriptional activity of NF-κB, with no substantial differences occurring between different dosages. SeV infection was able to activate the promoter activity, however, less potently compared to TNFα. TNFα-mediated activation of NF-κB was abrogated by the expression of MCV MC159. Based on these results, TNFα at final concentration of 5 ng/ml was used in following experiments.

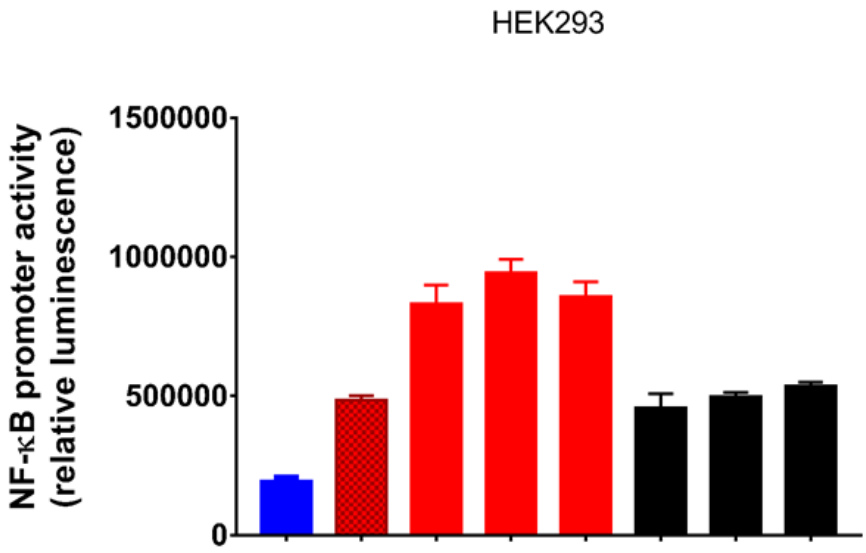

TNFα(ng/ml)	/	/	5	10	20	5	10	20
pcDNA(ng)	250	250	250	250	250	/	/	/
MC159(ng)	/	/	/	/	/	250	250	250
SeV	/	+	/	/	/	/	/	/

Figure 42. NF-κB induction in human HEK293 cell lines.

HEK293 were co-transfected with an empty vector (pcDNA3.1) or Molluscum Contagiosum Virus (MCV) MC159 along with an inducible firefly NF-κB reporter and a non-inducible *Renilla* plasmid. Cells were allowed to express plasmid-encoded protein for 24h and then treated with 5 ng/ml, 10 ng/ml or 20 ng/ml of TNFα or infected with Sendai virus to induce NF-κB transcription activity. 18h post-treatment cells were harvested and luciferase values were read. Data are provided as the means ± ranges of luciferase activity normalised to Renilla levels from one experiment with error bars representing standard deviation.

Once the inducibility of the NF-κB reporter had been established, HEK293 were co-transfected with p*K*B6tkluc, *Renilla* plasmid and a plasmid expressing either human (1M0, 18A and TC), porcine (G10P5, A8 and OSU), bovine (UKtc) or rhesus (RRV) NSP1. The MCV-MC159 plasmid and empty vector (pcDNA3.1) were used as positive and negative controls, respectively. 24h after co-transfection cells were either treated with 5 ng/µl of TNFα for 16 h or mock-treated. Cells were harvested and luciferase values were then determined (Figure 43). The human 1M0 ($P<0.0001$), the bovine UKtc ($P<0.0001$), the rhesus RRV ($P<0.0001$) and the porcine OSU ($P<0.01$) were all able to downregulate NF-κB activity to ~40%. The other human-derived NSP1 proteins (18A ($P<0.0001$)) and TC ($P<0.0001$)), together with the porcine A8 ($P<0.0001$) reduced luciferase activity to ~60%, while porcine G10P5 ($P<0.001$) reduced it to ~80%. The bovine UKtc and MCV-MC159 were able to reduce the transcriptional activity of NF-κB to ~30% ($P<0.0001$).

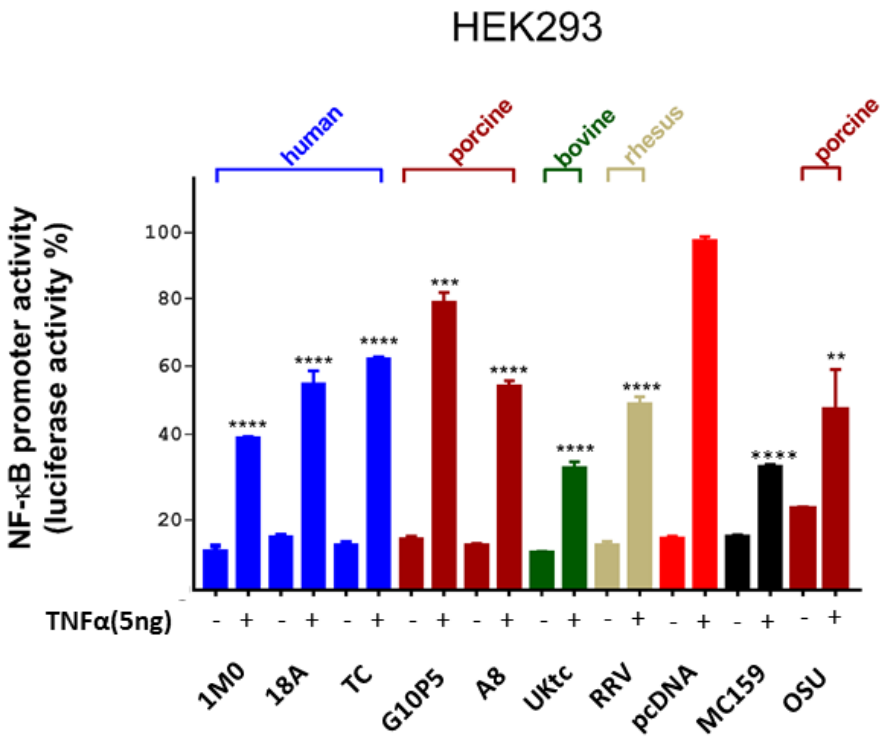

Figure 43. NF-kB downregulation by plasmid-encoded NSP1 in human HEK293 cell lines.

HEK293 cells were co-transfected with plasmid encoding either human (1M0, 18A, TC) porcine (G10P5, A8, OSU), bovine (UKtc), rhesus (RRV) NSP1 along with an NF-κB reporter and *Renilla* plasmid. Controls included transfection with an empty vector (pcDNA3.1) and plasmid expressing MCV-MC159. Plasmid-encoded proteins were allowed to express for 24h and cells were exposed to 5 ng/ml of pig TNFα or mock induced. 16h post-induction cells were harvested and luciferase values were read. NF-κB transcriptional activity (expressed in percentage) was determined by normalising the luciferase activity to *Renilla* and comparing the signals in cells transfected with NSP1 and cells expressing an empty vector. Data are presented as the mean of four independent experiments (+/- SD) and analysed with Student T-test **P<0.01, ***P<0.001, ****P<0.0001.

The ability of NSP1 to downregulate NF-κB transcriptional activity was investigated in other human cell lines, however, transfections of HT-29 and Caco-2 human-derived cell lines were unsuccessful, yielding non detectable luminescence values. The PK15 porcine cell line was next evaluated. Cells were transfected as previously described, treated with TNFα and luciferase activity was measured (Figure 44). The bovine UKtc was able to reduce NF-κB activity to ~30% ($P<0.0001$), while the rhesus RRV to ~60% ($P<0.0.1$). Of the porcine NSP1 proteins, only OSU ($P<0.01$) was able to block NF-κB activity, reducing it to ~80%, while the other porcine, together with the human strains, did not significantly change luciferase activity. In PK15 cell lines, MCV-MC159 appeared to knock down NF-κB activity to ~60% ($P<0.01$).

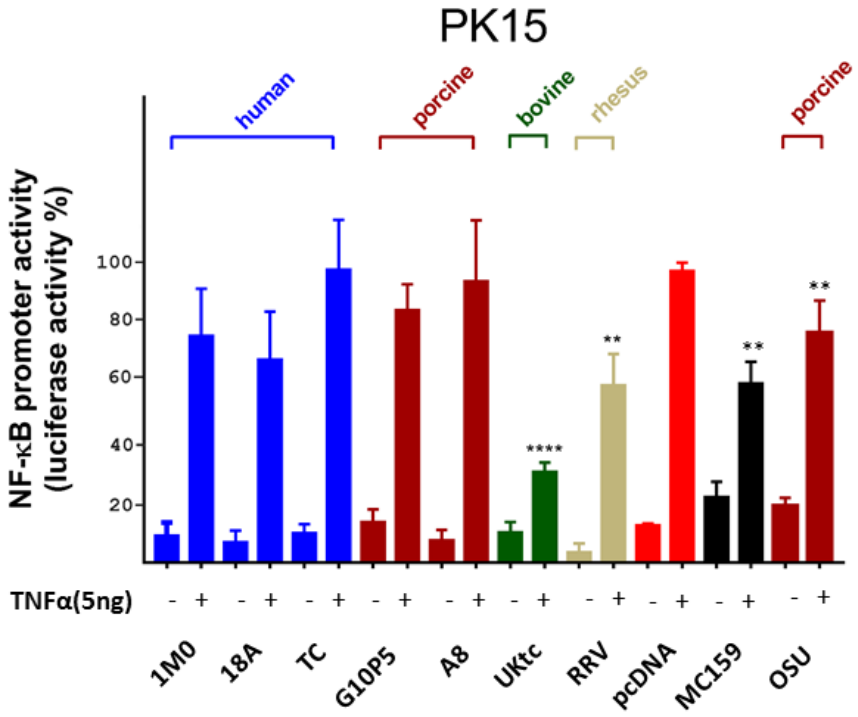

Figure 44. NF-kB downregulation by plasmid-encoded NSP1 in porcine PK15 cell lines.

PK15 cells were co-transfected with plasmid encoding either human (1M0, 18A, TC) porcine (G10P5, A8, OSU), bovine (UKtc), rhesus (RRV) NSP1 along with an NF-κB reporter and *Renilla* plasmid. Controls included transfection with an empty vector (pcDNA3.1) and plasmid expressing MCV-MC159. Plasmid-encoded proteins were allowed to express for 24h and cells were exposed to 5 ng/ml of pig TNFα or mock induced. 16h post-induction cells were harvested and luciferase values were read. NF-κB transcriptional activity (expressed in percentage) was determined by normalising the luciferase activity to *Renilla* and comparing the signals in cells transfected with NSP1 and cells expressing an empty vector. Data are presented as the mean of four independent experiments (+/- SD) and analysed with Student T-test **P<0.01, ****P<0.0001.

Next, the previously generated chimeric NSP1 plasmids (18AUKtc or UKtc18A) were used to assess the ability of the encoded proteins to inhibit the NF-κB promoter activity in HEK293 cells following TNFα treatment. Figure 45 shows that swapping domains between the human 18A and the bovine UKtc appeared not to compromise the functionality of the viral protein, which were still able to downregulate NF-κB activity. The chimeric 18AUktc, containing the 18A N-terminus and the UKtc C-terminus, showed a profile similar to that of the parental NSP1 UKtc protein, being able to reduce NF-κB activity to ~50% ($P<0.0001$). By contrast, the UKtc18A, which had the UKtc N-terminus and the 18A C-terminus, showed a profile similar to the parental strain 18A, showed a similar profile to the parental 18A, modulating the NF-κB activity down to ~30% ($P<0.001$). Consistent with previous results (Figure 43), MCV-MC159 appeared to knock down NF-κB activity to ~40% ($P<0.0001$).

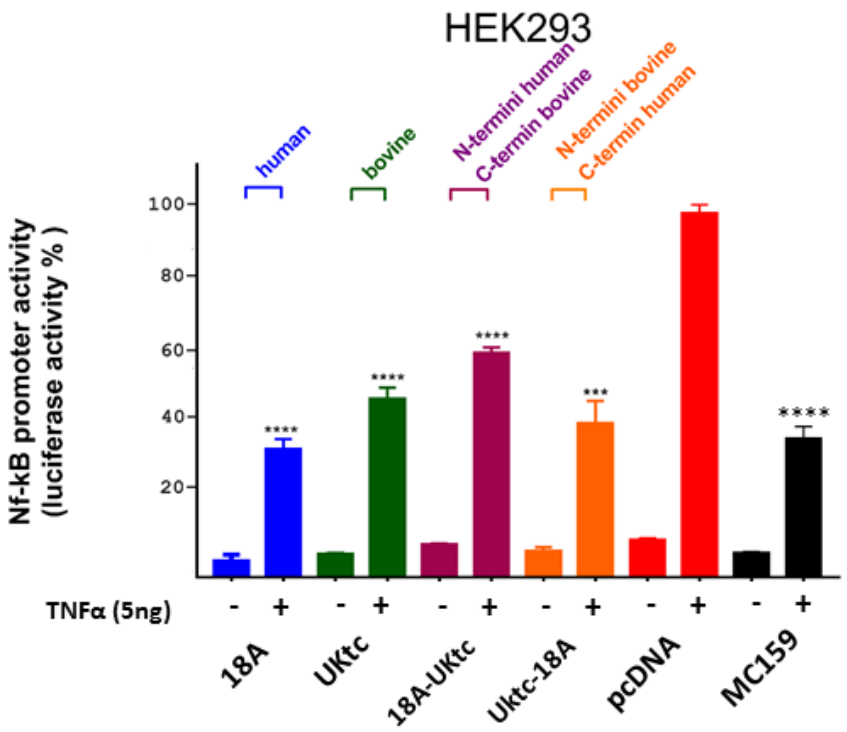

Figure 45. NF-κB downregulation by plasmid-encoded NSP1 in human HEK293 cell lines: swapped domains between the human 18A and the bovine UKtc.

HEK293 cells were co-transfected with plasmids encoding either the human NSP1 18A, the bovine NSP1 UKtc, the recombinant 18AUKtc or the recombinant UKt18A along with an NF-κB reporter and *Renilla* plasmid. Controls included transfection with an empty vector (pcDNA3.1) and plasmid expressing MCV-MC159. 24h post-transfection cells were treated with TNFα for 16h, before being harvested and luciferase values were read. Activation of the NF-κB transcriptional activity (expressed in percentage) was determined by normalising the luciferase activity to *Renilla* and comparing the signals in cells transfected with NSP1 and cells expressing an empty vector. Data are presented as the mean of two independent experiments (+/- SD) and analysed with Student T-test, ***P<0.001, ****P<0.0001.

The recombinant NSP1 18AUKtc of 499 aa in length has the N-terminus region (212 aa) from the human 18A and the C-terminus (287 aa) from the bovine UKtc. The recombinant UKtc18A of 487 aa in length has the N-terminus (220 aa) from the bovine UKtc and the C-terminus (267 aa) from the human 18A.

5.2.1.3.1 Dissecting the NF-KB pathway

Having identified the ability of NSP1 to downregulate the induction of IFN-λ (5.2.1.2) and having established that NSP1 is able to reduce TNFα-induced activation of the NF-κB promoter (5.2.1.3), which has been shown to be a responsible for a potent and sustained induction of type III IFN (Siegel *et al.*, 2011; Thomson *et al.*, 2009), the ability of NSP1 to target components of the NF-κB canonical pathway was investigated. In order to evaluate the effect of NSP1 on specific components involved in the activation of NF-κB transcriptional activity, preliminary experiments were performed in order to establish the responsiveness of the NF-κB reporter to ectopic expression of components involved in the canonical NF-κB pathway.

5.2.1.3.1.1 Ikkα

In order to evaluate the inducibility of the NF-κB reporter in response to variation in concentration of IKKα, HEK293 cells were co-transfected with an empty vector (pcDNA3.1) along with p*K*B6tkluc, R*enilla* plasmid and 50 ng, 100 ng or 200 ng of a plasmid encoding the IKKα protein. 16h after co-transfection cells were harvested and luciferase activity values were determined (Figure 46). NF-κB canonical activation with 5 ng/ml of porcine TNFα was used as a positive control. The exogenous expression of 50 ng of IKKα appeared to marginally induce NF-κB transcriptional activity, however, when the amount was doubled to 100 ng, a negative effect was observed. Due to the lack of response of NF-κB to IKKα in a dose dependent manner, the effect of NSP1 on the IKKα-mediated activation of NF-κB was not further investigated.

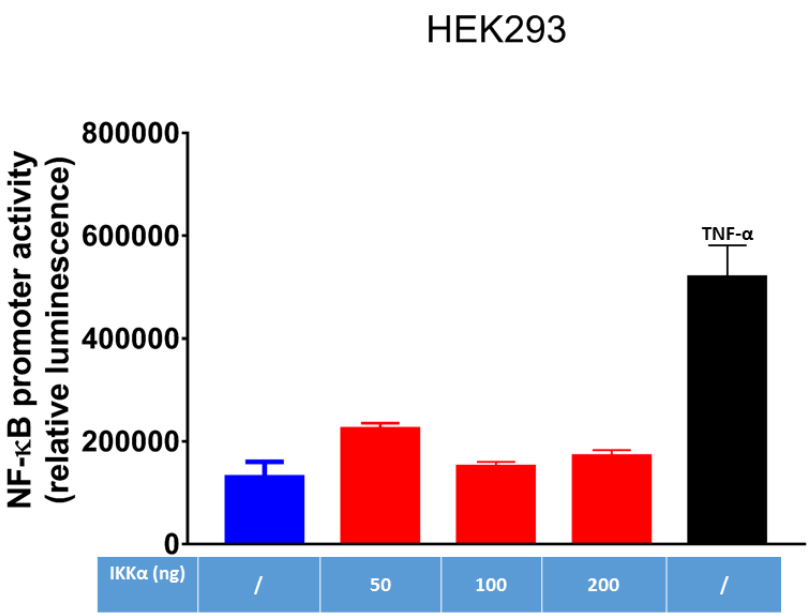

Figure 46. NF-κB promoter activity in response to exogenous expression of IKKα in human HEK293 cell line.

HEK293 cells were co-transfected with an empty vector pCDNA3.1, a NF-κB reporter and *Renilla* plasmid along with and 50 ng, 100 ng or 200 ng of IKKα. Equal amount of transfected DNA was reached with empty vector. Cells were allowed to express plasmid-encoded proteins 16h before being harvested and luciferase values were read. As positive control, cells were treated with 5 ng/ml of TNFα. Activation of the NF-κB transcriptional activity was determined by normalising the luciferase activity to *Renilla* and comparing the signals in cells transfected with IKKα and cells expressing an empty vector. Data are presented as the mean of one experiment (+/- SD).

5.2.1.3.1.2 Ikkβ

Next the ability of exogenous IKKβ to induce NF-κB transcriptional activity was investigated. HEK293 cells were co-transfected as previously described (5.2.1.3.1.1) along with 50 ng, 100 ng or 200 ng of IKKβ. 16 h after co-transfection cells were harvested and luciferase values were determined (Figure 47). NF-κB canonical activation with 5 ng/ml of porcine TNFα was used as a positive control. Co-transfection of 50 ng IKKβ was able to activate the transcriptional activity of NF-κB and a dosage-dependent increase was observed for increasing amounts of IKKβ.

Based on these results, the effect of NSP1 on the IKKβ-mediated activation of NF-κB was evaluated using 50 ng of IKKβ plasmid for co-transfections.

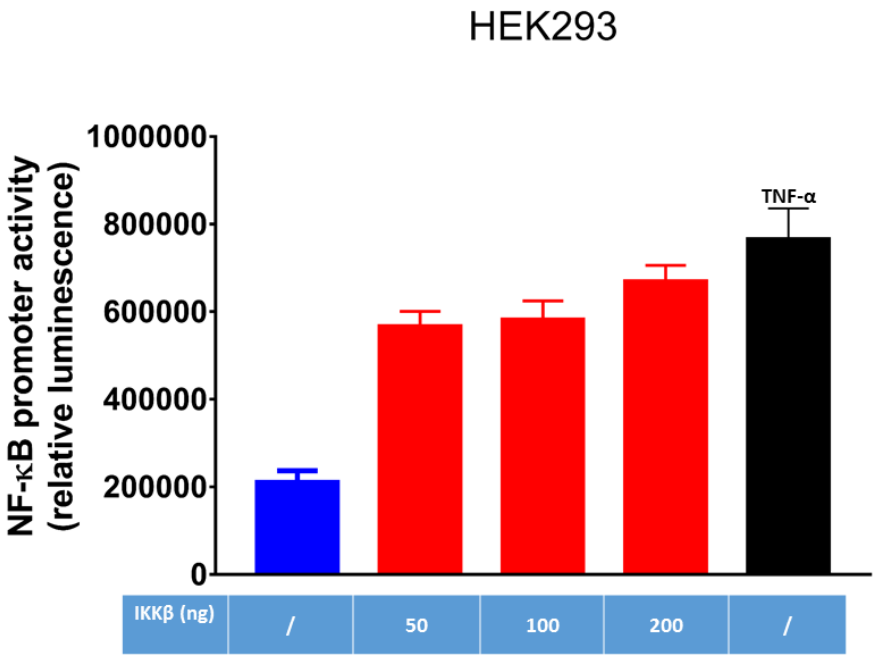

Figure 47. NF-κB promoter activity in response to exogenous expression of IKKβ in human HEK293 cell line.

HEK293 cells were co-transfected with an empty vector pCDNA3.1, a NF-κB reporter and *Renilla* plasmid along with and 50 ng, 100 ng or 200 ng of IKKβ. Equal amount of transfected DNA was reached with empty vector. Cells were allowed to express plasmid-encoded proteins 16h before being harvested and luciferase values were read. As a postive control, cells were treated with 5 ng/ml of TNFα. Activation of the NF-κB transcriptional activity was determined by normalising the luciferase activity to *Renilla* and comparing the signals in cells transfected with IKKα and cells expressing an empty vector. Data are presented as the mean of one experiment (+/- SD).

HEK293 cells were co-transfected with p*K*B6tkluc, *Renilla* plasmid and a plasmid expressing human (1M0, 18A and TC), porcine (G10P5, A8 and OSU), bovine (UKtc) or rhesus (RRV) NSP1 or an empty (vector pcDNA3.1). 24h after co-transfection cells were harvested and luciferase values were determined (Figure 48). The effect of NSP1 on the induction of NF-κB activity was evaluated by comparing

luciferase activity between cells expressing the viral protein and those expressing an empty vector. The human 1M0 (P<0.01) and TC (P<0.01), together with the porcine G10P5 (P<0.05) and the rhesus RRV (P<0.05) were able to knock down the IKKβ-mediated transcriptional activity of NF-κB to ~50%. The bovine UKtc (P<0.001) and the porcine OSU (P<0.001) showed a more potent effect, being able to downregulate NF-κB to ~30%. Downregulation observed for the porcine A8 was not statistically significant.

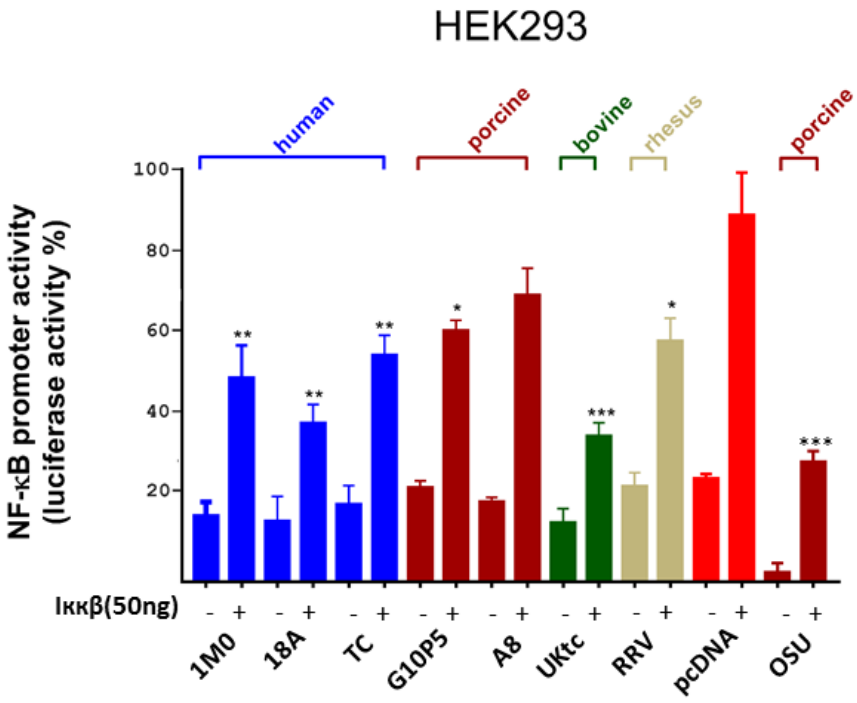

Figure 48. Effects of plasmids-encoded NSP1 on the Ikkβ-mediated activation of NF-κB transcriptional activity in human HEK293 cell line.

HEK293 cells were co-transfected with plasmids encoding either human (1M0, 18A, TC) porcine (G10P5, A8, OSU), bovine (UKtc) or rhesus (RRV) NSP1 proteins along with an NF-κB reporter and *Renilla* plasmid. Controls included transfection with an empty vector (pcDNA3.1). Activation of NF-κB transcriptional activity was achieved transfecting cells with 50 ng of IKKβ. 16h post-transfection cells were harvested and luciferase values were read. Activation of the NF-κB (expressed in percentage) was determined by normalising the luciferase activity to *Renilla* and comparing the signals in cells transfected with NSP1 and cells expressing an empty vector. Data are presented as the mean of three independent experiments (+/- SD) and analysed with Student T-test *P<0.05, **P<0.01, ***P<0.001.

5.2.1.3.1.3 β-TrCP

In order to evaluate if NF-κB transcriptional activity could be triggered in HEK293 through the exogenous expression of β-TrCP, cells were co-transfected with 250 ng of empty vector (pcDNA3.1) along with a reporter plasmid encoding firefly under the control of the human NF-κB promoter, R*enilla* plasmid and 50 ng, 100 ng or 200 ng of plasmid encoding the sequence for β-TrCP. 16h after co-transfection cells were treated with 5 ng/ml of TNFα to for a further 6h, 12h or 24h before being harvested and luciferase values determined (Figure 49). NF-κB canonical activation with 5 ng/ml of porcine TNFα was used as positive control. As previously shown (Figure 42) treatment of HEK293 cells with TNFα induced a strong response in NF-κB transcriptional activity at 6h post treatment. As expected, TNFα treatment led to a significant increase in luciferase activity (P<.0001), however, this was not improved by prior co-transfection of the β-TrCP plasmid. In fact, co-transfection of the β-TrCP and subsequent TNFα treatment for 6h and 12h led to relative luminescence values that were ~50% lower than those observed for TNFα treatment only. Co-transfection followed by TNFα treatment for 24h after led to further reductions in relative luminescence values when 100 ng and 200 ng of the β-TrCP plasmid were used.

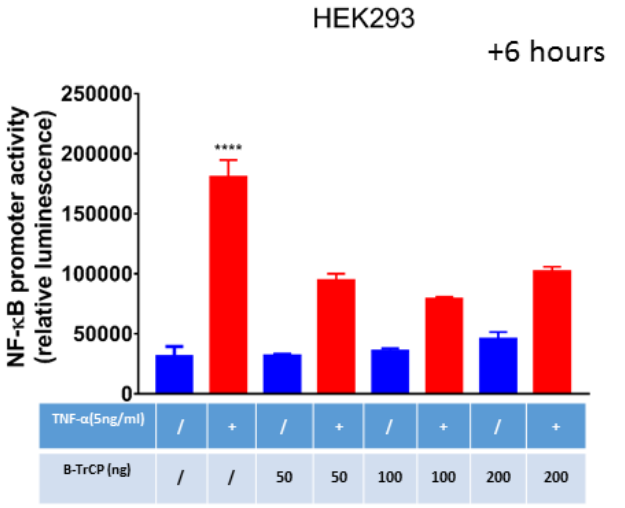
HEK293
+6 hours
NF-κB promoter activity (relative luminescence)
250000
200000
150000
100000
50000
0
****
TNF-α(5ng/ml) / + / + / + / +
B-TrCP (ng) / / 50 50 100 100 200 200

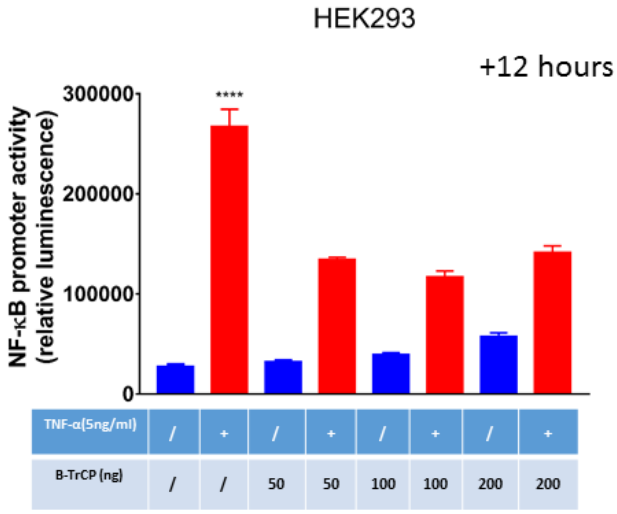
HEK293
+12 hours
NF-κB promoter activity (relative luminescence)
300000
200000
100000
0
****
TNF-α(5ng/ml) / + / + / + / +
B-TrCP (ng) / / 50 50 100 100 200 200

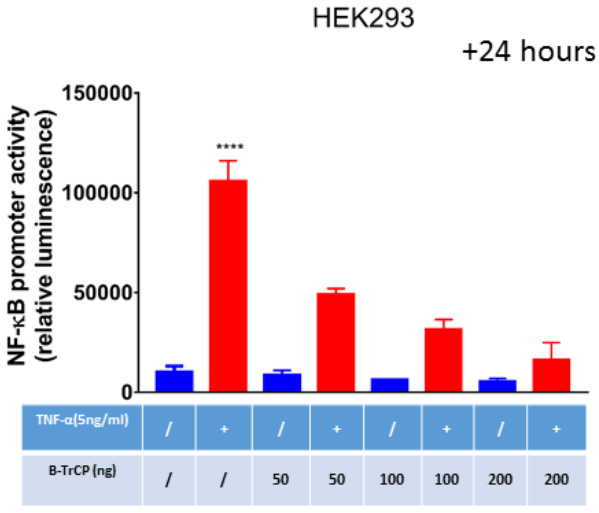
HEK293
+24 hours
NF-κB promoter activity (relative luminescence)
150000
100000
50000
0
****
TNF-α(5ng/ml) / + / + / + / +
B-TrCP (ng) / / 50 50 100 100 200 200

Figure 49. NF-κB promoter activity in response to exogenous expression of β-TrCP in human HEK293 cell lines.

HEK293 cells were co-transfected with 250ng of an empty vector (pCDNA3.1), a NF-κB reporter and *Renilla* plasmid, along and 50 ng, 100 ng or 200 ng of β-TrCP. Equal amount of transfected DNA was reached with empty vector. Cells were allowed to express plasmid-encoded proteins for 24 h and then exposed to 5ng/ml of pig TNFα. 6h, 12h and 24h post-induction, cells were harvested and luciferase values were read. Activation of NF-κB activity was determined by normalising the luciferase activity to *Renilla* and comparing the signals in cells transfected with β-TrCP and treated with TNFα. Data are presented as the mean of one experiment (+/- SD).

The activity of NF-κB needs to be strictly controlled and a negative feedback loop is in place. The exacerbating overexpression of one of the components involved in the NF-κB canonical induction pathway can result in NF-κB-mediated induction of IκB. Newly synthetized IκB moves to the nucleus, binds to NF-κB and translocates into the cytoplasm, thereby terminating NF-κB directed transcription (Fagerlund *et al.*, 2015). Based on that, the induction of NF-κB was investigated only in response to exogenous expression of β-TrCP, without TNFα treatment. Due to the fact that no difference was observed between cells transfected with 50 ng of β-TrCP and cells containing only media, $\leq$50 ng of β-TrCP plasmid was used for co-transfections. HEK293 cells were co-transfected with an empty vector (pcDNA3.1) along with a reporter plasmid encoding firefly under the control of the human NF-κB promoter, R*enilla* plasmid and 10 ng, 25 ng or 50 ng of β-TrCP plasmid. NF-κB canonical activation with 5 ng/ml of porcine TNFα was used as control. 16h after co-transfection cells were harvested and luciferase values were determined (Figure 50). Indeed the overexpression of β-TrCP was able to induce the NF-κB promoter leading to a significant increase ($P<0.001$) in luciferase activity. No substantial differences observed between 10 ng and 25 ng. Consistent with previously presented data (Figure 49), 50 ng appeared to be the highest amount of β-TrCP plasmid that could be transfected before a comparative decrease in relative luminescence was observed. Based on this, the effect of NSP1 on the β-TrCP-mediated activation of NF-κB was evaluated following co-transfection of 25 ng β-TrCP plasmid.

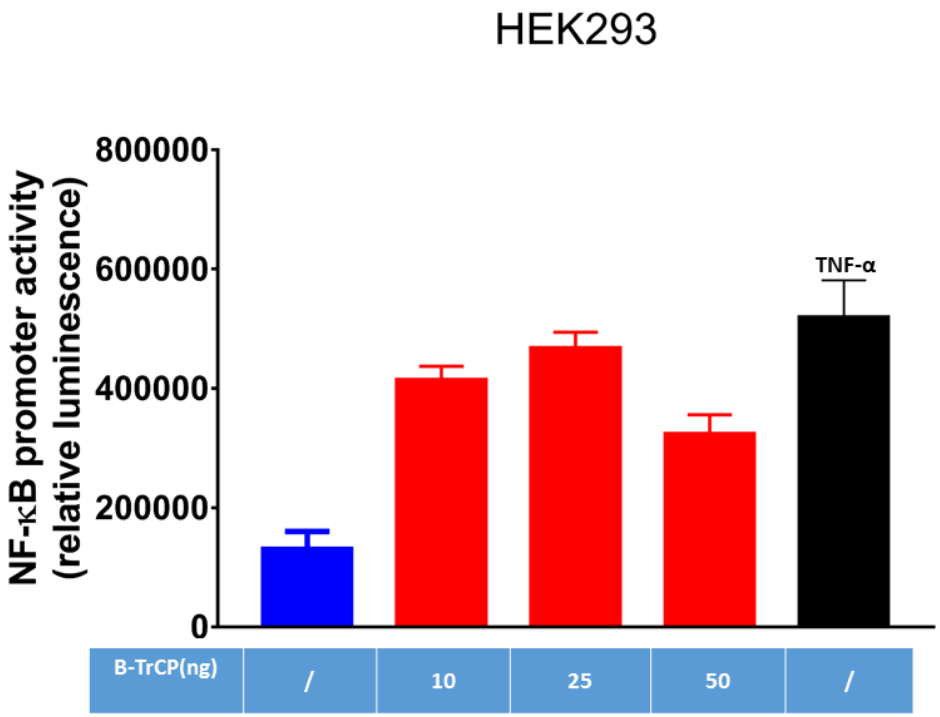

Figure 50. NF-κB promoter activity in response to exogenous expression of β-TrCP in human HEK293 cell lines.

HEK293 cells were co-transfected with an empty vector (pCDNA3.1), a NF-κB reporter and *Renilla* plasmid, along with 10 ng, 25 ng or 50 ng of for β-TrCP. Equal amount of transfected DNA was reached with empty vector. 16h post-transfection cells were harvested and luciferase values were read. As positive control, cells were treated with 5 ng/ml of TNFα. Activation of the NF-κB transcriptional activity was determined by normalising the luciferase activity to *Renilla* and comparing the signals in cells transfected with β-TrCP and cells expressing an empty vector. Data are presented as the mean of one experiment (+/- SD).

HEK293 cells were co-transfected with p*K*B6tkluc, *Renilla* plasmid and a plasmid expressing human (1M0, 18A and TC), porcine (G10P5, A8 and OSU), bovine (UKtc) or rhesus (RRV) NSP1 or an empty vector (pcDNA3.1). NF-κB transcription was activated by co-transfecting cells with 25 ng of β-TrCP or mock-transfected. 24h after co-transfection cells were harvested and luciferase values determined (Figure 51). The effect of NSP1 on the induction of NF-κB promoter activity was evaluated by comparing the relative luminescence between cells expressing the viral protein and those expressing an empty vector. The human 1M0 and TC ($P<0.001$), together with the porcine G10P5 ($P<0.001$) and OSU ($P<0.0001$), the bovine UKtc ($P<0.01$) and rhesus RRV ($P<0.01$) were all able to reduce luciferase activity to ~50%. The human 18A was able to further reduce the transcriptional activity to ~40% ($P<0.001$). By contrast, porcine A8 showed a lower efficiency, reducing luciferase activity to ~70% ($P<0.01$).

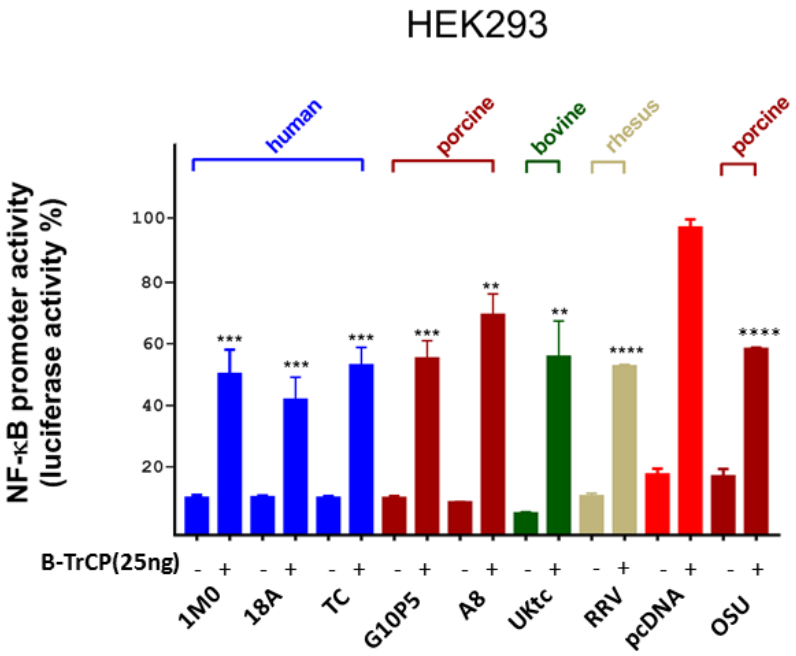

Figure 51. Effects of plasmids-encoded NSP1 on the β-TrCP-mediated activation of NF-κB transcriptional activity in human HEK293 cell line.

HEK293 cells were co-transfected with plasmids encoding either human (1M0, 18A, TC) porcine (G10P5, A8, OSU), bovine (UKtc) or rhesus (RRV) NSP1 proteins along with an NF-κB reporter and *Renilla* plasmid. Controls included transfection with an empty vector (pcDNA3.1). Activation of NF-κB transcriptional activity was achieved transfecting cells with25 ng of β-TrCP. 16h post-transfection cells were harvested and luciferase values were read. Activation of the NF-κB (expressed in percentage) was determined by normalising the luciferase activity to *Renilla* and comparing the signals in cells transfected with NSP1 and cells expressing an empty vector. Data are presented as the mean of three independent experiments (+/- SD) and analysed with Student T-test **P<0.01, ***P<0.001, ****P<0.0001.

5.2.1.3.1.4 p50

Given that p50–p65 is the most commonly detected NF-κB dimer, the ability of NSP1 to downregulate NF-κB transcriptional activity by targeting p50 or p65 was investigated. Preliminary experiments were performed to study inducibility of the NF-κB activity in response to increasing concentrations of p50 and p65. In order to do this HEK293 cells co-transfected with p*K*B6tkluc, R*enilla* plasmid and 50 ng, 100 ng or 200 ng of plasmid encoding the sequence for p50. 16h after co-transfection cells were treated with 5 ng/ml of TNFα for 6h, 12h or 24h before being harvested and luciferase values determined (Figure 52). p50 was unable to induce NF-κB activity, as an increase in luciferase activity was only observed when cells were subsequently treated with TNFα. In addition, increasing the concentration of co-transfected p50 appeared to have a negative feedback on NF-κB transcriptional activity following TNFα treatment. Based on results previously observed with β-TrCP (Figure 50), a reduced amount of p50 plasmid was co-transfected to induce the NF-κB promoter, and subsequent TNFα treatment was not used.

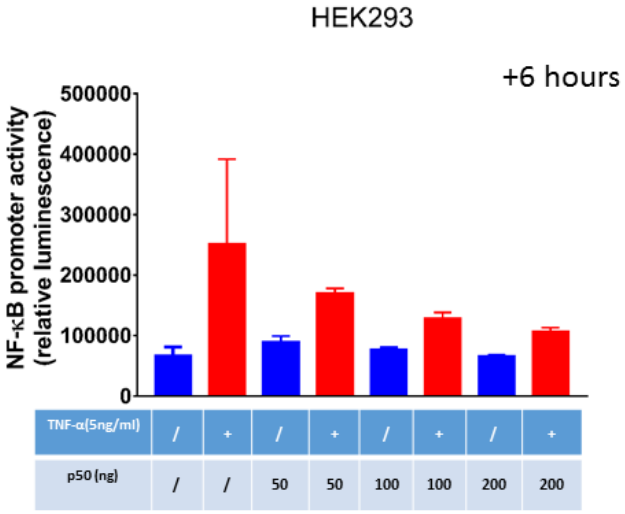
HEK293
+6 hours
NF-κB promoter activity (relative luminescence)
500000
400000
300000
200000
100000
0
TNF-α(5ng/ml) / + / + / + / +
p50 (ng) / / 50 50 100 100 200 200

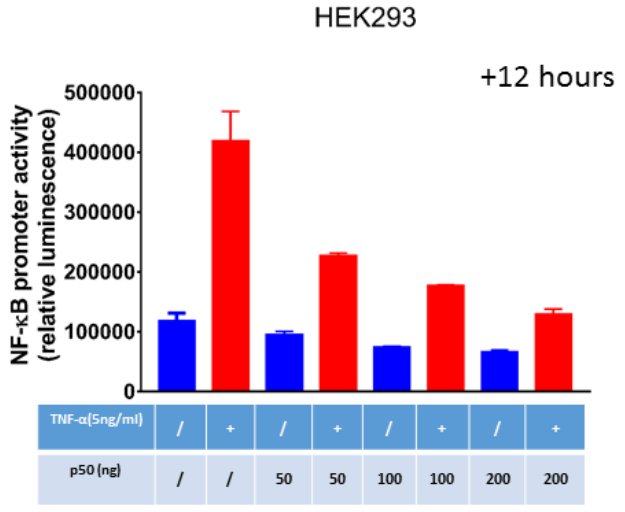
HEK293
+12 hours
NF-κB promoter activity (relative luminescence)
500000
400000
300000
200000
100000
0
TNF-α(5ng/ml) / + / + / + / +
p50 (ng) / / 50 50 100 100 200 200

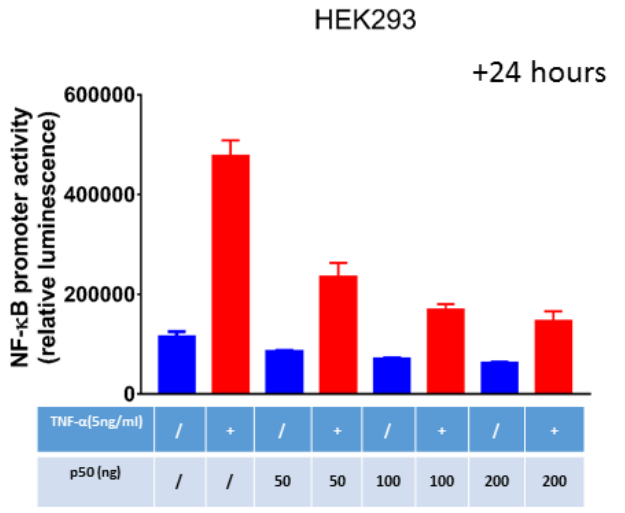
HEK293
+24 hours
NF-κB promoter activity (relative luminescence)
600000
400000
200000
0
TNF-α(5ng/ml) / + / + / + / +
p50 (ng) / / 50 50 100 100 200 200

Figure 52. NF-κB promoter activity in response to exogenous expression of p50 in human HEK293 cell lines.

HEK293 cells were co-transfected with 250ng of an empty vector (pCDNA3.1), NF-κB reporter and *Renilla* plasmid, along and 50 ng, 100 ng or 200 ng of p50. Equal amount of transfected DNA was reached with empty vector. Cells were allowed to express plasmid-encoded proteins for 24 h and then exposed to 5ng/ml of pig TNFα. 6h, 12h and 24h post-induction, cells were harvested and luciferase values were read. Activation of NF-κB activity was determined by normalising the luciferase activity to *Renilla* and comparing the signals in cells transfected with p50 and treated with TNFα. Data are presented as the mean of one experiment (+/- SD).

Figure 53 shows that co-transfection of 10 ng of p50 plasmid, in the absence of subsequent TNFα treatment, mediated an increase in luciferase activity in HEK293 cells ($P<0.05$). However, co-transfection of 25 ng and 50 ng of p50 plasmid both led to a decrease in luciferase activity. NF-κB canonical activation with 5 ng/ml of porcine TNFα, in the absence of co-transfection of the p50 plasmid, was used as control and led to the highest increase in luciferase activity ($P<0.05$). This data suggested that at lower concentration, p50 is potentially dimerising with itself or available p65, moving into the nucleus and initiate transcription (Tong *et al.*, 2004). However, when expression of p50 exceeded critical threshold, a negative feedback loop of NF-κB was induced. Based on these results, the overexpression of p50 was excluded from further investigation.

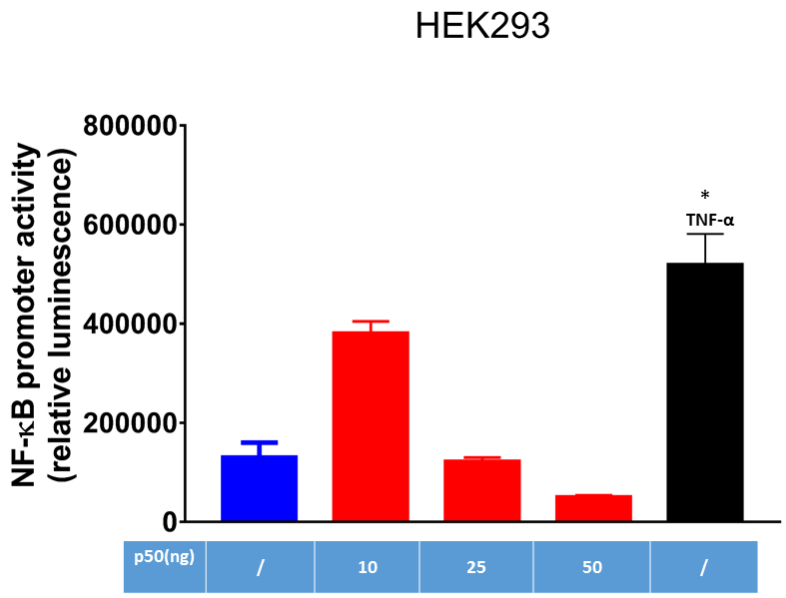

Figure 53. NF-κB promoter activity in response to exogenous expression of p50 in human HEK293 cell lines.

HEK293 cells were co-transfected with an empty vector pCDNA3.1, a NF-κB reporter and *Renilla* plasmid along with 10 ng, 25 ng or 50 ng of p50. Equal amount of transfected DNA was reached with empty vector. Cells were allowed to express plasmid-encoded proteins16h before being harvested and luciferase values were read. As positive control, cells were treated with 5 ng/ml of TNFα. Activation of the NF-κB transcriptional activity was determined by normalising the luciferase activity to *Renilla* and comparing the signals in cells transfected with p50 and cells expressing an empty vector. Data are presented as the mean of two experiments (+/- SD).

5.2.1.3.1.5 p65

p65 (known also as RelA) is the major transcriptional activating NF-κB subunit. In resting conditions, p65 nuclear signal is sequestered by IκB, however, upon phosphorylation and β-TrCP-mediated degradation of IκB, nuclear signal is exposed and p65 is able to translocate to the nucleus. In order to evaluate if RV NSP1 can target p65, preliminary experiments were performed in order to evaluate if NF-κB activity responded to a variation in the cellular concentration of p65. In order to do this HEK293 cells were co-transfected with an empty vector (pcDNA3.1) along with p*K*B6tkluc, R*enilla* plasmid and either 10 ng, 25 ng or 50 ng of plasmid encoding the

sequence for p65. 16h after co-transfection cells were harvested and luciferase values determined (Figure 54). NF-κB canonical activation with 5 ng/ml of porcine TNFα was used as control. The exogenous expression of p65 appeared to induce NF-κB activity in dose-dependent manner. Based on this, the effect of NSP1 on the p65-mediated activation of NF-κB was evaluated activating NF-κB promoter activity with the ectopic expression of 50 ng of p65.

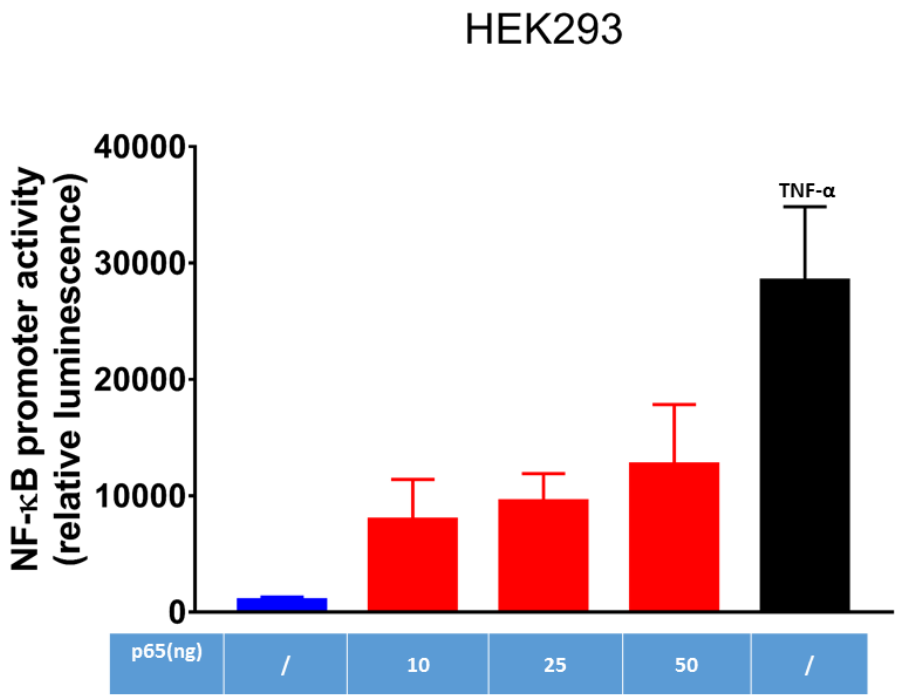

Figure 54. NF-κB promoter activity in response to exogenous expression of p65 in human HEK293 cell lines.

HEK293 cells were co-transfected with an empty vector pCDNA3.1, a NF-κB reporter and a *Renilla* plasmid along with 10 ng, 25 ng or 50 ng of p65. Equal amount of transfected DNA was reached with empty vector. Cells were allowed to express plasmid-encoded proteins16h before being harvested and luciferase values were read. As positive control, cells were treated with 5 ng/ml of TNFα. Activation of the NF-κB transcriptional activity was determined by normalising the luciferase activity to *Renilla* and comparing the signals in cells transfected with 65 and cells expressing an empty vector. Data are presented as the mean of two experiments (+/- SD).

HEK293 cells were co-transfected with p*K*B6tkluc, *Renilla* plasmid and a plasmid expressing either human (1M0, 18A and TC), porcine (G10P5, A8 and OSU), bovine (UKtc) and rhesus (RRV) NSP1 or empty vector (pcDNA3.1). NF-κB was activated with the exogenous expression of p65 or mock-transfected. 24h after co-transfection cells were harvested and luciferase values determined (Figure 55). The bovine UKtc and the porcine OSU were able to reduce NF-κB activity to ~60% ($P<0.01$), while the rhesus RRV showed an effect of the 20% ($P<0.01$). The human strain 1M0, 18A and TC and the porcine G10P5 and A8 appeared to have no effect on the p65-mediated activation of NF-κB transcriptional activity.

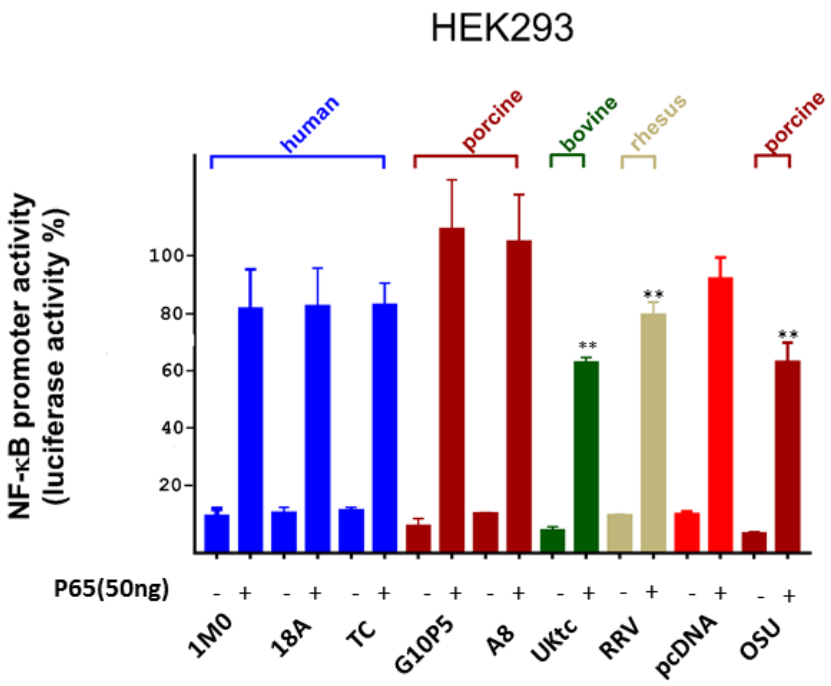

Figure 55. Effects of plasmids-encoded NSP1 on the p65-mediated activation of NF-κB transcriptional activity in human HEK293 cell lines.

HEK293 cells were co-transfected with plasmids encoding either human (1M0, 18A, TC) porcine (G10P5, A8, OSU), bovine (UKtc) or rhesus (RRV) NSP1 proteins along with a plasmid expressing luciferase under the control of mice NF-κB promoter and a non-inducible plasmid expressing *Renilla* and a plasmid expressing p65. Controls included transfection with an empty vector (pcDNA3.1). 24h post-transfection cells were harvested and luciferase values were read. Activation of the NF-

κB transcriptional activity (expressed in percentage) was determined by normalising the luciferase activity to *Renilla* and comparing the signals in cells transfected with NSP1 and cells expressing an empty vector. Data are presented as the mean of three independent experiments (+/- SD) and analysed with Student T-test **P<0.01.

5.2.1.4 NSP1-mediated antagonization of Mx promoter activity

It has been shown that the NSP1 protein encoded by the rhesus RV isolate (RRV) is able to affect the expression of ISGs by blocking STAT/1/2 nuclear translocation (Holloway *et al.*, 2014; Sen *et al.*, 2014). In order to investigate the ability of other NSP1 proteins to block the ISG induction a luciferase reporter assay was used in which the promoter sequence of the pig Mx_2 gene was inserted upstream of a firefly luciferase reporter plasmid.

Preliminary experiments were performed to evaluate the inducibility of Mx_2 reporter upon IFN treatment. HEK293 cells were co-transfected with Mx_2 reporter, R*enilla* plasmid and an empty vector (pcDNA3.1) or plasmid encoding Rinderpest virus (RPV) Saudi/81 V protein as positive control (Chinnakannan *et al.*, 2013). 24h after co-transfection cells were treated with 500 U/µl, 1000 U/µl, or 2000 U/µl of pig IFN-α (Abcam, #ab209114) for a further 6h or 8h, or were infected with SeV for 16h. Cells were then harvested and luciferase values determined (Figure 56). Treatment of HEK293 with IFN-α to induce Mx_2 transcription resulted in a small, but not significant increase inMx_2 promoter activation at 6h post-treatment, however, no substantial difference was observed in response to increasing concentrations of IFN-α. Activation of the Mx_2 promoter was also observed 18h post-treatment, however, this was unspecific the induction was observed in treated (red and purple bars) and mock-treated samples (blue bars).

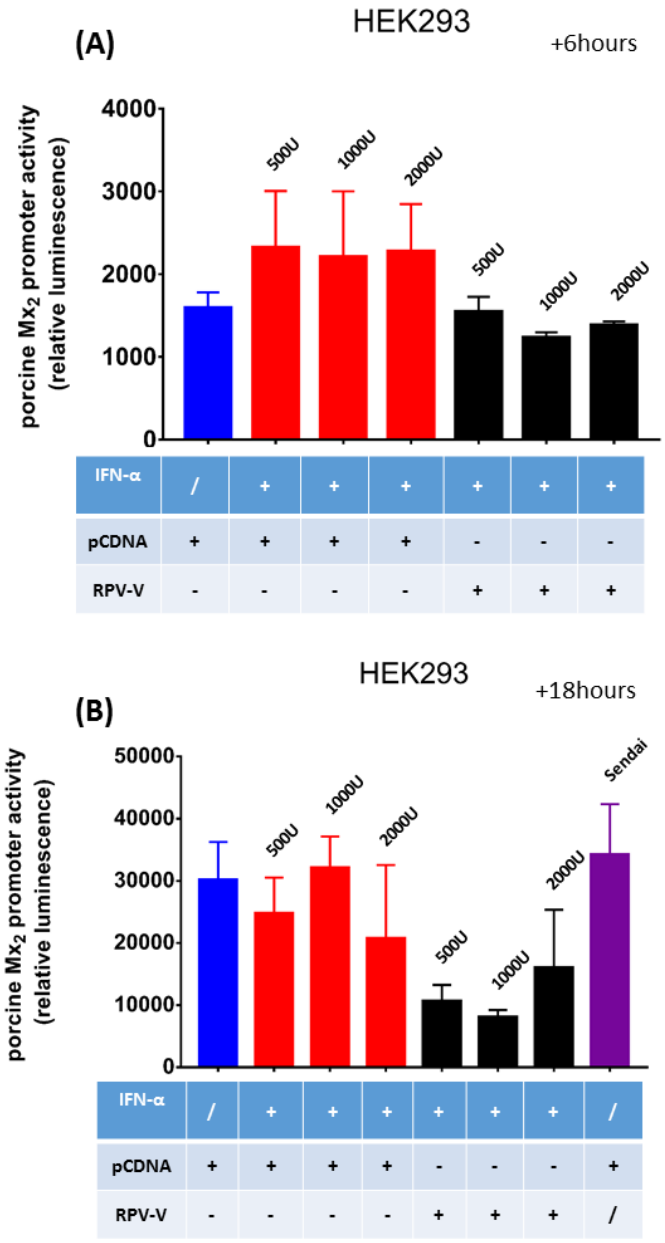

Figure 56. Porcine Mx_2 induction in human HEK293 cell lines.

HEK293 cells were co-transfected with an empty vector (pcDNA3.1) or Rinderpest virus (Saudi/80) V protein along with Mx_2 reporter and a *Renilla* plasmid. After 24h cells were exposed to 500 U/ml 1000 U/ml or 2000 U/ml of pig IFNα or infected with SeV. 6h or 18h post-treatment cells were harvested and luciferase values were read. Mx_2 relative promoter activity was evaluated comparing luciferase produced in cells treated with IFNα with those containing only media. Data are provided as the means ± ranges of luciferase activity normalised to Renilla levels from one experiment with error bars representing standard deviation.

Strong basal luciferase activity has previously been reported for the Mx_2 luciferase reporter in the absence of IFN stimulation by Jorns *et al* (Jorns *et al.*, 2006). They reported that a selective induction was achieved when the reporter gene was under the control of a 2.300 Kb-fragment of the mouse Mx_1 promoter (Hug *et al.*, 1988). Therefore,HEK293 cells were co-transfected with a reporter plasmid encoding firefly under the control of the mouse Mx_1 promoter (pGL3-Mx1P-luc, gift from Prof Kocks – Virology Institute of Freiburg), R*enilla* plasmid and a plasmid expressing either human (1M0, 18A and TC), porcine (G10P5 and A8), bovine (UKtc) or rhesus (RRV) NSP1. The RPV Saudi/81 V plasmid and empty vector (pcDNA3.1) were used as controls. 24h after co-transfection cells were treated with 500 U/ml of pig IFNα for a further 16 h to induce the Mx_1 promoter. Cells were then harvested and luciferase values determined (Figure 57). The human NSP1 1M0, 18A and TC ($P<0.0001$) and the rhesus RRV ($P<0.0001$) were all able to reduce luciferase activity to ~80%. The porcine G10P5 and A8 reduced luciferase activity to ~70% ($P<0.0001$), while the bovine reduced it to 50% ($P<0.001$). RPV-V appeared to completely abolish Mx_1 promoter activity ($P<0.0001$).

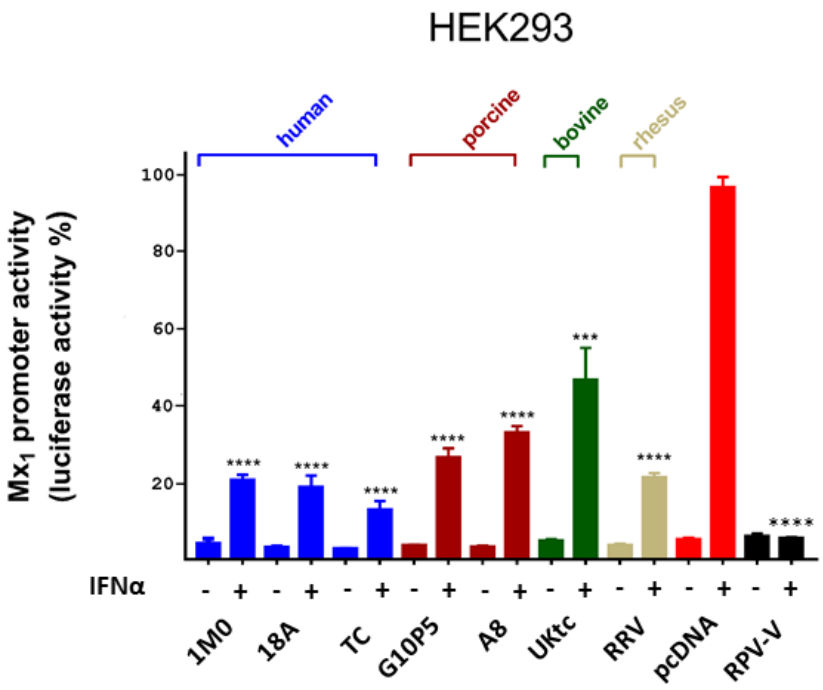

Figure 57. Murine Mx1 downregulation by plasmid-encoded NSP1 in human HEK293 cell lines.

HEK293 cells were co-transfected with plasmids encoding either human (1M0, 18A, TC) porcine (G10P5, A8), bovine (UKtc) or rhesus (RRV) NSP1 proteins along with a Mx_1 reporter and a *Renilla* plasmid. Controls included transfection with an empty vector (pcDNA3.1) and plasmid expressing Rinderpest virus V protein (RPV-V). 24h post-transfection cells were treated with pig IFNα for 16h, before being harvested and luciferase values were read. Activation of the Mx_1 promoter (expressed in percentage) was determined by normalising the luciferase activity to *Renilla* and comparing the signals in cells transfected with NSP1 and cells expressing an empty vector. Data are presented as the mean of three independent experiments (+/- SD) and analysed with Student T-test ***P<0.001, ****P<0.0001.

The ability of NSP1 to downregulate transcriptional activity of the Mx_1 promoter was investigated in other human cell lines, however, transfections of HT-29 and Caco-2 human-derived cell lines were unsuccessful, yielding non detectable luminescence values. The PK15 porcine cell line was next evaluated. Cells were co-transfected as previously described, treated with IFN-α and luciferase activity under the control of Mx_1 promoter was measured (Figure 58). The human NSP1 1M0 and TC were able to reduce luciferase activity to ~40% ($P<0.01$). Human 18A ($P<0.001$), together with the porcine G10P5 and A8 and the bovine UKtc ($P<0.001$) all reduced luciferase activity to ~30%, while the rhesus RRV reduced it to ~20% ($P<0.001$). Consistent with previous data (Figure 57), in PK15 cell lines, RPV-V appeared to knock down Mx_1 promoter to 10% ($P<0.001$).

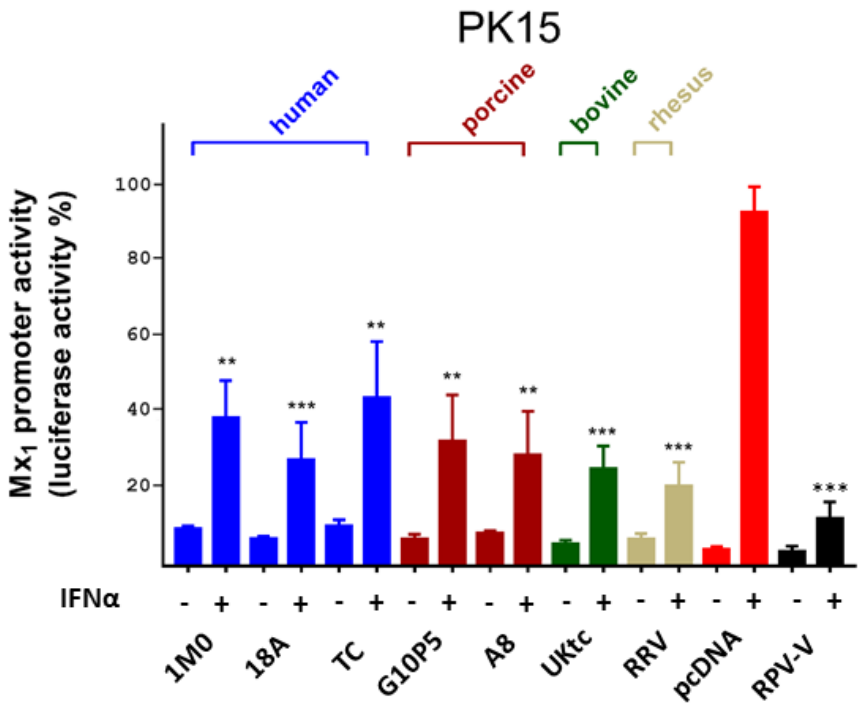

Figure 58. Murine Mx1 downregulation by plasmid-encoded NSP1 in porcinePK15 cell lines.

PK15 cells were co-transfected with plasmids encoding either human (1M0, 18A, TC) porcine (G10P5, A8), bovine (UKtc) or rhesus (RRV) NSP1 proteins along with a Mx_1 reporter and a *Renilla* plasmid. Controls included transfection with an empty vector (pcDNA3.1) and plasmid expressing Rinderpest virus V protein (RPV-V). 24h post-transfection cells were treated with pig IFNα for 16h, before being harvested and luciferase values were read. Activation of the Mx_1 promoter (expressed in percentage) was determined by normalising the luciferase activity to *Renilla* and comparing the signals in cells transfected with NSP1 and cells expressing an empty vector. Data are presented as the mean of three independent experiments (+/- SD) and analysed with Student T-test **P<0.01, ***P<0.001.

5.3 Summary of the luciferase reporters

Results obtained in this chapter have reported a strain-specific ability of RV NSP1 to target the induction of type I and type III IFNs and their signalling pathway (Table 12). With the exception of the porcine-derived A8, all the NSP1 considered in this study appeared to be able to modulate the induction of type I IFN, IFN-β but not IFN-α. More pronounced effect in the downregulation of type III IFN was observed among different strains. In contrast, a more potent and conservative ability to target the transcriptional activity of NF-κB and the induction of Mx_1 was observed.

Table 12. Summary of the luciferase reporters.

Host origin	HUMAN			PORCINE		BOVINE	RHESUS
NSP1 strains	1M0	18A	TC	G10P5	A8	UKtc	RRV
Reporter							
IFN-β	++	++	++	++	NE	++	+++
IFN-α	NE	NE	NE	NE	+	++	NE
IFN-λ_1	++	++	++	+++	+	++	+++
IFN-λ_3	+	NE	NE	+	NE	++	+
NF-κB	++	++	++	+	++	+++	++
Mx_1	+++	+++	+++	+++	+++	++	+++

Table indicating the effects of plasmid-encoded NSP1 on the reporter activity of type I IFN (IFN-β and IFN-α), type III IFN (IFN-λ_1 and IFN-λ_3), NF-κB and Mx_1 in human cell lines HEK293. "+" indicates potency of downregulation: "+++" >70%, "++" 40%-60%, "+" 70%-90%. "NE" no effects.

6 Discussion

NSP1 is the most variable RV protein, with an amino acid sequence much more variable even then outer capsid proteins VP7 and VP4 (Dunn *et al.*, 1994). The functionality of NSP1 in downregulating the host innate immune response suggests that the viral protein is expressed during the early stages of RV replication soon after the infection. NSP1 expression throughout the course of infection is very low (Johnson *et al.*, 1989; Pina-Vazquez *et al.*, 2007) and the protein does not appear to be essential for RV replication in cell culture as mutants encoding a truncated version of the protein can still replicate, however, producing smaller virus plaques (Kanai *et al.*, 2017; K. Taniguchi *et al.*, 1996). The NSP1-mediated ability of RV to counteract the IFN response is conserved between strains infecting different species, however, targets within the induction and signalling pathways may vary (Arnold, 2016). NSP1 from bovine (UKtc), rhesus (RRV) and murine (EW) have been shown to target IRF-3 inducing its proteasome-mediated degradation (Barro et al., 2005; Sen et al., 2009). In contrast, the OSU-derived NSP1 has been reported to target the NF-kB pathway, inducing the degradation of β-TrCP (Di Fiore et al., 2015; Graff et al., 2009).

To understand if NSP1 derived from different RV strains are capable of down-regulating the induction of IFN in a host-specific manner, the Y-2-H system was employed to assess potential strain-specific interactions (Fields et al., 1989), which has been used in the past to screen for potential partner of NSP1 (Graff *et al.*, 2002).Y-2-H interaction assays carried out between NSP1 proteins derived from human (18A, 1M0, TC), porcine (G10P5, A8), bovine (UKtc) and rhesus (RRV) RV strains did not identify interactions with human MAVS, TBK1, RIG-I MDA5 and β-TrCP proteins under high stringency conditions (Figure 14, Figure 15, Figure 19). In contrast with Y-2-H screening, co-IP experiments reported that NSP1 encoded by pig (OSU), cattle (UKtc), human (Wa), mice (EW) and rhesus (RRV) RV strains interacted with human MAVS, driving its degradation (Nandi *et al.*, 2014). The same experimental approach was used to confirm an interaction between NSP1 derived from pig (OSU) and simian (SA-11) RV strains and RIG-I (Broquet *et al.*, 2011; Qin *et*

al., 2011). The interaction between β-TrCP and human NSP1 Wa was also confirmed by co-IP (Ding *et al.*, 2016) or pull-down (Lutz *et al.*, 2016), however, not by Y-2-H.

Y-2-H analysis performed in this study showed a strain-specific interaction occurring between IRF-3 and NSP1 encoded by different species. Some NSP1 were able to interact with IRF-3 from disparate host species even under high stringency conditions, while other NSP1 showed no interaction with any of the TF (Figure 14, Figure 15, Figure 16, Figure 17, Figure 18 and Figure 19). By contrast, other NSP1/IRF-3 interactions were detectable only under lower stringency conditions (Figure 20). The bovine UKtc showed a more promiscuous activity, being able to strongly interact with the IRF-3 encoded by human, pigs, cattle and monkeys. Swine NSP1 G10P5 was able to target both pig and monkey IRF-3, while no interactions were confirmed for swine NSP1 A8 due to its ability to self-activate the system (Figure 13). Lower stringency screening revealed how the human 1MO was weakly interacting with the human, bovine and monkey-derived IRF-3. The same stringency conditions revealed a weak or transient interaction between the human TC NSP1 and the monkey and cattle-derived IRF-3. The other human (18A) and the rhesus (RRV) NSP1 proteins showed no interactions, even under lower stringency conditions (Table 11).

The adaptor proteins STING, MAVS, and TRIF contain a conserved motif, pLxIS (in which p represents the hydrophilic residue, x represents any residue, and S represents the phosphorylation site), that is phosphorylated by TBK1 or IKKε and mediates the recruitment of IRF-3 to the signalling complexes (S. Liu *et al.*, 2015). Because the *p*L*x*IS motif plays a critical role in mediating the recruitment of IRF-3 in the cGAS-, RLR-, and TLR-signalling pathways, NSP1 employs this motif to sequester IRF-3 and induce its degradation (B. Zhao *et al.*, 2016). A BLAST homology search revealed that RV NSP1 also contains a *p*L*x*IS motif within its C-terminal 17 residues (B. Zhao *et al.*, 2016). Interestingly, of the NSP1 considered in this study, only rhesus NSP1 RRV contains a complete pLxIS motif (alignment not shown); however, it was not able to interact with any of the IRF-3 under the stringency conditions tested.

Y-2-H screening involving chimeric NSP1 suggested that both the amino and carboxyl termini regions of NSP1 cooperate for an optimal interaction with IRF-3. Those two regions carry respectively the putative RING domain (located in the N-terminus) and the pLxIS motif (located in the C-terminus). Proper folding and structure of NSP1 are important for IRF-3 interaction and experiments involving mutations in the zinc-binding RING domain have reported a reduction of 30% in IRF-3 binding ability (Graff *et al.*, 2007).

Luciferase reporters have shown the ability of all NSP1 to downregulate the IFN-β induction, targeting components that bind the PDR elements in the promoter region of type I IFN (Figure 30 and Figure 32). The bovine UKtc and the rhesus RRV mediated the highest reduction in IFN- β promoter activity. In contrast with Y-2-H assays, the use of a PDRIII firefly luciferase reporter (a functional reporter whose expression is dependent on an IRF-3 sensitive promoter element (Fitzgerald *et al.*, 2003), showed that all NSP1 were able to target IRF-3-mediated induction of the IFN-β promoter (Figure 31). The ability of the porcine-derived NSP1 to downregulate a PDRIII-driven IFN-β expression was greater than the human, and similar to that of UKtc and RRV NSP1. Arnold and colleagues reported the ability of NSP1 to target IRF-3 is a three-factor event, which depends on the viral strain, the host species and the experimental context (Arnold *et al.*, 2009).

Results obtained with wild-type and PDRIII driven IFN-β promoter reporters showed contrasting results with previously published data. Simian-derived NSP1s have been shown to downregulate IFN-β by targeting IRF-3. Work by Barro showed how the simian SA-11 RV strain was able to suppress the IFN induction in $FRhL_2$ cell lines (monkey) and how this was achieved by targeting IRF-3 (Barro *et al.*, 2007). In the same work, they generated a series of truncated simian NSP1 which were unable target IRF-3 and to inhibit the expression of IFN-β. The same simian strain, together with the rhesus RRV, the bovine NCDV and the porcine OSU, were used by Arnold to show how the downregulation of IFN-β was not strictly correlated with IRF-3 degradation: all the strains were able to modulate type I IFN, however, only the simian, rhesus and bovine but not OSU were targeting IRF-3 (Arnold *et al.*, 2011).

MA104 infection with OSU RV or exogenous expression of OSU NSP1 results in IRF-3 phosphorylation and nuclear translocation (Graff et al., 2009; Graff et al., 2007). In contrast with its inability to induce IRF-3 degradation, OSU infection of MA104 did not induce IFN-β. Recombinant strain carrying OSU NSP1 showed how the IFN downregulation was due to NSP1 (Graff et al., 2009). Similar results were obtained in different cell lines of different host origin, excluding the cellular context as a potential factor.

The interplayed role of strain/host/cells in the NSP1-IRF-3 degradation and subsequent modulation of IFN-β was further investigated by Greenberg's group, trying to identify the role of IFN-β response in regulation of heterologous and homologous RV infections in mouse embryonic fibroblasts (MEFs) (Feng *et al.*, 2009). The virus yields of bovine (UK and NCDV) and porcine (OSU) RV from wild-type MEFs were more than 2 log units lower than that from IFN-deficient MEFs, indicating the IFN sensitivity of these strains in wild-type MEFs. In contrast, the replication rates of rhesus RRV and homologous murine ETD and EHP strains were similar in both wild-type and IFN-deficient MEFs. The growth of another simian strain, SA-11, was reduced 8- to 10-fold in wild-type compared to IFN-deficient MEFs. These experiments indicated that the heterologous bovine and porcine RV strains were highly sensitive to the antiviral effects of the murine IFN system, while the two homologous strains together with the rhesus RRV strain, replicate optimally despite the presence of an intact IFN signalling system. MEFs infected with the bovine UKtc strain, or with RV reassortants carrying UKtc gene 5 (encoding NSP1) induced a robust IFN-β response. In contrast, rhesus RRV, RRV-like reassortant for gene 5 and EDT strains significantly reduced IFN-β secretion in wild-type MEFs.

Infection of MEFs with bovine UKtc and NCDV or porcine OSU resulted in stable levels of IRF-3. By contrast, during RRV or EDT infection, IRF-3 was susceptible to proteasome-mediated degradation or unable to move to the nucleus. The inability of UKtc to target IRF-3 in MEFs cells was maybe due to intrinsic characteristics of the strain and/or to extrinsic host factors. In support to this, Sen *et al* found that infection of COS7 cell lines (simian) with the bovine UKtc and NCDV strains resulted in IRF-3

degradation (Sen *et al.*, 2009). However, porcine OSU was still unable to target IRF-3 even in COS7. In the same cell lines, using a PDRIII reporter, they showed how rhesus RRV, murine EW and bovine UKtc NSP1 strongly inhibited PDRIII activity upon poly(I:C) transfection. Increasing concentrations of ectopic IRF-3 alleviated this effect in a dose dependent manner, confirming the hypothesis that in COS7 the NSP1 inhibition of poly(I:C) response occurs primarily by degradation of IRF-3. Moreover, they were able to identify the ability of RRV, EW and UKtc NSP1 to downregulate PDRIII activity upon activation of the reporter with the activator TBK1, confirming that in COS7 those NSP1 were able to inhibit IRF-3 function following the activation of the IRF-3 C-terminal cluster of 5-phospho acceptors sites, maybe targeting phosphorylated/dimerized IRF-3.

In has been shown that in non-permissive cell lines bovine UKtc RV infection and UKtc NSP1 expression are not able to induce degradation of IRF-3, leading to in a strong IFN-β response (Feng *et al.*, 2009). Same effect was obtained when UKtc NSP1 was expressed in 3T3 murine cell lines. However when 3T3 were infected with UKtc RV, a significant reduction in PDRIII IFN-β reporter was observed. Same effects were observed for Rhesus RRV and murine EW RV infection (Sen *et al.*, 2009). These founding suggest that NSP1 may encodes additional mechanisms to inhibit IRF-3 function that are independent of IRF-3 degradation.

Infection of Caco-2 and $FRhL_2$ cell lines with the simian SA-11 RV strain resulted in co-immunoprecipitation of NSP1 with IRF-3. A function of time decrease in IRF-3 levels was observed such that by 9–12 hpi, IRF-3 levels were considerably lower than those levels present in mock-infected cells (Barro *et al.*, 2005). In the same cellular context, using an IFN-β luciferase reporter, they showed how infection with the simian strain SA-11 resulted in a 4-fold decrease in the IFN-β induction compared to cells infected with a virus carrying a C-truncated NSP1. SA-11 infection resulted in accumulation of IRF-3 in the cytoplasm, while a mutant carrying a C-truncated NSP1 was unable to prevent IRF-3 nuclear translocation. They also showed how the simian NSP1 targets the phosphorylated forms of IRF-3 dimers, as previously shown by Sen (Sen *et al.*, 2009). The ability of bovine RV B641 and simian RV SA-11 to induce the

degradation of IRF-3 has been also reported in MA104 cell lines (Graff *et al.*, 2007), and is consistent with previously published data (Barro *et al.*, 2005).

MA104 infected with B641 carrying a rearrangement in gene 5 (strain A5-16) resulted in IRF-3 being activated and stable during the course of infection (Graff *et al.*, 2007). Same effect on IRF-3 was observed when MA104 were infected with porcine OSU RV. To exclude that the inability of NSP1 to target IRF-3 was due to its low expression levels, Graff investigated the effect of transient expression of NSP1. In KEH293 cell lines, exogenous expression of OSU NSP1 resulted in IRF-3 being stable, further confirming the inability of the swine-derived NSP1 to target IRF-3, independently of the cellular context.

Y-2-H analyses have shown how the porcine G10P5 interacts with the homologous IRF-3, plus the one encoded by human and monkey (Figure 15, Figure 17 and Figure 18). Analyses of the amino acid sequences of the porcine G10P5 and OSU (data not shown) revealed that the OSU carries only 1 out of 5 of the amino acid of the PDL motif necessary for the interaction with IRF-3 (B. Zhao *et al.*, 2016). Interestingly, the RRV NSP1, which has a full PDL motif is not interacting with any of the IRF-3s screened against, and the bovine UKtc NSP1, which present only a partial motif (1 out of 5 amino acid), is interacting with all IRF-3s. These findings suggest that the interaction between NSP1 and IRF-3 cannot be addressed to a single motif, but are more likely to be a synergic event involving more than one viral protein region. GST pull-downs revealed that UKtc and OSU NSP1 interact with monkey derived IRF-3, however, UKtc precipitated comparatively more IRF-3 (Graff *et al.*, 2007). This could explain that the stability of IRF-3 in cells infected with OSU or transfected OSU NSP1 could be due to a weak or transient interaction between NSP1 and IRF-3 human or monkey cell lines.

Tandem affinity purification coupled with high-resolution mass spectrometry has revealed a strain-specific interaction between NSP1 and IRF-3 or β-TrCP (Ding *et al.*, 2016). NSP1s from rhesus (RRV) and murine (ETD) RV strains exclusively bind to human IRF-3 while those from the two human (Wa, ST3) strains bind to human β-

TrCP. As reported in this study, the UKtc NSP1 interacts with human IRF-3 (Figure 17). Ding showed how UKtc interacted with both human IRF-3 and β-TrCP likely representing an evolutionarily intermediate viral protein. In this study, no interaction between RRV NSP1 and any of the IRF-3s tested was observed using the Y-2-H system (Figure 14, Figure 17 and Figure 18). In agreement with the Y-2-H data described herein (Figure 14, Figure 15, Figure 16 and Figure 19), Ding reported that MAVS did not interact with NSP1 (Ding *et al.*, 2016). However, it has been previously shown using co-IP that the simian Sa-11 NSP1 interact with MAVS (Nandi *et al.*, 2014) and that bovine A5-13 with TRAF2 (Bagchi, Bhowmick*, et al.*, 2013).

Type I IFN also plays a role in driving the generation of adaptive immune responses (Le Bon *et al.*, 2006; Le Bon *et al.*, 2002), a process during which dendritic cells (DCs) play a central role. Studies have shown that virus exposure stimulates DCs to upregulate the surface expression of costimulatory molecules (Brimnes *et al.*, 2003; C. B. Lopez *et al.*, 2004) and that type I IFN is important for mediating this effect (Hidmark *et al.*, 2006; Honda *et al.*, 2003). Viruses that encode type I IFN antagonists may therefore induce suboptimal immune responses not only in the early phase of the infection but also in terms of long-term adaptive responses, as recently discussed for influenza virus and its type I IFN antagonist, non-structural protein 1 (NS1) (Fernandez-Sesma *et al.*, 2006).

Infection of murine bone-morrow derived DCs (mDCs) with the rhesus RRV RV strain resulted in induction of type I IFN and a similar response was obtained when cells were exposed to triple-layered particles (TPLs) which contain all structural proteins thus being infectious (entry competent) (Douagi *et al.*, 2007). Immunofluorescence and western blot analysis showed how IRF-3 levels were profoundly lost in mouse embryonic fibroblast (MEFs) and MA104 cells infected with RRV, as previously reported (Barro *et al.*, 2007). RRV infection of mDCs resulted in viral growth, but no cytopathic effect was observed, as previously reported (Narvaez *et al.*, 2005). In contrast with the detection of new viral protein production, there was no measurable release of newly synthesized infectious viral particles, suggesting that viral replication cycle is aborted at a stage prior to viral assembly or release,

maybe due to the higher immune response of DCs compared to other cells (Hidmark *et al.*, 2005).

IRF-3 expression in RRV-infected mDCs revealed no detectable loss of IRF-3 expression over the time of infection. However, bulk measurement of IRF-3 degradation will mask a small fraction of cells which actually express NSP1 and degrade IRF-3. mDCs may restrict viral proteins, thus the effect of a viral-encoded protein antagonist of type I IFN induction in DCs can be less profound compared to other cell lines, as MEFs. The use of transgenic mice lacking a functional gene for IRF-3 (IRF-3$^{-/-}$) revealed an induction of IFN-β by other IRFs, such as IRF-7.

The secretion of type I IFN can be initiated by a cascade of events upon detection of PAMPs by TLR receptors: TLR8, through MyD88 and Ικκα/β leading to the activation of NF-κB, and TLR3 through TBK1 with the activation of IRFs (Thwaites *et al.*, 2014). The use of MyD88$^{-/-}$, and TLR3$^{-/-}$ mDCs showed no difference in IFN-β induction, suggesting that RRV infection induces type I IFN induction in a TLR-independent manner, and cytosolic recognition events mediate type I IFN induction in response to RRV infection. TLR (7/8 and 9) have been reported to play a pivotal role in the induction of type I IFN in response to viral infection or synthetic ligands in plasmacytoid dendritic cells (pDCs) (Bao *et al.*, 2013), maybe due to the constitutive expression of IRF-7 (Barchet *et al.*, 2002), which is normally expressed at low levels in resting conditions, but enhanced upon IFNAR signalling in other cell lines (Huye *et al.*, 2007). Infection of pDCs with RRC RV resulted in induction of type I IFN-α.

As professional antigen-presenting cells (APCs), DCs effectively link the innate recognition of invading pathogens to the generation of adaptive immune responses (Osmola-Mankowska *et al.*, 2015; Steinman *et al.*, 2006). DCs initiate a maturation process and then induce the activation and differentiation of naïve T cells into functional subtypes for the elimination of the relevant pathogen (Y. Wang *et al.*, 2014). It has been shown that the infection of murine bone marrow-derived DCs (BMDCs) with porcine PRV RV does not result in cell death but leads to cell maturation, with enhanced expression of MHC II and costimulatory molecules (CD40,

CD80, CD86 and CD83) (Ye *et al.*, 2017). Moreover, PRV infection resulted in increased levels of TRL2, 3, 4, 7 and 8, leading to a MyD88-independent (TLR3) and MyD88-dependent (TLR2) maturation of BMDCs. Analysis of secreted cytokines revealed a predominant production of IFN-ɣ, indicating that PRV infection of BMDCs preferentially promoted a Th1-type T cell response (Ye *et al.*, 2017).

In order to obtain an efficient and sustained IFN response, a quick inducible system needs to be in place. In the early phase of infection, the immune response is mostly IRF-3 mediated, with the IFN expressed at very low levels. Sensed incoming infections are detected by PRRs and through the activation of IRF-3, IFN-β and IFN-λ are secreted. The IFNs induction results in the activation a full set of ISGs, including IRF-7. IRF-7 transcription is then rapidly increased through the expression of IFN (Hwang *et al.*, 2013; Sato *et al.*, 1998; Sato *et al.*, 2000). In late phase, IRF-3 and IRF-7 cooperate with each other for the amplification of IFN gene induction, resulting in full procurement of all IFN family members, including IFN-α (Figure 7). Thus, the induction of IRF-7 in response to IFNs and its activation after viral infection provide a positive feedback for the production of IFNs. The ability of RV to spread from the site of infection to surrounding cells and tissues suggests the ability of the virus to antagonise not only the induction, but also the paracrine action of IFN, blocking the activation of the ISGs.

Work by Barro has shown how the simian-derived NSP1 targets not only IRF-3, but IRF-5 and IRF-7, inducing their proteasome-mediated degradation (Barro *et al.*, 2007). Similar results were obtained by Arnold (Arnold, Barro*, et al.*, 2013), which was able to identify a C-proximal IRF association domain (IAD), which mediates IRF dimerization, as the region required for NSP1 interaction. The IAD was mapped in IRF-3, IRF-5 and IRF-7, while IRF-9 contains an IAD-like domain, but not in IRF-1which was not targeted for degradation (Arnold, Barro*, et al.*, 2013). Transient expression assays have shown how the simian NSP1 Sa-11 was able to induce the degradation of IRF-5 and IRF-7 through a proteasome dependent process, allowing NSP1 to block the IFN pathway at different stages of an immune response (Arnold, Barro*, et al.*, 2013).

As previously reported (Osterlund *et al.*, 2007), the ectopic expression of IRF-7 is able to induce the expression of IFN-α in HEK293 cell lines, which do not express the TF (Huye *et al.*, 2007). Based on the sequence analogies present in the promoter regions of IFN genes, Osterlund classified them as either IFN-α type (IFN-α_1, IFN-α_4, and IFN-λ_3) or IFN-β type (IFN-β and IFN-λ_1) promoters. Analogies corresponded to common regulation: SeV was able to activate the transcription of IFN-β and IFN-λ_1 (IFN-β type), however, no effects on the transcription levels of IFN-α_1, IFN-α_4, and IFN-λ_3 (IFN-α type) promoter were observed. By contrast, the exogenous expression of IRF-7 was able to increase the activity of all promoters (IFN-α_1, IFN-α_4, IFN-λ_3, IFN-β and IFN-λ_1) without SeV infection.

Cells that have been pre-treated with IFNs and which have induced ISGs, produce other IFNs, mainly α subtype, leading to a super-stimulation of ISGs, a phenomenon that is called "IFN type I receptor mediated feed-forward" (Marie *et al.*, 1998). Despite the fact that the type I IFNs constitute a family of related cytokines that all recognize the same receptor, differences in action have been shown *in vitro* and *in vivo (van Boxel-Dezaire et al., 2006).* Although target cells are identical, the kinetics of the different type I IFNs varies, *with the sub-class* IFN-α being expressed later (Pulverer *et al.*, 2010).

The inability of RRV to modulate type I IFN in pDCs (Douagi *et al.*, 2007) together with the observed inability of RRV NSP1 to modulate IFN-α-promoter reporter activity (Figure 36) suggest that the ability of NSP1 to induce the degradation of IRF-7 (Barro *et al.*, 2007) could be strain dependent. The inability of NSP1 to target induction of IFN-α could explain why IFN-α treatment in new-born mice is sufficient to prevent biliary and hepatic disease (Petersen *et al.*, 1997), however, the administration of the virus through the tail vein did not reflect the real site of infection of RV. For this reason, IFN-mediated antiviral effects in other cells lines rather than small intestine-derived cells should be carefully considered.

The ability of NSP1 to target IRF-7 has been further investigated by Di Fiore, comparing the effect of some human RV strains to antagonise the IRF-7-mediated

IFN-α_1 promoter activity (Di Fiore *et al.*, 2015). In support of the data generated in this thesis, IRF-7 was able to strongly induce IFN-α_1 promoter activity (Figure 35). In the presence of a Wa-like or DS-1 like human strain, IFN-α_1 promoter activity was reduced from 20% to 40% depending on the strain. In comparison, porcine CRW-8 RV was not able to target IRF-7. In contrast, the simian SA-11 strongly inhibited IRF-7-mediated IFN-α_1 gene expression and was also able to downregulate IκKϵ-stimulated IFN-β Luc gene expression. IκKϵ is an activator of IRF-3 and acts downstream of virus-sensing innate immune activators including RIG-I and MDA5. Human and porcine derived NSP1 were not able to target IκKϵ. These findings show a degree of inhibition of IRF-7 signalling by NSP1 from some human rotaviruses.

The epithelium is the main entry point of many viruses, such as hepatitis B virus, hepatitis C virus, human immunodeficiency virus, influenza virus, poliovirus and rotavirus (Bomsel *et al.*, 2003). Previous studies have reported how a synergic cooperation of IL-22 and IFN-λ receptors, both of which are highly expressed in intestinal epithelial cells (IECs), is required for an optimal activation of the transcriptional factor STAT1 and expression of interferon stimulated genes (ISGs) (Pott *et al.*, 2011). Epithelium-rich organs such as the intestine, stomach, skin and lungs show a high expression of IFNLR-1 and respond to IFN-λ (Brand *et al.*, 2005; Doyle *et al.*, 2006; Ioannidis *et al.*, 2012; Kotenko *et al.*, 2003; Zahn *et al.*, 2011).

While type I and type III IFNs and their receptors are only distantly related (Kotenko *et al.*, 2003), they show virtually identical signalling behaviour in that they activate the STAT1-STAT2 transcription factor signalling pathway, which leads to the formation of the ternary interferon-stimulated gene factor-3 (ISGF3) complex (consisting of STAT1, STAT2 and IRF-9) that controls transcription of more than 300 interferon-stimulated genes (ISGs) acting in concert to restrict replication of viruses (Aaronson *et al.*, 2002; Leonard, 2001; Villarino *et al.*, 2017). Recent studies have investigated the role of type I and type III IFN *in vivo* in clearance of virus infection, and they have demonstrated a high degree of redundancy and suggested that type III can support type I activity, however, it cannot replace its functionality (Mordstein *et al.*, 2010).

Infection of STAT1-deficient mice with RRV RV results in higher viral shed compared to wild-type mice (Vancott *et al.*, 2003) and IFNAR1-deficient mice exhibit no enhanced susceptibility to RV infection (Angel *et al.*, 1999). Work by Pott showed a distinct and critical role of IFN-λ in the vaginal mucosal in preventing RV infection that cannot be compensated for by IFN-α/β (Pott *et al.*, 2011). These findings are unique, compared to other respiratory viruses (Mordstein *et al.*, 2010). The apparent discrepancy between the conclusions of the current and previous studies may be a result of the exceptional tissue tropism of RV, which replicates mostly, if not exclusively in epithelial cells of the small intestine (Boshuizen et al., 2003). Using knock out mice for *IFN-β (*IFNAR1$^{0/0}$) and IFN-λ (IL28Rα$^{0/0}$) receptors, they showed how epithelial cells respond far more strongly to IFN-λ rather to type I IFN, maybe due to restricted receptor expression (Sommereyns et al., 2008), and treatment of mice with IFN-λ, but not IFN-β, repressed RV replication (Hernandez *et al.*, 2015; Mahlakoiv *et al.*, 2015).

Moreover, while humans have three or four functional *IFNL* genes, mice have only two (*Ifnl2* and *Ifnl3*), because the *IFNL4* genomic region is absent in mice and mouse *Ifnl1* is a pseudogene (Donnelly et al., 2010). Therefore, studies involving the IFN-λ murine model should be carefully considered since the lack of IFN-λ_1 may lead to an under estimation of the overall effect of type III IFN (Hermant et al., 2014; Pulverer et al., 2010).

IFN-λ and the IFN-λ receptor (IFN-λR) share homologies with IL-10 family cytokines and their receptors. In particular, the gene encoding the α-chain of the IL-22 receptor (*Il22ra1*) is the closest relative of the gene encoding the IFN-λR1 chain (*Ifnlr1*) (Kotenko *et al.*, 2003). The close relationship between IFN-λR and IL-22R is interesting because both receptors are preferentially expressed by epithelial cells (Sommereyns *et al.*, 2008), indicating a designated role in controlling epithelial function in response to infections. Given the important role of type III IFN in curtailing early RV replication *(Pott et al., 2011)* and the close homology occurring between IFN-λ and IL-22, it is not surprising that the two evolutionarily related mucosal cytokines cooperate synergistically to activate the transcriptional factor STAT1 and

express ISGs, curtailing RV homologous replication (Hernandez et al., 2015). The ability of NSP1 to downregulate the IFN-λ to a greater extent than IFN-β could be explained with the high tropism of the virus. However, later in the infection, spreading from intestinal epithelium to the *lamina propria*, the virus needs to be able to downregulate IFN-β, which is highly expressed in connective tissue (Mahlakoiv et al., 2015).

The induction of IFN-λ is a synergic and cooperative action of different transcriptional factors. The promoter region of IFN-λ presents a series of NF-κB (PDRII) and IRF-3 (PDRIII or ISRE) binding element sequences, which synergistically act to ensure a potent transcription. Sequences analyses have shown a more distal NF-κB binding site within the IFN-λ promoter region (-1137 to -1182 bp) (Thomson *et al.*, 2009). Based on the presence of multiple NF-κB binding sites compared to IRF-3 ones, it is not surprising that a full procurement of IFN-λ induction is more linked to the transcriptional activity of NF-κB rather than to IRF family members (Odendall *et al.*, 2015).

NF-κB is a critical regulator of the immediate early pathogen response which plays an important role in promoting inflammation, regulating cell proliferation and survival (Hayden *et al.*, 2012). The inactive NF-κB complex is activated in response to a variety of stimuli, including viral and bacterial infection, exposure to pro-inflammatory cytokines, mitogens and growth factors and stress-inducing agents. Some of the cell membrane sensors involved in NF-κB activation have been characterized in more depth, as in the case of dsRNA virus infection which are sensed by Toll-like receptors (TLRs) and trigger the recruitment of the death domain-containing adaptor protein myeloid differentiation primary response gene 88 (MyD88) (Iordanov *et al.*, 2001). One of the best characterised NF-κB induction signalling pathways is the one triggered by the pro-inflammatory cytokine tumour necrosis factor-α (TNFα). TNF-induced activation of NF-κB mostly relies on phosphorylation, ubiquitination and subsequent degradation of inhibitor of kappa B (IkB) proteins. The inhibitor of kappa B kinase (IKK) complex, a multiprotein kinase complex containing IKKα and IKKβ, is responsible for the TNFα-induced

phosphorylation of IkB. Following recognition by an E3 ligase complex containing β-TrCP, polyubiquitination and degradation of IkB releases free NF-κB dimers to translocate to the nucleus and induces expression of certain genes (Kanarek *et al.*, 2012) (Figure 59).

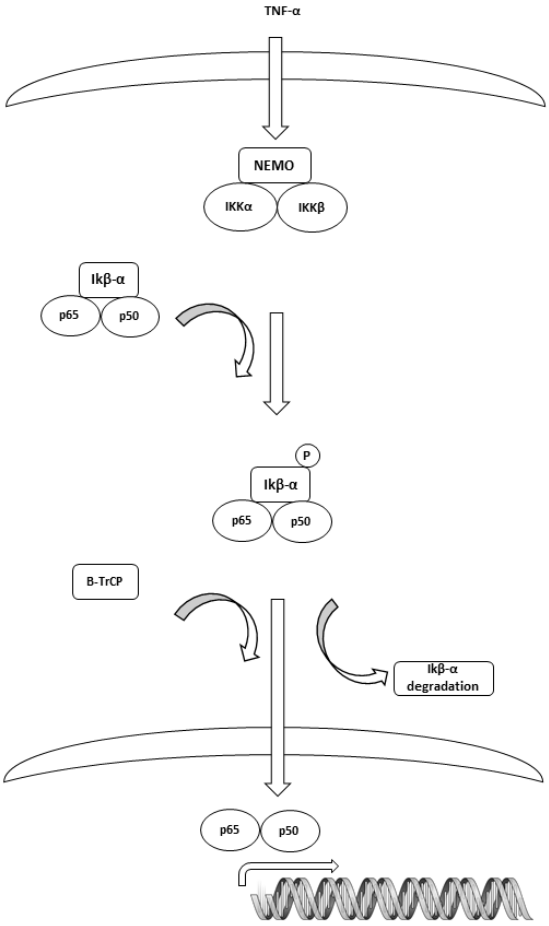

Figure 59. Schematic representation of NF-KB canonical induction pathway.

A wide range of soluble and membrane-bound extracellular ligands activate the NF-κB pathway, as members of TNFR, TLR, IL-1R. The engagement of TNFα with its receptors initiates a cascade of events which end with the transcriptional activation of NF-κB. Under resting conditions, NF-κB dimers are bound to inhibitory IκB proteins, which sequester inactive NF-κB complexes in the cytoplasm. Stimulus-induced degradation of IκB proteins is initiated through phosphorylation by the IκB kinase (IKK) complex, which consists of two catalytically active kinases, IKKα and IKKβ, and the regulatory subunit IKKγ (NEMO). Phosphorylated IκB proteins are targeted for ubiquitination and proteasome-mediated degradation by β-TrCP, which thus releases the bound NF-κB dimers so they can translocate to the nucleus, activating transcription.

The high tropism of RV, with the ability to downregulate IFN-λ induction and the ability of NSP1 to target β-TrCP (Davis *et al.*, 2017a; Graff *et al.*, 2009), together with a strong dependence of IFN-λ on NF-κB, prompted the investigation of the effect of NSP1 on the transcriptional activity of NF-κB (5.2.1.3). Previously works have reported that β-TrCP is preferentially targeted by human and porcine RV (Di Fiore *et al.*, 2015; Graff *et al.*, 2009) and that NF-κB transcriptional activity was targeted by NSP1 of bovine and monkey origin in the presence of a potent inducer such as TNFα (Graff *et al.*, 2009). The ability to trigger NF-κB reporter with the ectopic expression of Ikkβ reported in this thesis (5.2.1.3.1) is consistent with previously published data (Gates *et al.*, 2016; Israel, 2010; C. M. Randall *et al.*, 2012). The presence of phosphorylated Ikk complex during the course of OSU and NCDV infection indicated that the kinase activity was not disrupted by either viruses with the downregulation of NF-κB happening at some point downstream of kinase phosphorylation (5.2.1.3.1.2).

β-transducing repeat-containing protein (β-TrCP, encoded by BTRC) is the core substrate recognition component of the Skp1-Cul1-F-box $(SCF)^{\beta\text{-}TrCP}$ E3 ubiquitin ligase complex, which plays essential roles in a variety of biological processes, including apoptosis, cell cycle, carcinogenesis and innate immunity (Low et al., 2014). Modification of eukaryotic proteins with ubiquitin (Ub) prior to proteasome degradation requires an E1 activating enzyme, E2 conjugating enzyme, and an E3 ligase that transfers Ub from E2 to the target substrate (Takayama *et al.*, 2017). E3 ligases fall into two major classes of proteins that contain either a catalytic HECT domain or a RING domain. Typical RING domains consist of cysteine and histidine residues spaced in a C3HC4 pattern that coordinately bind two zinc ions. The pattern of cysteine and histidine residues in the zinc finger motif of NSP1 is similar, but not identical, to RING finger domains in cellular E3 ubiquitin ligases (Graff *et al.*, 2007). The RING domain variant of NSP1 could address a potential E3 ubiquitin ligase activity to the viral protein, attaching ubiquitin chains to host proteins to drive their proteasome-mediate degradation.

An associated inhibitor of κB protein (IκB) regulates NF-κB activation. IκB contains a degron motif (DSGΦxS, Φ, hydrophobic residue) (PD) that undergoes phosphorylation following pathogen recognition or other proinflammatory signals (Fortmann *et al.*, 2015). Signals from PRRs or other receptors activate the IκB kinase (IKK) complex, which phosphorylates IκBs on a pair of serine residues within the degron motif DSGΦxS (Kanarek et al., 2012) . $SCF^{\beta\text{-}TrCP}$ recognizes this phosphodegron through its β-TrCP (Ghosh et al., 1998). In association with the E2 ubiquitin-conjugating enzyme UBCH5, $SCF^{\beta\text{-}TrCP}$ polyubiquitinates phosphorylated IκB driving its proteasome-mediated degradation, releasing dimeric NF-κB to translocate to the nucleus, where it binds κB sites in the promoter and enhancer regions of target genes. The $SCF^{\beta\text{-}TrCP}$ E3 ligase complex mediates proteasome-dependent degradation of several proteins with roles in regulating cell proliferation, including IκBα, NF-κB subunits p100 and p105, cyclin dependent kinases, and β-catenin, among others (Frescas *et al.*, 2008). Aside from the IκB family, $SCF^{\beta\text{-}TrCP}$ mediates the degradation of other proteins involved in NF-κB activation, as IFN-α receptor 1 (IFNAR1) (Kumar *et al.*, 2004) and IL-1R-associated kinase 1 (IRAK1) (Cui *et al.*, 2012) and of a number of cell cycle and pro-apoptotic regulatory factors (Frescas *et al.*, 2008). NSP1-mediated degradation of β-TrCP is expected to arrest the turnover of these proteins, which should have manifold implications for RV replication.

Sequences analyses have revealed the presence of a similar sequence (DSGΦS) in several human proteins (IκBα, IκBβ, β-catenin, NRF2, YAP) (Diehl *et al.*, 2013) which turnover is mediated by the ubiquitin-proteasome system. The same motif is present in a number of unrelated virus proteins which mimic the PDL motif to sequester β-TrCP and thereby inhibit NF-κB activity, as Epstein-Barr virus (EBV) LMP1 (Tang *et al.*, 2003), human immunodeficiency virus type 1 (HIV-1) Vpu (Bour *et al.*, 2001) and vaccinia virus (VACV) A49 (Mansur *et al.*, 2013). NSP1 proteins of most human and porcine RV strains conserve a C-terminal phosphodegron-like (PDL) motif, DSGΦS (Di Fiore *et al.*, 2015). The PDL motif, present in most of the human (both Wa and DS-1 derived) and porcine strains but missing in cattle and murine proteins, is employed by NSP1 to sequester β-TrCP, as shown by co-IP experiments (Davis *et al.*,

2017a, 2017b; Morelli, Dennis*, et al.*, 2015). Deletion of this motif or mutation of its serine residues disrupts the ability of viral proteins to interact with its target (Di Fiore *et al.*, 2015). Point mutation within the PD β-TrCP-binding pocket protects the protein from NSP1-mediated turnover (Morelli, Dennis*, et al.*, 2015). Morelli proposed that the site of polyubiquitination on cellular targets of $SCF^{\beta\text{-}TrCP}$ is a lysine located 9 to 14 residues N-terminal to the PDL motif. A conserved lysine (K465) is common in most of the human strains, but missing in NSP1 derived from virus infecting cattle and monkeys (Morelli, Dennis*, et al.*, 2015). The functional role of this lysine is confirmed by the fact that NSP1 derived from pigs (Gottfried-U08431) and monkey (SA-11f-AF290881) strains, which are lacking a complete PDL or a conserved lysine in 465 position, lack the ability to target β-TrCP. Of the strains considered in this study, only the human 1M0, 18A and TC together with the porcine OSU NSP1 had a complete PDL motif and a conserved upstream lysine in position 465. Same lysine is present in the porcine A8, which carries a partial PDL motif. The other porcine G10P5 together with bovine UKtc and rhesus RRV are missing the lysine and a complete PDL (alignment not shown). However, all of them are capable to modulate NF-κB activity (Figure 43).

The interaction between β-TrCP and NSP1 requires in first instance the phosphorylation of RV protein at least in one of the serine present in the PDL (Davis *et al.*, 2017b). It is possible to speculate that the lack of interaction observed with the porcine G10P5 and A8, the bovine UKtc and rhesus RRV was due to the absence of a complete PDL motif of NSP1. However, the presence of a full PDL in human-derived NSP1 did not result in interaction with β-TrCP in the Y-2-H system. However, luciferase reporter experiments showed that NSP1 had effects on the β-TrCP-mediated activation of NF-kB transcriptional activity (Figure 51). The ectopic expression of β-TrCP to induce NF-κB transcriptional activity has been proved as a reliable way to identify the point at which NSP1 is targeting the NF-κB pathway (Frescas *et al.*, 2008; Muerkoster *et al.*, 2005). This could be the result of interactions which were not detectable using a Y-2-H assay, or the stringency conditions used (Figure 14, Figure 15, Figure 16 and Figure 19). Co-IP experiments showed how the

NCDV or OSU derived NSP1 were interacting with β-TrCP (Di Fiore *et al.*, 2015) and β-TrCP was not detected in either NCDV or OSU infected cells, however, its expression was stabilized when cells were treated with the proteasome inhibitor MG132.

The interaction between β-TrCP with NSP1 reported by *Morelli* did not result in its degradation for all different isolates (Morelli, Dennis*, et al.*, 2015), suggesting that some strains may target NF-κB through a mechanism independent to β-TrCP degradation. The employment of alternative ways to modulate the IFN response could be a common mechanism between different RV strains, as reported for bovine UK NSP1, which mediates the degradation of IRF-3 in a host-cell-specific manner but can also block IRF-3 transcriptional activity without inducing its degradation (Sen *et al.*, 2009). Furthermore EBV LMP1 (Tang *et al.*, 2003), HIV-1 Vpu (Bour *et al.*, 2001) and VACV A49 (Mansur *et al.*, 2013) all interact with β-TrCP to block NF-κB activation, without inducing β-TrCP turnover.

Despite significant sequence variability occurring between different RV strains (Dunn *et al.*, 1994), all full-length RVA NSP1 proteins are thought to utilize an N-terminal RING domain to interact with a cellular E2 ubiquitin-conjugating enzyme and a C-terminal sequence element to provide binding specificity for a host innate immune target (Graff *et al.*, 2007). Formation of such a complex is predicted to induce polyubiquitination of the target, followed by its degradation by the proteasome. NSP1 may conserve its architecture across strains, with one of two C-terminal motifs (PDL or pLxIS) mediating target specificity. In this study, when domains were swapped between the human 18A and the bovine UKtc NSP1, data showed how the C-terminus was responsible for the ability of the viral protein to interact with their targets and downregulate NF-κB response (Figure 45).

Chimeric NSP1 in which the PDL motif of the simian Sa-4f NSP1, which specifically targets IRFs (Arnold *et al.*, 2011), was replaced with the PDL of OSU NSP1 showed that the recombinant NSP1 was still able to downregulate NF-κB, however less potently than the OSU, indicating that regions outside the C-terminal PDL motif

likely contribute to NF-κB antagonism by OSU NSP1 and are not fully captured by SA11-4F NSP1 (Morelli, Dennis*, et al.*, 2015). Work by Di Fiore showed how truncation and point mutations in the PDL motif hampered the ability of NSP1 to target β-TrCP and inhibit NF-κB-driven reporter gene expression (Di Fiore *et al.*, 2015). This finding suggests that the PDL motif, when paired with an intact RING domain, is sufficient to target $SCF^{\beta\text{-}TrCP}$, and that SA11-4F and OSU NSP1 proteins conserve an architecture and mechanism similar enough to permit this transfer of functionality. This data supports results generated in this work, where swapping domains did not alter the functionality of NSP1 (Figure 39, Figure 45). The interplaying role of the RING domain and PDL motif in orchestrating recognition and degradation of NSP1 targets has been further investigated by *Ding,* identifying a COPII signal domain within the N-terminal RING-finger domain and the other at the very C-terminus (Ding *et al.*, 2016). COPII coated vesicles are responsible for sorting and trafficking cargo out of the ER and into the Golgi apparatus (Campbell *et al.*, 1997), and their presence on NSP1 suggest that the interaction NSP1/CUL3/β-TrCP results in Golgi re-localization, where proteasome-mediated degradation takes place. Cullin-RING ubiquitin ligases (CRLs) comprise the largest known category of ubiquitin ligases. CRLs regulate an extensive number of dynamic cellular processes, including multiple aspects of the cell cycle, transcription, signal transduction, and development (Bosu *et al.*, 2008).

Proteomic analyses revealed how NSP1 of simian, murine, bovine and human origin were interacting with proteins belonging to the CRL complexes, including Cullins 1–7, the shared E3 ligase subunit Rbx1 and other CRL-associated components and regulatory factors (Ding *et al.*, 2016). Cul3 has been observed to interact with porcine OSU-NSP1 (Pichlmair *et al.*, 2012) and more recently with NSP1s from several human and animal RV strains (Lutz *et al.*, 2016). Proteomics analyses were confirmed by co-IP experiments and by expression of NSP1 or in the context of viral infection. Ding also showed that NSP1 precipitated with E2 ubiquitin-conjugating enzyme.

Fluorescence microscopy experiments have shown how during viral infection NSP1 is localised in proximity of the Golgi (Ding *et al.*, 2016). Mutants lacking the

RING domain are unable to localize to the Golgi and they have lost their binding ability toward β-TrCP. Point mutations which partially restored the RING domain conferred to NSP1 the ability to bind again to β-TrCP and colocalize to the Golgi, however, binding affinity and NF-κB downregulation were less potent than the wild type NSP1 carrying a full RING domain. The fact that some strains (RRV) show an interaction between NSP1 and CUL3 and localization to the Golgi, but not β-TrCP degradation support the hypothesis that the specific functionality of NSP1 is strain specific, and within the tri-complex NSP1/CUL3/β-TrCP NSP1 acts more as an adaptor protein which mediated CUL3-β-TrCP interaction at the Golgi, rather being an E3 ligase. Therefore, it appears that Wa-NSP1 does not function as an E3 ligase on its own but instead usurps the host CRL to degrade β-TrCP. The use of lactacystin as an irreversible inhibitor (Bogyo *et al.*, 1997) confirmed that β-TrCP was degraded through the ubiquitin–proteasome pathway.

The ability of some RV strains to target IRF-3 for degradation is independent of CUL3 (Bosu *et al.*, 2008; Davis *et al.*, 2017b), highlighting a major difference of NSP1 dependence on host control during RV evolution and emphasizing the versatility of various RV strains in identifying substrates.

The interaction occurring between NSP1 and CUL3 has been further investigated by *Lutz et al*, however, their work showed contrasting results with Ding (Ding *et al.*, 2016). The interaction between the two proteins was confirmed, however knocking down of CUL3 resulted in degradation of β-TrCP and IRF-3, suggesting that CUL3 played only a marginal role in the degradation (Lutz *et al.*, 2016). However, it is possible that a certain level of degradation was observed since knock down cells may still express sufficient CUL3 complex to interact with NSP1, or the viral protein could use other components of the CRL complex, such as CUL1. CUL3 has been reported to be important for RV infection (Silva-Ayala *et al.*, 2013) and its interaction with NSP1 raises the possibility that RV employs the NSP1-CUL3 interaction to mediate degradation of other host proteins involved in immunity. Contrasting results showed by the two different groups might be due to the differences in methodology, including the use of stable cell lines by Ding, versus

transient transfection by Lutz. The use of siRNA to silence selective Cullins revealed a strain-specific ability of NSP1 to induce β-TrCP degradation (Ding *et al.*, 2016; Lutz *et al.*, 2016). In support of the data generated in this thesis, they showed how the bovine UKtc NSP1 was able to strongly induce β-TrCP degradation.

The role of the PDL motif has been further investigated with point mutations that disrupt the N-termini domain, showing how mutation in the putative RING domain affected not only IRF-3 binding ability of NSP1 (Arnold *et al.*, 2011) but also failed to block NF-κB activation. However, it is not established whether disruption of the RING domain may have perturbed the overall structure of NSP1 and affected functions other than its putative E3 ubiquitin ligase activity.

The interaction of β-TrCP with Iκβ requires phosphorylation of two serine residues in the Iκβ motif (Fortmann *et al.*, 2015). Since NSP1 employs a PDL motif to interact with β-TrCP mimicking Iκβ, it is possible that before the interaction its serine residues within the motif need to be phosphorylated. Indeed, phosphorylation of NSP1 is strictly required before interaction with CUL3 or β-TrCP takes place (Davis *et al.*, 2017b). The phosphorylation is strain independent, however, is occurring in NSP1 derived from RV infecting different animals (Davis *et al.*, 2017b). In contrast with Iκβ which is phosphorylated by Iκκβ subunits (Israel, 2010), NSP1 carries recognition motifs for the constitutively expressed casein kinase II (CKII) (Davis *et al.*, 2017a).

Consistent with previously published data, although the RING domain and PDL motif cooperate together, their functionalities are not strictly correlated for β-TrCP interaction (Ding *et al.*, 2016). NSP1 RING mutants which carried an intact PDL motif that could be phosphorylated, retained their ability to interact with β-TrCP, however, interaction was not followed by β-TrCP degradation. This finding suggests that β-TrCP may not be the only mechanism employed by RV to downregulate NF-κB activity. Alternatively, NSP1 could physically sequester β-TrCP prior to allocation with CUL3 to prevent Iκβ degradation. The employment of a constitutively expressed kinase, such as CKII, for NSP1 phosphorylation would facilitate NSP1 to be primed for interaction with β-TrCP immediately after expression. In contrast, Iκβ

phosphorylation relies on upstream phosphorylation events. It has been shown that early in OSU infection phosphorylated levels of Iκβ increase, even in presence of β-TrCP, suggesting that NSP1 may block NF-κB activation by sequestering β-TrCP. In support to this hypothesis, IκBα was detected in lysates from NCDV and OSU infected cells throughout a ten hour time-point experiment (Graff *et al.*, 2009). Although IκBα was present at each time point, degradation of the NF-κB inhibitor was still observed in the early stages of infection, when viral-encoded proteins levels were low and not sufficient to block NF-κB activity.

In support to the hypothesis that the presence of a PDL motif is not strictly correlated with the ability of NSP1 to downregulate NF-κB activity thought the degradation of β-TrCP, Graff showed, using a luciferase reporter, how the OSU NSP1 was able to downregulate NF-κB activity in MA104 cells treated with polyI:C (Graff *et al.*, 2009). In contrast, the NSP1 encoded by NCVD lacked this ability. Differences observed were not due to different expression levels of the two viral proteins, which showed a similar profile. Results of the bovine NCDV strain are in contrast with data generated in this work, since the bovine UKtc NSP1 was potently able to downregulate NF-κB activity (Figure 43). The two NSP1 encoded by RV infecting cattle are remarkably similar in their amino acid sequences, and they are 100% identical in the PDL motif (alignment not shown) which has been shown to be responsible for mediating the interaction (Davis *et al.*, 2017a, 2017b). One of the possible reason could be the employment of two different cell lines, Ma104 by Graff, HEK293 in this work. Since NSP1 expression levels are very low during early stages of infection, it is possible that RV use this mechanism to reduce the level of active NF-κB without a long-term interaction between NSP1 and β-TrCP. Later in infection, when NSP1 levels have risen, a more long-term interaction may occur.

The ability of human and porcine strains to preferentially target NF-κB rather than IRFs to modulate the host immunity had been further investigated by Coulson's lab (Di Fiore *et al.*, 2015). They selected a panel of human and porcine RV isolates and compared their respective activates to simian ones. CRW-8 swine RV shares 96% nucleotide sequence to the OSU, and clusters closely with the A8 used in this study.

They also considered a human WA-like (as 1M0 and TC) and a DS-1 like (like 18A) RV isolate. Consistent with previous results (Arnold *et al.*, 2011; Graff *et al.*, 2009), IκBα levels were stable during the course of the CRW-8, WA-like and a DS-1 like RV infection, indicating a block in the NF-κB pathway. In contrast, simian infection (SA-11) showed a decrease in IκBα levels (Di Fiore *et al.*, 2015). An opposite trend was observed when IRF-3 levels were analysed, with the simian strain being able to target IRF-3 and human and porcine not, as previously reported (Barro *et al.*, 2005, 2007; Graff *et al.*, 2002).

TRAF6 induces canonical NF-κB pathway activation upstream of TBK1 and IκK. The ability to induce NF-κB activation through the ectopic expression of TRAF6, further supported the evidence that NSP1 of human and porcine origin were responsible for the stabilization of IκB observed during infection (Di Fiore *et al.*, 2015). The ability to induce NF-κB transcriptional activity with the ectopic expression of members involved in its regulation allowed a further species-specific dissection of the pathway. The human, porcine, bovine and rhesus NSP1 appeared to target NF-κB between the phosphorylation of IKβ-α by IKKβ and its attachment with a polyubiquitin chain by β-TrCP (Figure 48, Figure 51). However, the bovine UKtc appeared to have an effect downstream in the pathway, acting on p65 NF-κB subunit (Figure 55). The inability of rhesus RRV to target downstream of p65 (Figure 55) was consistent with published data, in which infection of murine MEFs with the simian RV resulted in nuclear translocation of p65 (Douagi *et al.*, 2007). Similar results were obtained for human RV strains, however, information of the different genotypes were not indicated, with the two strains defined as human RV1 and human RV2 (Hakim *et al.*, 2018).

Treatment of MA104 and HT29 cells with TNFα results in increased levels of phosphorylated p65 which is able to translocate to the nucleus. However, RRV and Wa infection of cells previously exposed to TNFα resulted in phosphorylation of p65 that was unable to translocate to the nucleus (Holloway *et al.*, 2009). The mechanism through which RV prevents nuclear accumulation of p65 is unknown. Since p65 is activated and its levels remain constant thought the course of infection, it is possible

that RV sequesters p65 to the cytoplasm or interferes with its mode of translocation. Consistent with the inability of NF-κB to translocate to the nucleus, RRV and Wa infection of MA104 cells previously treated with TNFα, showed a substantial decrease (9 fold reduction) in NF-κB transcriptional activity (Holloway *et al.*, 2009). The inability of RRV to prevent nuclear translocation of p65 supports findings of this thesis, where NSP1 appeared to have marginal effects on the p65-mediated activation of NF-κB activity (Figure 55), suggesting that the viral protein is acting between β-TrCP degradation and p50/p65 release.

The production of cytokines in RV-infected cells depend on the relative timing of cell response to infection and potency of RV disruption of gene expression, both of which may vary between cell types. Contrasting results have been obtained in mouse embryonic fibroblast (MEFs), where RRV infection resulted in nuclear translocation of NF-κB (Douagi *et al.*, 2007). It is possible that NF-κB is activated in MEFs before RRV can inhibit its nuclear accumulation, or that RRV does not inhibit the nuclear accumulation of NF-κB in cells of mouse origin.

The NF-κB transcription factor family in mammals consists of five proteins, p65 (RelA), RelB, c-Rel, p105/p50 (NF-κB1), and p100/52 (NF-κB2) that associate with each other to form distinct transcriptionally active homo- and heterodimeric complexes. The p50/65 heterodimer clearly represents the most abundant of Rel dimers, being found in almost all cell types. NF-κB p50 subunit mostly form dimers with p65 and it can form homodimers that act as repressor when they bound to the promoter, since they lack a trans-activator domain (Plaksin *et al.*, 1993).

MA104 cells infected with NCSV and A5-15 RV strains revealed high levels of active p50 (Graff *et al.*, 2009). Analysis of the expression levels of the two subunits in RV infected cells revealed that viral infection with OSU or NCDV did not result in degradation of p50/p65. In contrast with their stability, the two subunits showed different activation profiles upon infection, with p50 activated and p65 inactivated. The latter was not able to translocate to the nucleus and accumulated in OSU and NCDV-encoded viroplasms (Graff *et al.*, 2009).

Work by Hakim *et al* showed how TNF-α treatment of SA-11 RV infected Caco-2 cell lines resulted in the production of IL32, IL8, CXCL11 and CCL20 which potently inhibited rotavirus replication (Hakim *et al.*, 2018). Thus, the ability of NSP1 to modulate NF-κB transcriptional activity, prevents the secretion of cytokines with potent antiviral effect.

Incoming viral infections trigger a cascade of events which in the end result in the production of type I IFN (α and β) and type III IFN (λ). IFN bind to their specific receptors and signalling thought the JAK/STAT pathway recruit IRF-9, forming the heterotrimeric complex Interferon-stimulated gene factor 3 (ISGF3). The ISGF3 transcriptional factor enters the nucleus and binds to the IFN stimulated response element (ISRE) to activate the transcription of interferon stimulated genes (IGGs) (R. E. Randall *et al.*, 2008). Of the many ISGs, one of the most studied and characterized is *Mx*.

RV infection of intestinal hemapoietic cells compartment induces significant secretion of type I IFN (Ramig, 2004). However, the virus is able to spread from the site of infection to bystander cells, despite exogenous stimulation of the STAT pathway. It has been shown that IFN-α and IFN-γ signalling is required for the resolution of viral replication and extra-intestinal pathology in mice infected with certain RV strains but not others (Feng *et al.*, 2008; Vancott *et al.*, 2003). In MA104 cell lines, RRV and Wa infection resulted in 50% decrease of ISGs expression upon stimulation with IFN-α or IFN-γ, and 8hpi a further 20% decrease was observed (Holloway *et al.*, 2009). Interestingly, when the same experimental approach was performed in Caco-2 cell lines, while the human Wa retained its capacity, RRV lost its ability to block ISGs during the course of infection (Holloway *et al.*, 2009). Despite differences in antagonising ISGs production later in the infection, both RRV, Wa and UKtc blocked their transcription preventing STAT nuclear translocation when cells were treated with IFN-α or IFN-γ (Holloway *et al.*, 2009).

The activation of STAT follows its phosphorylation at tyrosine Y701 by JAK (Villarino *et al.*, 2017). Work by Sen has shown how RRV, EW, OSU and UKtc RV were

capable of inhibiting Y701 phosphorylation and how this was independent of the NSP1 RING domain (Holloway *et al.*, 2014; Sen *et al.*, 2014). Work by Holloway also suggested that the ability of blocking nuclear translocation of STAT was conserved among different strains of RV infecting human and pigs (Holloway *et al.*, 2014). In contrast with previous findings, the authors suggested that the inhibition of ISG expression is due to the inability of STAT to translocate to the nucleus, rather than prevention of its phosphorylation. Some viruses inhibit STAT nuclear translocation by interfering with the importin machinery, as reported for Ebola VP24 (Reid *et al.*, 2006), however expression of RV proteins appeared not to compromise nuclear localization of MPα5 and IMPβ1 (Holloway *et al.*, 2014). It is possible that RV employs a novel uncharacterised mechanism to prevent ISG expression.

Upon Activation, STAT associate with IRF-9 forming the *ISGF3* heterotrimeric complex. It has been reported that NSP1 can induce degradation of IRF-9 (Arnold, Barro*, et al.*, 2013) however, the authors describe how a truncated form of NSP1 was unable to degrade IRF-9, but still prevented STAT delocalization to the nucleus. In support of this, it has been reported that activated STAT is able to translocate to the nucleus without IRF-9 (Banninger *et al.*, 2004).

The varied ways in which NSP1 modulates the induction of different IFNs (type I and type III), by targeting different pathway components (IRF-3 and NF-κB) in a strain-dependent manner most likely contributes to the differences observed in homologous and heterologous infections. Rhesus RRV infection of type I and type II IFN-deficient suckling mice resulted in a prolonged infection in multiple extra-intestinal organs (liver, bile duct, and pancreas), supporting the essential role of STAT-dependent IFN signalling response to control systematic replication. However, infection of type I and type II IFN-deficient suckling mice with other heterologous strains, such as simian SA, bovine NCDV or porcine OSU, or homologous infection with murine EW triggered a robust type I and II IFN induction and resulted in mild or absent effects, with the infection contained in the intestinal lumen (Feng *et al.*, 2008). Different homologous murine strains have shown variable responses to the absence of IFN signalling, such as EC, that despite showing a similar pathogenicity to EW, is

able to spread from the site of infection to surrounding organs (Broome *et al.*, 1993). A possible explanation could be that the NSP1 encoded by the two different RV strains could differentially target IRF-3 or NF-κB.

Mouse biliary tract is high susceptible to rhesus RRV infection (Feng *et al.*, 2008) but not to bovine UKtc. Reassortments between RRV and UKtc have been able to identify *in vivo* that the high infectivity of RRV was facilitated by VP4, which provided an enhanced viral entry capacity, and NSP1 which was able to strongly suppress the host immune response compared to the parental strain (Feng *et al.*, 2011). Only reassortants that carried VP4 and NSP1 of RRV origin were able to grow to a titer similar to the parental virus. These results support previously generated data that showed NSP1 derived from UKtc and RRV were able to degrade IRF-3 with different efficiencies in MEFs (Feng *et al.*, 2009; Sen *et al.*, 2009). Understanding the impact of each viral protein in modulation of host innate immunity could be beneficial for development of a better vaccine since UKtc and RRV strains have been used as heterologous backbone strains for human RV vaccine (Flores *et al.*, 1993; Midthun *et al.*, 1985). However, infection of mice with the homologous EW, the heterologous UKtc or reassortants EWxUKtc revealed that an efficient infection and replication of EW was due to a constellation of murine genes expressing VP3, NSP2 and NSP3 along with VP4 and NSP1 (Feng *et al.*, 2013).

Bulk measurement of the IFN response cannot reveal hierarchical, temporal and spatial response to virus infection. A single cell approach facilitates detailed dissection of the differences occurring in infected and bystander cells. This approach has been used to show how the homologous murine RV infection resulted in an induction of IRFs and NF-κB transcripts early in the infection (Sen *et al.*, 2012). In contrast, rhesus RRV appeared to be able to block secretion of type I IFN early in infection. Interestingly, the activation of the NF-κB pathway was further reduced in bystander cells compared to the site of infection, with increased levels of Iκβα, in comparison with IRF-3 levels. These findings further corroborate the hypothesis that the ability of RV to successfully infect its host is related to its ability to modulate type III rather than type I IFN, as previously discussed (Hernandez *et al.*, 2015; Pott *et al.*,

2011). However, work by *Lin et al* has shown that RV sensitivity to IFN treatment is strain dependent and varies between hosts, and both type I and type III IFN cooperate synergistically for an optimal protection of the gastro-intestinal tract (J. D. Lin *et al.*, 2016).

The successful infection of the host requires virus dissemination from the site of infection to surrounding cells and tissues. This is translated in its capacity to mask its presence, prevent and/or downregulate immune response and keep the cells alive for sufficient time to support its replication. Antagonism of specific mediators of the apoptotic response is a survival mechanism adopted by many viruses (Best, 2008). For example, RSV selectively targets NF-κB (Bitko *et al.*, 2007), whilst poliovirus (Autret *et al.*, 2008), influenza A virus (Ehrhardt *et al.*, 2007) and dengue virus (Lee *et al.*, 2005) have all been shown to target phosphoinositide 3-kinase (PI3K)/Akt,. The activation of PI3K/Akt has been shown to support viral replication during acute infection inhibiting apoptosis (Diehl *et al.*, 2013).

During early stages of infection, RV creates a favourable environment for its replication by preventing apoptosis within infected cells. It has been reported that NSP1, through is RING domain, interacts with PI3K/Akt activating pro-survival pathways (Bagchi *et al.*, 2010; Bagchi, Nandi*, et al.*, 2013) and induces the proteasome-mediated degradation of p53 to prevent cell-cycle arrest (Bhowmick *et al.*, 2013). In addition, degradation of β-TrCP prevents the secretion of a number of cell cycle and pro-apoptotic regulatory factors (Frescas *et al.*, 2008). Later in the infection, when virus progeny have reached a lytic threshold, the level of NSP1 decreases, leading to the inactivation of PI3K/Akt and the restoration of p53 levels, and subsequent initiation of pro-apoptotic signals.

The high tropism of RV for mature enterocytes of the small intestine, means that upon infection the virus mainly faces a type III IFN-mediated host immune response. In early stages of infection, NSP1 levels and stability are not sufficient to inhibit the transcriptional activity of NF-κB and IRF-3, leading to the induction of IFNs,

which are secreted in an autocrine and a paracrine manner to other epithelial cells, inducing the transcription of ISG. ISG are able to boost the activity of NF-κB and IRF-3, and together with the activation of IRF-7, procure the expression of other IFNs family members, as INF-α and IFN-λ_3.

In advanced stages of infection, with the expression of all RV-encoded proteins, NSP1 stability is increased, and the viral protein is able to target both NF-κB and IRF-3, resulting in modulation of the IFN expression. The block of NF-κB also leads to a reduction of pro-apoptotic signals and together with the binding to p53 and Akt, results in a favourable environment for viral growth. The subsequent decrease in NSP1 levels, reduces Akt activation and allows p53 to activate pro-apoptotic pathways, resulting in cell death and virus release. Released virions can then infect bystander cells. The ability of NSP1 to modulate the JAK/STAT pathways help facilitate the spread. It has been shown that RV is able to systematically infect susceptible animals, spreading from the site of infection to surrounding tissues (Adeyi *et al.*, 2010; Crawford *et al.*, 2017). Crossing the barrier of epithelial cells, the virus needs to spread across the *lamina propria* tissue. In contrast with epithelial cells, *lamina propria* cells are more susceptible to INF-β rather than INF-λ. Thus, to cross this barrier, RV needs to be able to downregulate type I IFN expression rather than type III (Figure 60).

The ability to modulate the host innate immune response appears conserved among different RV strains, with viruses isolated from different hosts being to downregulate the IFN response (5.2). Through the expression of NSP1, RV is able to modulate both the induction and signalling of IFN; by targeting PPRs and IRFs NSP1 blocks the production and secretion of cytokines and by targeting the JACK/STAT pathway NSP1 affects their signalling action. Here we have reported that the NSP1 encoded from different species (human, pigs, cattle and monkeys) are able to downregulate IFN-λ induction (5.2.1.2) targeting NF-κB (5.2.1.3). Epithelial cells mainly express type III IFN, however, due to similitudes in the promoter regions of

type III and type I IFN, viral infection results in a partial secretion of INF-β too. Thus, the ability of some NSP1 to be able to strongly downregulate both IFN-λ and INF-β could reflect the ability of some RV strains to establish a successful infection earlier compared to others.

Together with the inhibition of IFN-λ, a conserved ability to interfere with the JAK/STAT pathway was observed (5.2.1.4). However, in contrast with the IFN induction pathway, we were not able to identify specific host proteins of the signalling pathway targeted by NSP1. Indeed the downregulation of ISG offers an advantageous scenario for the virus, preventing the boosting of IFN induction in infected cells and the activation of bystander cells, offering an easier target to infect. Interestingly, NSP1 appears to only marginally affect IFN-α (5.2.1.1.2) and IFN-λ_3 (5.2.1.2.2) induction. The expression of these two IFNs dos not take place directly upon viral infection through the activation of NF-κB or IRF-3, but they require IRF-7 expression (Figure 35, Figure 40). A possible scenario could be that by the time IFN-α and IFN-λ_3 are activated, viral progeny has reached cell lyses threshold, and the block on IFN induction in infected cells in not required anymore. In contrast, the potential paracrine action of IFN-α and IFN-λ_3 is compensated by the ability of NSP1 to target the JAK/STAT pathway.

In order to better define the observed host range restriction further comparative analysis are required. However, based on the finding of this work, it appears that successful infection of different host may not be solely dependent on the ability of RV to target different host proteins, but more related to the capacity of NSP1 to strongly interact early in the infection with its target (IRF-3, β-TrCP), preventing their activation and blocking or delaying the establishment of the antiviral state.

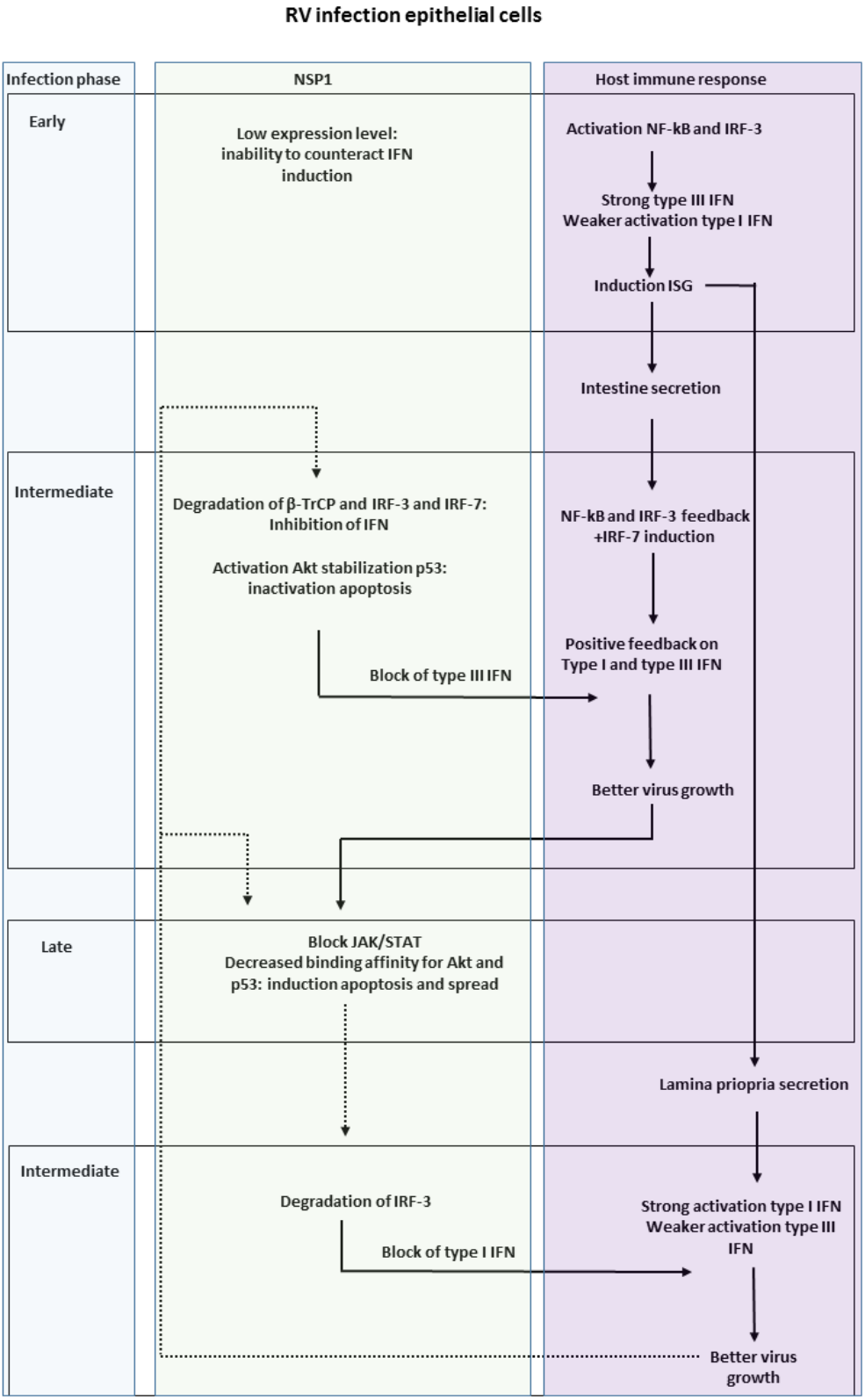

Figure 60. Putative mechanism of action NSP1 during RV infection

Schematic representation of NSP1 mediated downregulation of the IFN induction and signalling.

7 Future work

Viruses constitute a fascinating example of simple complexity.

RV encodes only 12 proteins, of which six are non-structural (Desselberger, 2014). With such a limited repertoire of functional tools, the virus is able to set up a complex cascade of events to establish a successful infection. Masking its presence, downregulating the immune response, controlling cellular trafficking, requesting translational machinery for its own advantage and using host components to assemble mature virions constitute only a few examples of the strategies pursued by the virus using a limited number of self-encoded proteins (Crawford *et al.*, 2017). In such scenario, it is likely that virus-encoded proteins are multi-functional, thus other functions of NSP1 remain to be determined.

Y-2-H screening revealed strain-dependent interactions between NSP1 derived from RV infecting different species and IRF-3 (Table 11). Those interactions may reflect possible scenario of a homologous or heterologous infection, with differences in potency of the interaction been reported. Some NSP1s showed a strong interaction with their targets, by contrast, others were able to target IRF-3 only under lower stringency conditions (Figure 20 and Figure 21). The Y-2-H system is one of the most popular, preferred, cost effective and scalable *in vivo* genetic approaches for screening protein-protein interactions (Aho *et al.*, 1997). One of the possible, and maybe most significant, drawbacks of this technique is that relies on transcription: in order to assess a positive interaction the two proteins need to be able to initiate transcription, but only when they are in close association with each other (Causier *et al.*, 2002). The employment of chimeras, with the fusion of the proteins to yeast DNA-BD and DNA-AD domain always pose a possible risk of altering the actual symmetrical arrangement of the bait or prey and, therefore, modifying its functionalities. This might also result in limited activity or in the inaccessibility to binding sites. Moreover, it needs to take into account that some protein interactions depend on post-translational modifications, such as glycosylation, formation of di-sulfide bonds, and phosphorylation, and these may not occur, or occur unsuitably, in

yeast. In addition, the “bait” and the “protein” may not interact directly, but part of a larger complex of interacting proteins. In this case, the activation of the reporter genes does not reflect a direct interaction. Thus false positive and false negative interactions can occur. Since the employment of other techniques has shown that NSP1 interacts with RIG-I, β-TrCP and STAT1, Y-2-H interactions could be further investigated using alternative systems, such as pull-down or co-IP assays. Since lower stringency conditions in Y-2-H revealed a strain-specific ability of human NSP1 to interact with IRF-3 (Figure 21), same conditions could be used to screen for transient or weak interactions with MAVS and β-TrCP, which have been previously reported to interact with NSP1 (Di Fiore *et al.*, 2015; Nandi *et al.*, 2014). Moreover, since chimeric NSP1 were still able to downregulate type I, type III induction and NF-κB activity (Figure 33, Figure 39 and Figure 45), their ability to interact with IRf-3s could be further investigated.

NSP1 showed a strain-dependent level of expression from transfected plasmids. A possible explanation for the differences observed for the various reporter assays could be due not to strain-specific ability of NSP1 to differentially target the induction of the relative promoter regions, but simply the result of differential levels of expression of NSP1 proteins. The employment of cell lines stably expressing NSP1 will help to decipher the relative strain-specific ability to modulate immune response. Indeed a better understanding of the comparative expressions of different NSP1 in different mammalian cell lines is needed. NSP1 is the most variable protein encoded by RV (Dunn *et al.*, 1994), however sequences analysis have identified highly conserved residues or domains (Bremont *et al.*, 1993; Hua *et al.*, 1994; Mitchell *et al.*, 1990; Okada *et al.*, 1999) which can be used for the production of specific antibodies against NSP1. Western Blot analysis couple with TandT (4.2) would better define the strain-specific half-live of NSP1 and its levels of expression during the course of infection.

The ability of NSP1 to target IRF-3 and NF-κB to downregulate the induction of type I and III IFN appears to be related to its ability to interact through specific NSP1 domains (Davis *et al.*, 2017a; Di Fiore *et al.*, 2015; Ding *et al.*, 2016; Graff *et al.*,

2007; Kanai *et al.*, 2017; Lutz *et al.*, 2016; Morelli, Dennis*, et al.*, 2015; B. Zhao *et al.*, 2016). A RING domain in the N-termini region and a PDL or pLxIS motif in the carboxyl-termini are reported to coordinate NSP1 function. Contrasting results were obtained on the role of these motifs in inducing degradation of their targets. Since chimeric NSP1 were still functional, the generation of NSP1 containing targeted mutations in these motifs would be able to better define their role in IFN downregulation. Upon infection, IRF-3 proteins dimerise, trans-phosphorylate and subsequently translocating to the nucleus. Since NSP1 has been shown to have a strain-specific ability to interact with IRF-3 and downregulate IFN-β (Table 11, Figure 30, Figure 31, Figure 32) (which is mostly IRF-3 driven) production, it would be interesting to determine if NSP1 targets IRF-3 monomers or activated dimers. It has been proposed that an alternative way of NSP1 to affect β-TrCP is not driving its proteasome-mediated degradation, but sitting in its PD motif, preventing recognition with IκBβα (Ding *et al.*, 2016). Similarly, NSP1 could prevent IRF-3 monomers interaction, occupying their respective docking sites. The use of chimeric NSP1 and investigation in IRF-3 phosphorylated levels would better characterize NSP1 ability.

Modulation of NF-κB transcriptional activity has cast a new light on the ability of NSP1 (Figure 43 and Figure 44). Luciferase reporters suggested that the activity of NSP1 in the downregulation of NF-κB activity appears located upstream of p65/p50 (Figure 55) nuclear translocation and downstream of β-TrCP (Figure 51). However, differences between strains were observed. To further elucidate possible steps targeted by NSP1, a series of alternative approaches can be used to detect NF-κB activation, such as band-shifts. The ability of NSP1 to target β-TrCP resulting in stable IκBβα levels could be investigated by measuring the levels of phosphorylated IκBβα or its degradation by Western blot analysis. Confocal microscopy analysis have revealed contrasting results regarding nuclear translocation of p65 in the nucleus (Graff *et al.*, 2009; Holloway *et al.*, 2009). Nuclear fraction Western Blot analysis will help to better elucidate the effect of NSP1 on the release of IκBβα and NF-κB subunits. The presence of NSP1 appears to not affect the activation of the IKK complex (Figure 48) (Graff *et al.*, 2009). However, the employment of an IKKβ Kinase

Assay would be beneficial to better understand if the viral protein employs another system to block the NF-κB pathway.

Mx CAT assay has provided a versatile and powerful tool to assess the IFN induction (Fray *et al.*, 2001), and the assay does allow a classification of the type of IFN induced (Kugel *et al.*, 2011) . As reported, the dual role of IFN-β and IFN-λ in clearance and control of RV infection has shown contrasting results and further analysis are required. SeV infection has been able to trigger both type I and III IFN (Figure 30 and Figure 37). Since the IFN-λ produced in response to infection is acid labile (Kugel *et al.*, 2011), the employment of a MX CAT assay of acid-treated supernatant collected from cells infected with SeV would allow to understand which type if IFN is blocked in presence of NSP1. The employment of a luciferase reporter under the control of the Mx_1 promoter identified a conserved ability of NSP1 isolates from RV infecting different species to block the IFN signalling targeting the JAK/STAT pathway (Figure 57 and Figure 58). A series of studies have reported how different RV strains are capable of blocking the ISGs induction targeting different steps of the JACK/STAT pathway, as at level of STAT phosphorylation (Sen *et al.*, 2014), or preventing its nuclear translocation (Holloway *et al.*, 2014). Since RF-9 has a crucial role in formation of the *ISGF3* complex, would be interesting investigated the strain-specific ability of NSP1 to target IRF-9. The ectopic expression of components of the NF-κB pathways has allowed a better understanding of which stages of the NF-κB induction could be targeted by NSP1 (5.2.1.3.1). A similar approach could be employed to narrow the window of action of NSP1 in the JAK/STAT pathway.

To conclude, a better understanding of the downregulation of the host immune response could come from infectious studies using full RV viruses rather than plasmid-encoded proteins. A fully functional reverse-genetic system is in place, allowing the study of RV replication, pathogenicity and downregulation of the immune response by NSP1 related to a different gene constellation.

8 List of abbreviations

+RNA	positive-sense RNA
aa	amino acid
BD	dna-binding domain
BLAST	basic local alignment search tool
BSA	bovine serum albumin
BVT	Bluetongue virus
CARD	cysteine-aspartic protease (caspase)-recruiting domain
CAT	chloramphenicol acetyltransferase
cDCs	classical dendritic cells
CFP	cell-free protein synthesis
complementary DNA	cDNA
CSFV	Classical Sswine Fever Virus
CTD	c-terminal domain
CTD	carboxy-terminal domain
DDO	double drop-out
distilled water	dH_2O
DLP	double layered particle
DLR	dual-luciferase reporter
DMEM	dulbecco's modified eagle medium
DNA	deoxyribonucleic acid
dNTPs	deoxynucleotide triphosphates
dsRNA	double-stranded RNA
e1F4E	eukaryotic initiation factor 4e
EDTA	ethylenediaminetetraacetic acid
ELISA	enzyme-linked immunosorbent assay
ELISA	enzyme-linked immunosorbent assay
ENS	enteric nervous system
GFP	green fluorescent protein
GPI	glycophosphatidylinositol
GSLs	glycosphingolipids
GTs	glycosyltransferases
h	hour
HA	haemagglutinin
HIV	Human Immunodeficiency Virus
hpi	hours post infection
hsc	heat-shock cognate protein
IEM	immunoelectron-microscopy
IF	immune-fluorescence
IFN	interferon
IFNAR	ifn α/β receptors
IFNLR	ifn λ receptors
IFNRG	ifn ɣ receptors
IL	interleukin
IM	inhibitory motif
IPS-1	interferon promoter stimulator

IRAKs	interleukin-1 receptor-associated kinases
IRF	interferon regulatory factor
ISGF3	ifn-stimulated gene factor 3
ISGs	interferon stimulated genes
ISREs	ifn-stimulated response elements
Iκβ	inhibitor of kappa b
Iκβα	inhibitor of kappa b alpha
JAK	cytoplasmic –associated protein from the janus kinase
JAK/STAT	janus kinase/signal transducers and activators of transcription
kb	kilobase
kDa	kilodalton
LB	luria both
LGP2	laboratory of genetics and physiology 2
LRR	leucine-rich repeat
MAPKs	mitogen-activated protein kinases
MAVS	mitochondrial antiviral-signalling protein
MDA5	melanoma differentiation-associated antigen 5
MEFs	mouse embryonic fibroblast
mg	milligram
min	minute
ml	millilitre
mL	millilitre
mM	millimolar
mRNA	Messenger RNA
MVA	Modified Vaccinia Virus Ankara
MxA	Myxovirus resistance gene a
MyD88	myeloid differentiation primary response gene 88
N/A	not applicable
NF-κB	nuclear factor kappa-light-chain-enhancer of activated b cells
ng	nanogram
NLRs	nucleotide-binding oligomerization domain-like receptors nod-like receptors
N^{pro}	n-terminal autoprotease
NS	viral non-structural protein
ORF	open reading frame
PABP	poly-a binding protein
PABP	cellular poly-a binding protein
PAGE	polyacrylamide gel electrophoresis
PAMPs	pathogen-associated molecular patterns
PBS	phosphate buffered saline
pCDs	plasmacytoid dendritic cells
PCR	polymerase chain reaction
PD	phosphodegron motif
PDL	phosphodegron-like motif
Pm	picommolar
PRDs	positive regulatory domains
PRRs	pattern recognition receptors
QDO	quadruple drop-out

RD	repressor domain
RdRp	RNA dependent RNA polymerase
RER	rough endoplasmic reticulum
RHD	rel homology domain
RI	replication intermediates
RIG-I	retinoic acid-inducible gene i product
RIP-1	receptor-interacting protein 1
RLRs	RIG-I-like receptors
RNA	ribonucleic acid
RNAi	RNAinterference
rpm	revolution per minute
RT	room temperature
RV	rotaviruses
RVA	group A rotaviruses
RVGE	Rotavirus-induced acute and recurrent gastroenteritis
s	second
SDS-PAGE	sodium dodecyl sulphate polyacrylamide gel electrophoresis
SeV	Sendai Virus
siRNA	small interfering RNA
SLP	single layered particle
ssRNA	single stranded rna
STAT	signal transducer and activator of transcription
TADs	transactivation domains
TAE	tris-acetate edta
TBE	tris-borate edta
tc	tissue-culture adapted
TD	transcriptional-activation domain
TDO	triple drop-out
TF	transcriptional factor
TGF-β	tumour growth factor beta
TLP	triple layered particle
TLRs	membrane-bound toll-like receptors
TLRs	toll-like receptors
TM	transmembrane domain
TNFα	tumour necrosis factor alpha
TnT	transcription and translation
TRAF6	tnf receptor-associated factor 6
TRIF	tir-domain-containing adapter-inducing interferon-β
TRR	tetratricopeptide repeat region
UTRs	untranslated regions
VISA	virus-induced signalling adapter
VP	viral structural protein
WT	wild type
Y-2-H	yeast-2-hybrid
β-TrCP	β-transducin repeat-containing protein
µg	microgram
µl	microliter
µM	micromolar

9 Bibliography

Aaronson, D. S., & Horvath, C. M. (2002). A road map for those who don't know JAK-STAT. *Science, 296*(5573), 1653-1655. doi:10.1126/science.1071545

Abdelhakim, A. H., Salgado, E. N., Fu, X., Pasham, M., Nicastro, D., Kirchhausen, T., & Harrison, S. C. (2014). Structural correlates of rotavirus cell entry. *PLoS Pathog, 10*(9), e1004355. doi:10.1371/journal.ppat.1004355

Ablasser, A., Poeck, H., Anz, D., Berger, M., Schlee, M., Kim, S., . . . Hornung, V. (2009). Selection of molecular structure and delivery of RNA oligonucleotides to activate TLR7 versus TLR8 and to induce high amounts of IL-12p70 in primary human monocytes. *J Immunol, 182*(11), 6824-6833. doi:10.4049/jimmunol.0803001

Adeyi, O. A., Costa, G., Abu-Elmagd, K. M., & Wu, T. (2010). Rotavirus infection in adult small intestine allografts: a clinicopathological study of a cohort of 23 patients. *Am J Transplant, 10*(12), 2683-2689. doi:10.1111/j.1600-6143.2010.03311.x

Affranchino, J. L., & Gonzalez, S. A. (1997). Deletion mapping of functional domains in the rotavirus capsid protein VP6. *J Gen Virol, 78 (Pt 8)*, 1949-1955. doi:10.1099/0022-1317-78-8-1949

Afrikanova, I., Fabbretti, E., Miozzo, M. C., & Burrone, O. R. (1998). Rotavirus NSP5 phosphorylation is up-regulated by interaction with NSP2. *J Gen Virol, 79 (Pt 11)*, 2679-2686. doi:10.1099/0022-1317-79-11-2679

Afrikanova, I., Miozzo, M. C., Giambiagi, S., & Burrone, O. (1996). Phosphorylation generates different forms of rotavirus NSP5. *J Gen Virol, 77 (Pt 9)*, 2059-2065. doi:10.1099/0022-1317-77-9-2059

Aho, S., Arffman, A., Pummi, T., & Uitto, J. (1997). A novel reporter gene MEL1 for the yeast two-hybrid system. *Anal Biochem, 253*(2), 270-272. doi:10.1006/abio.1997.2394

Altenburg, B. C., Graham, D. Y., & Estes, M. K. (1980). Ultrastructural study of rotavirus replication in cultured cells. *J Gen Virol, 46*(1), 75-85. doi:10.1099/0022-1317-46-1-75

Angel, J., Franco, M. A., & Greenberg, H. B. (2007). Rotavirus vaccines: recent developments and future considerations. *Nature Reviews Microbiology, 5*(7), 529-U518. doi:10.1038/nrmicro1692

Angel, J., Franco, M. A., & Greenberg, H. B. (2012). Rotavirus immune responses and correlates of protection. *Current Opinion in Virology, 2*(4), 419-425. doi:10.1016/j.coviro.2012.05.003

Angel, J., Franco, M. A., Greenberg, H. B., & Bass, D. (1999). Lack of a role for type I and type II interferons in the resolution of rotavirus-induced diarrhea and infection in mice. *J Interferon Cytokine Res, 19*(6), 655-659. doi:10.1089/107999099313802

Anthony, I. D., Bullivant, S., Dayal, S., Bellamy, A. R., & Berriman, J. A. (1991). Rotavirus spike structure and polypeptide composition. *J Virol, 65*(8), 4334-4340.

Araujo, A. P., Oliva, G., Henrique-Silva, F., Garratt, R. C., Caceres, O., & Beltramini, L. M. (2000). Influence of the histidine tail on the structure and activity of recombinant chlorocatechol 1,2-dioxygenase. *Biochem Biophys Res Commun, 272*(2), 480-484. doi:10.1006/bbrc.2000.2802

Arias, C. F., Silva-Ayala, D., & Lopez, S. (2015). Rotavirus entry: a deep journey into the cell with several exits. *J Virol, 89*(2), 890-893. doi:10.1128/JVI.01787-14

Armah, G. E., Sow, S. O., Breiman, R. F., Dallas, M. J., Tapia, M. D., Feikin, D. R., . . . Neuzil, K. M. (2010). Efficacy of pentavalent rotavirus vaccine against severe rotavirus gastroenteritis in infants in developing countries in sub-Saharan Africa: a randomised, double-blind, placebo-controlled trial. *Lancet, 376*(9741), 606-614. doi:10.1016/S0140-6736(10)60889-6

Arnold, M. M. (2016). The Rotavirus Interferon Antagonist NSP1: Many Targets, Many Questions. *J Virol, 90*(11), 5212-5215. doi:10.1128/JVI.03068-15

Arnold, M. M., Barro, M., & Patton, J. T. (2013). Rotavirus NSP1 mediates degradation of interferon regulatory factors through targeting of the dimerization domain. *J Virol, 87*(17), 9813-9821. doi:10.1128/jvi.01146-13

Arnold, M. M., & Patton, J. T. (2009). Rotavirus antagonism of the innate immune response. *Viruses, 1*(3), 1035-1056. doi:10.3390/v1031035

Arnold, M. M., & Patton, J. T. (2011). Diversity of interferon antagonist activities mediated by NSP1 proteins of different rotavirus strains. *J Virol, 85*(5), 1970-1979. doi:10.1128/JVI.01801-10

Arnold, M. M., Sen, A., Greenberg, H. B., & Patton, J. T. (2013). The Battle between Rotavirus and Its Host for Control of the Interferon Signaling Pathway. *PLoS Pathog, 9*(1). doi:ARTN e1003064

DOI 10.1371/journal.ppat.1003064
Arnoldi, F., Campagna, M., Eichwald, C., Desselberger, U., & Burrone, O. R. (2007). Interaction of rotavirus polymerase VP1 with nonstructural protein NSP5 is stronger than that with NSP2. *J Virol, 81*(5), 2128-2137. doi:10.1128/JVI.01494-06
Au, K. S., Chan, W. K., Burns, J. W., & Estes, M. K. (1989). Receptor activity of rotavirus nonstructural glycoprotein NS28. *J Virol, 63*(11), 4553-4562.
Au, K. S., Mattion, N. M., & Estes, M. K. (1993). A subviral particle binding domain on the rotavirus nonstructural glycoprotein NS28. *Virology, 194*(2), 665-673. doi:10.1006/viro.1993.1306
Autret, A., Martin-Latil, S., Brisac, C., Mousson, L., Colbere-Garapin, F., & Blondel, B. (2008). Early phosphatidylinositol 3-kinase/Akt pathway activation limits poliovirus-induced JNK-mediated cell death. *J Virol, 82*(7), 3796-3802. doi:10.1128/JVI.02020-07
Ayala-Breton, C., Arias, M., Espinosa, R., Romero, P., Arias, C. F., & Lopez, S. (2009). Analysis of the kinetics of transcription and replication of the rotavirus genome by RNA interference. *J Virol, 83*(17), 8819-8831. doi:10.1128/JVI.02308-08
Bagchi, P., Bhowmick, R., Nandi, S., Kant Nayak, M., & Chawla-Sarkar, M. (2013). Rotavirus NSP1 inhibits interferon induced non-canonical NFkappaB activation by interacting with TNF receptor associated factor 2. *Virology, 444*(1-2), 41-44. doi:10.1016/j.virol.2013.07.003
Bagchi, P., Dutta, D., Chattopadhyay, S., Mukherjee, A., Halder, U. C., Sarkar, S., . . . Chawla-Sarkar, M. (2010). Rotavirus nonstructural protein 1 suppresses virus-induced cellular apoptosis to facilitate viral growth by activating the cell survival pathways during early stages of infection. *J Virol, 84*(13), 6834-6845. doi:10.1128/JVI.00225-10
Bagchi, P., Nandi, S., Nayak, M. K., & Chawla-Sarkar, M. (2013). Molecular mechanism behind rotavirus NSP1-mediated PI3 kinase activation: interaction between NSP1 and the p85 subunit of PI3 kinase. *J Virol, 87*(4), 2358-2362. doi:10.1128/JVI.02479-12
Baldwin, A. S., Jr. (1996). The NF-kappa B and I kappa B proteins: new discoveries and insights. *Annu Rev Immunol, 14*, 649-683. doi:10.1146/annurev.immunol.14.1.649
Banninger, G., & Reich, N. C. (2004). STAT2 nuclear trafficking. *J Biol Chem, 279*(38), 39199-39206. doi:10.1074/jbc.M400815200
Bao, M., & Liu, Y. J. (2013). Regulation of TLR7/9 signaling in plasmacytoid dendritic cells. *Protein Cell, 4*(1), 40-52. doi:10.1007/s13238-012-2104-8
Barchet, W., Cella, M., Odermatt, B., Asselin-Paturel, C., Colonna, M., & Kalinke, U. (2002). Virus-induced interferon alpha production by a dendritic cell subset in the absence of feedback signaling in vivo. *J Exp Med, 195*(4), 507-516.
Barro, M., & Patton, J. T. (2005). Rotavirus nonstructural protein 1 subverts innate immune response by inducing degradation of IFN regulatory factor 3. *Proc Natl Acad Sci U S A, 102*(11), 4114-4119. doi:10.1073/pnas.0408376102
Barro, M., & Patton, J. T. (2007). Rotavirus NSP1 inhibits expression of type I interferon by antagonizing the function of interferon regulatory factors IRF3, IRF5, and IRF7. *J Virol, 81*(9), 4473-4481. doi:10.1128/JVI.02498-06
Bashirullah, A., Cooperstock, R. L., & Lipshitz, H. D. (2001). Spatial and temporal control of RNA stability. *Proc Natl Acad Sci U S A, 98*(13), 7025-7028. doi:10.1073/pnas.111145698
Bergmann, C. C., Maass, D., Poruchynsky, M. S., Atkinson, P. H., & Bellamy, A. R. (1989). Topology of the non-structural rotavirus receptor glycoprotein NS28 in the rough endoplasmic reticulum. *EMBO J, 8*(6), 1695-1703.
Berkova, Z., Crawford, S. E., Blutt, S. E., Morris, A. P., & Estes, M. K. (2007). Expression of rotavirus NSP4 alters the actin network organization through the actin remodeling protein cofilin. *J Virol, 81*(7), 3545-3553. doi:10.1128/Jvi.01080-06
Bernstein, D. I., Sack, D. A., Rothstein, E., Reisinger, K., Smith, V. E., O'Sullivan, D., . . . Ward, R. L. (1999). Efficacy of live, attenuated, human rotavirus vaccine 89-12 in infants: a randomised placebo-controlled trial. *Lancet, 354*(9175), 287-290. doi:10.1016/S0140-6736(98)12106-2
Berois, M., Sapin, C., Erk, I., Poncet, D., & Cohen, J. (2003). Rotavirus nonstructural protein NSP5 interacts with major core protein VP2. *J Virol, 77*(3), 1757-1763.
Best, S. M. (2008). Viral subversion of apoptotic enzymes: escape from death row. *Annu Rev Microbiol, 62*, 171-192. doi:10.1146/annurev.micro.62.081307.163009

Bhowmick, R., Halder, U. C., Chattopadhyay, S., Nayak, M. K., & Chawla-Sarkar, M. (2013). Rotavirus-encoded nonstructural protein 1 modulates cellular apoptotic machinery by targeting tumor suppressor protein p53. *J Virol, 87*(12), 6840-6850. doi:10.1128/JVI.00734-13

Bican, P., Cohen, J., Charpilienne, A., & Scherrer, R. (1982). Purification and characterization of bovine rotavirus cores. *J Virol, 43*(3), 1113-1117.

Bishop, R. F., & Davidson, G. P. (1973). Virus-Particles in Epithelial-Cells of Duodenal Mucosa from Children with Acute Non-Bacterial Gastroenteritis. *Lancet, 2*(7841), 1281-1283.

Bishop, R. F., Davidson, G. P., Holmes, I. H., & Ruck, B. J. (1974). Detection of a new virus by electron microscopy of faecal extracts from children with acute gastroenteritis. *Lancet, 1*(7849), 149-151.

Bitko, V., Shulyayeva, O., Mazumder, B., Musiyenko, A., Ramaswamy, M., Look, D. C., & Barik, S. (2007). Nonstructural proteins of respiratory syncytial virus suppress premature apoptosis by an NF-kappaB-dependent, interferon-independent mechanism and facilitate virus growth. *J Virol, 81*(4), 1786-1795. doi:10.1128/JVI.01420-06

Bogyo, M., McMaster, J. S., Gaczynska, M., Tortorella, D., Goldberg, A. L., & Ploegh, H. (1997). Covalent modification of the active site threonine of proteasomal beta subunits and the Escherichia coli homolog HslV by a new class of inhibitors. *Proc Natl Acad Sci U S A, 94*(13), 6629-6634.

Bohm, R., Fleming, F. E., Maggioni, A., Dang, V. T., Holloway, G., Coulson, B. S., . . . Haselhorst, T. (2015). Revisiting the role of histo-blood group antigens in rotavirus host-cell invasion. *Nat Commun, 6*, 5907. doi:10.1038/ncomms6907

Bomsel, M., & Alfsen, A. (2003). Entry of viruses through the epithelial barrier: pathogenic trickery. *Nat Rev Mol Cell Biol, 4*(1), 57-68. doi:10.1038/nrm1005

Booth, W. T., Schlachter, C. R., Pote, S., Ussin, N., Mank, N. J., Klapper, V., . . . Chruszcz, M. (2018). Impact of an N-terminal Polyhistidine Tag on Protein Thermal Stability. *ACS Omega, 3*(1), 760-768. doi:10.1021/acsomega.7b01598

Borodavka, A., Dykeman, E. C., Schrimpf, W., & Lamb, D. C. (2017). Protein-mediated RNA folding governs sequence-specific interactions between rotavirus genome segments. *Elife, 6*. doi:10.7554/eLife.27453

Borodavka, A., Singaram, S. W., Stockley, P. G., Gelbart, W. M., Ben-Shaul, A., & Tuma, R. (2016). Sizes of Long RNA Molecules Are Determined by the Branching Patterns of Their Secondary Structures. *Biophys J, 111*(10), 2077-2085. doi:10.1016/j.bpj.2016.10.014

Boshuizen, J. A., Reimerink, J. H., Korteland-van Male, A. M., van Ham, V. J., Koopmans, M. P., Buller, H. A., . . . Einerhand, A. W. (2003). Changes in small intestinal homeostasis, morphology, and gene expression during rotavirus infection of infant mice. *J Virol, 77*(24), 13005-13016.

Bosu, D. R., & Kipreos, E. T. (2008). Cullin-RING ubiquitin ligases: global regulation and activation cycles. *Cell Div, 3*, 7. doi:10.1186/1747-1028-3-7

Both, G. W., Siegman, L. J., Bellamy, A. R., & Atkinson, P. H. (1983). Coding assignment and nucleotide sequence of simian rotavirus SA11 gene segment 10: location of glycosylation sites suggests that the signal peptide is not cleaved. *J Virol, 48*(2), 335-339.

Bour, S., Perrin, C., Akari, H., & Strebel, K. (2001). The human immunodeficiency virus type 1 Vpu protein inhibits NF-kappa B activation by interfering with beta TrCP-mediated degradation of Ikappa B. *J Biol Chem, 276*(19), 15920-15928. doi:10.1074/jbc.M010533200

Boyce, M., McCrae, M. A., Boyce, P., & Kim, J. T. (2016). Inter-segment complementarity in orbiviruses: a driver for co-ordinated genome packaging in the Reoviridae? *J Gen Virol, 97*(5), 1145-1157. doi:10.1099/jgv.0.000400

Boyle, J. F., & Holmes, K. V. (1986). RNA-binding proteins of bovine rotavirus. *J Virol, 58*(2), 561-568.

Brand, S., Beigel, F., Olszak, T., Zitzmann, K., Eichhorst, S. T., Otte, J. M., . . . Dambacher, J. (2005). IL-28A and IL-29 mediate antiproliferative and antiviral signals in intestinal epithelial cells and murine CMV infection increases colonic IL-28A expression. *Am J Physiol Gastrointest Liver Physiol, 289*(5), G960-968. doi:10.1152/ajpgi.00126.2005

Bremont, M., Chabanne-Vautherot, D., & Cohen, J. (1993). Sequence analysis of three non structural proteins of a porcine group C (Cowden strain) rotavirus. *Arch Virol, 130*(1-2), 85-92.

Bresee, J. S., Hummelman, E., Nelson, E. A., & Glass, R. I. (2005). Rotavirus in Asia: the value of surveillance for informing decisions about the introduction of new vaccines. *J Infect Dis, 192 Suppl 1*, S1-5. doi:10.1086/431515

Bridger, J. C., & Oldham, G. (1987). Avirulent rotavirus infections protect calves from disease with and without inducing high levels of neutralizing antibody. *J Gen Virol, 68 (Pt 9)*, 2311-2317. doi:10.1099/0022-1317-68-9-2311

Bridger, J. C., Pedley, S., & McCrae, M. A. (1986). Group C rotaviruses in humans. *J Clin Microbiol, 23*(4), 760-763.

Brimnes, M. K., Bonifaz, L., Steinman, R. M., & Moran, T. M. (2003). Influenza virus-induced dendritic cell maturation is associated with the induction of strong T cell immunity to a coadministered, normally nonimmunogenic protein. *J Exp Med, 198*(1), 133-144. doi:10.1084/jem.20030266

Broome, R. L., Vo, P. T., Ward, R. L., Clark, H. F., & Greenberg, H. B. (1993). Murine rotavirus genes encoding outer capsid proteins VP4 and VP7 are not major determinants of host range restriction and virulence. *J Virol, 67*(5), 2448-2455.

Broquet, A. H., Hirata, Y., McAllister, C. S., & Kagnoff, M. F. (2011). RIG-I/MDA5/MAVS are required to signal a protective IFN response in rotavirus-infected intestinal epithelium. *J Immunol, 186*(3), 1618-1626. doi:10.4049/jimmunol.1002862

Brottier, P., Nandi, P., Bremont, M., & Cohen, J. (1992). Bovine rotavirus segment 5 protein expressed in the baculovirus system interacts with zinc and RNA. *J Gen Virol, 73 (Pt 8)*, 1931-1938. doi:10.1099/0022-1317-73-8-1931

Brunet, J. P., Jourdan, N., Cotte-Laffite, J., Linxe, C., Geniteau-Legendre, M., Servin, A., & Quero, A. M. (2000). Rotavirus infection induces cytoskeleton disorganization in human intestinal epithelial cells: Implication of an increase in intracellular calcium concentration. *J Virol, 74*(22), 10801-10806. doi:Doi 10.1128/Jvi.74.22.10801-10806.2000

Buchholz, U. J., Finke, S., & Conzelmann, K. K. (1999). Generation of bovine respiratory syncytial virus (BRSV) from cDNA: BRSV NS2 is not essential for virus replication in tissue culture, and the human RSV leader region acts as a functional BRSV genome promoter. *J Virol, 73*(1), 251-259.

Cabral-Romero, C., & Padilla-Noriega, L. (2006). Association of rotavirus viroplasms with microtubules through NSP2 and NSP5. *Mem Inst Oswaldo Cruz, 101*(6), 603-611.

Campagna, M., Eichwald, C., Vascotto, F., & Burrone, O. R. (2005). RNA interference of rotavirus segment 11 mRNA reveals the essential role of NSP5 in the virus replicative cycle. *J Gen Virol, 86*(Pt 5), 1481-1487. doi:10.1099/vir.0.80598-0

Campbell, J. L., & Schekman, R. (1997). Selective packaging of cargo molecules into endoplasmic reticulum-derived COPII vesicles. *Proc Natl Acad Sci U S A, 94*(3), 837-842.

Cao, W., & Liu, Y. J. (2007). Innate immune functions of plasmacytoid dendritic cells. *Curr Opin Immunol, 19*(1), 24-30. doi:10.1016/j.coi.2006.11.004

Carpio, R. V., Gonzalez-Nilo, F. D., Jayaram, H., Spencer, E., Prasad, B. V., Patton, J. T., & Taraporewala, Z. F. (2004). Role of the histidine triad-like motif in nucleotide hydrolysis by the rotavirus RNA-packaging protein NSP2. *J Biol Chem, 279*(11), 10624-10633. doi:10.1074/jbc.M311563200

Causier, B., & Davies, B. (2002). Analysing protein-protein interactions with the yeast two-hybrid system. *Plant Mol Biol, 50*(6), 855-870.

Charpilienne, A., Lepault, J., Rey, F., & Cohen, J. (2002). Identification of rotavirus VP6 residues located at the interface with VP2 that are essential for capsid assembly and transcriptase activity. *J Virol, 76*(15), 7822-7831. doi:10.1128/Jvi.76.15.7822-7831.2002

Chemello, M. E., Aristimuno, O. C., Michelangeli, F., & Ruiz, M. C. (2002). Requirement for vacuolar H+ -ATPase activity and Ca2+ gradient during entry of rotavirus into MA104 cells. *J Virol, 76*(24), 13083-13087.

Chen, C. M., Hung, T., Bridger, J. C., & McCrae, M. A. (1985). Chinese adult rotavirus is a group B rotavirus. *Lancet, 2*(8464), 1123-1124.

Chen, D., Gombold, J. L., & Ramig, R. F. (1990). Intracellular RNA synthesis directed by temperature-sensitive mutants of simian rotavirus SA11. *Virology, 178*(1), 143-151.

Chen, D., Luongo, C. L., Nibert, M. L., & Patton, J. T. (1999). Rotavirus open cores catalyze 5'-capping and methylation of exogenous RNA: evidence that VP3 is a methyltransferase. *Virology, 265*(1), 120-130. doi:10.1006/viro.1999.0029

Chen, D., Zeng, C. Q., Wentz, M. J., Gorziglia, M., Estes, M. K., & Ramig, R. F. (1994). Template-dependent, in vitro replication of rotavirus RNA. *J Virol, 68*(11), 7030-7039.

Chinnakannan, S. K., Nanda, S. K., & Baron, M. D. (2013). Morbillivirus v proteins exhibit multiple mechanisms to block type 1 and type 2 interferon signalling pathways. *PLoS One, 8*(2), e57063. doi:10.1371/journal.pone.0057063

Chowdary, D. R., Dermody, J. J., Jha, K. K., & Ozer, H. L. (1994). Accumulation of p53 in a mutant cell line defective in the ubiquitin pathway. *Mol Cell Biol, 14*(3), 1997-2003.

Ciarlet, M., & Estes, M. K. (2001). Interactions between rotavirus and gastrointestinal cells. *Curr Opin Microbiol, 4*(4), 435-441.

Clapp, L. L., & Patton, J. T. (1991). Rotavirus morphogenesis: domains in the major inner capsid protein essential for binding to single-shelled particles and for trimerization. *Virology, 180*(2), 697-708.

Clark, S. M., Roth, J. R., Clark, M. L., Barnett, B. B., & Spendlove, R. S. (1981). Trypsin enhancement of rotavirus infectivity: mechanism of enhancement. *J Virol, 39*(3), 816-822.

Clarke, I. N., & McCrae, M. A. (1981). A rapid and sensitive method for analysing the genome profiles of field isolates of rotavirus. *J Virol Methods, 2*(4), 203-209.

Cohen, J., Laporte, J., Charpilienne, A., & Scherrer, R. (1979). Activation of rotavirus RNA polymerase by calcium chelation. *Arch Virol, 60*(3-4), 177-186.

Colomina, J., Gil, M. T., Codoner, P., & Buesa, J. (1998). Viral proteins VP2, VP6, and NSP2 are strongly precipitated by serum and fecal antibodies from children with rotavirus symptomatic infection. *J Med Virol, 56*(1), 58-65.

Condemine, W., Eguether, T., Courousse, N., Etchebest, C., Gardet, A., Trugnan, G., & Chwetzoff, S. (2018). The C-terminus of rotavirus VP4 protein contains an actin binding domain which requires co-operation with the coiled-coil domain for actin remodeling. *J Virol*. doi:10.1128/JVI.01598-18

Contin, R., Arnoldi, F., Campagna, M., & Burrone, O. R. (2010). Rotavirus NSP5 orchestrates recruitment of viroplasmic proteins. *J Gen Virol, 91*(Pt 7), 1782-1793. doi:10.1099/vir.0.019133-0

Contreras-Trevino, H. I., Reyna-Rosas, E., Leon-Rodriguez, R., Ruiz-Ordaz, B. H., Dinkova, T. D., Cevallos, A. M., & Padilla-Noriega, L. (2017). Species A rotavirus NSP3 acquires its translation inhibitory function prior to stable dimer formation. *PLoS One, 12*(7), e0181871. doi:10.1371/journal.pone.0181871

Crawford, S. E., Ramani, S., Tate, J. E., Parashar, U. D., Svensson, L., Hagbom, M., . . . Estes, M. K. (2017). Rotavirus infection. *Nat Rev Dis Primers, 3*, 17083. doi:10.1038/nrdp.2017.83

Criglar, J. M., Hu, L., Crawford, S. E., Hyser, J. M., Broughman, J. R., Prasad, B. V., & Estes, M. K. (2014). A novel form of rotavirus NSP2 and phosphorylation-dependent NSP2-NSP5 interactions are associated with viroplasm assembly. *J Virol, 88*(2), 786-798. doi:10.1128/JVI.03022-13

Crosas, B., Hanna, J., Kirkpatrick, D. S., Zhang, D. P., Tone, Y., Hathaway, N. A., . . . Finley, D. (2006). Ubiquitin chains are remodeled at the proteasome by opposing ubiquitin ligase and deubiquitinating activities. *Cell, 127*(7), 1401-1413. doi:10.1016/j.cell.2006.09.051

Cuadras, M. A., Arias, C. F., & Lopez, S. (1997). Rotaviruses induce an early membrane permeabilization of MA104 cells and do not require a low intracellular Ca2+ concentration to initiate their replication cycle. *J Virol, 71*(12), 9065-9074.

Cui, W., Xiao, N., Xiao, H., Zhou, H., Yu, M., Gu, J., & Li, X. (2012). beta-TrCP-mediated IRAK1 degradation releases TAK1-TRAF6 from the membrane to the cytosol for TAK1-dependent NF-kappaB activation. *Mol Cell Biol, 32*(19), 3990-4000. doi:10.1128/MCB.00722-12

Darnell, J. E., Jr. (1997). Phosphotyrosine signaling and the single cell:metazoan boundary. *Proc Natl Acad Sci U S A, 94*(22), 11767-11769.

Davis, K. A., Morelli, M., & Patton, J. T. (2017a). Rotavirus NSP1 as a phosphorylated substrate adaptor of hijacked Cullin-RING ligases. *Faseb Journal, 31*.

Davis, K. A., Morelli, M., & Patton, J. T. (2017b). Rotavirus NSP1 Requires Casein Kinase II-Mediated Phosphorylation for Hijacking of Cullin-RING Ligases. *MBio, 8*(4). doi:10.1128/mBio.01213-17

De Lorenzo, G., Drikic, M., Papa, G., Eichwald, C., Burrone, O. R., & Arnoldi, F. (2016). An Inhibitory Motif on the 5'UTR of Several Rotavirus Genome Segments Affects Protein Expression and Reverse Genetics Strategies. *PLoS One, 11*(11), e0166719. doi:10.1371/journal.pone.0166719

De Nardo, D. (2015). Toll-like receptors: Activation, signalling and transcriptional modulation. *Cytokine, 74*(2), 181-189. doi:10.1016/j.cyto.2015.02.025

Deo, R. C., Groft, C. M., Rajashankar, K. R., & Burley, S. K. (2002). Recognition of the rotavirus mRNA 3' consensus by an asymmetric NSP3 homodimer. *Cell, 108*(1), 71-81.

Desai, R., Esposito, D. H., Lees, C., Goodin, K., Harris, M., Blostein, J., & Parashar, U. D. (2011). Rotavirus-Coded Deaths in Children, United States, 1999-2007. *Pediatric Infectious Disease Journal, 30*(11), 986-988. doi:10.1097/INF.0b013e318220fe20

Desselberger, U. (2014). Rotaviruses. *Virus Res, 190*, 75-96. doi:10.1016/j.virusres.2014.06.016

Desselberger, U., Richards, J., Tchertanov, L., Lepault, J., Lever, A., Burrone, O., & Cohen, J. (2013). Further characterisation of rotavirus cores: Ss(+)RNAs can be packaged in vitro but packaging lacks sequence specificity. *Virus Res, 178*(2), 252-263. doi:10.1016/j.virusres.2013.09.034

Di Fiore, I. J., Pane, J. A., Holloway, G., & Coulson, B. S. (2015). NSP1 of human rotaviruses commonly inhibits NF-kappaB signaling by inducing beta-TrCP degradation. *J Gen Virol*. doi:10.1099/vir.0.000093

Dias Junior, A. G., Sampaio, N. G., & Rehwinkel, J. (2018). A Balancing Act: MDA5 in Antiviral Immunity and Autoinflammation. *Trends Microbiol*. doi:10.1016/j.tim.2018.08.007

Diaz-Salinas, M. A., Romero, P., Espinosa, R., Hoshino, Y., Lopez, S., & Arias, C. F. (2013). The spike protein VP4 defines the endocytic pathway used by rotavirus to enter MA104 cells. *J Virol, 87*(3), 1658-1663. doi:10.1128/JVI.02086-12

Diaz, Y., Pena, F., Aristimuno, O. C., Matteo, L., De Agrela, M., Chemello, M. E., . . . Ruiz, M. C. (2012). Dissecting the Ca(2)(+) entry pathways induced by rotavirus infection and NSP4-EGFP expression in Cos-7 cells. *Virus Res, 167*(2), 285-296. doi:10.1016/j.virusres.2012.05.012

Dickensheets, H., Sheikh, F., Park, O., Gao, B., & Donnelly, R. P. (2013). Interferon-lambda (IFN-lambda) induces signal transduction and gene expression in human hepatocytes, but not in lymphocytes or monocytes. *J Leukoc Biol, 93*(3), 377-385. doi:10.1189/jlb.0812395

Dickman, K. G., Hempson, S. J., Anderson, J., Lippe, S., Zhao, L. M., Burakoff, R., & Shaw, R. D. (2000). Rotavirus alters paracellular permeability and energy metabolism in Caco-2 cells. *American Journal of Physiology-Gastrointestinal and Liver Physiology, 279*(4), G757-G766.

Diehl, N., & Schaal, H. (2013). Make Yourself at Home: Viral Hijacking of the PI3K/Akt Signaling Pathway. *Viruses-Basel, 5*(12), 3192-3212. doi:10.3390/v5123192

Ding, S., Mooney, N., Li, B., Kelly, M. R., Feng, N., Loktev, A. V., . . . Greenberg, H. B. (2016). Comparative Proteomics Reveals Strain-Specific beta-TrCP Degradation via Rotavirus NSP1 Hijacking a Host Cullin-3-Rbx1 Complex. *PLoS Pathog, 12*(10), e1005929. doi:10.1371/journal.ppat.1005929

Ding, S., Zhu, S., Ren, L., Feng, N., Song, Y., Ge, X., . . . Greenberg, H. B. (2018). Rotavirus VP3 targets MAVS for degradation to inhibit type III interferon expression in intestinal epithelial cells. *Elife, 7*. doi:10.7554/eLife.39494

Donnelly, R. P., & Kotenko, S. V. (2010). Interferon-lambda: a new addition to an old family. *J Interferon Cytokine Res, 30*(8), 555-564. doi:10.1089/jir.2010.0078

Donnelly, R. P., Sheikh, F., Kotenko, S. V., & Dickensheets, H. (2004). The expanded family of class II cytokines that share the IL-10 receptor-2 (IL-10R2) chain. *J Leukoc Biol, 76*(2), 314-321. doi:10.1189/jlb.0204117

Douagi, I., McInerney, G. M., Hidmark, A. S., Miriallis, V., Johansen, K., Svensson, L., & Karlsson Hedestam, G. B. (2007). Role of interferon regulatory factor 3 in type I interferon responses in rotavirus-infected dendritic cells and fibroblasts. *J Virol, 81*(6), 2758-2768. doi:10.1128/JVI.01555-06

Doyle, S. E., Schreckhise, H., Khuu-Duong, K., Henderson, K., Rosler, R., Storey, H., . . . Klucher, K. M. (2006). Interleukin-29 uses a type 1 interferon-like program to promote antiviral responses in human hepatocytes. *Hepatology, 44*(4), 896-906. doi:10.1002/hep.21312

Dunn, S. J., Cross, T. L., & Greenberg, H. B. (1994). Comparison of the rotavirus nonstructural protein NSP1 (NS53) from different species by sequence analysis and northern blot hybridization. *Virology, 203*(1), 178-183. doi:10.1006/viro.1994.1471

Durfee, T., Becherer, K., Chen, P. L., Yeh, S. H., Yang, Y., Kilburn, A. E., . . . Elledge, S. J. (1993). The retinoblastoma protein associates with the protein phosphatase type 1 catalytic subunit. *Genes Dev, 7*(4), 555-569.

Dyall-Smith, M. L., Azad, A. A., & Holmes, I. H. (1983). Gene mapping of rotavirus double-stranded RNA segments by northern blot hybridization: application to segments 7, 8, and 9. *J Virol, 46*(1), 317-320.

Ehrhardt, C., Wolff, T., Pleschka, S., Planz, O., Beermann, W., Bode, J. G., . . . Ludwig, S. (2007). Influenza A virus NS1 protein activates the PI3K/Akt pathway to mediate antiapoptotic signaling responses. *J Virol, 81*(7), 3058-3067. doi:10.1128/JVI.02082-06

Eichwald, C., Arnoldi, F., Laimbacher, A. S., Schraner, E. M., Fraefel, C., Wild, P., . . . Ackermann, M. (2012). Rotavirus viroplasm fusion and perinuclear localization are dynamic processes requiring stabilized microtubules. *PLoS One, 7*(10), e47947. doi:10.1371/journal.pone.0047947

Eichwald, C., Rodriguez, J. F., & Burrone, O. R. (2004). Characterization of rotavirus NSP2/NSP5 interactions and the dynamics of viroplasm formation. *J Gen Virol, 85*(Pt 3), 625-634. doi:10.1099/vir.0.19611-0

Ericson, B. L., Graham, D. Y., Mason, B. B., & Estes, M. K. (1982). Identification, synthesis, and modifications of simian rotavirus SA11 polypeptides in infected cells. *J Virol, 42*(3), 825-839.

Estes, & Greenberg, H. B. (2007). Rotaviruses. In B. N. Fields, D. M. Knipe, & P. M. Howley (Eds.), *Fields' virology*

(5th ed., pp. 1347-1395). Philadelphia: Wolters Kluwer Health/Lippincott Williams & Wilkins.

Estes, M. K., & Cohen, J. (1989). Rotavirus gene structure and function. *Microbiol Rev, 53*(4), 410-449.

Estrozi, L. F., Settembre, E. C., Goret, G., McClain, B., Zhang, X., Chen, J. Z., . . . Harrison, S. C. (2013). Location of the dsRNA-dependent polymerase, VP1, in rotavirus particles. *J Mol Biol, 425*(1), 124-132. doi:10.1016/j.jmb.2012.10.011

Fabbretti, E., Afrikanova, I., Vascotto, F., & Burrone, O. R. (1999). Two non-structural rotavirus proteins, NSP2 and NSP5, form viroplasm-like structures in vivo. *J Gen Virol, 80 (Pt 2)*, 333-339. doi:10.1099/0022-1317-80-2-333

Fagerlund, R., Behar, M., Fortmann, K. T., Lin, Y. E., Vargas, J. D., & Hoffmann, A. (2015). Anatomy of a negative feedback loop: the case of IkappaBalpha. *J R Soc Interface, 12*(110), 0262. doi:10.1098/rsif.2015.0262

Fajardo, T., Jr., Sung, P. Y., & Roy, P. (2015). Disruption of Specific RNA-RNA Interactions in a Double-Stranded RNA Virus Inhibits Genome Packaging and Virus Infectivity. *PLoS Pathog, 11*(12), e1005321. doi:10.1371/journal.ppat.1005321

Faul, E. J., Wanjalla, C. N., Suthar, M. S., Gale, M., Wirblich, C., & Schnell, M. J. (2010). Rabies virus infection induces type I interferon production in an IPS-1 dependent manner while dendritic cell activation relies on IFNAR signaling. *PLoS Pathog, 6*(7), e1001016. doi:10.1371/journal.ppat.1001016

Feng, N., Kim, B., Fenaux, M., Nguyen, H., Vo, P., Omary, M. B., & Greenberg, H. B. (2008). Role of interferon in homologous and heterologous rotavirus infection in the intestines and extraintestinal organs of suckling mice. *J Virol, 82*(15), 7578-7590. doi:10.1128/JVI.00391-08

Feng, N., Sen, A., Nguyen, H., Vo, P., Hoshino, Y., Deal, E. M., & Greenberg, H. B. (2009). Variation in antagonism of the interferon response to rotavirus NSP1 results in differential infectivity in mouse embryonic fibroblasts. *J Virol, 83*(14), 6987-6994. doi:10.1128/JVI.00585-09

Feng, N., Sen, A., Wolf, M., Vo, P., Hoshino, Y., & Greenberg, H. B. (2011). Roles of VP4 and NSP1 in determining the distinctive replication capacities of simian rotavirus RRV and bovine rotavirus UK in the mouse biliary tract. *J Virol, 85*(6), 2686-2694. doi:10.1128/JVI.02408-10

Feng, N., Yasukawa, L. L., Sen, A., & Greenberg, H. B. (2013). Permissive replication of homologous murine rotavirus in the mouse intestine is primarily regulated by VP4 and NSP1. *J Virol, 87*(15), 8307-8316. doi:10.1128/JVI.00619-13

Fernandez-Sesma, A., Marukian, S., Ebersole, B. J., Kaminski, D., Park, M. S., Yuen, T., . . . Moran, T. M. (2006). Influenza virus evades innate and adaptive immunity via the NS1 protein. *J Virol, 80*(13), 6295-6304. doi:10.1128/JVI.02381-05

Fiebach, A. R., Guzylack-Piriou, L., Python, S., Summerfield, A., & Ruggli, N. (2011). Classical swine fever virus N(pro) limits type I interferon induction in plasmacytoid dendritic cells by interacting with interferon regulatory factor 7. *J Virol, 85*(16), 8002-8011. doi:10.1128/JVI.00330-11

Fields, S., & Song, O. (1989). A novel genetic system to detect protein-protein interactions. *Nature, 340*(6230), 245-246. doi:10.1038/340245a0

Fiore, L., Greenberg, H. B., & Mackow, E. R. (1991). The Vp8 Fragment of Vp4 Is the Rhesus Rotavirus Hemagglutinin. *Virology, 181*(2), 553-563. doi:Doi 10.1016/0042-6822(91)90888-I

Fischer, T. K., Viboud, C., Parashar, U., Malek, M., Steiner, C., Glass, R., & Simonsen, L. (2007). Hospitalizations and deaths from diarrhea and rotavirus among children < 5 years of age in the United States, 1993-2003. *Journal of Infectious Diseases, 195*(8), 1117-1125. doi:10.1086/512863

Fitzgerald, K. A., McWhirter, S. M., Faia, K. L., Rowe, D. C., Latz, E., Golenbock, D. T., . . . Maniatis, T. (2003). IKKepsilon and TBK1 are essential components of the IRF3 signaling pathway. *Nat Immunol, 4*(5), 491-496. doi:10.1038/ni921

Fleming, F. E., Graham, K. L., Takada, Y., & Coulson, B. S. (2011). Determinants of the specificity of rotavirus interactions with the alpha2beta1 integrin. *J Biol Chem, 286*(8), 6165-6174. doi:10.1074/jbc.M110.142992

Flewett, T. H., Bryden, A. S., & Davies, H. (1973). Letter: Virus particles in gastroenteritis. *Lancet, 2*(7844), 1497.

Flewett, T. H., Bryden, A. S., Davies, H., Woode, G. N., Bridger, J. C., & Derrick, J. M. (1974). Relation between viruses from acute gastroenteritis of children and newborn calves. *Lancet, 2*(7872), 61-63.

Flores, J., Perez-Schael, I., Blanco, M., Rojas, A. M., Alfonzo, E., Crespo, I., . . . Kapikian, A. Z. (1993). Reactogenicity and immunogenicity of a high-titer rhesus rotavirus-based quadrivalent rotavirus vaccine. *J Clin Microbiol, 31*(9), 2439-2445.

Fortmann, K. T., Lewis, R. D., Ngo, K. A., Fagerlund, R., & Hoffmann, A. (2015). A Regulated, Ubiquitin-Independent Degron in IkappaBalpha. *J Mol Biol, 427*(17), 2748-2756. doi:10.1016/j.jmb.2015.07.008

Fray, M. D., Mann, G. E., & Charleston, B. (2001). Validation of an Mx/CAT reporter gene assay for the quantification of bovine type-I interferon. *J Immunol Methods, 249*(1-2), 235-244.

Fredericksen, B. L., Keller, B. C., Fornek, J., Katze, M. G., & Gale, M., Jr. (2008). Establishment and maintenance of the innate antiviral response to West Nile Virus involves both RIG-I and MDA5 signaling through IPS-1. *J Virol, 82*(2), 609-616. doi:10.1128/JVI.01305-07

Frescas, D., & Pagano, M. (2008). Deregulated proteolysis by the F-box proteins SKP2 and beta-TrCP: tipping the scales of cancer. *Nat Rev Cancer, 8*(6), 438-449. doi:10.1038/nrc2396

Fu, X. Y., Kessler, D. S., Veals, S. A., Levy, D. E., & Darnell, J. E., Jr. (1990). ISGF3, the transcriptional activator induced by interferon alpha, consists of multiple interacting polypeptide chains. *Proc Natl Acad Sci U S A, 87*(21), 8555-8559.

Fujita, T., Miyamoto, M., Kimura, Y., Hammer, J., & Taniguchi, T. (1989). Involvement of a cis-element that binds an H2TF-1/NF kappa B like factor(s) in the virus-induced interferon-beta gene expression. *Nucleic Acids Res, 17*(9), 3335-3346.

Fukuhara, N., Yoshie, O., Kitaoka, S., & Konno, T. (1988). Role of VP3 in human rotavirus internalization after target cell attachment via VP7. *J Virol, 62*(7), 2209-2218.

Gack, M. U. (2014). Mechanisms of RIG-I-Like Receptor Activation and Manipulation by Viral Pathogens. *J Virol, 88*(10), 5213-5216. doi:10.1128/jvi.03370-13

Gallegos, C. O., & Patton, J. T. (1989). Characterization of rotavirus replication intermediates: a model for the assembly of single-shelled particles. *Virology, 172*(2), 616-627.

Garcés Suárez, Y., Martínez, J. L., Torres Hernández, D., Hernández, H. O., Méndez, M., Wood, C., . . . Arias, C. F. (2018). Nanoscale organization of rotavirus replication machineries. *bioRxiv*. doi:10.1101/445262

Gardet, A., Breton, M., Trugnan, G., & Chwetzoff, S. (2007). Role for actin in the polarized release of rotavirus. *J Virol, 81*(9), 4892-4894. doi:10.1128/Jvi.02698-06

Gates, L. T., & Shisler, J. L. (2016). cFLIPL Interrupts IRF3-CBP-DNA Interactions To Inhibit IRF3-Driven Transcription. *J Immunol, 197*(3), 923-933. doi:10.4049/jimmunol.1502611

Gentsch, J. R., Laird, A. R., Bielfelt, B., Griffin, D. D., Banyai, K., Ramachandran, M., . . . Glass, R. I. (2005). Serotype diversity and reassortment between human and animal rotavirus strains: implications for rotavirus vaccine programs. *J Infect Dis, 192 Suppl 1*, S146-159. doi:10.1086/431499

Ghosh, S., May, M. J., & Kopp, E. B. (1998). NF-kappa B and Rel proteins: evolutionarily conserved mediators of immune responses. *Annu Rev Immunol, 16*, 225-260. doi:10.1146/annurev.immunol.16.1.225

Giardino Torchia, M. L., Conze, D. B., Jankovic, D., & Ashwell, J. D. (2013). Balance between NF-kappaB p100 and p52 regulates T cell costimulation dependence. *J Immunol, 190*(2), 549-555. doi:10.4049/jimmunol.1201697

Goerke, A. R., & Swartz, J. R. (2008). Development of cell-free protein synthesis platforms for disulfide bonded proteins. *Biotechnology and Bioengineering, 99*(2), 351-367. doi:10.1002/bit.21567

Gombold, J. L., Estes, M. K., & Ramig, R. F. (1985a). Assignment of Simian Rotavirus Sa11 Temperature-Sensitive Mutant Group-B and Group-E to Genome Segments. *Virology, 143*(1), 309-320. doi:Doi 10.1016/0042-6822(85)90118-7

Gombold, J. L., Estes, M. K., & Ramig, R. F. (1985b). Assignment of simian rotavirus SA11 temperature-sensitive mutant groups B and E to genome segments. *Virology, 143*(1), 309-320.

Gombold, J. L., & Ramig, R. F. (1987). Assignment of simian rotavirus SA11 temperature-sensitive mutant groups A, C, F, and G to genome segments. *Virology, 161*(2), 463-473.

Gonzalez, R. A., Torres-Vega, M. A., Lopez, S., & Arias, C. F. (1998). In vivo interactions among rotavirus nonstructural proteins. *Arch Virol, 143*(5), 981-996.

Gonzalez, S. A., & Burrone, O. R. (1989). Porcine OSU rotavirus segment II sequence shows common features with the viral gene of human origin. *Nucleic Acids Res, 17*(15), 6402.

Goodbourn, S., & Maniatis, T. (1988). Overlapping positive and negative regulatory domains of the human beta-interferon gene. *Proc Natl Acad Sci U S A, 85*(5), 1447-1451.

Gorziglia, M., Larrea, C., Liprandi, F., & Esparza, J. (1985). Biochemical evidence for the oligomeric (possibly trimeric) structure of the major inner capsid polypeptide (45K) of rotaviruses. *J Gen Virol, 66 (Pt 9)*, 1889-1900. doi:10.1099/0022-1317-66-9-1889

Gorziglia, M., Nishikawa, K., & Fukuhara, N. (1989). Evidence of duplication and deletion in super short segment 11 of rabbit rotavirus Alabama strain. *Virology, 170*(2), 587-590.

Gottipati, K., Holthauzen, L. M., Ruggli, N., & Choi, K. H. (2016). Pestivirus Npro Directly Interacts with Interferon Regulatory Factor 3 Monomer and Dimer. *J Virol, 90*(17), 7740-7747. doi:10.1128/JVI.00318-16

Graff, J. W., Ettayebi, K., & Hardy, M. E. (2009). Rotavirus NSP1 inhibits NFkappaB activation by inducing proteasome-dependent degradation of beta-TrCP: a novel mechanism of IFN antagonism. *PLoS Pathog, 5*(1), e1000280. doi:10.1371/journal.ppat.1000280

Graff, J. W., Ewen, J., Ettayebi, K., & Hardy, M. E. (2007). Zinc-binding domain of rotavirus NSP1 is required for proteasome-dependent degradation of IRF3 and autoregulatory NSP1 stability. *J Gen Virol, 88*(Pt 2), 613-620. doi:10.1099/vir.0.82255-0

Graff, J. W., Mitzel, D. N., Weisend, C. M., Flenniken, M. L., & Hardy, M. E. (2002). Interferon regulatory factor 3 is a cellular partner of rotavirus NSP1. *J Virol, 76*(18), 9545-9550.

Graham, D. Y., & Estes, M. K. (1985). Proposed Working Serologic Classification-System for Rotaviruses. *Annales De L Institut Pasteur-Virology, 136E*(1), 5-12. doi:Doi 10.1016/S0769-2617(85)80108-8

Graham, K. L., Halasz, P., Tan, Y., Hewish, M. J., Takada, Y., Mackow, E. R., . . . Coulson, B. S. (2003). Integrin-using rotaviruses bind alpha2beta1 integrin alpha2 I domain via VP4 DGE sequence and recognize alphaXbeta2 and alphaVbeta3 by using VP7 during cell entry. *J Virol, 77*(18), 9969-9978.

Gratia, M., Sarot, E., Vende, P., Charpilienne, A., Baron, C. H., Duarte, M., . . . Poncet, D. (2015). Rotavirus NSP3 Is a Translational Surrogate of the Poly(A) Binding Protein-Poly(A) Complex. *J Virol, 89*(17), 8773-8782. doi:10.1128/JVI.01402-15

Gratia, M., Vende, P., Charpilienne, A., Baron, H. C., Laroche, C., Sarot, E., . . . Poncet, D. (2016). Challenging the Roles of NSP3 and Untranslated Regions in Rotavirus mRNA Translation. *PLoS One, 11*(1), e0145998. doi:10.1371/journal.pone.0145998

Greenberg, H. B., Flores, J., Kalica, A. R., Wyatt, R. G., & Jones, R. (1983). Gene coding assignments for growth restriction, neutralization and subgroup specificities of the W and DS-1 strains of human rotavirus. *J Gen Virol, 64 (Pt 2)*, 313-320. doi:10.1099/0022-1317-64-2-313

Gridley, C. L., & Patton, J. T. (2014). Regulation of rotavirus polymerase activity by inner capsid proteins. *Current Opinion in Virology, 9*, 31-38. doi:10.1016/j.coviro.2014.08.008

Guerrero, C. A., Bouyssounade, D., Zarate, S., Isa, P., Lopez, T., Espinosa, R., . . . Arias, C. F. (2002). Heat shock cognate protein 70 is involved in rotavirus cell entry. *J Virol, 76*(8), 4096-4102.

Guzman, E., & McCrae, M. A. (2005). Molecular characterization of the rotavirus NSP4 enterotoxin homologue from group B rotavirus. *Virus Res, 110*(1-2), 151-160. doi:10.1016/j.virusres.2005.02.005

Hakim, M. S., Ding, S., Chen, S., Yin, Y., Su, J., van der Woude, C. J., . . . Wang, W. (2018). TNF-alpha exerts potent anti-rotavirus effects via the activation of classical NF-kappaB pathway. *Virus Res, 253*, 28-37. doi:10.1016/j.virusres.2018.05.022

Hansen, J. D., Vojtech, L. N., & Laing, K. J. (2011). Sensing disease and danger: a survey of vertebrate PRRs and their origins. *Dev Comp Immunol, 35*(9), 886-897. doi:10.1016/j.dci.2011.01.008

Hayden, M. S., & Ghosh, S. (2012). NF-kappaB, the first quarter-century: remarkable progress and outstanding questions. *Genes Dev, 26*(3), 203-234. doi:10.1101/gad.183434.111

Hermant, P., Demarez, C., Mahlakoiv, T., Staeheli, P., Meuleman, P., & Michiels, T. (2014). Human but Not Mouse Hepatocytes Respond to Interferon-Lambda In Vivo. *PLoS One, 9*(1). doi:ARTN e87906

10.1371/journal.pone.0087906

Hernandez, P. P., Mahlakoiv, T., Yang, I., Schwierzeck, V., Nguyen, N., Guendel, F., . . . Diefenbach, A. (2015). Interferon-lambda and interleukin 22 act synergistically for the induction of interferon-stimulated genes and control of rotavirus infection. *Nat Immunol, 16*(7), 698-707. doi:10.1038/ni.3180

Hershko, A., Ciechanover, A., Heller, H., Haas, A. L., & Rose, I. A. (1980). Proposed role of ATP in protein breakdown: conjugation of protein with multiple chains of the polypeptide of ATP-dependent proteolysis. *Proc Natl Acad Sci U S A, 77*(4), 1783-1786.

Hidmark, A. S., McInerney, G. M., Nordstrom, E. K., Douagi, I., Werner, K. M., Liljestrom, P., & Karlsson Hedestam, G. B. (2005). Early alpha/beta interferon production by myeloid dendritic cells in response to UV-inactivated virus requires viral entry and interferon regulatory factor 3 but not MyD88. *J Virol, 79*(16), 10376-10385. doi:10.1128/JVI.79.16.10376-10385.2005

Hidmark, A. S., Nordstrom, E. K., Dosenovic, P., Forsell, M. N., Liljestrom, P., & Karlsson Hedestam, G. B. (2006). Humoral responses against coimmunized protein antigen but not against alphavirus-encoded antigens require alpha/beta interferon signaling. *J Virol, 80*(14), 7100-7110. doi:10.1128/JVI.02579-05

Hilton, L., Moganeradj, K., Zhang, G., Chen, Y. H., Randall, R. E., McCauley, J. W., & Goodbourn, S. (2006). The NPro product of bovine viral diarrhea virus inhibits DNA binding by interferon regulatory factor 3 and targets it for proteasomal degradation. *J Virol, 80*(23), 11723-11732. doi:10.1128/JVI.01145-06

Hinz, M., Arslan, S. C., & Scheidereit, C. (2012). It takes two to tango: IkappaBs, the multifunctional partners of NF-kappaB. *Immunol Rev, 246*(1), 59-76. doi:10.1111/j.1600-065X.2012.01102.x

Holloway, G., & Coulson, B. S. (2013). Innate cellular responses to rotavirus infection. *J Gen Virol, 94*(Pt 6), 1151-1160. doi:10.1099/vir.0.051276-0

Holloway, G., Dang, V. T., Jans, D. A., & Coulson, B. S. (2014). Rotavirus inhibits IFN-induced STAT nuclear translocation by a mechanism that acts after STAT binding to importin-alpha. *J Gen Virol, 95*(Pt 8), 1723-1733. doi:10.1099/vir.0.064063-0

Holloway, G., Truong, T. T., & Coulson, B. S. (2009). Rotavirus antagonizes cellular antiviral responses by inhibiting the nuclear accumulation of STAT1, STAT2, and NF-kappaB. *J Virol, 83*(10), 4942-4951. doi:10.1128/JVI.01450-08

Honda, K., Sakaguchi, S., Nakajima, C., Watanabe, A., Yanai, H., Matsumoto, M., . . . Taniguchi, T. (2003). Selective contribution of IFN-alpha/beta signaling to the maturation of dendritic cells induced by double-stranded RNA or viral infection. *Proc Natl Acad Sci U S A, 100*(19), 10872-10877. doi:10.1073/pnas.1934678100

Hoshino, Y., & Kapikian, A. Z. (1996). Classification of rotavirus VP4 and VP7 serotypes. *Arch Virol Suppl, 12*, 99-111.

Hoshino, Y., Wyatt, R. G., Greenberg, H. B., Flores, J., & Kapikian, A. Z. (1984). Serotypic Similarity and Diversity of Rotaviruses of Mammalian and Avian Origin as Studied by Plaque-Reduction Neutralization. *Journal of Infectious Diseases, 149*(5), 694-702.

Hou, Z., Huang, Y., Huan, Y., Pang, W., Meng, M., Wang, P., . . . Wu, K. K. (2008). Anti-NSP4 antibody can block rotavirus-induced diarrhea in mice. *J Pediatr Gastroenterol Nutr, 46*(4), 376-385. doi:10.1097/MPG.0b013e3181661ae4

Hough, R., Pratt, G., & Rechsteiner, M. (1987). Purification of two high molecular weight proteases from rabbit reticulocyte lysate. *J Biol Chem, 262*(17), 8303-8313.

Hu, L., Crawford, S. E., Czako, R., Cortes-Penfield, N. W., Smith, D. F., Le Pendu, J., . . . Prasad, B. V. (2012). Cell attachment protein VP8* of a human rotavirus specifically interacts with A-type histo-blood group antigen. *Nature, 485*(7397), 256-259. doi:10.1038/nature10996

Hua, J., Chen, X., & Patton, J. T. (1994). Deletion mapping of the rotavirus metalloprotein NS53 (NSP1): the conserved cysteine-rich region is essential for virus-specific RNA binding. *J Virol, 68*(6), 3990-4000.

Hug, H., Costas, M., Staeheli, P., Aebi, M., & Weissmann, C. (1988). Organization of the murine Mx gene and characterization of its interferon- and virus-inducible promoter. *Mol Cell Biol, 8*(8), 3065-3079.

Huye, L. E., Ning, S., Kelliher, M., & Pagano, J. S. (2007). Interferon regulatory factor 7 is activated by a viral oncoprotein through RIP-dependent ubiquitination. *Mol Cell Biol, 27*(8), 2910-2918. doi:10.1128/MCB.02256-06

Hwang, S. Y., Hur, K. Y., Kim, J. R., Cho, K. H., Kim, S. H., & Yoo, J. Y. (2013). Biphasic RLR-IFN-beta response controls the balance between antiviral immunity and cell damage. *J Immunol, 190*(3), 1192-1200. doi:10.4049/jimmunol.1202326

Imai, M., Akatani, K., Ikegami, N., & Furuichi, Y. (1983). Capped and conserved terminal structures in human rotavirus genome double-stranded RNA segments. *J Virol, 47*(1), 125-136.

Imataka, H., Gradi, A., & Sonenberg, N. (1998). A newly identified N-terminal amino acid sequence of human eIF4G binds poly(A)-binding protein and functions in poly(A)-dependent translation. *EMBO J, 17*(24), 7480-7489. doi:10.1093/emboj/17.24.7480

International Committee on Taxonomy of, V., & King, A. M. Q. (2012). *Virus taxonomy : classification and nomenclature of viruses : ninth report of the International Committee on Taxonomy of Viruses*. London: Elsevier Academic Press.

Ioannidis, I., McNally, B., Willette, M., Peeples, M. E., Chaussabel, D., Durbin, J. E., . . . Flano, E. (2012). Plasticity and virus specificity of the airway epithelial cell immune response during respiratory virus infection. *J Virol, 86*(10), 5422-5436. doi:10.1128/JVI.06757-11

Iordanov, M. S., Wong, J., Bell, J. C., & Magun, B. E. (2001). Activation of NF-kappaB by double-stranded RNA (dsRNA) in the absence of protein kinase R and RNase L demonstrates the existence of two separate dsRNA-triggered antiviral programs. *Mol Cell Biol, 21*(1), 61-72. doi:10.1128/MCB.21.1.61-72.2001

Iosef, C., Van Nguyen, T., Jeong, K., Bengtsson, K., Morein, B., Kim, Y., . . . Saif, L. J. (2002). Systemic and intestinal antibody secreting cell responses and protection in gnotobiotic pigs immunized orally with attenuated Wa human rotavirus and Wa 2/6-rotavirus-like-particles associated with immunostimulating complexes. *Vaccine, 20*(13-14), 1741-1753.

Israel, A. (2010). The IKK complex, a central regulator of NF-kappaB activation. *Cold Spring Harb Perspect Biol, 2*(3), a000158. doi:10.1101/cshperspect.a000158

Ivashkiv, L. B., & Donlin, L. T. (2014). Regulation of type I interferon responses. *Nat Rev Immunol, 14*(1), 36-49. doi:10.1038/nri3581

Iversen, M. B., Ank, N., Melchjorsen, J., & Paludan, S. R. (2010). Expression of type III interferon (IFN) in the vaginal mucosa is mediated primarily by dendritic cells and displays stronger dependence on NF-kappaB than type I IFNs. *J Virol, 84*(9), 4579-4586. doi:10.1128/JVI.02591-09

Iversen, M. B., & Paludan, S. R. (2010). Mechanisms of type III interferon expression. *J Interferon Cytokine Res, 30*(8), 573-578. doi:10.1089/jir.2010.0063

Jagannath, M. R., Kesavulu, M. M., Deepa, R., Sastri, P. N., Kumar, S. S., Suguna, K., & Rao, C. D. (2006). N- and C-terminal cooperation in rotavirus enterotoxin: novel mechanism of modulation of the properties of a multifunctional protein by a structurally and functionally overlapping conformational domain. *J Virol, 80*(1), 412-425. doi:10.1128/JVI.80.1.412-425.2006

Jansen, R. P. (2001). mRNA localization: message on the move. *Nat Rev Mol Cell Biol, 2*(4), 247-256. doi:10.1038/35067016

Jayaram, H., Estes, M. K., & Prasad, B. V. (2004). Emerging themes in rotavirus cell entry, genome organization, transcription and replication. *Virus Res, 101*(1), 67-81. doi:10.1016/j.virusres.2003.12.007

Johnson, M. A., & McCrae, M. A. (1989). Molecular biology of rotaviruses. VIII. Quantitative analysis of regulation of gene expression during virus replication. *J Virol, 63*(5), 2048-2055.

Jorns, C., Holzinger, D., Thimme, R., Spangenberg, H. C., Weidmann, M., Rasenack, J., . . . Kochs, G. (2006). Rapid and simple detection of IFN-neutralizing antibodies in chronic hepatitis C non-responsive to IFN-alpha. *J Med Virol, 78*(1), 74-82. doi:10.1002/jmv.20506

Josephson, K., Logsdon, N. J., & Walter, M. R. (2001). Crystal structure of the IL-10/IL-10R1 complex reveals a shared receptor binding site. *Immunity, 15*(1), 35-46.

Jourdan, N., Maurice, M., Delautier, D., Quero, A. M., Servin, A. L., & Trugnan, G. (1997). Rotavirus is released from the apical surface of cultured human intestinal cells through nonconventional vesicular transport that bypasses the Golgi apparatus. *J Virol, 71*(11), 8268-8278.

Kabcenell, A. K., & Atkinson, P. H. (1985). Processing of the rough endoplasmic reticulum membrane glycoproteins of rotavirus SA11. *J Cell Biol, 101*(4), 1270-1280.

Kalica, A. R., James, J. D., Jr., & Kapikian, A. Z. (1978). Hemagglutination by simian rotavirus. *J Clin Microbiol, 7*(3), 314-315.

Kaljot, K. T., Shaw, R. D., Rubin, D. H., & Greenberg, H. B. (1988). Infectious rotavirus enters cells by direct cell membrane penetration, not by endocytosis. *J Virol, 62*(4), 1136-1144.

Kamada, R., Yang, W., Zhang, Y., Patel, M. C., Yang, Y., Ouda, R., . . . Ozato, K. (2018). Interferon stimulation creates chromatin marks and establishes transcriptional memory. *Proceedings of the National Academy of Sciences, 115*(39), E9162-E9171. doi:10.1073/pnas.1720930115

Kanai, Y., Komoto, S., Kawagishi, T., Nouda, R., Nagasawa, N., Onishi, M., . . . Kobayashi, T. (2017). Entirely plasmid-based reverse genetics system for rotaviruses. *Proc Natl Acad Sci U S A, 114*(9), 2349-2354. doi:10.1073/pnas.1618424114

Kanarek, N., & Ben-Neriah, Y. (2012). Regulation of NF-kappaB by ubiquitination and degradation of the IkappaBs. *Immunol Rev, 246*(1), 77-94. doi:10.1111/j.1600-065X.2012.01098.x

Kantharidis, P., Dyall-Smith, M. L., Tregear, G. W., & Holmes, I. H. (1988). Nucleotide sequence of UK bovine rotavirus segment 4: possible host restriction of VP3 genes. *Virology, 166*(2), 308-315.

Kapikian, A. Z., Kim, H. W., Wyatt, R. G., Rodrigue.Wj, Ross, S., Cline, W. L., . . . Chanock, R. M. (1974). Reovirus-Like Agent in Stools - Association with Infantile Diarrhea and Development of Serologic Tests. *Science, 185*(4156), 1049-1053. doi:DOI 10.1126/science.185.4156.1049

Kapikian, A. Z., Simonsen, L., Vesikari, T., Hoshino, Y., Morens, D. M., Chanock, R. M., . . . Murphy, B. R. (2005). A hexavalent human rotavirus-bovine rotavirus (UK) reassortant vaccine designed for use in developing countries and delivered in a schedule with the potential to eliminate the risk of intussusception. *J Infect Dis, 192 Suppl 1*, S22-29. doi:10.1086/431510

Kato, H., Sato, S., Yoneyama, M., Yamamoto, M., Uematsu, S., Matsui, K., . . . Akira, S. (2005). Cell type-specific involvement of RIG-I in antiviral response. *Immunity, 23*(1), 19-28. doi:10.1016/j.immuni.2005.04.010

Kato, H., Takeuchi, O., Mikamo-Satoh, E., Hirai, R., Kawai, T., Matsushita, K., . . . Akira, S. (2008). Length-dependent recognition of double-stranded ribonucleic acids by retinoic acid–inducible gene-I and melanoma differentiation–associated gene 5. *The Journal of Experimental Medicine, 205*(7), 1601-1610. doi:10.1084/jem.20080091

Kattoura, M. D., Chen, X., & Patton, J. T. (1994). The rotavirus RNA-binding protein NS35 (NSP2) forms 10S multimers and interacts with the viral RNA polymerase. *Virology, 202*(2), 803-813. doi:10.1006/viro.1994.1402

Katzen, F., Chang, G., & Kudlicki, W. (2005). The past, present and future of cell-free protein synthesis. *Trends Biotechnol, 23*(3), 150-156. doi:10.1016/j.tibtech.2005.01.003

Katzen, F., Peterson, T. C., & Kudlicki, W. (2009). Membrane protein expression: no cells required. *Trends in Biotechnology, 27*(8), 455-460. doi:10.1016/j.tibtech.2009.05.005

Kawai, T., & Akira, S. (2008). Toll-like receptor and RIG-I-like receptor signaling. *Ann N Y Acad Sci, 1143*, 1-20. doi:10.1196/annals.1443.020

Kawai, T., Takahashi, K., Sato, S., Coban, C., Kumar, H., Kato, H., . . . Akira, S. (2005). IPS-1, an adaptor triggering RIG-I- and Mda5-mediated type I interferon induction. *Nat Immunol, 6*(10), 981-988. doi:10.1038/ni1243

Kearney, K., Chen, D., Taraporewala, Z. F., Vende, P., Hoshino, Y., Tortorici, M. A., . . . Patton, J. T. (2004). Cell-line-induced mutation of the rotavirus genome alters expression of an IRF3-interacting protein. *EMBO J, 23*(20), 4072-4081. doi:10.1038/sj.emboj.7600408

Kessler, D. S., Veals, S. A., Fu, X. Y., & Levy, D. E. (1990). Interferon-alpha regulates nuclear translocation and DNA-binding affinity of ISGF3, a multimeric transcriptional activator. *Genes Dev, 4*(10), 1753-1765.

Keswick, B. H., Pickering, L. K., DuPont, H. L., & Woodward, W. E. (1983). Survival and detection of rotaviruses on environmental surfaces in day care centers. *Appl Environ Microbiol, 46*(4), 813-816.

Kim, Y. K., Shin, J. S., & Nahm, M. H. (2016). NOD-Like Receptors in Infection, Immunity, and Diseases. *Yonsei Med J, 57*(1), 5-14. doi:10.3349/ymj.2016.57.1.5

Kojima, K., Taniguchi, K., Urasawa, T., & Urasawa, S. (1996). Sequence analysis of normal and rearranged NSP5 genes from human rotavirus strains isolated in nature: implications for the occurrence of the rearrangement at the step of plus strand synthesis. *Virology, 224*(2), 446-452. doi:10.1006/viro.1996.0551

Komoto, S., Kanai, Y., Fukuda, S., Kugita, M., Kawagishi, T., Ito, N., . . . Taniguchi, K. (2017). Reverse Genetics System Demonstrates that Rotavirus Nonstructural Protein NSP6 Is Not Essential for Viral Replication in Cell Culture. *J Virol, 91*(21). doi:10.1128/JVI.00695-17

Kotenko, S. V., Gallagher, G., Baurin, V. V., Lewis-Antes, A., Shen, M., Shah, N. K., . . . Donnelly, R. P. (2003). IFN-lambdas mediate antiviral protection through a distinct class II cytokine receptor complex. *Nat Immunol, 4*(1), 69-77. doi:10.1038/ni875

Kotredes, K. P., & Gamero, A. M. (2013). Interferons as Inducers of Apoptosis in Malignant Cells. *Journal of Interferon and Cytokine Research, 33*(4), 162-170. doi:10.1089/jir.2012.0110

Kouvelos, K., Petric, M., & Middleton, P. J. (1984). Comparison of bovine, simian and human rotavirus structural glycoproteins. *J Gen Virol, 65 (Pt 7)*, 1211-1214. doi:10.1099/0022-1317-65-7-1211

Kugel, D., Pulverer, J. E., Koster, M., Hauser, H., & Staeheli, P. (2011). Novel nonviral bioassays for mouse type I and type III interferon. *J Interferon Cytokine Res, 31*(4), 345-349. doi:10.1089/jir.2010.0079

Kumar, K. G., Krolewski, J. J., & Fuchs, S. Y. (2004). Phosphorylation and specific ubiquitin acceptor sites are required for ubiquitination and degradation of the IFNAR1 subunit of type I interferon receptor. *J Biol Chem, 279*(45), 46614-46620. doi:10.1074/jbc.M407082200

Labbe, M., Baudoux, P., Charpilienne, A., Poncet, D., & Cohen, J. (1994). Identification of the nucleic acid binding domain of the rotavirus VP2 protein. *J Gen Virol, 75 (Pt 12)*, 3423-3430. doi:10.1099/0022-1317-75-12-3423

Labbe, M., Charpilienne, A., Crawford, S. E., Estes, M. K., & Cohen, J. (1991). Expression of rotavirus VP2 produces empty corelike particles. *J Virol, 65*(6), 2946-2952.

LaMonica, R., Kocer, S. S., Nazarova, J., Dowling, W., Geimonen, E., Shaw, R. D., & Mackow, E. R. (2001). VP4 differentially regulates TRAF2 signaling, disengaging JNK activation while directing NF-kappa B to effect rotavirus-specific cellular responses. *J Biol Chem, 276*(23), 19889-19896. doi:10.1074/jbc.M100499200

Lanata, C. F., Fischer-Walker, C. L., Olascoaga, A. C., Torres, C. X., Aryee, M. J., Black, R. E., . . . Unicef. (2013). Global causes of diarrheal disease mortality in children <5 years of age: a systematic review. *PLoS One, 8*(9), e72788. doi:10.1371/journal.pone.0072788

Landschulz, W. H., Johnson, P. F., & McKnight, S. L. (1988). The leucine zipper: a hypothetical structure common to a new class of DNA binding proteins. *Science, 240*(4860), 1759-1764.

Lapaque, N., Jahnke, M., Trowsdale, J., & Kelly, A. P. (2009). The HLA-DRalpha chain is modified by polyubiquitination. *J Biol Chem, 284*(11), 7007-7016. doi:10.1074/jbc.M805736200

Lappalainen, S., Blazevic, V., Malm, M., & Vesikari, T. (2017). Rotavirus vaccination and infection induce VP6-specific IgA responses. *J Med Virol, 89*(2), 239-245. doi:10.1002/jmv.24636

Lasfar, A., Lewis-Antes, A., Smirnov, S. V., Anantha, S., Abushahba, W., Tian, B., . . . Kotenko, S. V. (2006). Characterization of the mouse IFN-lambda ligand-receptor system: IFN-lambdas exhibit antitumor activity against B16 melanoma. *Cancer Res, 66*(8), 4468-4477. doi:10.1158/0008-5472.CAN-05-3653

Lausch, K. R., Westh, L., Kristensen, L. H., Lindberg, J., Tarp, B., & Larsen, C. S. (2017). Rotavirus is frequent among adults hospitalised for acute gastroenteritis. *Dan Med J, 64*(1).

Lawton, J. A., Estes, M. K., & Prasad, B. V. (2001). Identification and characterization of a transcription pause site in rotavirus. *J Virol, 75*(4), 1632-1642. doi:10.1128/JVI.75.4.1632-1642.2001

Lawton, J. A., Zeng, C. Q., Mukherjee, S. K., Cohen, J., Estes, M. K., & Prasad, B. V. (1997). Three-dimensional structural analysis of recombinant rotavirus-like particles with intact and amino-terminal-deleted VP2: implications for the architecture of the VP2 capsid layer. *J Virol, 71*(10), 7353-7360.

Le Bon, A., Durand, V., Kamphuis, E., Thompson, C., Bulfone-Paus, S., Rossmann, C., . . . Tough, D. F. (2006). Direct stimulation of T cells by type I IFN enhances the CD8+ T cell response during cross-priming. *J Immunol, 176*(8), 4682-4689.

Le Bon, A., & Tough, D. F. (2002). Links between innate and adaptive immunity via type I interferon. *Current Opinion in Immunology, 14*(4), 432-436. doi:Doi 10.1016/S0952-7915(02)00354-0

Leblanc, J. F., Cohen, L., Rodrigues, M., & Hiscott, J. (1990). Synergism between distinct enhanson domains in viral induction of the human beta interferon gene. *Mol Cell Biol, 10*(8), 3987-3993.

Ledent, P., Duez, C., Vanhove, M., Lejeune, A., Fonze, E., Charlier, P., . . . Frere, J. M. (1997). Unexpected influence of a C-terminal-fused His-tag on the processing of an enzyme and on the kinetic and folding parameters. *FEBS Lett, 413*(2), 194-196.

Lee, C. J., Liao, C. L., & Lin, Y. L. (2005). Flavivirus activates phosphatidylinositol 3-kinase signaling to block caspase-dependent apoptotic cell death at the early stage of virus infection. *J Virol, 79*(13), 8388-8399. doi:10.1128/JVI.79.13.8388-8399.2005

Leonard, W. J. (2001). Role of Jak kinases and STATs in cytokine signal transduction. *Int J Hematol, 73*(3), 271-277.

Leshem, E., Lopman, B., Glass, R., Gentsch, J., Banyai, K., Parashar, U., & Patel, M. (2014). Distribution of rotavirus strains and strain-specific effectiveness of the rotavirus vaccine after its introduction: a systematic review and meta-analysis. *Lancet Infectious Diseases, 14*(9), 847-856. doi:10.1016/S1473-3099(14)70832-1

Lewin, B. (1975). Units of transcription and translation: the relationship between heterogeneous nuclear RNA and messenger RNA. *Cell, 4*(1), 11-20.

Li, B., & Fields, S. (1993). Identification of mutations in p53 that affect its binding to SV40 large T antigen by using the yeast two-hybrid system. *FASEB J, 7*(10), 957-963.

Li, Y., Xue, M., Yu, L., Luo, G., Yang, H., Jia, L., . . . Xia, N. (2018). Expression and characterization of a novel truncated rotavirus VP4 for the development of a recombinant rotavirus vaccine. *Vaccine, 36*(16), 2086-2092. doi:10.1016/j.vaccine.2018.03.011

Li, Z., Baker, M. L., Jiang, W., Estes, M. K., & Prasad, B. V. (2009). Rotavirus architecture at subnanometer resolution. *J Virol, 83*(4), 1754-1766. doi:10.1128/JVI.01855-08

Lin, J. D., Feng, N., Sen, A., Balan, M., Tseng, H. C., McElrath, C., . . . Kotenko, S. V. (2016). Distinct Roles of Type I and Type III Interferons in Intestinal Immunity to Homologous and Heterologous Rotavirus Infections. *PLoS Pathog, 12*(4), e1005600. doi:10.1371/journal.ppat.1005600

Lin, S. L., & Tian, P. (2003). Detailed computational analysis of a comprehensive set of group A rotavirus NSP4 proteins. *Virus Genes, 26*(3), 271-282.

Liu, G., Lu, Y., Thulasi Raman, S. N., Xu, F., Wu, Q., Li, Z., . . . Zhou, Y. (2018). Nuclear-resident RIG-I senses viral replication inducing antiviral immunity. *Nat Commun, 9*(1), 3199. doi:10.1038/s41467-018-05745-w

Liu, M., Mattion, N. M., & Estes, M. K. (1992). Rotavirus VP3 expressed in insect cells possesses guanylyltransferase activity. *Virology, 188*(1), 77-84.

Liu, M., Offit, P. A., & Estes, M. K. (1988). Identification of the simian rotavirus SA11 genome segment 3 product. *Virology, 163*(1), 26-32.

Liu, S., Cai, X., Wu, J., Cong, Q., Chen, X., Li, T., . . . Chen, Z. J. (2015). Phosphorylation of innate immune adaptor proteins MAVS, STING, and TRIF induces IRF3 activation. *Science, 347*(6227), aaa2630. doi:10.1126/science.aaa2630

Long, C. P., & McDonald, S. M. (2017). Rotavirus genome replication: Some assembly required. *PLoS Pathog, 13*(4), e1006242. doi:10.1371/journal.ppat.1006242

Loo, Y. M., Fornek, J., Crochet, N., Bajwa, G., Perwitasari, O., Martinez-Sobrido, L., . . . Gale, M., Jr. (2008). Distinct RIG-I and MDA5 signaling by RNA viruses in innate immunity. *J Virol, 82*(1), 335-345. doi:10.1128/JVI.01080-07

Lopez-Guerrero, D. V., Arias, N., Gutierrez-Xicotencatl, L., Chihu-Amparan, L., Gonzalez, A., Pedroza-Saavedra, A., . . . Esquivel-Guadarrama, F. (2018). Enhancement of VP6 immunogenicity and protective efficacy against rotavirus by VP2 in a genetic immunization. *Vaccine, 36*(22), 3072-3078. doi:10.1016/j.vaccine.2017.03.104

Lopez, C. B., Moltedo, B., Alexopoulou, L., Bonifaz, L., Flavell, R. A., & Moran, T. M. (2004). TLR-independent induction of dendritic cell maturation and adaptive immunity by negative-strand RNA viruses. *J Immunol, 173*(11), 6882-6889.

Lopez, S., & Arias, C. F. (2004). Multistep entry of rotavirus into cells: a Versaillesque dance. *Trends Microbiol, 12*(6), 271-278. doi:10.1016/j.tim.2004.04.003

Lopez, S., & Arias, C. F. (2006). Early steps in rotavirus cell entry. *Curr Top Microbiol Immunol, 309*, 39-66.

Lopez, S., Oceguera, A., & Sandoval-Jaime, C. (2016). Stress Response and Translation Control in Rotavirus Infection. *Viruses, 8*(6). doi:10.3390/v8060162

Lopez, S., Sanchez-Tacuba, L., Moreno, J., & Arias, C. F. (2016). Rotavirus Strategies Against the Innate Antiviral System. *Annu Rev Virol, 3*(1), 591-609. doi:10.1146/annurev-virology-110615-042152

Lopez, T., Camacho, M., Zayas, M., Najera, R., Sanchez, R., Arias, C. F., & Lopez, S. (2005). Silencing the morphogenesis of rotavirus. *J Virol, 79*(1), 184-192. doi:10.1128/JVI.79.1.184-192.2005

Lopez, T., Rojas, M., Ayala-Breton, C., Lopez, S., & Arias, C. F. (2005). Reduced expression of the rotavirus NSP5 gene has a pleiotropic effect on virus replication. *J Gen Virol, 86*(Pt 6), 1609-1617. doi:10.1099/vir.0.80827-0

Low, T. Y., Peng, M., Magliozzi, R., Mohammed, S., Guardavaccaro, D., & Heck, A. J. (2014). A systems-wide screen identifies substrates of the SCFbetaTrCP ubiquitin ligase. *Sci Signal, 7*(356), rs8. doi:10.1126/scisignal.2005882

Ludert, J. E., Michelangeli, F., Gil, F., Liprandi, F., & Esparza, J. (1987). Penetration and uncoating of rotaviruses in cultured cells. *Intervirology, 27*(2), 95-101.

Lundgren, O., Peregrin, A. T., Persson, K., Kordasti, S., Uhnoo, I., & Svensson, L. (2000). Role of the enteric nervous system in the fluid and electrolyte secretion of rotavirus diarrhea. *Science, 287*(5452), 491-495.

Lutz, L. M., Pace, C. R., & Arnold, M. M. (2016). Rotavirus NSP1 Associates with Components of the Cullin RING Ligase Family of E3 Ubiquitin Ligases. *J Virol, 90*(13), 6036-6048. doi:10.1128/JVI.00704-16

Ma, X., Li, D. D., Li, X. P., & Duan, Z. J. (2014). [Research progress in receptors involved in rotavirus infection]. *Bing Du Xue Bao, 30*(3), 303-309.

Maass, D. R., & Atkinson, P. H. (1990). Rotavirus proteins VP7, NS28, and VP4 form oligomeric structures. *J Virol, 64*(6), 2632-2641.

Mackett, M., Smith, G. L., & Moss, B. (1992). Vaccinia virus: a selectable eukaryotic cloning and expression vector. 1982. *Biotechnology, 24*, 495-499.

Madin, K., Sawasaki, T., Ogasawara, T., & Endo, Y. (2000). A highly efficient and robust cell-free protein synthesis system prepared from wheat embryos: Plants apparently contain a suicide system directed at ribosomes. *Proc Natl Acad Sci U S A, 97*(2), 559-564. doi:DOI 10.1073/pnas.97.2.559

Maes, P., Matthijnssens, J., Rahman, M., & Van Ranst, M. (2009). RotaC: a web-based tool for the complete genome classification of group A rotaviruses. *BMC Microbiol, 9*, 238. doi:10.1186/1471-2180-9-238

Mahlakoiv, T., Hernandez, P., Gronke, K., Diefenbach, A., & Staeheli, P. (2015). Leukocyte-derived IFN-alpha/beta and epithelial IFN-lambda constitute a compartmentalized mucosal defense system that restricts enteric virus infections. *PLoS Pathog, 11*(4), e1004782. doi:10.1371/journal.ppat.1004782

Majorek, K. A., Kuhn, M. L., Chruszcz, M., Anderson, W. F., & Minor, W. (2014). Double trouble-Buffer selection and His-tag presence may be responsible for nonreproducibility of biomedical experiments. *Protein Sci, 23*(10), 1359-1368. doi:10.1002/pro.2520

Malik, J., Bhan, M. K., & Ray, P. (2008). Natural immunity to rotavirus infection in children. *Indian J Biochem Biophys, 45*(4), 219-228.

Mansell, E. A., & Patton, J. T. (1990). Rotavirus Rna Replication - Vp2, but Not Vp6, Is Necessary for Viral Replicase Activity. *J Virol, 64*(10), 4988-4996.

Mansur, D. S., Maluquer de Motes, C., Unterholzner, L., Sumner, R. P., Ferguson, B. J., Ren, H., . . . Smith, G. L. (2013). Poxvirus targeting of E3 ligase beta-TrCP by molecular mimicry: a mechanism to inhibit NF-kappaB activation and promote immune evasion and virulence. *PLoS Pathog, 9*(2), e1003183. doi:10.1371/journal.ppat.1003183

Marie, I., Durbin, J. E., & Levy, D. E. (1998). Differential viral induction of distinct interferon-alpha genes by positive feedback through interferon regulatory factor-7. *EMBO J, 17*(22), 6660-6669. doi:10.1093/emboj/17.22.6660

Martella, V., Banyai, K., Matthijnssens, J., Buonavoglia, C., & Ciarlet, M. (2010). Zoonotic aspects of rotaviruses. *Vet Microbiol, 140*(3-4), 246-255. doi:10.1016/j.vetmic.2009.08.028

Martin, D., Charpilienne, A., Parent, A., Boussac, A., D'Autreaux, B., Poupon, J., & Poncet, D. (2013). The rotavirus nonstructural protein NSP5 coordinates a [2Fe-2S] iron-sulfur cluster that modulates interaction to RNA. *FASEB J, 27*(3), 1074-1083. doi:10.1096/fj.12-217182

Martin, D., Duarte, M., Lepault, J., & Poncet, D. (2010). Sequestration of free tubulin molecules by the viral protein NSP2 induces microtubule depolymerization during rotavirus infection. *J Virol, 84*(5), 2522-2532. doi:10.1128/JVI.01883-09

Mason, B. B., Graham, D. Y., & Estes, M. K. (1980). In vitro transcription and translation of simian rotavirus SA11 gene products. *J Virol, 33*(3), 1111-1121.

Mathieu, M., Petitpas, I., Navaza, J., Lepault, J., Kohli, E., Pothier, P., . . . Rey, F. A. (2001). Atomic structure of the major capsid protein of rotavirus: implications for the architecture of the virion. *EMBO J, 20*(7), 1485-1497. doi:10.1093/emboj/20.7.1485

Matthijnssens, J., Ciarlet, M., Heiman, E., Arijs, I., Delbeke, T., McDonald, S. M., . . . Van Ranst, M. (2008). Full genome-based classification of rotaviruses reveals a common origin between human Wa-Like and porcine rotavirus strains and human DS-1-like and bovine rotavirus strains. *J Virol, 82*(7), 3204-3219. doi:10.1128/JVI.02257-07

Matthijnssens, J., Ciarlet, M., McDonald, S. M., Attoui, H., Banyai, K., Brister, J. R., . . . Van Ranst, M. (2011). Uniformity of rotavirus strain nomenclature proposed by the Rotavirus Classification Working Group (RCWG). *Arch Virol, 156*(8), 1397-1413. doi:10.1007/s00705-011-1006-z

Mattion, N. M., Cohen, J., Aponte, C., & Estes, M. K. (1992). Characterization of an oligomerization domain and RNA-binding properties on rotavirus nonstructural protein NS34. *Virology, 190*(1), 68-83.

Mattion, N. M., Mitchell, D. B., Both, G. W., & Estes, M. K. (1991). Expression of rotavirus proteins encoded by alternative open reading frames of genome segment 11. *Virology, 181*(1), 295-304.

McCrae, M. A., & Faulkner-Valle, G. P. (1981). Molecular biology of rotaviruses. I. Characterization of basic growth parameters and pattern of macromolecular synthesis. *J Virol, 39*(2), 490-496.

McCrae, M. A., & McCorquodale, J. G. (1983). Molecular biology of rotaviruses. V. Terminal structure of viral RNA species. *Virology, 126*(1), 204-212.

McDonald, S. M., Nelson, M. I., Turner, P. E., & Patton, J. T. (2016). Reassortment in segmented RNA viruses: mechanisms and outcomes. *Nat Rev Microbiol, 14*(7), 448-460. doi:10.1038/nrmicro.2016.46

McDonald, S. M., & Patton, J. T. (2011). Rotavirus VP2 core shell regions critical for viral polymerase activation. *J Virol, 85*(7), 3095-3105. doi:10.1128/JVI.02360-10

Mebus, C. A., Kono, M., Underdahl, N. R., & Twiehaus, M. J. (1971). Cell culture propagation of neonatal calf diarrhea (scours) virus. *Can Vet J, 12*(3), 69-72.

Mebus, C. A., Underdahl, N. R., Rhodes, M. B., & Twiehaus, M. J. (1969). Further studies on neonatal calf diarrhea virus. *Proc Annu Meet U S Anim Health Assoc, 73*, 97-99.

Meylan, E., Burns, K., Hofmann, K., Blancheteau, V., Martinon, F., Kelliher, M., & Tschopp, J. (2004). RIP1 is an essential mediator of Toll-like receptor 3-induced NF-kappa B activation. *Nat Immunol, 5*(5), 503-507. doi:10.1038/ni1061

Middleto.Pj, Szymansk.Mt, Abbott, G. D., Bortolus.R, & Hamilton, J. R. (1974). Orbivirus Acute Gastroenteritis of Infancy. *Lancet, 1*(7869), 1241-1244.

Midthun, K., Greenberg, H. B., Hoshino, Y., Kapikian, A. Z., Wyatt, R. G., & Chanock, R. M. (1985). Reassortant rotaviruses as potential live rotavirus vaccine candidates. *J Virol, 53*(3), 949-954.

Mitchell, D. B., & Both, G. W. (1990). Conservation of a potential metal binding motif despite extensive sequence diversity in the rotavirus nonstructural protein NS53. *Virology, 174*(2), 618-621.
Mitzel, D. N., Weisend, C. M., White, M. W., & Hardy, M. E. (2003). Translational regulation of rotavirus gene expression. *J Gen Virol, 84*(Pt 2), 383-391. doi:10.1099/vir.0.18558-0
Mogensen, T. H. (2009). Pathogen recognition and inflammatory signaling in innate immune defenses. *Clin Microbiol Rev, 22*(2), 240-273, Table of Contents. doi:10.1128/CMR.00046-08
Mohanty, A. K., & Wiener, M. C. (2004). Membrane protein expression and production: effects of polyhistidine tag length and position. *Protein Expr Purif, 33*(2), 311-325.
Mohanty, S. K., Donnelly, B., Dupree, P., Lobeck, I., Mowery, S., Meller, J., . . . Tiao, G. (2017). A Point Mutation in the Rhesus Rotavirus VP4 Protein Generated through a Rotavirus Reverse Genetics System Attenuates Biliary Atresia in the Murine Model. *J Virol, 91*(15). doi:10.1128/JVI.00510-17
Montero, H., Arias, C. F., & Lopez, S. (2006). Rotavirus Nonstructural Protein NSP3 is not required for viral protein synthesis. *J Virol, 80*(18), 9031-9038. doi:10.1128/JVI.00437-06
Moorthy, A. K., Savinova, O. V., Ho, J. Q., Wang, V. Y., Vu, D., & Ghosh, G. (2006). The 20S proteasome processes NF-kappaB1 p105 into p50 in a translation-independent manner. *EMBO J, 25*(9), 1945-1956. doi:10.1038/sj.emboj.7601081
Mordstein, M., Neugebauer, E., Ditt, V., Jessen, B., Rieger, T., Falcone, V., . . . Staeheli, P. (2010). Lambda interferon renders epithelial cells of the respiratory and gastrointestinal tracts resistant to viral infections. *J Virol, 84*(11), 5670-5677. doi:10.1128/JVI.00272-10
Morelli, M., Dennis, A. F., & Patton, J. T. (2015). Putative E3 Ubiquitin Ligase of Human Rotavirus Inhibits NF-kappaB Activation by Using Molecular Mimicry To Target beta-TrCP. *MBio, 6*(1). doi:10.1128/mBio.02490-14
Morelli, M., Ogden, K. M., & Patton, J. T. (2015). Silencing the alarms: Innate immune antagonism by rotavirus NSP1 and VP3. *Virology, 479-480*, 75-84. doi:10.1016/j.virol.2015.01.006
Muerkoster, S., Arlt, A., Sipos, B., Witt, M., Grossmann, M., Kloppel, G., . . . Schafer, H. (2005). Increased expression of the E3-ubiquitin ligase receptor subunit betaTRCP1 relates to constitutive nuclear factor-kappaB activation and chemoresistance in pancreatic carcinoma cells. *Cancer Res, 65*(4), 1316-1324. doi:10.1158/0008-5472.CAN-04-1626
Musalem, C., & Espejo, R. T. (1985). Release of Progeny Virus from Cells Infected with Simian Rotavirus Sa11. *Journal of General Virology, 66*, 2715-2724. doi:Doi 10.1099/0022-1317-66-12-2715
Nandi, S., Chanda, S., Bagchi, P., Nayak, M. K., Bhowmick, R., & Chawla-Sarkar, M. (2014). MAVS protein is attenuated by rotavirus nonstructural protein 1. *PLoS One, 9*(3), e92126. doi:10.1371/journal.pone.0092126
Narvaez, C. F., Angel, J., & Franco, M. A. (2005). Interaction of rotavirus with human myeloid dendritic cells. *J Virol, 79*(23), 14526-14535. doi:10.1128/JVI.79.23.14526-14535.2005
Nirenberg, M. W., & Matthaei, J. H. (1961). The dependence of cell-free protein synthesis in E. coli upon naturally occurring or synthetic polyribonucleotides. *Proc Natl Acad Sci U S A, 47*, 1588-1602.
Obert, G., Peiffer, I., & Servin, A. L. (2000). Rotavirus-induced structural and functional alterations in tight junctions of polarized intestinal caco-2 cell monolayers. *J Virol, 74*(10), 4645-4651. doi:Doi 10.1128/Jvi.74.10.4645-4651.2000
Odendall, C., Dixit, E., Stavru, F., Bierne, H., Franz, K. M., Durbin, A. F., . . . Kagan, J. C. (2014). Diverse intracellular pathogens activate type III interferon expression from peroxisomes. *Nat Immunol, 15*(8), 717-726. doi:10.1038/ni.2915
Odendall, C., & Kagan, J. C. (2015). The unique regulation and functions of type III interferons in antiviral immunity. *Current Opinion in Virology, 12*, 47-52. doi:10.1016/j.coviro.2015.02.003
Oeckinghaus, A., & Ghosh, S. (2009). The NF-kappaB family of transcription factors and its regulation. *Cold Spring Harb Perspect Biol, 1*(4), a000034. doi:10.1101/cshperspect.a000034
Oeckinghaus, A., Hayden, M. S., & Ghosh, S. (2011). Crosstalk in NF-kappaB signaling pathways. *Nat Immunol, 12*(8), 695-708. doi:10.1038/ni.2065
Offit, P. A., Blavat, G., Greenberg, H. B., & Clark, H. F. (1986). Molecular basis of rotavirus virulence: role of gene segment 4. *J Virol, 57*(1), 46-49.

Okada, J., Kobayashi, N., Taniguchi, K., & Urasawa, S. (1999). Analysis on reassortment of rotavirus NSP1 genes lacking coding region for cysteine-rich zinc finger motif. *Arch Virol, 144*(2), 345-353.

Onoguchi, K., Yoneyama, M., Takemura, A., Akira, S., Taniguchi, T., Namiki, H., & Fujita, T. (2007). Viral infections activate types I and III interferon genes through a common mechanism. *J Biol Chem, 282*(10), 7576-7581. doi:10.1074/jbc.M608618200

Osborne, M. P., Haddon, S. J., Spencer, A. J., Collins, J., Starkey, W. G., Wallis, T. S., . . . Stephen, J. (1988). An electron microscopic investigation of time-related changes in the intestine of neonatal mice infected with murine rotavirus. *J Pediatr Gastroenterol Nutr, 7*(2), 236-248.

Osmola-Mankowska, A., Teresiak-Mikolajczak, E., Danczak-Pazdrowska, A., Kowalczyk, M., Zaba, R., & Adamski, Z. (2015). The role of dendritic cells and regulatory T cells in the pathogenesis of morphea. *Cent Eur J Immunol, 40*(1), 103-108. doi:10.5114/ceji.2015.50841

Osterlund, P. I., Pietila, T. E., Veckman, V., Kotenko, S. V., & Julkunen, I. (2007). IFN regulatory factor family members differentially regulate the expression of type III IFN (IFN-lambda) genes. *J Immunol, 179*(6), 3434-3442.

Padilla-Noriega, L., Paniagua, O., & Guzman-Leon, S. (2002). Rotavirus protein NSP3 shuts off host cell protein synthesis. *Virology, 298*(1), 1-7.

Panek, A., Pietrow, O., Filipkowski, P., & Synowiecki, J. (2013). Effects of the polyhistidine tag on kinetics and other properties of trehalose synthase from Deinococcus geothermalis. *Acta Biochim Pol, 60*(2), 163-166.

Panne, D. (2008). The enhanceosome. *Curr Opin Struct Biol, 18*(2), 236-242. doi:10.1016/j.sbi.2007.12.002

Parashar, U. D., Burton, A., Lanata, C., Boschi-Pinto, C., Shibuya, K., Steele, D., . . . Glass, R. I. (2009). Global mortality associated with rotavirus disease among children in 2004. *J Infect Dis, 200 Suppl 1*, S9-S15. doi:10.1086/605025

Parashar, U. D., Gibson, C. J., Bresee, J. S., & Glass, R. I. (2006a). Rotavirus and severe childhood diarrhea. *Emerg Infect Dis, 12*(2), 304-306.

Parashar, U. D., Gibson, C. J., Bresee, J. S., & Glass, R. I. (2006b). Rotavirus and severe childhood diarrhea. *Emerg Infect Dis, 12*(2), 304-306. doi:10.3201/eid1202.050006

Parashar, U. D., Hummelman, E. G., Bresee, J. S., Miller, M. A., & Glass, R. I. (2003). Global illness and deaths caused by rotavirus disease in children. *Emerg Infect Dis, 9*(5), 565-572.

Patel, M. M., Glass, R., Desai, R., Tate, J. E., & Parashar, U. D. (2012). Fulfilling the promise of rotavirus vaccines: how far have we come since licensure? *Lancet Infectious Diseases, 12*(7), 561-570.

Patton, J., & Barro, M. (2009). *Rna Viruses: Host Gene Responses To Infections*.

Patton, J. T. (1995). Structure and function of the rotavirus RNA-binding proteins. *J Gen Virol, 76 (Pt 11)*, 2633-2644. doi:10.1099/0022-1317-76-11-2633

Patton, J. T. (2012). Rotavirus diversity and evolution in the post-vaccine world. *Discov Med, 13*(68), 85-97.

Patton, J. T., & Chen, D. (1999). RNA-binding and capping activities of proteins in rotavirus open cores. *J Virol, 73*(2), 1382-1391.

Patton, J. T., & Gallegos, C. O. (1990). Rotavirus RNA replication: single-stranded RNA extends from the replicase particle. *J Gen Virol, 71 (Pt 5)*, 1087-1094. doi:10.1099/0022-1317-71-5-1087

Patton, J. T., Jones, M. T., Kalbach, A. N., He, Y. W., & Xiaobo, J. (1997). Rotavirus RNA polymerase requires the core shell protein to synthesize the double-stranded RNA genome. *J Virol, 71*(12), 9618-9626.

Patton, J. T., Silvestri, L. S., Tortorici, M. A., Vasquez-Del Carpio, R., & Taraporewala, Z. F. (2006). Rotavirus genome replication and morphogenesis: role of the viroplasm. *Curr Top Microbiol Immunol, 309*, 169-187.

Patton, J. T., & Spencer, E. (2000). Genome replication and packaging of segmented double-stranded RNA viruses. *Virology, 277*(2), 217-225. doi:10.1006/viro.2000.0645

Patton, J. T., Taraporewala, Z., Chen, D., Chizhikov, V., Jones, M., Elhelu, A., . . . Gouvea, V. (2001). Effect of intragenic rearrangement and changes in the 3' consensus sequence on NSP1 expression and rotavirus replication. *J Virol, 75*(5), 2076-2086. doi:10.1128/JVI.75.5.2076-2086.2001

Patton, J. T., Vasquez-Del Carpio, R., & Spencer, E. (2004). Replication and transcription of the rotavirus genome. *Curr Pharm Des, 10*(30), 3769-3777.

Patton, J. T., Wentz, M., Xiaobo, J., & Ramig, R. F. (1996). cis-Acting signals that promote genome replication in rotavirus mRNA. *J Virol, 70*(6), 3961-3971.

Pedley, S., Bridger, J. C., Chasey, D., & McCrae, M. A. (1986). Definition of two new groups of atypical rotaviruses. *J Gen Virol, 67 (Pt 1)*, 131-137. doi:10.1099/0022-1317-67-1-131

Pedley, S., Hundley, F., Chrystie, I., Mccrae, M. A., & Desselberger, U. (1984). The Genomes of Rotaviruses Isolated from Chronically Infected Immunodeficient Children. *Journal of General Virology, 65*(Jul), 1141-1150. doi:Doi 10.1099/0022-1317-65-7-1141

Perez, J. F., Chemello, M. E., Liprandi, F., Ruiz, M. C., & Michelangeli, F. (1998). Oncosis in MA104 cells is induced by rotavirus infection through an increase in intracellular Ca2+ concentration. *Virology, 252*(1), 17-27. doi:DOI 10.1006/viro.1998.9433

Periz, J., Celma, C., Jing, B., Pinkney, J. N., Roy, P., & Kapanidis, A. N. (2013). Rotavirus mRNAS are released by transcript-specific channels in the double-layered viral capsid. *Proc Natl Acad Sci U S A, 110*(29), 12042-12047. doi:10.1073/pnas.1220345110

Perron-Savard, P., De Crescenzo, G., & Le Moual, H. (2005). Dimerization and DNA binding of the Salmonella enterica PhoP response regulator are phosphorylation independent. *Microbiology, 151*(Pt 12), 3979-3987. doi:10.1099/mic.0.28236-0

Petersen, C., Bruns, E., Kuske, M., & von Wussow, P. (1997). Treatment of extrahepatic biliary atresia with interferon-alpha in a murine infectious model. *Pediatr Res, 42*(5), 623-628. doi:10.1203/00006450-199711000-00013

Petrie, B. L., Estes, M. K., & Graham, D. Y. (1983). Effects of tunicamycin on rotavirus morphogenesis and infectivity. *J Virol, 46*(1), 270-274.

Petrie, B. L., Greenberg, H. B., Graham, D. Y., & Estes, M. K. (1984). Ultrastructural localization of rotavirus antigens using colloidal gold. *Virus Res, 1*(2), 133-152.

Pham, T., Perry, J. L., Dosey, T. L., Delcour, A. H., & Hyser, J. M. (2017). The Rotavirus NSP4 Viroporin Domain is a Calcium-conducting Ion Channel. *Sci Rep, 7*, 43487. doi:10.1038/srep43487

Phua, K. B., Quak, S. H., Lee, B. W., Emmanuel, S. C., Goh, P., Han, H. H., . . . Bock, H. L. (2005). Evaluation of RIX4414, a live, attenuated rotavirus vaccine, in a randomized, double-blind, placebo-controlled phase 2 trial involving 2464 Singaporean infants. *J Infect Dis, 192 Suppl 1*, S6-S16. doi:10.1086/431511

Pichlmair, A., Kandasamy, K., Alvisi, G., Mulhern, O., Sacco, R., Habjan, M., . . . Superti-Furga, G. (2012). Viral immune modulators perturb the human molecular network by common and unique strategies. *Nature, 487*(7408), 486-490. doi:10.1038/nature11289

Pina-Vazquez, C., De Nova-Ocampo, M., Guzman-Leon, S., & Padilla-Noriega, L. (2007). Post-translational regulation of rotavirus protein NSP1 expression in mammalian cells. *Arch Virol, 152*(2), 345-368. doi:10.1007/s00705-006-0850-8

Pippig, D. A., Hellmuth, J. C., Cui, S., Kirchhofer, A., Lammens, K., Lammens, A., . . . Hopfner, K. P. (2009). The regulatory domain of the RIG-I family ATPase LGP2 senses double-stranded RNA. *Nucleic Acids Res, 37*(6), 2014-2025. doi:10.1093/nar/gkp059

Plaksin, D., Baeuerle, P. A., & Eisenbach, L. (1993). KBF1 (p50 NF-kappa B homodimer) acts as a repressor of H-2Kb gene expression in metastatic tumor cells. *J Exp Med, 177*(6), 1651-1662.

Poncet, D., Aponte, C., & Cohen, J. (1993). Rotavirus protein NSP3 (NS34) is bound to the 3' end consensus sequence of viral mRNAs in infected cells. *J Virol, 67*(6), 3159-3165.

Poncet, D., Laurent, S., & Cohen, J. (1994). Four nucleotides are the minimal requirement for RNA recognition by rotavirus non-structural protein NSP3. *EMBO J, 13*(17), 4165-4173.

Poruchynsky, M. S., Maass, D. R., & Atkinson, P. H. (1991). Calcium depletion blocks the maturation of rotavirus by altering the oligomerization of virus-encoded proteins in the ER. *J Cell Biol, 114*(4), 651-656.

Pott, J., Mahlakoiv, T., Mordstein, M., Duerr, C. U., Michiels, T., Stockinger, S., . . . Hornef, M. W. (2011). IFN-lambda determines the intestinal epithelial antiviral host defense. *Proc Natl Acad Sci U S A, 108*(19), 7944-7949. doi:10.1073/pnas.1100552108

Prasad, B. V., Burns, J. W., Marietta, E., Estes, M. K., & Chiu, W. (1990). Localization of VP4 neutralization sites in rotavirus by three-dimensional cryo-electron microscopy. *Nature, 343*(6257), 476-479. doi:10.1038/343476a0

Prasad, B. V., & Chiu, W. (1994). Structure of rotavirus. *Curr Top Microbiol Immunol, 185*, 9-29.

Prasad, B. V., Rothnagel, R., Zeng, C. Q., Jakana, J., Lawton, J. A., Chiu, W., & Estes, M. K. (1996). Visualization of ordered genomic RNA and localization of transcriptional complexes in rotavirus. *Nature, 382*(6590), 471-473. doi:10.1038/382471a0

Prasad, B. V., Wang, G. J., Clerx, J. P., & Chiu, W. (1988). Three-dimensional structure of rotavirus. *J Mol Biol, 199*(2), 269-275.

Preiss, T., & Hentze, M. W. (1998). Dual function of the messenger RNA cap structure in poly(A)-tail-promoted translation in yeast. *Nature, 392*(6675), 516-520. doi:10.1038/33192

Prokunina-Olsson, L., Muchmore, B., Tang, W., Pfeiffer, R. M., Park, H., Dickensheets, H., . . . O'Brien, T. R. (2013). A variant upstream of IFNL3 (IL28B) creating a new interferon gene IFNL4 is associated with impaired clearance of hepatitis C virus. *Nat Genet, 45*(2), 164-171. doi:10.1038/ng.2521

Pulverer, J. E., Rand, U., Lienenklaus, S., Kugel, D., Zietara, N., Kochs, G., . . . Koster, M. (2010). Temporal and Spatial Resolution of Type I and III Interferon Responses In Vivo. *J Virol, 84*(17), 8626-8638. doi:10.1128/Jvi.00303-10

Qin, L., Ren, L., Zhou, Z., Lei, X., Chen, L., Xue, Q., . . . Hung, T. (2011). Rotavirus nonstructural protein 1 antagonizes innate immune response by interacting with retinoic acid inducible gene I. *Virol J, 8*, 526. doi:10.1186/1743-422X-8-526

Rainsford, E. W., & McCrae, M. A. (2007). Characterization of the NSP6 protein product of rotavirus gene 11. *Virus Res, 130*(1-2), 193-201. doi:10.1016/j.virusres.2007.06.011

Raj, N. B., Israeli, R., Kellum, M., & Pitha, P. M. (1989). Upstream regulatory elements of murine alpha 4-interferon gene confer inducibility and cell type-restricted expression. *J Biol Chem, 264*(19), 11149-11157.

Ramig, R. F. (2004). Pathogenesis of intestinal and systemic rotavirus infection. *J Virol, 78*(19), 10213-10220. doi:10.1128/JVI.78.19.10213-10220.2004

Ramig, R. F., & Petrie, B. L. (1984). Characterization of Temperature-Sensitive Mutants of Simian Rotavirus-Sa11 - Protein-Synthesis and Morphogenesis. *J Virol, 49*(3), 665-673.

Randall, C. M., Jokela, J. A., & Shisler, J. L. (2012). The MC159 protein from the molluscum contagiosum poxvirus inhibits NF-kappaB activation by interacting with the IkappaB kinase complex. *J Immunol, 188*(5), 2371-2379. doi:10.4049/jimmunol.1100136

Randall, R. E., & Goodbourn, S. (2008). Interferons and viruses: an interplay between induction, signalling, antiviral responses and virus countermeasures. *J Gen Virol, 89*(Pt 1), 1-47. doi:10.1099/vir.0.83391-0

Reid, S. P., Leung, L. W., Hartman, A. L., Martinez, O., Shaw, M. L., Carbonnelle, C., . . . Basler, C. F. (2006). Ebola virus VP24 binds karyopherin alpha1 and blocks STAT1 nuclear accumulation. *J Virol, 80*(11), 5156-5167. doi:10.1128/JVI.02349-05

Rheingans, R. D., Antil, L., Dreibelbis, R., Podewils, L. J., Bresee, J. S., & Parashar, U. D. (2009). Economic costs of rotavirus gastroenteritis and cost-effectiveness of vaccination in developing countries. *J Infect Dis, 200 Suppl 1*, S16-27. doi:10.1086/605026

Ruggeri, F. M., & Greenberg, H. B. (1991). Antibodies to the trypsin cleavage peptide VP8 neutralize rotavirus by inhibiting binding of virions to target cells in culture. *J Virol, 65*(5), 2211-2219.

Ruiz, M. C., Diaz, Y., Pena, F., Aristimuno, O. C., Chemello, M. E., & Michelangeli, F. (2005). Ca2+ permeability of the plasma membrane induced by rotavirus infection in cultured cells is inhibited by tunicamycin and brefeldin A. *Virology, 333*(1), 54-65. doi:10.1016/j.virol.2004.12.032

Ryals, J., Dierks, P., Ragg, H., & Weissmann, C. (1985). A 46-nucleotide promoter segment from an IFN-alpha gene renders an unrelated promoter inducible by virus. *Cell, 41*(2), 497-507.

Sabara, M., Barrington, A., & Babiuk, L. A. (1985). Immunogenicity of a bovine rotavirus glycoprotein fragment. *J Virol, 56*(3), 1037-1040.

Sabara, M., Ready, K. F., Frenchick, P. J., & Babiuk, L. A. (1987). Biochemical evidence for the oligomeric arrangement of bovine rotavirus nucleocapsid protein and its possible significance in the immunogenicity of this protein. *J Gen Virol, 68 (Pt 1)*, 123-133. doi:10.1099/0022-1317-68-1-123

Sabaty, M., Grosse, S., Adryanczyk, G., Boiry, S., Biaso, F., Arnoux, P., & Pignol, D. (2013). Detrimental effect of the 6 His C-terminal tag on YedY enzymatic activity and influence of the TAT signal sequence on YedY synthesis. *BMC Biochem, 14*, 28. doi:10.1186/1471-2091-14-28

Said, E. A., Tremblay, N., Al-Balushi, M. S., Al-Jabri, A. A., & Lamarre, D. (2018). Viruses Seen by Our Cells: The Role of Viral RNA Sensors. *Journal of Immunology Research, 2018*, 14. doi:10.1155/2018/9480497

Salgado, E. N., Garcia Rodriguez, B., Narayanaswamy, N., Krishnan, Y., & Harrison, S. C. (2018). Visualization of Ca(2+) loss from rotavirus during cell entry. *J Virol*. doi:10.1128/JVI.01327-18

Sandino, A. M., Jashes, M., Faundez, G., & Spencer, E. (1986). Role of the inner protein capsid on in vitro human rotavirus transcription. *J Virol, 60*(2), 797-802.

Sanekata, T., Ahmed, M. U., Kader, A., Taniguchi, K., & Kobayashi, N. (2003). Human group B rotavirus infections cause severe diarrhea in children and adults in Bangladesh. *J Clin Microbiol, 41*(5), 2187-2190.

Santos, N., Volotao, E. M., Soares, C. C., Campos, G. S., Sardi, S. I., & Hoshino, Y. (2005). Predominance of rotavirus genotype G9 during the 1999, 2000, and 2002 seasons among hospitalized children in the city of Salvador, Bahia, Brazil: implications for future vaccine strategies. *J Clin Microbiol, 43*(8), 4064-4069. doi:10.1128/JCM.43.8.4064-4069.2005

Sapin, C., Colard, O., Delmas, O., Tessier, C., Breton, M., Enouf, V., . . . Trugnan, G. (2002). Rafts promote assembly and atypical targeting of a nonenveloped virus, rotavirus, in Caco-2 cells. *J Virol, 76*(9), 4591-4602. doi:10.1128/Jvi.76.9.4591-4602

Sastri, N. P., Viskovska, M., Hyser, J. M., Tanner, M. R., Horton, L. B., Sankaran, B., . . . Estes, M. K. (2014). Structural plasticity of the coiled-coil domain of rotavirus NSP4. *J Virol, 88*(23), 13602-13612. doi:10.1128/JVI.02227-14

Satheshkumar, P. S., Anton, L. C., Sanz, P., & Moss, B. (2009). Inhibition of the ubiquitin-proteasome system prevents vaccinia virus DNA replication and expression of intermediate and late genes. *J Virol, 83*(6), 2469-2479. doi:10.1128/JVI.01986-08

Sato, M., Hata, N., Asagiri, M., Nakaya, T., Taniguchi, T., & Tanaka, N. (1998). Positive feedback regulation of type I IFN genes by the IFN-inducible transcription factor IRF-7. *FEBS Lett, 441*(1), 106-110.

Sato, M., Suemori, H., Hata, N., Asagiri, M., Ogasawara, K., Nakao, K., . . . Taniguchi, T. (2000). Distinct and essential roles of transcription factors IRF-3 and IRF-7 in response to viruses for IFN-alpha/beta gene induction. *Immunity, 13*(4), 539-548.

Saxena, K., Blutt, S. E., Ettayebi, K., Zeng, X. L., Broughman, J. R., Crawford, S. E., . . . Estes, M. K. (2016). Human Intestinal Enteroids: a New Model To Study Human Rotavirus Infection, Host Restriction, and Pathophysiology. *J Virol, 90*(1), 43-56. doi:10.1128/JVI.01930-15

Schembri, L., Dalibart, R., Tomasello, F., Legembre, P., Ichas, F., & De Giorgi, F. (2007). The HA tag is cleaved and loses immunoreactivity during apoptosis. *Nat Methods, 4*(2), 107-108. doi:10.1038/nmeth0207-107

Schneider, W. M., Chevillotte, M. D., & Rice, C. M. (2014). Interferon-stimulated genes: a complex web of host defenses. *Annu Rev Immunol, 32*, 513-545. doi:10.1146/annurev-immunol-032713-120231

Schoggins, J. W., & Rice, C. M. (2011). Interferon-stimulated genes and their antiviral effector functions. *Current Opinion in Virology, 1*(6), 519-525. doi:10.1016/j.coviro.2011.10.008

Schuck, P., Taraporewala, Z., McPhie, P., & Patton, J. T. (2001). Rotavirus nonstructural protein NSP2 self-assembles into octamers that undergo ligand-induced conformational changes. *J Biol Chem, 276*(13), 9679-9687. doi:10.1074/jbc.M009398200

Seago, J., Hilton, L., Reid, E., Doceul, V., Jeyatheesan, J., Moganeradj, K., . . . Goodbourn, S. (2007). The Npro product of classical swine fever virus and bovine viral diarrhea virus uses a conserved mechanism to target interferon regulatory factor-3. *J Gen Virol, 88*(Pt 11), 3002-3006. doi:10.1099/vir.0.82934-0

Sen, A., Feng, N., Ettayebi, K., Hardy, M. E., & Greenberg, H. B. (2009). IRF3 inhibition by rotavirus NSP1 is host cell and virus strain dependent but independent of NSP1 proteasomal degradation. *J Virol, 83*(20), 10322-10335. doi:10.1128/JVI.01186-09

Sen, A., Pruijssers, A. J., Dermody, T. S., Garcia-Sastre, A., & Greenberg, H. B. (2011). The early interferon response to rotavirus is regulated by PKR and depends on MAVS/IPS-1, RIG-I, MDA-5, and IRF3. *J Virol, 85*(8), 3717-3732. doi:10.1128/jvi.02634-10

Sen, A., Rothenberg, M. E., Mukherjee, G., Feng, N., Kalisky, T., Nair, N., . . . Greenberg, H. B. (2012). Innate immune response to homologous rotavirus infection in the small intestinal villous epithelium at single-cell resolution. *Proc Natl Acad Sci U S A, 109*(50), 20667-20672. doi:10.1073/pnas.1212188109

Sen, A., Rott, L., Phan, N., Mukherjee, G., & Greenberg, H. B. (2014). Rotavirus NSP1 protein inhibits interferon-mediated STAT1 activation. *J Virol, 88*(1), 41-53. doi:10.1128/JVI.01501-13

Settembre, E. C., Chen, J. Z., Dormitzer, P. R., Grigorieff, N., & Harrison, S. C. (2011). Atomic model of an infectious rotavirus particle. *EMBO J, 30*(2), 408-416. doi:10.1038/emboj.2010.322

Shahrabadi, M. S., & Lee, P. W. K. (1986). Bovine Rotavirus Maturation Is a Calcium-Dependent Process. *Virology, 152*(2), 298-307. doi:Doi 10.1016/0042-6822(86)90133-9

Shaw, A. L., Rothnagel, R., Chen, D., Ramig, R. F., Chiu, W., & Prasad, B. V. (1993). Three-dimensional visualization of the rotavirus hemagglutinin structure. *Cell, 74*(4), 693-701.

Sheridan, J. F., Aurelian, L., Barbour, G., Santosham, M., Sack, R. B., & Ryder, R. W. (1981). Traveler's diarrhea associated with rotavirus infection: analysis of virus-specific immunoglobulin classes. *Infect Immun, 31*(1), 419-429.

Shors, T., Keck, J. G., & Moss, B. (1999). Down regulation of gene expression by the vaccinia virus D10 protein. *J Virol, 73*(1), 791-796.

Siegel, R., Eskdale, J., & Gallagher, G. (2011). Regulation of IFN-lambda1 promoter activity (IFN-lambda1/IL-29) in human airway epithelial cells. *J Immunol, 187*(11), 5636-5644. doi:10.4049/jimmunol.1003988

Silva-Ayala, D., Lopez, T., Gutierrez, M., Perrimon, N., Lopez, S., & Arias, C. F. (2013). Genome-wide RNAi screen reveals a role for the ESCRT complex in rotavirus cell entry. *Proc Natl Acad Sci U S A, 110*(25), 10270-10275. doi:10.1073/pnas.1304932110

Silverman, R. H., & Weiss, S. R. (2014). Viral phosphodiesterases that antagonize double-stranded RNA signaling to RNase L by degrading 2-5A. *J Interferon Cytokine Res, 34*(6), 455-463. doi:10.1089/jir.2014.0007

Silvestri, L. S., Taraporewala, Z. F., & Patton, J. T. (2004). Rotavirus replication: plus-sense templates for double-stranded RNA synthesis are made in viroplasms. *J Virol, 78*(14), 7763-7774. doi:10.1128/JVI.78.14.7763-7774.2004

Sommereyns, C., Paul, S., Staeheli, P., & Michiels, T. (2008). IFN-lambda (IFN-lambda) is expressed in a tissue-dependent fashion and primarily acts on epithelial cells in vivo. *PLoS Pathog, 4*(3), e1000017. doi:10.1371/journal.ppat.1000017

Soriano-Gabarro, M., Mrukowicz, J., Vesikari, T., & Verstraeten, T. (2006). Burden of rotavirus disease in European Union countries. *Pediatric Infectious Disease Journal, 25*(1 Suppl), S7-S11.

Spencer, E., & Arias, M. L. (1981). In vitro transcription catalyzed by heat-treated human rotavirus. *J Virol, 40*(1), 1-10.

Stacy-Phipps, S., & Patton, J. T. (1987). Synthesis of plus- and minus-strand RNA in rotavirus-infected cells. *J Virol, 61*(11), 3479-3484.

Stanley, P. (2011). Golgi glycosylation. *Cold Spring Harb Perspect Biol, 3*(4). doi:10.1101/cshperspect.a005199

Steele, A. D., Neuzil, K. M., Cunliffe, N. A., Madhi, S. A., Bos, P., Ngwira, B., . . . Han, H. H. (2012). Human rotavirus vaccine Rotarix provides protection against diverse circulating rotavirus strains in African infants: a randomized controlled trial. *BMC Infect Dis, 12*, 213. doi:10.1186/1471-2334-12-213

Steger, C. L., Boudreaux, C. E., LaConte, L. E., Pease, J. B., & McDonald, S. M. (2018). Group A Rotavirus VP1 Polymerase and VP2 Core Shell Proteins: Intergenotypic Sequence Variation and In vitro Functional Compatibility. *J Virol*. doi:10.1128/JVI.01642-18

Steinman, R. M., & Hemmi, H. (2006). Dendritic cells: translating innate to adaptive immunity. *Curr Top Microbiol Immunol, 311*, 17-58.

Strahle, L., Garcin, D., Le Mercier, P., Schlaak, J. F., & Kolakofsky, D. (2003). Sendai virus targets inflammatory responses, as well as the interferon-induced antiviral state, in a multifaceted manner. *J Virol, 77*(14), 7903-7913.

Structural Genomics, C., China Structural Genomics, C., Northeast Structural Genomics, C., Graslund, S., Nordlund, P., Weigelt, J., . . . Gunsalus, K. C. (2008). Protein production and purification. *Nat Methods, 5*(2), 135-146. doi:10.1038/nmeth.f.202

Strunk, B. S., Loucks, C. R., Su, M., Vashisth, H., Cheng, S., Schilling, J., . . . Skiniotis, G. (2011). Ribosome assembly factors prevent premature translation initiation by 40S assembly intermediates. *Science, 333*(6048), 1449-1453. doi:10.1126/science.1208245

Su, C. Q., Wu, Y. L., Shen, H. K., Wang, D. B., Chen, Y. H., Wu, D. M., . . . Yang, Z. L. (1986). An outbreak of epidemic diarrhoea in adults caused by a new rotavirus in Anhui Province of China in the summer of 1983. *J Med Virol, 19*(2), 167-173.

Sutter, G., Ohlmann, M., & Erfle, V. (1995). Non-replicating vaccinia vector efficiently expresses bacteriophage T7 RNA polymerase. *FEBS Lett, 371*(1), 9-12.

Suzuki, H., Kitaoka, S., Konno, T., Sato, T., & Ishida, N. (1985). Two modes of human rotavirus entry into MA 104 cells. *Arch Virol, 85*(1-2), 25-34.

Swartz, J. (2006). Developing cell-free biology for industrial applications. *J Ind Microbiol Biotechnol, 33*(7), 476-485. doi:10.1007/s10295-006-0127-y

Szabo, A., Magyarics, Z., Pazmandi, K., Gopcsa, L., Rajnavolgyi, E., & Bacsi, A. (2014). TLR ligands upregulate RIG-I expression in human plasmacytoid dendritic cells in a type I IFN-independent manner. *Immunol Cell Biol, 92*(8), 671-678. doi:10.1038/icb.2014.38

Takai, K., Sawasaki, T., & Endo, Y. (2010). Practical cell-free protein synthesis system using purified wheat embryos. *Nature Protocols, 5*(2), 227-238. doi:10.1038/nprot.2009.207

Takayama, K., Matsuura, A., & Itakura, E. (2017). Dissection of ubiquitinated protein degradation by basal autophagy. *FEBS Lett, 591*(9), 1199-1211. doi:10.1002/1873-3468.12641

Takeuchi, O., & Akira, S. (2010). Pattern recognition receptors and inflammation. *Cell, 140*(6), 805-820. doi:10.1016/j.cell.2010.01.022

Tang, W., Pavlish, O. A., Spiegelman, V. S., Parkhitko, A. A., & Fuchs, S. Y. (2003). Interaction of Epstein-Barr virus latent membrane protein 1 with SCFHOS/beta-TrCP E3 ubiquitin ligase regulates extent of NF-kappaB activation. *J Biol Chem, 278*(49), 48942-48949. doi:10.1074/jbc.M307962200

Taniguchi, K., Kojima, K., & Urasawa, S. (1996). Nondefective rotavirus mutants with an NSP1 gene which has a deletion of 500 nucleotides, including a cysteine-rich zinc finger motif-encoding region (nucleotides 156 to 248), or which has a nonsense codon at nucleotides 153-155. *J Virol, 70*(6), 4125-4130.

Taniguchi, T., Ogasawara, K., Takaoka, A., & Tanaka, N. (2001). IRF family of transcription factors as regulators of host defense. *Annu Rev Immunol, 19*, 623-655. doi:10.1146/annurev.immunol.19.1.623

Taraporewala, Z., Chen, D., & Patton, J. T. (1999). Multimers formed by the rotavirus nonstructural protein NSP2 bind to RNA and have nucleoside triphosphatase activity. *J Virol, 73*(12), 9934-9943.

Taraporewala, Z. F., & Patton, J. T. (2001). Identification and characterization of the helix-destabilizing activity of rotavirus nonstructural protein NSP2. *J Virol, 75*(10), 4519-4527. doi:10.1128/JVI.75.10.4519-4527.2001

Taraporewala, Z. F., & Patton, J. T. (2004). Nonstructural proteins involved in genome packaging and replication of rotaviruses and other members of the Reoviridae. *Virus Res, 101*(1), 57-66. doi:10.1016/j.virusres.2003.12.006

Taraporewala, Z. F., Schuck, P., Ramig, R. F., Silvestri, L., & Patton, J. T. (2002). Analysis of a temperature-sensitive mutant rotavirus indicates that NSP2 octamers are the functional form of the protein. *J Virol, 76*(14), 7082-7093.

Tarun, S. Z., Jr., & Sachs, A. B. (1995). A common function for mRNA 5' and 3' ends in translation initiation in yeast. *Genes Dev, 9*(23), 2997-3007.

Tate, J. E., Burton, A. H., Boschi-Pinto, C., Parashar, U. D., & World Health Organization-Coordinated Global Rotavirus Surveillance, N. (2016). Global, Regional, and National Estimates of Rotavirus Mortality in Children <5 Years of Age, 2000-2013. *Clin Infect Dis, 62 Suppl 2*, S96-S105. doi:10.1093/cid/civ1013

Taylor, J. A., Meyer, J. C., Legge, M. A., O'Brien, J. A., Street, J. E., Lord, V. J., . . . Bellamy, A. R. (1992). Transient expression and mutational analysis of the rotavirus intracellular receptor: the C-terminal methionine residue is essential for ligand binding. *J Virol, 66*(6), 3566-3572.

Thanos, D., & Maniatis, T. (1995). Virus induction of human IFN beta gene expression requires the assembly of an enhanceosome. *Cell, 83*(7), 1091-1100.

Thomson, S. J., Goh, F. G., Banks, H., Krausgruber, T., Kotenko, S. V., Foxwell, B. M., & Udalova, I. A. (2009). The role of transposable elements in the regulation of IFN-lambda1 gene expression. *Proc Natl Acad Sci U S A, 106*(28), 11564-11569. doi:10.1073/pnas.0904477106

Thwaites, R., Chamberlain, G., & Sacre, S. (2014). Emerging role of endosomal toll-like receptors in rheumatoid arthritis. *Front Immunol, 5*, 1. doi:10.3389/fimmu.2014.00001

Tian, P., Ball, J. M., Zeng, C. Q., & Estes, M. K. (1996). Rotavirus protein expression is important for virus assembly and pathogenesis. *Arch Virol Suppl, 12*, 69-77.

Tian, P., Hu, Y., Schilling, W. P., Lindsay, D. A., Eiden, J., & Estes, M. K. (1994). The nonstructural glycoprotein of rotavirus affects intracellular calcium levels. *J Virol, 68*(1), 251-257.

Tong, X., Yin, L., Washington, R., Rosenberg, D. W., & Giardina, C. (2004). The p50-p50 NF-kappaB complex as a stimulus-specific repressor of gene activation. *Mol Cell Biochem, 265*(1-2), 171-183.

Torres-Vega, M. A., Gonzalez, R. A., Duarte, M., Poncet, D., Lopez, S., & Arias, C. F. (2000). The C-terminal domain of rotavirus NSP5 is essential for its multimerization, hyperphosphorylation and interaction with NSP6. *J Gen Virol, 81*(Pt 3), 821-830. doi:10.1099/0022-1317-81-3-821

Tosser, G., Labbe, M., Bremont, M., & Cohen, J. (1992). Expression of the major capsid protein VP6 of group C rotavirus and synthesis of chimeric single-shelled particles by using recombinant baculoviruses. *J Virol, 66*(10), 5825-5831.

Traenckner, E. B., Pahl, H. L., Henkel, T., Schmidt, K. N., Wilk, S., & Baeuerle, P. A. (1995). Phosphorylation of human I kappa B-alpha on serines 32 and 36 controls I kappa B-alpha proteolysis and NF-kappa B activation in response to diverse stimuli. *EMBO J, 14*(12), 2876-2883.

Trask, S. D., McDonald, S. M., & Patton, J. T. (2012). Structural insights into the coupling of virion assembly and rotavirus replication. *Nat Rev Microbiol, 10*(3), 165-177. doi:10.1038/nrmicro2673

Trask, S. D., Ogden, K. M., & Patton, J. T. (2012). Interactions among capsid proteins orchestrate rotavirus particle functions. *Current Opinion in Virology, 2*(4), 373-379. doi:DOI 10.1016/j.coviro.2012.04.005

Trask, S. D., Wetzel, J. D., Dermody, T. S., & Patton, J. T. (2013). Mutations in the rotavirus spike protein VP4 reduce trypsin sensitivity but not viral spread. *J Gen Virol, 94*(Pt 6), 1296-1300. doi:10.1099/vir.0.050674-0

Trojnar, E., Otto, P., Roth, B., Reetz, J., & Johne, R. (2010). The genome segments of a group D rotavirus possess group A-like conserved termini but encode group-specific proteins. *J Virol, 84*(19), 10254-10265. doi:10.1128/JVI.00332-10

Tucker, A. W., Haddix, A. C., Bresee, J. S., Holman, R. C., Parashar, U. D., & Glass, R. I. (1998). Cost-effectiveness analysis of a rotavirus immunization program for the United States. *Jama-Journal of the American Medical Association, 279*(17), 1371-1376. doi:DOI 10.1001/jama.279.17.1371

Uhlen, M., Forsberg, G., Moks, T., Hartmanis, M., & Nilsson, B. (1992). Fusion proteins in biotechnology. *Curr Opin Biotechnol, 3*(4), 363-369.

Uzri, D., & Greenberg, H. B. (2013). Characterization of rotavirus RNAs that activate innate immune signaling through the RIG-I-like receptors. *PLoS One, 8*(7), e69825. doi:10.1371/journal.pone.0069825

Valenzuela, S., Pizarro, J., Sandino, A. M., Vasquez, M., Fernandez, J., Hernandez, O., . . . Spencer, E. (1991). Photoaffinity labeling of rotavirus VP1 with 8-azido-ATP: identification of the viral RNA polymerase. *J Virol, 65*(7), 3964-3967.

van Boxel-Dezaire, A. H., Rani, M. R., & Stark, G. R. (2006). Complex modulation of cell type-specific signaling in response to type I interferons. *Immunity, 25*(3), 361-372. doi:10.1016/j.immuni.2006.08.014

van der Velden, A. W., & Thomas, A. A. (1999). The role of the 5' untranslated region of an mRNA in translation regulation during development. *Int J Biochem Cell Biol, 31*(1), 87-106.
van Gaalen, R. D., van de Kassteele, J., Hahne, S. J. M., Bruijning-Verhagen, P., & Wallinga, J. (2017). Determinants of Rotavirus Transmission: A Lag Nonlinear Time Series Analysis. *Epidemiology, 28*(4), 503-513. doi:10.1097/EDE.0000000000000654
Vancott, J. L., McNeal, M. M., Choi, A. H., & Ward, R. L. (2003). The role of interferons in rotavirus infections and protection. *J Interferon Cytokine Res, 23*(3), 163-170. doi:10.1089/107999003321532501
Vascotto, F., Campagna, M., Visintin, M., Cattaneo, A., & Burrone, O. R. (2004). Effects of intrabodies specific for rotavirus NSP5 during the virus replicative cycle. *J Gen Virol, 85*(Pt 11), 3285-3290. doi:10.1099/vir.0.80075-0
Vasquez-Del Carpio, R., Gonzalez-Nilo, F. D., Riadi, G., Taraporewala, Z. F., & Patton, J. T. (2006). Histidine triad-like motif of the rotavirus NSP2 octamer mediates both RTPase and NTPase activities. *J Mol Biol, 362*(3), 539-554. doi:10.1016/j.jmb.2006.07.050
Vazquez, C., & Horner, S. M. (2015). MAVS Coordination of Antiviral Innate Immunity. *J Virol, 89*(14), 6974-6977. doi:10.1128/jvi.01918-14
Vende, P., Piron, M., Castagne, N., & Poncet, D. (2000). Efficient translation of rotavirus mRNA requires simultaneous interaction of NSP3 with the eukaryotic translation initiation factor eIF4G and the mRNA 3' end. *J Virol, 74*(15), 7064-7071.
Vende, P., Taraporewala, Z. F., & Patton, J. T. (2002). RNA-binding activity of the rotavirus phosphoprotein NSP5 includes affinity for double-stranded RNA. *J Virol, 76*(10), 5291-5299.
Vidya, M. K., Kumar, V. G., Sejian, V., Bagath, M., Krishnan, G., & Bhatta, R. (2018). Toll-like receptors: Significance, ligands, signaling pathways, and functions in mammals. *Int Rev Immunol, 37*(1), 20-36. doi:10.1080/08830185.2017.1380200
Villarino, A. V., Kanno, Y., & O'Shea, J. J. (2017). Mechanisms and consequences of Jak-STAT signaling in the immune system. *Nat Immunol, 18*(4), 374-384. doi:10.1038/ni.3691
Vitour, D., Lindenbaum, P., Vende, P., Becker, M. M., & Poncet, D. (2004). RoXaN, a novel cellular protein containing TPR, LD, and zinc finger motifs, forms a ternary complex with eukaryotic initiation factor 4G and rotavirus NSP3. *J Virol, 78*(8), 3851-3862.
Wack, A., Terczynska-Dyla, E., & Hartmann, R. (2015). Guarding the frontiers: the biology of type III interferons. *Nat Immunol, 16*(8), 802-809. doi:10.1038/ni.3212
Walker, C. L. F., Rudan, I., Liu, L., Nair, H., Theodoratou, E., Bhutta, Z. A., . . . Black, R. E. (2013). Global burden of childhood pneumonia and diarrhoea. *Lancet, 381*(9875), 1405-1416. doi:10.1016/S0140-6736(13)60222-6
Walther, A., Mohanty, S. K., Donnelly, B., Coots, A., Lages, C. S., Lobeck, I., . . . Tiao, G. (2015). Rhesus rotavirus VP4 sequence-specific activation of mononuclear cells is associated with cholangiopathy in murine biliary atresia. *Am J Physiol Gastrointest Liver Physiol, 309*(6), G466-474. doi:10.1152/ajpgi.00079.2015
Wang, C., Deng, L., Hong, M., Akkaraju, G. R., Inoue, J., & Chen, Z. J. (2001). TAK1 is a ubiquitin-dependent kinase of MKK and IKK. *Nature, 412*(6844), 346-351. doi:10.1038/35085597
Wang, W., Donnelly, B., Bondoc, A., Mohanty, S. K., McNeal, M., Ward, R., . . . Tiao, G. (2011). The rhesus rotavirus gene encoding VP4 is a major determinant in the pathogenesis of biliary atresia in newborn mice. *J Virol, 85*(17), 9069-9077. doi:10.1128/JVI.02436-10
Wang, Y., Cao, Y., Meng, Y., You, Z., Liu, X., & Liu, Z. (2014). The novel role of thymopentin in induction of maturation of bone marrow dendritic cells (BMDCs). *Int Immunopharmacol, 21*(2), 255-260. doi:10.1016/j.intimp.2014.05.011
Ward, R. L., Knowlton, D. R., & Pierce, M. J. (1984). Efficiency of human rotavirus propagation in cell culture. *J Clin Microbiol, 19*(6), 748-753.
Wells, A. I., & Coyne, C. B. (2018). Type III Interferons in Antiviral Defenses at Barrier Surfaces. *Trends in Immunology, 39*(10), 848-858. doi:https://doi.org/10.1016/j.it.2018.08.008
Wentz, M. J., Patton, J. T., & Ramig, R. F. (1996). The 3'-terminal consensus sequence of rotavirus mRNA is the minimal promoter of negative-strand RNA synthesis. *J Virol, 70*(11), 7833-7841.
Wentz, M. J., Zeng, C. Q., Patton, J. T., Estes, M. K., & Ramig, R. F. (1996). Identification of the minimal replicase and the minimal promoter of (-)-strand synthesis, functional in rotavirus RNA replication in vitro. *Arch Virol Suppl, 12*, 59-67.

WHO. (2016). WHO: Immunization surveillance, assessment and monitoring. Retrieved from http://www.who.int/immunization/topics/rotavirus/en/

Wu, H., Taniguchi, K., Urasawa, T., & Urasawa, S. (1998). Serological and genomic characterization of human rotaviruses detected in China. *J Med Virol, 55*(2), 168-176.

Wyatt, R. G., James, W. D., Bohl, E. H., Theil, K. W., Saif, L. J., Kalica, A. R., . . . Chanock, R. M. (1980). Human Rotavirus Type-2 - Cultivation Invitro. *Science, 207*(4427), 189-191. doi:DOI 10.1126/science.6243190

Yang, Y., Kitagaki, J., Dai, R. M., Tsai, Y. C., Lorick, K. L., Ludwig, R. L., . . . Weissman, A. M. (2007). Inhibitors of ubiquitin-activating enzyme (E1), a new class of potential cancer therapeutics. *Cancer Res, 67*(19), 9472-9481. doi:10.1158/0008-5472.CAN-07-0568

Ye, L., Jiang, Y., Yang, G., Yang, W., Hu, J., Cui, Y., . . . Wang, C. (2017). Murine bone marrow-derived DCs activated by porcine rotavirus stimulate the Th1 subtype response in vitro. *Microb Pathog, 110*, 325-334. doi:10.1016/j.micpath.2017.07.015

Yin, Z., Dai, J., Deng, J., Sheikh, F., Natalia, M., Shih, T., . . . Fitzgerald-Bocarsly, P. (2012). Type III IFNs are produced by and stimulate human plasmacytoid dendritic cells. *J Immunol, 189*(6), 2735-2745. doi:10.4049/jimmunol.1102038

Yolken, R., Arango-Jaramillo, S., Eiden, J., & Vonderfecht, S. (1988). Lack of genomic reassortment following infection of infant rats with group A and group B rotaviruses. *J Infect Dis, 158*(5), 1120-1123.

Yoneyama, M., Kikuchi, M., Matsumoto, K., Imaizumi, T., Miyagishi, M., Taira, K., . . . Fujita, T. (2005). Shared and unique functions of the DExD/H-box helicases RIG-I, MDA5, and LGP2 in antiviral innate immunity. *J Immunol, 175*(5), 2851-2858.

Yow, M. D., Melnick, J. L., Blattner, R. J., Stephenson, W. B., Robinson, N. M., & Burkhardt, M. A. (1970). The association of viruses and bacteria with infantile diarrhea. *Am J Epidemiol, 92*(1), 33-39.

Yu, X., Mishra, R., Holloway, G., von Itzstein, M., Coulson, B. S., & Blanchard, H. (2015). Substantial Receptor-induced Structural Rearrangement of Rotavirus VP8*: Potential Implications for Cross-Species Infection. *Chembiochem, 16*(15), 2176-2181. doi:10.1002/cbic.201500360

Zahn, S., Rehkamper, C., Kummerer, B. M., Ferring-Schmidt, S., Bieber, T., Tuting, T., & Wenzel, J. (2011). Evidence for a pathophysiological role of keratinocyte-derived type III interferon (IFNlambda) in cutaneous lupus erythematosus. *J Invest Dermatol, 131*(1), 133-140. doi:10.1038/jid.2010.244

Zarate, S., Cuadras, M. A., Espinosa, R., Romero, P., Juarez, K. O., Camacho-Nuez, M., . . . Lopez, S. (2003). Interaction of rotaviruses with Hsc70 during cell entry is mediated by VP5. *J Virol, 77*(13), 7254-7260.

Zarate, S., Espinosa, R., Romero, P., Mendez, E., Arias, C. F., & Lopez, S. (2000). The VP5 domain of VP4 can mediate attachment of rotaviruses to cells. *J Virol, 74*(2), 593-599. doi:Doi 10.1128/Jvi.74.2.593-599.2000

Zarate, S., Romero, P., Espinosa, R., Arias, C. F., & Lopez, S. (2004). VP7 mediates the interaction of rotaviruses with integrin alphavbeta3 through a novel integrin-binding site. *J Virol, 78*(20), 10839-10847. doi:10.1128/JVI.78.20.10839-10847.2004

Zeng, C. Q., Estes, M. K., Charpilienne, A., & Cohen, J. (1998). The N terminus of rotavirus VP2 is necessary for encapsidation of VP1 and VP3. *J Virol, 72*(1), 201-208.

Zeng, C. Q., Wentz, M. J., Cohen, J., Estes, M. K., & Ramig, R. F. (1996). Characterization and replicase activity of double-layered and single-layered rotavirus-like particles expressed from baculovirus recombinants. *J Virol, 70*(5), 2736-2742.

Zhang, R., Jha, B. K., Ogden, K. M., Dong, B., Zhao, L., Elliott, R., . . . Weiss, S. R. (2013). Homologous 2',5'-phosphodiesterases from disparate RNA viruses antagonize antiviral innate immunity. *Proc Natl Acad Sci U S A, 110*(32), 13114-13119. doi:10.1073/pnas.1306917110

Zhang, S., Kodys, K., Li, K., & Szabo, G. (2013). Human type 2 myeloid dendritic cells produce interferon-lambda and amplify interferon-alpha in response to hepatitis C virus infection. *Gastroenterology, 144*(2), 414-425 e417. doi:10.1053/j.gastro.2012.10.034

Zhang, X., Friedman, A., Heaney, S., Purcell, P., & Maas, R. L. (2002). Meis homeoproteins directly regulate Pax6 during vertebrate lens morphogenesis. *Genes Dev, 16*(16), 2097-2107. doi:10.1101/gad.1007602

Zhao, B., Shu, C., Gao, X., Sankaran, B., Du, F., Shelton, C. L., . . . Li, P. (2016). Structural basis for concerted recruitment and activation of IRF-3 by innate immune adaptor proteins. *Proc Natl Acad Sci U S A, 113*(24), E3403-3412. doi:10.1073/pnas.1603269113

Zhao, J., Zhai, B., Gygi, S. P., & Goldberg, A. L. (2015). mTOR inhibition activates overall protein degradation by the ubiquitin proteasome system as well as by autophagy. *Proc Natl Acad Sci U S A, 112*(52), 15790-15797. doi:10.1073/pnas.1521919112